universität uulm

Fault diagnosis for distributed-parameter systems using integral transformations and trajectory planning methods

DISSERTATION

zur Erlangung des akademischen Grades eines

DOKTOR-INGENIEURS
(Dr.-Ing.)

der Fakultät für Ingenieurwissenschaften, Informatik
und Psychologie der Universität Ulm

von

Ferdinand Fischer
aus Berlin

Gutachter: Prof. Dr.-Ing. habil. Joachim Deutscher
PD Dr.-Ing. habil. Paul Kotyczka

Amtierender Dekan: Prof. Dr.-Ing. Maurits Ortmanns

Ulm, 07.02.2022

Acknowledgements

This thesis was written during my work as a research assistant at the Institute of Measurement, Control and Microtechnology (MRM) at Ulm University. However, many of the results described in this work were obtained during my time as a research assistant at the Institute of Automatic Control (LRT) of the Friedrich-Alexander-Universität Erlangen-Nürnberg.

At this point, I would like to thank my thesis advisor Prof. Dr.-Ing. habil. Joachim Deutscher, who supervised this work with extraordinary interest and commitment both at LRT and MRM. His always highly valuable suggestions and enriching discussions have contributed in the highest degree to the success of this work. I would like to thank him for his trust, which allowed me to devote myself to this interesting and enriching research topic. Special thanks go to PD Dr.-Ing. habil. Paul Kotyczka for his commitment as a reviewer of my dissertation and for his constructive comments. I would also like to thank the examiners of the doctoral committee, Prof. Dr.-Ing. Jürgen Freudenberger and Prof. Dr.-Ing. Albrecht Rothermel.

My thanks also go to the chairholder of the LRT Prof. Dr.-Ing. Knut Graichen and the retired chairholder Prof. Dr.-Ing. habil. Günter Roppenecker for giving me the necessary freedom to work on my dissertation. In addition, I would like to express my sincere thanks to my esteemed colleagues, both at the LRT and the MRM, for the outstanding cooperation and the excellent working atmosphere. In particular, I would like to express my heartfelt thanks to my dear colleagues Jakob Gabriel and Alexander Lomakin for the countless inspiring technical discussions and the proofreading of this work.

Abstract

A unified method is presented for the fault diagnosis for a large class of distributed-parameter systems that does not require a system approximation. The considered system class includes parabolic, biharmonic, and heterodirectional hyperbolic ODE-PDE systems. A residual generator is derived for the detection of additive and multiplicative actuator, process and sensor faults with unknown signal form. This residual generator is decoupled from disturbances that are described by a signal model in the form of a finite-dimensional linear time-invariant system. With this signal model, a large class of relevant signal forms for disturbances can be considered. In addition to the modeled disturbances, also unknown but bounded disturbances are taken into account by introducing a threshold for the fault detection residual signal. Moreover, the fault diagnosis, i.e., the fault detection, isolation, and identification, is regarded for additive actuator, process, and sensor faults with known signal form. For the fault diagnosis, the signal form of both the fault and the disturbance are assumed to be described also by a signal model. The fault identification is achieved in finite time. If additionally the unknown but bounded disturbance is present, then fault detection, isolation and estimation with a bounded estimation error are achieved.

By applying integral transformations to the system description, an input-output relation is established. From this expression, residual generators that are dedicated to the fault detection and the fault diagnosis can be derived in the form of moving horizon integrals. The used integral kernels are determined as the solution of a feedforward control problem for an ODE-PDE system, which is solved by flatness-based trajectory planning. Existing degrees of freedom in the trajectory planning are utilized to make the resulting residual generator less sensitive with respect to the unknown but bounded disturbance. In addition to systematically determining the residual generators, the flatness-based approach also leads to conditions to easily check the detectability and identifiability of the faults. For the implementation of the resulting residual generators in discrete-time, finite impulse response filters can be used. Simulation results for models motivated from engineering applications of a cantilever with load at the free end and a cable with payload in constant flowing water illustrate the theoretical results for the fault detection and diagnosis.

Kurzfassung

Zur Fehlerdiagnose für eine große Klasse verteilt-parametrischer Systeme wird eine einheitliche Methode vorgestellt, die keine Systemapproximation erfordert. Die betrachtete Systemklasse umfasst parabolische, biharmonische und heterodirektionale hyperbolische ODE-PDE Systeme. Zur dedizierten Detektion von additiven und multiplikativen Aktor-, Prozess- sowie Sensorfehlern mit unbekannter Signalform wird ein Residuengenerator hergeleitet. Dieser Residuengenerator kann von Störungen entkoppelt werden, die sich durch ein endlich-dimensionales lineares zeitinvariantes Signalmodell beschreiben lassen. Dieses Signalmodell ermöglicht die Berücksichtigung einer großen Klasse von relevanten Signalformen für die Störung. Zusätzlich lassen sich auch unbekannte Störungen mit bekannter oberer Schranke durch die Einführung eines Schwellenwertes für das zur Fehlerdetektion genutzte Residuum berücksichtigen. Des Weiteren, wird die Fehlerdiagnose, d. h. die Fehlerdetektion, -isolation und -identifikation, für additive Aktor-, Prozess- und Sensorfehler mit bekannter Signalform behandelt. Zur Fehlerdiagnose wird angenommen, dass sich die Signalform des Fehlers und der Störung durch ein endlich-dimensionales lineares zeitinvariantes Signalmodell beschreiben lassen. Wenn zusätzlich unbekannte aber betragsmäßig beschränkte Störungen auftreten, ist die Fehlerdetektion, -isolation und -schätzung mit beschränktem und bekannten Schätzfehler dennoch möglich.

Durch Anwendung von Integraltransformationen auf die Systembeschreibung wird eine Eingangs-Ausgangs-Beziehung aufgestellt. Aus diesem Zusammenhang lassen sich Residuengeneratoren die speziell für die Fehlerdetektion und die Fehlerdiagnose vorgesehen sind in Form von Integralen über einem gleitenden Horizont bestimmen. Die verwendeten Integralkerne werden als Lösung eines Steuerungsproblems für ein ODE-PDE-System bestimmt, das mit flachheitsbasierter Trajektorienplanung gelöst wird. Vorhandene Freiheitsgrade in der Trajektorienplanung werden genutzt, um den resultierenden Residuengenerator gegenüber der unbekannten, aber begrenzten Störung unempfindlicher zu machen. Neben der systematischen Bestimmung der Residuengeneratoren führt der flachheitsbasierte Ansatz auch zu Bedingungen zur einfachen Überprüfung der Detektier- und Identifizierbarkeit der Fehler. Die Implementierung der resultierenden Residuengeneratoren in diskreter Zeit erfolgt durch Filter mit endlicher Impulsantwort. Simulationsergebnisse für aus technischen Anwendungen motivierte Modelle eines Auslegers mit Last am freien Ende und eines schweren Seils mit Last in konstant fließendem Wasser veranschaulichen die theoretischen Ergebnisse zur Fehlererkennung und -diagnose.

Contents

Chapter 1

Introduction

The development of control methods enables the automation of more and more complex tasks, increase process efficiency and improve product quality. However, with the resulting increase in the automation, also the issues of operational safety, availability and reliability become more and more important. In safety critical systems, the occurrence of a fault can lead to serious consequences such as economic loss, endangerment of people and ecological destruction. *Faults* are unpermitted deviations of the system from standard conditions, which can cause a failure or malfunction, i.e., a permanent or intermittent irregularity of the required function (see, e.g., [43]). Thus, an essential step in avoiding the possible consequences of failures or malfunctions is the early detection of a fault so that countermeasures can be taken. Further information about the location and magnitude of the fault can help to make the automated system more resilient by means of fault-tolerant control methods, or to support and simplify maintenance. The detection of a fault, the isolation of different faults and the identification of the magnitude of a fault are summarized as *fault diagnosis* (see, e.g., [43]). To be specific, the fault diagnosis consists of the fault detection, isolation and identification. *Fault detection* is primarily concerned with determining the occurrence of a fault, *fault isolation* is about distinguishing between different faults and *fault identification* addresses the determination of the magnitude of a fault. Thus, the on-line supervision of automated systems by a fault detection is a key technology to avoid catastrophic consequences in safety-critical systems. In addition, the fault diagnosis can improve the availability, reliability and maintainability of technical systems.

In the model-based fault diagnosis approaches, a mathematical model of the technical process is used to derive a residual generator for a residual signal. The latter indicates the presence of a fault and can be used for the fault isolation and identification. When the dynamics of the technical process can be described by linear ordinary differential equations (ODEs), a linear lumped-parameter system (LPS) is derived as a model. For this system class, the model-based fault diagnosis approaches are a

well-developed field (see, e.g., the monographs [12, 16, 28, 42]). However, whenever a relevant quantity of the technical process does not only change in time but is also continuously distributed over a spatial domain, the modeling of the technical process leads to partial differential equations (PDEs). The derived system model is then a distributed-parameter system (DPS). A spatial dependence of system variables occurs in many models for technical processes. Examples are diffusion, heat transfer, vibrations in flexible structures and wave propagation. The reaction-diffusion equation and the heat equation are PDEs of *parabolic* type, which describe balancing processes like matter diffusion or heat transfer. Important application examples that are modeled by parabolic PDEs originate from the field of chemical and biochemical engineering (see, e.g., [6, 44]). A specific example is a tubular reactor as described in [45]. The typical PDE of the *biharmonic* type is the Euler-Bernoulli-beam equation, which describes the distributed vibrations in a beam. The latter is a relevant model in the field of smart materials (see, e.g., [8]) and flexible structures (see, e.g., [7]). As discussed in [30], flexible robot manipulators in particular can be modeled by biharmonic PDEs. With *hyperbolic* PDEs like the wave equation or the transport equation, for example, vibrations in a string, transport processes, but also time delays are described. An important subclass are the *heterodirectional hyperbolic PDE* systems. They consist of transport PDEs propagating in both the negative and positive direction of the spatial coordinate. Many hyperbolic PDE systems can be rewritten into this form, including models for coupled string networks (see, e.g., [59]), transmission lines, networks of open channels and further application examples described in [10]. Moreover, when the model of the technical system contains coupled subsystems with lumped and distributed parameters, ODE-PDE systems are derived. Examples are a flexible robot arm (see, e.g., [3]), a cable with a payload (see, e.g., [68]), a pneumatic system with a tank (see [47]) or a dual-cable elevator (see [88]). Although the modeling often leads to nonlinear system models, in many cases it is sufficient to consider a linearization of these. Recently, efficient control design approaches have been developed for DPSs (see, e.g., [29, 52, 59, 62]), which increases also the need for a systematic fault diagnosis method for this system class.

1.1 Fault diagnosis for distributed-parameter systems

In contrast to the well-developed methods for the LPSs, the fault diagnosis methods for DPSs are so far predominantly based on observers. In an early-lumping approach, the observer used for the fault diagnosis is designed for a finite-dimensional model of the DPS (see, e.g., [9, 32, 37, 39]). Thus, in principle, the well-developed fault diagnosis methods for LPSs become accessible for the residual generator design,

but the neglected dynamics must be additionally taken into account. The latter introduces further complexity in the residual generator design and can also lead to high-order models, which can further complicate the design process. In particular, as discussed in [37], the approximation of some boundary controlled DPSs can become challenging. The fault localization, which is also relevant for DPSs, is solved in [34] based on a finite-dimensional observer used as a residual generator for a spatially distributed residual signal.

In the late-lumping approaches, the residual generator is designed directly for the DPS. A general fault diagnosis approach based on a late-lumping observer is described in [20] for estimating process faults. However, the distributed state must be known, which is rarely possible in real-world applications. For positive-real linear infinite-dimensional systems, the fault detection for actuator faults is presented in [22], where a late-lumping observer is used. Moreover, some nonlinearities have been taken into account by observer-based approaches, shown in [4] and [21]. For parabolic PDE systems with constant coefficients, boundary inputs and measurements, fault diagnosis approaches are regarded in [15, 27], by using backstepping-based observers as residual generators. Both approaches take into account distributed disturbances but consider specific boundary conditions (BCs) and specific fault scenarios, which limits the application of the method. Another observer-based fault diagnosis approach in which measurements in the spatial domain and at the boundary are used is presented in [33] for scalar parabolic PDE systems with constant coefficients. For hyperbolic PDE systems, fault diagnosis residual generators based on observers that are designed by the backstepping method can be found in [1, 26, 97]. To be specific, the fault detection, identification and localization problem is solved in [1] for a 2×2 heterodirectional hyperbolic PDE system. Multiplicative actuator and sensor faults with constant fault parameters in a scalar first-order hyperbolic PDE system with an additional integral term are considered in [97]. An additive distributed fault affecting a wave equation subject to a distributed disturbance is taken into account in [26]. These late lumping approaches have in common that no approximation error has to be considered in the construction of the residual generator. However, since the residual generator is based on an infinite-dimensional observer, at least for the realization of this observer an approximation is required. An approach that omits the latter drawback is the functional observer designed in [23] for the fault detection in Riesz-spectral systems. However, only systems with in-domain input and measurement can be regarded. An alternative to the observer-based approaches is shown in [35], by using the Laplace transform and algebraic manipulations to derive a residual generator for the detection and localization of a fault in an electrical transmission line.

This non-exhaustive overview for the fault diagnosis for DPS shows that a lot of relevant fault diagnosis problems have been already taken into account. However, all the presented solutions are only applicable for a specific problem setting or

require restrictive assumptions. In particular, no late-lumping approach for parabolic and biharmonic PDE systems with spatially varying coefficients for boundary and in-domain control inputs as well as measurements is available in the literature. There are also no such results for general heterodirectional hyperbolic ODE-PDE systems. Moreover, only a few of the existing fault diagnosis approaches take disturbances into account.

Recently, a new approach for the design of the residual generator based on integral transformations has been introduced in [98] for a simple parabolic system. It was extended in [102] for a large system class including DPS with parabolic and biharmonic PDEs, general BCs, boundary and in-domain inputs, measurements as well as disturbances. In this approach, additive actuator, sensor and process faults with a signal form that can be modeled by a polynomial are taken into account. This approach was transferred to a faulty wave equation in [103] and generalized to heterodirectional hyperbolic ODE-PDE systems in [104]. In the latter contribution, also the signal class of the faults and disturbances is extended. Both, the fault and the disturbance signals are assumed to be solutions of a *signal model* in form of a lumped-parameter linear time-invariant (LTI) system, which enables the modeling of polynomial and trigonometric signals as well as combinations thereof. Thus, a significantly larger signal class can be taken into account that includes relevant and frequently occurring signal types. A further result, based on the integral transformation-based method, is the dedicated fault detection approach for LPS in [106] that requires no knowledge of the fault signal form. In all these contributions, the resulting residual generators consist of integral expressions on a moving horizon for the control input and the measurement. Since the latter are usually only available at sampled time points, the integral expressions must be approximated in discrete-time. This approximation yields finite-impulse response (FIR) filters, which are easy to implement with low computational effort.

1.2 Contribution

A fault detection and a fault diagnosis approach based on integral transformations for linear parabolic, biharmonic and heterodirectional hyperbolic ODE-PDE systems is presented in this thesis. Both, for fault detection and diagnosis, no system approximation is required. In [102] and [104], the fault diagnosis problem is solved with the focus on the identification, which requires the assumption that the fault signals can be described by a signal model. As has been shown for LPSs in [106], this restrictive assumption can be omitted if only fault detection is required. Thus, the approach in [106] is transferred in this thesis to the DPSs to solve the fault detection problem under less restrictive assumptions. A fault detection residual generator is

designed to detect faults of additive and multiplicative type, which does not require a known signal form for the fault. The corresponding residual signal is decoupled from disturbances with known signal form that are modeled by lumped-parameter LTI signal models. Unknown but bounded disturbances can be taken into account by a threshold. The fault diagnosis problem, i.e., the fault detection, isolation and identification, is solved for additive faults that have a known signal form and can be described by a lumped-parameter LTI signal model. Similar to the fault detection, the residual generator for the fault diagnosis can also be decoupled from disturbances, which are described by a signal model of the same type. Because integral transformations on a moving horizon are used, the fault identification is achieved in finite time. If an unknown but bounded disturbance is present, the fault detection, isolation and estimation with bounded estimation error can still be achieved. For both, the fault detection and the fault diagnosis residual generator, available degrees of freedom are used to make the residual signal less sensitive to the unknown but bounded disturbances. This sensitivity optimization allows the detection of small faults even in the presence of disturbances with unknown signal forms and for the fault estimation, a low fault estimation error is achieved. To verify the fault detectability and identifiability, conditions are derived that are simple to evaluate and depend solely on the system parameters as well as the assumed signal models for the faults and the disturbances. Note that the resulting residual generators do not require a system approximation and no observer must be designed. The resulting residual generators can be efficiently implemented in discrete-time by FIR filters.

The fault diagnosis for DPSs with parabolic or biharmonic PDEs is already considered in [102], but extended in this thesis to systems with general ODE-PDE couplings. These couplings can occur both in the spatial domain and at the boundaries so that the fault diagnosis becomes available for further relevant technical systems such as, e.g., flexible robot arms [3]. Moreover, only fault and disturbance signals that can be described by polynomials have been taken into account in [102]. To further increase the flexibility of the proposed method and make it applicable to more fault diagnosis settings, also the signal class of the faults and disturbances is extended. Similar to [104], these signals are assumed to be described by lumped-parameter LTI signal models in this thesis. Thus, also trigonometric signals or combinations of these and polynomial signals can be taken into account.

The proposed approaches for the fault detection and diagnosis are based on integral transformations on a moving horizon. The integral kernels of these transformations can be determined so that an input-output relation is derived, which is decoupled from the disturbance with known signal form. Based on this input-output relation, the fault detection residual generator is obtained in form of integral expressions on a moving horizon for the control input and the measurement signal. To derive this residual generator, requirements on the integral kernels are imposed, which

yield *kernel equations* in the form of an ODE-PDE system with initial and end conditions, an algebraic constraint and a freely assignable input. The PDE subsystem of this kernel equations is of the same type as the original system, i.e., it is either of the parabolic, the biharmonic or the heterodirectional hyperbolic type. Because of the given initial and end points, the kernel equations are a two-point initial-boundary value problem. The latter can be solved by the determination of a suitable feedforward control for the freely assignable input that drives the kernel equations system from the initial point to the end point. To compute this transition, results from the flatness-based trajectory planning are used. The flatness-based approach was originally developed for LPS (see, e.g., [54, 74, 82]) and generalized to DPS in, e.g., [53, 62, 73, 75, 93]. It uses a differential parametrization to express any system variable in terms of a freely assignable parametrizing variable. If the components of the latter are differentially independent, then it is a flat output and the system is called flat. For such systems, the planning of a transition between given initial and end points can be reformulated into an algebraic interpolation problem for a reference trajectory that is assigned to the flat output. Since this interpolation can be achieved by solving a linear system of equations, the solution of the two-point initial-boundary value problem is significantly facilitated. Finally, the trajectories for the system variables are obtained by the evaluation of the differential parametrizations with the computed reference trajectory. Note that for the solution of the kernel equations, only transitions for specific initial and end points have to be realized, which does not necessarily require a differentially independent parametrizing variable. In particular, for the fault detection problem, the obtained initial and end points are homogeneous. Thus, it suffices to plan a reference trajectory for this specific transition under consideration of the additional algebraic constraint. To verify the existence of such a trajectory, a condition based on the coefficient matrices of the differential expressions is derived in this thesis. On the one hand, this condition is significantly simpler to evaluate than a flatness analysis of the DPS of the kernel equations and on the other hand, it directly ensures the detectability of the fault. In contrast to the fault detection, the fault diagnosis kernel equations ICs are inhomogeneous and in general do not correspond to an equilibrium point of the corresponding ODE-PDE system. Although this nonequilibrium point makes the trajectory planning more difficult, it suffices to show that the required transition can be parametrized by a suitable reference trajectory. For the planning of the latter, this thesis proposes a constructive approach that provides also an easily verifiable condition.

Since the flatness analysis of the kernel equations system is avoided, the derived formal differential parametrizations are called differential expressions and the corresponding quantity to the flat output is called a parametrizing variable. Nevertheless, the required differential expressions can still be derived by employing results from the literature. To be specific, for kernel equations with a subsystem described by a PDE of parabolic or biharmonic type, results from [75, 93] are used to determine the differential expressions. However, this approach considers only dynamic BCs. To

determine the differential expressions for the more general ODE-PDE couplings that can occur in the kernel equations system the results from [75, 93] are supplemented in this thesis. For faulty heterodirectional hyperbolic ODE-PDE systems, a kernel equation with a PDE subsystem of the same type is obtained. The few flatness-based trajectory planning approaches for this system class (see, e.g., [93, 94]) are not suitable for the solution of the kernel equations. In particular, the approach in [93] requires a fixpoint iteration and the approach in [94] is only described for systems with constant coefficients. Thus, an alternative approach following the idea in [83] is proposed in this thesis. In [83], the flatness-based motion planning for a DPS with scalar parabolic PDE with varying coefficients is facilitated by mapping the original system into a more suitable form by a backstepping transformation. The latter is an established method for the feedback controller design of boundary controlled DPSs and an introduction to it can be found, e.g., in [52]. In the sense of [83], the backstepping transformation described in [41] is used to map the heterodirectional hyperbolic ODE-PDE system of the kernel equations into a target system with a cascade structure. Due to the latter, the differential expressions can be determined explicitly (see [104]), which gives rise to a systematic solution of the kernel equations.

By making use of results from the flatness-based trajectory planning methods, an interesting connection between the flatness and the fault detection as well as the fault diagnosis is established. This connection makes already existing results in the literature applicable to solve the fault detection and diagnosis problems systematically for a large system class. Vice versa, this connection also allows to transfer results derived for the solution of the kernel equations back to the motion planning for DPSs. In addition to the extended results for the determination of the differential expressions, a trade-off design for a residual generator is shown in this thesis that is sensitive to the fault and less sensitive to the disturbance. This trade-off design is derived by utilizing degrees of freedom in the reference trajectory planning, which might also be useful in other transition planning tasks.

1.3 Relation to other integral transformation based methods

Similar integral transformations as used in the proposed approach are also used in the modulating functions method, for which an overview can be found in [70]. The modulating function method is an algebraic method, originally developed in [81] for the parameter identification in LPS, which has been transferred to other system classes. Examples are nonlinear LPS (see, e.g., [17]), fractional LPS (see, e.g., [31]) and also DPS (see, e.g., [2, 56, 67]). Moreover, the modulating functions

method has also been applied to state estimation problems (see, e.g., [46, 69, 90]) and source estimation in DPS (see, e.g., [5, 105]). For the derivative estimation, approaches based on similar integral transformations are, e.g., [55, 61, 91]. Note that such approaches for the derivative estimation have also been used to solve fault detection problems for nonlinear systems in [57, 58, 66]. In contrast to the proposed method in this thesis, the previously mentioned approaches are based on integral transformations with prescribed integral kernels. Thus, available degrees of freedom are not systematically chosen to achieve additional objectives as the sensitivity optimization in this contribution. However, a systematic design for the determination of the integral kernels that imposes a desired transfer behavior on the derivative estimator is presented in [49, 65]. Moreover, in [77, 78], the modulating functions method is presented for the parameter identification for linear LPSs, where the determination of the modulating functions is firstly formulated in terms of a transition problem for a dynamical system. Since the latter is solved by trajectory planning methods, it shows interesting similarities to the presented approach in this thesis.

Moreover, the integral transformation based approach introduced in [98] is also used in [105] to reconstruct the source-term in a transport equation with time-varying transportation speed. A further interesting extension of the proposed approach can be found in [36], where it was modified to estimate the distributed state in a parabolic system.

1.4 Outline of the thesis

In Chapter 2, the fault detection and diagnosis problem is solved for parabolic and biharmonic ODE-PDE systems. At first, the considered system class as well as the fault and disturbance signals are introduced in Section 2.1 and Section 2.2. Based on this problem setting, the fault detection problem for parabolic and biharmonic ODE-PDE systems is solved in Section 2.3. After a detailed problem formulation in Section 2.3.1, the integral expressions are used to derive an input-output expression in Section 2.3.2 from which the residual generator is derived in Section 2.3.3. For this residual generator, the kernels of the applied integral transformations must be computed as a solution of the fault detection kernel equations, which are determined in Section 2.3.4 employing results of the flatness-based trajectory planning methods. The fault detection results are demonstrated for a simulation example of an Euler-Bernoulli beam as model for a cantilever beam with a tip load in Section 2.3.5.

Subsequently, the fault diagnosis approach for the parabolic and biharmonic ODE-PDE systems is presented in Section 2.4. After the introduction of the fault diagnosis

problem formulation in Section 2.4.1, the fault diagnosis equation for the fault identification respectively estimation is derived in Section 2.4.2. To make use of the resulting residual generator, the fault diagnosis kernel equations are solved in Section 2.4.3. Finally, the described fault diagnosis method is demonstrated for an Euler-Bernoulli beam in Section 2.4.4.

In the Chapter 3, the fault detection and diagnosis problem is solved for hetero-directional hyperbolic ODE-PDE systems, which are introduced in Section 3.1. The fault detection for this system class presented in Section 3.2 follows basically the same outline as the solution of the fault detection problem for the parabolic and biharmonic ODE-PDE systems. This procedure leads to the input-output expression described in Section 3.2.1 and the residual generator described in Section 3.2.2. However, the solution of the fault detection kernel equation in Section 3.2.3 is more involved due to the transport character of the hyperbolic PDEs. A backstepping transformation is used to map the ODE-PDE system of the corresponding fault detection kernel equations into a target system of cascade structure, which facilitates the solution of the feedforward control problem. The described results are verified for a 4×4 heterodirectional ODE-PDE system as a model for a hanging cable with a payload that is immersed in water with constant flow.

In Section 3.3, the fault diagnosis problem for the heterodirectional hyperbolic ODE-PDE system is solved. For this, the fault diagnosis equation is derived in Section 3.3.1. The corresponding fault diagnosis kernel equations are taken into account in Section 3.3.2. Simulation results in Section 3.3.3 demonstrate the effectiveness of the fault diagnosis method for a simulation example of a hanging cable with a payload immersed in water with constant flow.

A brief summary of the presented methods and an outlook on possible research fields for extensions of the proposed method will conclude the thesis in Chapter 4.

1.5 Remarks on the notation

The identity matrix is denoted by I and is always assumed to be of appropriate dimension. When the dimension of I does not result from the context, it is explicitly specified, i.e., $I_n \in \mathbb{R}^{n \times n}$ is the identity matrix of dimension $n \times n$. By $e_{i,n} \in \mathbb{R}^n$, the ith unit vector of dimension n is denoted. The zero matrix is denoted by 0, which is always assumed to be of appropriate dimension. With $A \otimes B$ the Kronecker product is referred to, i.e., $A \otimes B = [a_{ij}] \otimes B = [a_{ij}B]$ for matrices $A \in \mathbb{R}^{m \times n}$ and $B \in \mathbb{R}^{p \times q}$ of arbitrary dimension (see, e.g., [11, Def. 7.1.2]). Derivatives are written in the notation $\mathrm{d}_z h(z) = \frac{\mathrm{d}}{\mathrm{d}z} h(z)$ respectively $\mathrm{d}_t h(t) = \dot{h}(t) = \frac{\mathrm{d}}{\mathrm{d}t} h(t)$. Partial derivatives with respect

to space and time are shortened by $\partial_z h(z,t) = \frac{\partial}{\partial z} h(z,t)$ and $\partial_t h(z,t) = \frac{\partial}{\partial t} h(z,t)$. The pointwise evaluation of the derivative $\partial_z x(z,t)|_{z=z_i}$ at a point z_i is abbreviated by $\partial_z x(z_i,t)$. With $\mathbb{R}^+$ the positive real numbers are denoted, i.e., $\mathbb{R}^+ = \{x \in \mathbb{R} | x > 0\}$, with $\mathbb{R}_0^+$ the nonnegative real numbers, i.e., $\mathbb{R}_0^+ = \{x \in \mathbb{R} | x \geq 0\}$ and with $\mathbb{R}^-$ the negative real numbers, i.e., $\mathbb{R}^- = \{x \in \mathbb{R} | x < 0\}$. For a vector $h(t) \in \mathbb{R}^n$, $|h(t)|$ is the vector of absolute values, i.e., $|h(t)| = \mathrm{col}\,(|h_1(t)|, \ldots, |h_n(t)|) \in (\mathbb{R}_0^+)^n$.

Chapter 2

Parabolic and biharmonic ODE-PDE systems

In this chapter, the fault diagnosis problem is solved for ODE-PDE systems with PDEs of parabolic or biharmonic type. Application examples that are modeled by parabolic PDEs come from chemical and biochemical engineering (see, e.g., [6, 44]). Important examples are chemical fixed-bed and tubular reactors (see, e.g., [45, 71]). Moreover, for battery management systems, thermoelectrical models in the form of parabolic PDEs are derived (see, e.g., [38, 84]). Typical real-world systems that are modeled by the Euler-Bernoulli beam equation, i.e., a biharmonic PDE, originate from the field of flexible and smart structures (see, e.g., [7, 8]). Specific application examples are a piezo-actuated flexible structure considered in [80] or a flexible robot arm (see, e.g., [3]). This non-exhaustive overview shows that a wide range of technical processes can be modeled by parabolic and biharmonic ODE-PDE systems, for which a unified description is introduced in the following section. The fault and disturbance signals that are considered for the fault diagnosis are described in Section 2.2. To ensure a safe and reliable operation of these systems, a fault detection and diagnosis scheme for this system class is proposed in Section 2.3 respectively Section 2.4.

2.1 System description

Consider the faulty linear ODE-PDE system, which may be of the parabolic or biharmonic type and is described by

$$\partial_z x(z,t) = \mathcal{A}[x(z)](t) + H_1(z)w(t) + B_1(z)u(t)$$
$$+ G_1(z)d(t) + E_1(z)f(t), \qquad\qquad (z,t) \in (0,1) \times \mathbb{R}^+ \quad (2.1a)$$
$$K_0 x(0,t) + K_1 x(1,t) + H_2 w(t)$$
$$= B_2 u(t) + G_2 d(t) + E_2 f(t), \qquad\qquad t > 0 \qquad\qquad (2.1b)$$

$$\dot{w}(t) = F w(t) + \int_0^1 L_1(z) x(z,t)\mathrm{d}z + L_2 x(0,t) + L_3 x(1,t) + B_3 u(t)$$
$$+ G_3 d(t) + E_3 f(t), \qquad\qquad t > 0 \qquad\qquad (2.1c)$$

$$y(t) = \int_0^1 C_1(z) x(z,t)\mathrm{d}z + C_2 x(0,t) + C_3 x(1,t) + C_4 w(t) + G_4 d(t)$$
$$+ E_4 f(t), \qquad\qquad t \geq 0 \qquad\qquad (2.1d)$$

with the distributed state $x(z,t) \in \mathbb{R}^{n_x}$, the lumped state $w(t) \in \mathbb{R}^{n_w}$, the input $u(t) \in \mathbb{R}^{n_u}$, the disturbance $d(t) \in \mathbb{R}^{n_d}$, the fault $f(t) \in \mathbb{R}^{n_f}$ and the measurement $y(t) \in \mathbb{R}^{n_y}$. From these signals, only the input $u(t)$ and the measurement $y(t)$ are assumed to be known. In (2.1a), the formal differential operator of the order $n_A \in \mathbb{N}^+$ is given by

$$\mathcal{A}[x(z)](t) = \sum_{i=0}^{n_A} A_i(z) \partial_t^i x(z,t) \qquad\qquad (2.2)$$

with $A_i \in (C^1[0,1])^{n_x \times n_x}$, $i = 0, \ldots, n_A$. The unknown initial conditions (ICs) are $\partial_t^i x(z,t)|_{t=0} = x_{i,0}(z) \in \mathbb{R}^{n_x}$, $z \in [0,1]$, $i = 0, \ldots, n_A-1$, as well as $w(0) = w_0 \in \mathbb{R}^{n_w}$ and assumed to be compatible with the BCs (2.1b). With (2.1b), the required n_x BCs for the PDE subsystem (2.1a) and (2.1b) are specified by $K_0, K_1 \in \mathbb{R}^{n_x \times n_x}$ where $K = [\, K_0 \;\; K_1 \,] \in \mathbb{R}^{n_x \times 2n_x}$ satisfies

$$\mathrm{rank}\, K = n_x. \qquad\qquad (2.3)$$

The system matrix of the ODE (2.1c) is $F \in \mathbb{R}^{n_w \times n_w}$ and the coupling from the PDE to the ODE is given by $L_1 \in (L_2(0,1))^{n_w \times n_x}$ and $L_2, L_3 \in \mathbb{R}^{n_w \times n_x}$. The ODE subsystem affects the PDE subsystem (2.1a) via $H_1 \in (L_2(0,1))^{n_x \times n_w}$ and $H_2 \in \mathbb{R}^{n_x \times n_w}$. The input $u(t)$, the disturbance $d(t)$ and the fault $f(t)$ act via $B_1 \in (L_2(0,1))^{n_x \times n_u}$, $G_1 \in (L_2(0,1))^{n_x \times n_d}$, $E_1 \in (L_2(0,1))^{n_x \times n_f}$ and the real

valued matrices of appropriate dimensions B_i, $i = 2, 3$, G_j, $j = 2, 3, 4$, as well as E_j on the system. According to (2.1d), the output $y(t)$ can contain in-domain, boundary and ODE state measurements, which are characterized by $C_1 \in (L_2(0, 1))^{n_y \times n_x}$, $C_2, C_3 \in \mathbb{R}^{n_y \times n_x}$ and $C_4 \in \mathbb{R}^{n_y \times n_w}$. In the following, all system parameters are assumed to be known. Note that the specified function classes for $B_1(z)$ and $C_1(z)$ exclude pointwise inputs respectively measurements. However, this restriction is only made for the sake of brevity, but is not a general limitation of the proposed method. An example for the consideration of pointwise measurements can be found in [98, 99]. Furthermore, this restriction is also justified by the fact that such inputs and measurements can usually be well approximated by suitable spatial characteristics.

A general discussion for the well-posedness of the system (2.1) is out of the scope of this thesis. However, in the following it is assumed that the faulty system under consideration is well-posed in the sense of Hadamard (see, e.g., [18, Chapter 2.1]). This assumption is justified since the modeling of technical systems usually leads to such systems. Note that with (2.1a), PDEs of parabolic, biharmonic and hyperbolic type can be described in general. However, in this section only parabolic and biharmonic PDEs are taken into account, since these can be treated in a common framework. For PDEs of the hyperbolic type a more suitable system representation is introduced in Section 3.

The representation of the PDE subsystem given by (2.1a) and (2.1b) as system of first order PDEs with respect to the spatial variable z was originally introduced in [75, 93] to facilitate the flatness-based solution of the motion planning problem for DPSs realizing a setpoint change. This system representation for the PDE subsystem has already been shown in [102] to be suitable to solve the fault diagnosis problem for parabolic or biharmonic PDE systems. To consider also ODE-PDE couplings, the PDE subsystem (2.1a) and (2.1b) is extended by the ODE (2.1c), which differs from the system representation in [75, 93]. Although dynamic BCs can already be accounted for in [75, 93] by differential operators, the form (2.1) with the explicit ODE (2.1c) allows more general ODE-PDE couplings and is thus well suited to solve fault detection and diagnosis problems.

To illustrate how a parabolic PDE system with an actuator dynamic described by an ODE fits into the system description (2.1), the following example is given.

Example 2.1 *(Faulty parabolic system with actuator dynamics).*
Consider the parabolic system

$$\partial_t v(z,t) = \partial_z(\alpha(z)\partial_z v(z,t)) + \beta(z)v(z,t) + g_1^\top(z)d(t), \ (z,t) \in (0,1) \times \mathbb{R}^+ \quad (2.4a)$$
$$\partial_z v(0,t) = h_2^\top w(t), \qquad\qquad\qquad\qquad t > 0 \qquad\qquad (2.4b)$$
$$\partial_z v(1,t) = g_2^\top d(t), \qquad\qquad\qquad\qquad t > 0 \qquad\qquad (2.4c)$$

with the distributed state $v(z,t) \in \mathbb{R}$ and the lumped state $w(t) \in \mathbb{R}^{n_w}$ described by the ODE

$$\dot{w}(t) = Fw(t) + B_3(u(t) + f_1(t)), \qquad\qquad t > 0 \qquad\qquad (2.4d)$$

with the ICs $v(z,0) = v_0 \in \mathbb{R}$ and $w(0) = w_0 \in \mathbb{R}^{n_w}$ as well as input $u(t) \in \mathbb{R}$. The measurement $y(t) \in \mathbb{R}$ is given by

$$y(t) = c_1 v(1,t) + f_2(t), \qquad\qquad\qquad t \geq 0. \qquad\qquad (2.4e)$$

The system is subject to the disturbance $d(t) \in \mathbb{R}^2$ and the faults to be considered are $f(t) = \mathrm{col}\,(f_1(t), f_2(t)) \in \mathbb{R}^2$. The system parameters $\alpha(z), \beta(z)$ satisfy $\alpha, \beta \in C^1[0,1]$ and $\alpha(z) > 0$, $z \in [0,1]$. The remaining parameters are real valued vectors respectively matrices of appropriate size. Hence, (2.4a) can be rewritten to

$$\partial_z^2 v(z,t) = \frac{1}{\alpha(z)}\partial_t v(z,t) - \frac{\mathrm{d}_z\alpha(z)}{\alpha(z)}\partial_z v(z,t) - \frac{\beta(z)}{\alpha(z)}v(z,t) - \frac{g_1^\top(z)}{\alpha(z)}d(t). \quad (2.5)$$

Introducing $x(z,t) = \mathrm{col}\,(\partial_z v(z,t), v(z,t))$, the first order differential operator $\mathcal{A}$ (see (2.2)) has the coefficients

$$A_0(z) = \begin{bmatrix} -\frac{\mathrm{d}_z\alpha(z)}{\alpha(z)} & -\frac{\beta(z)}{\alpha(z)} \\ 1 & 0 \end{bmatrix} \qquad \text{and} \qquad A_1(z) = \begin{bmatrix} 0 & \frac{1}{\alpha(z)} \\ 0 & 0 \end{bmatrix}. \qquad (2.6)$$

Furthermore, $G_1(z) = \mathrm{col}\left(-\frac{g_1^\top(z)}{\alpha(z)}, 0^\top\right)$,

$$K_0 = \begin{bmatrix} 1 & 0 \\ 0 & 0 \end{bmatrix}, \qquad\qquad\qquad K_1 = \begin{bmatrix} 0 & 0 \\ 1 & 0 \end{bmatrix}, \qquad\qquad (2.7)$$

$H_2 = \mathrm{col}\left(-h_2^\top, 0^\top\right)$, $G_2 = \mathrm{col}\left(0^\top, g_2^\top\right)$ and $C_3 = [\,0 \ c_1\,]$ are obtained. Due to the two independent BCs (2.4b) and (2.4c), K satisfies (2.3). The fault $f_1(t)$ is an actuator fault with $E_3 = B_3[\,1 \ 0\,]$ and $f_2(t)$ is a sensor fault with $E_4 = [\,0 \ 1\,]$. ◁

Also biharmonic PDEs with dynamic BCs can be described in the form of (2.1), which is shown in Section 2.3.5 and Section 2.4.4. Hence, a large class of DPSs
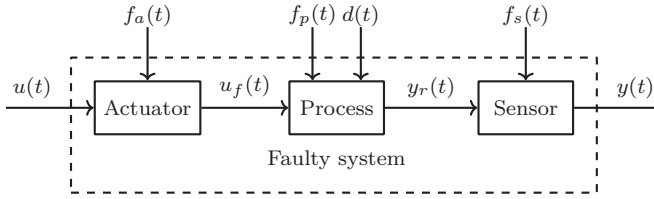
Figure 2.1: Separation of a faulty system into the actuator, process and sensor part, which are subject to the actuator fault $f_a(t)$, the process fault $f_p(t)$, the sensor fault $f_s(t)$ and the disturbance $d(t)$.

can be modeled by (2.1) and thus are considered for the fault diagnosis. For a less abstract description of the following fault detection method, the interested reader is encouraged to consult [100]. In this article, a similar fault diagnosis method for a diffusion-reaction system is shown directly on the basis of the parabolic PDE.

2.2 Faults and disturbances

A technical system can be separated into the actuator, process and sensor parts, which is shown in Figure 2.1. According to the component in which a fault occurs, the fault is called an actuator fault, a process fault, or a sensor fault (see, e.g., [28]). To be specific, a fault $f_i(t) = e_{i,n_f}^\top f(t)$, $i \in \{1, \ldots, n_f\}$, is called an *actuator fault* if the system is subject to the faulty input signal

$$u_{f,j}(t) = u_j(t) + f_i(t) \tag{2.8}$$

where only $u_j(t)$ is known, which is the jth component of $u(t)$. The fault $f_i(t)$ can be taken into account in the setting of (2.1) by the fault input matrices E_k, $k = 1, 2, 3$, which follow from

$$B_k e_{j,n_u} u_{f,j}(t) = B_k e_{j,n_u} u_j(t) + B_k e_{j,n_u} f_i(t), \tag{2.9}$$

and are given by $E_k e_{i,n_f} = B_k e_{j,n_u}$. To describe the sensor faults, let $y_{r,j}(t)$ be the jth component of the fault free measurement $y_r(t) = y(t) - E_4 f(t)$ (see (2.1d)). Then, a fault $f_i(t)$ is called a *sensor fault* if the jth component

$$y_j(t) = y_{r,j}(t) + f_i(t), \tag{2.10}$$

of the measurement $y(t)$ is corrupted by a fault $f_i(t)$. According to (2.1d), this is modeled by $e_{j,n_y}^\top E_4 e_{i,n_f} = 1$. If a fault $f_i(t)$ does not correspond to an actuator or

a sensor fault, it is called a *process fault*. Depending on whether such a fault occurs in the distributed- or the lumped-parameter subsystem, the fault input in (2.1) is described by the matrices E_i, $i = 1, 2, 3$.

Moreover, a distinction between additive and multiplicative faults must be made. *Additive faults* are unknown exogenous signals, which are independent of system variables. This can be, e.g., an offset in an actuator, a drift in a sensor or when the system is subject to an unknown exogenous signals (e.g., disturbances) that could provoke a malfunction or damage to the technical process that must therefore be monitored.

In contrast, a fault that leads to a change in a system parameter is called a *multiplicative fault*. Thus, the effect of a multiplicative fault on the system depends on a corrupted system variable, i.e., $u(t), x(z, t), w(t)$ or $y(t)$ (see, e.g., [28, Section 3.5]). The influence of a *multiplicative actuator fault* $\Delta f_i(t)$ can be described by

$$u_{f,j}(t) = (1 + \Delta f_i(t)) u_j(t), \quad i \in \{1, \ldots, n_f\}. \tag{2.11}$$

In order to consider this type of faults in the setting of (2.1), it is reformulated into the form given in (2.8) by introducing $f_i(t) = \Delta f_i(t) u_j(t)$. Similarly, a *multiplicative sensor fault* $\Delta f_i(t)$ affecting the measurement by

$$y_j(t) = (1 + \Delta f_i(t)) y_{r,j}(t), \tag{2.12}$$

is regarded with $f_i(t) = \Delta f_i(t) y_{r,j}(t)$ as additive sensor fault in (2.1). Distributed multiplicative process faults would require the introduction of a space and time dependent fault expression, which would make the system description and derivation of the residual generator unnecessarily cumbersome. Thus, only multiplicative process faults in lumped quantities are considered in the following. To be specific, a *multiplicative process fault* $\Delta f_i(t)$ in the jth component $w_j(t)$ of $w(t)$ is rewritten into an additive process fault by $f_i(t) = \Delta f_i(t) w_j(t)$ and corresponding entries in the fault input matrices E_i, $i = 1, \ldots, 4$. Similarly, a multiplicative process fault $\Delta f_i(t)$ in the boundary values $x(0, t)$ or $x(1, t)$ can be rewritten into an additive process fault by $f_i(t) = \Delta f_i(t) x_j(0, t)$ respectively $f_i(t) = \Delta f_i(t) x_j(1, t)$, $j \in \{1, \ldots, n_x\}$, and corresponding entries in E_i, $i = 2, 3, 4$. Note that in the following it is assumed that the system is at first in a healthy state, i.e., $f(t) \equiv 0$ for $0 \leq t < t_f$, where t_f is the *fault occurrence time*.

In addition to faults, technical systems are in general also subject to disturbances. The latter are unknown exogenous signals that influence the system but do not cause failures or malfunctions. Unlike faults, the occurrence of a disturbance during operation must be tolerated. Thus, a major challenge in the fault diagnosis is the reliable diagnosis or detection of faults even though disturbances are present.

Although a disturbance $d(t)$ must be assumed to be unknown, often some information is still available that allows to specifically consider their influence on the fault detection. To use this information in the following fault detection approach, assume that $d(t)$ is composed of two components $\tilde{d}(t) \in \mathbb{R}^{n_{\tilde{d}}}$ and $\bar{d}(t) \in \mathbb{R}^{n_{\bar{d}}}$, so that it satisfies

$$d(t) = \tilde{G}\tilde{d}(t) + \bar{G}\bar{d}(t) \tag{2.13}$$

with the known matrices $\tilde{G} \in \mathbb{R}^{n_d \times n_{\tilde{d}}}$ and $\bar{G} \in \mathbb{R}^{n_d \times n_{\bar{d}}}$. The components $\bar{d}_i(t)$ of $\bar{d}(t)$ are absolutely bounded by

$$|\bar{d}_i(t)| \le \delta_i, \quad i = 1, 2, \ldots, n_{\bar{d}}, t \ge 0, \tag{2.14}$$

with known bound $\delta = \mathrm{col}(\delta_1, \ldots, \delta_{n_{\bar{d}}}) \in \mathbb{R}^{n_{\bar{d}}}$. The component $\tilde{d}(t)$ is assumed to be described by the *signal model*

$$\dot{v}_d(t) = S_d v_d(t), \qquad\qquad t > 0 \tag{2.15a}$$
$$\tilde{d}(t) = R_d v_d(t), \qquad\qquad t \ge 0 \tag{2.15b}$$

with $v_d(t) \in \mathbb{R}^{n_{vd}}$ and the known matrices $S_d \in \mathbb{R}^{n_{vd} \times n_{vd}}$ as well as $R_d \in \mathbb{R}^{n_{\tilde{d}} \times n_{vd}}$, where (R_d, S_d) is observable. Note that the spectrum of S_d satisfies $\sigma(S_d) \subset \mathrm{j}\mathbb{R}$ and S_d is not required to be diagonalizable. The signal model (2.15) describes only the specific form of the signal, but the actual form (e.g., offset and slope for a drifting fault or amplitude and phase in case of trigonometric signals) is determined by the unknown IC $v_d(0) = v_d^0 \in \mathbb{R}^{n_{vd}}$ and thus $\tilde{d}(t)$ is unknown. With the signal model (2.15) signals of polynomial form, trigonometric signals or also combinations thereof can be described (see, e.g., the examples in Section 2.3.5 and 2.4.4). Hence, commonly occurring disturbance signals can be considered. In view of (2.13), the component $\tilde{d}(t)$ of a disturbance must only hold approximately on the moving horizon $\mathrm{I}_t = [t - T, t]$ with finite length $T \in \mathbb{R}^+$, since the approximation error can be readily taken into account by the bounded disturbance $\bar{d}(t)$. The length T of the moving horizon is a design parameter that will be considered in Section 2.3.

2.3 Fault detection

A key technology to ensure the safety of automated systems is the reliable detection of faults. This detection should be possible with as few assumptions as necessary so that it can be used for a wide range of failure scenarios. Therefore, a residual generator for fault detection is presented that does not require knowledge of the fault signal form and reliably detects both additive and multiplicative faults. The specific
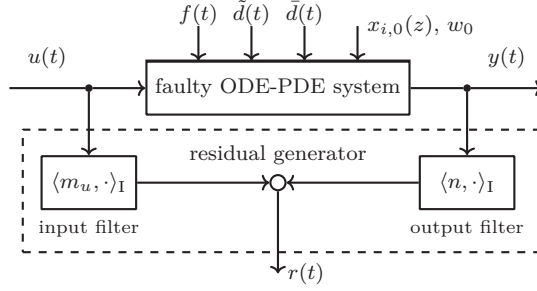
Figure 2.2: Structure of the residual generator for the fault detection with
an input filter $\langle m_u, u(t)\rangle_I$ and an output filter $\langle n, y(t)\rangle_I$.

fault detection problem is introduced in Section 2.3.1. Subsequently, an input-output
relation is determined in Section 2.3.2, from which the fault detection residual
generator is derived in Section 2.3.3. The required kernel equations are solved in
Section 2.3.4 by a flatness-based trajectory planning. Finally, a simulation example
for an Euler-Bernoulli beam in Section 2.3.5 visualizes the theoretical results.

2.3.1 Problem formulation

The fault detection problem consists in detecting the occurrence of a fault by means
of a residual signal. This problem is solved using a residual generator with the
structure shown in Figure 2.2 for the *residual signal* $r(t) \in \mathbb{R}$. In accordance with
[12, Problem 6.2], the *residual generator* must

- consist of an input and an output filter,

- be independent of the operating point of the system,

- be independent of the ICs of the system,

- be independent of the disturbance $\tilde{d}(t)$

- and satisfy

$$r(t) \not\equiv 0 \qquad \text{for} \qquad f(t) \not\equiv 0, \qquad t \geq T \qquad (2.16\text{a})$$
$$r(t) \equiv 0 \qquad \text{for} \qquad f(t) \equiv 0, \qquad t \geq T. \qquad (2.16\text{b})$$

Based on (2.16), the definition of *weak fault detectability* is introduced.

> **Definition 1 (Weak fault detectability [12, Definition 6.1]).** A fault $f_i(t) \not\equiv 0$, where $f_i(t)$ is the ith component of $f(t)$, is weakly detectable if there exists a residual generator such that the residual signal $r(t)$ is affected by $f_i(t)$ (see (2.16)).

A fault detection in sense of Definition 1 is called weak, since it is possible that the residual signal $r(t)$ may return to zero after a transient phase although a fault is still present. For a residual signal $r(t)$ to reliably indicate the presence of a fault $f_i(t)$ even after the transient phase, *strong fault detectability* is required. The latter is specified in the following definition.

> **Definition 2 (Strong fault detectability [12, Definition 6.2]).** A fault $f_i(t)$ is strongly detectable if there exists a residual generator such that $r(t)$ reaches a nonzero steady-state value for a fault signal that has a bounded steady-state value different from zero.

However, (2.16) can only be achieved if $\bar{d}(t) \equiv 0$. If a disturbance $\bar{d}(t)$ is present, i.e, $\bar{d}(t) \not\equiv 0$, a threshold value $r_B > 0$ must be introduced for secured fault detection, i.e.,

$$|r(t)| \leq r_B, \qquad \text{for} \qquad f(t) \equiv 0, \qquad t \geq T \qquad (2.17)$$

must hold, so that $|r(t)| > r_B$ necessarily indicates the presence of a fault $f(t) \not\equiv 0$.

2.3.2 Determination of the input-output expression

In the following, an input-output expression is determined by the application of integral transformations, from which the residual generator can be derived. For this, the *integral transformation* for the PDE (2.1a)

$$\mathcal{M}[x](t) = \int\limits_0^1 \int\limits_0^T m^\top(z,\tau) x(z, t-\tau) \mathrm{d}\tau \mathrm{d}z = \langle m, x(t) \rangle_{\Omega,\mathrm{I}} \qquad (2.18\mathrm{a})$$

with $\Omega = [0,1]$ and $\mathrm{I} = [0,T]$, $T \in \mathbb{R}^+$, for the BC (2.1b)

$$\mathcal{P}[h](t) = \int_0^T p^\top(\tau)h(t-\tau)\mathrm{d}\tau = \langle p, h(t)\rangle_{\mathrm{I}}, \quad h(t) \in \mathbb{R}^{n_x}, \tag{2.18b}$$

for the ODE (2.1c)

$$\mathcal{Q}_w[w](t) = \langle q_w, w(t)\rangle_{\mathrm{I}}, \tag{2.18c}$$

for the output equation (2.1d)

$$\mathcal{N}[y](t) = \langle n, y(t)\rangle_{\mathrm{I}} \tag{2.18d}$$

and for the signal model (2.15) of the disturbance $\tilde{d}(t)$

$$\mathcal{Q}_d[v_d](t) = \langle q_d, v_d(t)\rangle_{\mathrm{I}} \tag{2.18e}$$

are introduced. The *moving horizon length T* is a design parameter addressed more in detail in Section 2.3.5. Due to the timeshift in the arguments of the transformations in (2.18), these are evaluated on the *moving horizon* $\mathrm{I}_t = [t-T, t]$. This becomes obvious by a simple substitution $\tilde{\tau} = t - \tau$, which yields, e.g.,

$$\int_0^T n^\top(\tau)y(t-\tau)\mathrm{d}\tau = \int_{t-T}^t n^\top(t-\tilde{\tau})y(\tilde{\tau})\mathrm{d}\tilde{\tau}, \quad t \geq T \tag{2.19}$$

for (2.18d) and is illustrated in Figure 2.3. The *integral kernels* $m(z,\tau) \in \mathbb{R}^{n_x}$, $n(\tau) \in \mathbb{R}^{n_y}$, $q_w(\tau) \in \mathbb{R}^{n_w}$, $q_d(\tau) \in \mathbb{R}^{n_{vd}}$ and $p(\tau) \in \mathbb{R}^{n_x}$ are degrees of freedom which are utilized to solve the fault detection problem. Note that similar integral transformations are used in the modulating functions method for the parameter, state and derivative estimation (see, e.g., [46, 49, 70, 78]). However, in these approaches, the integral transformations are applied to treat derivatives of known signals. In contrast, the integral kernels in the presented approach are used to eliminate unknown system variables in order to derive an input-output expression from which the residual generators are determined.

Apply the transformations (2.18) to the corresponding equations of (2.1), which
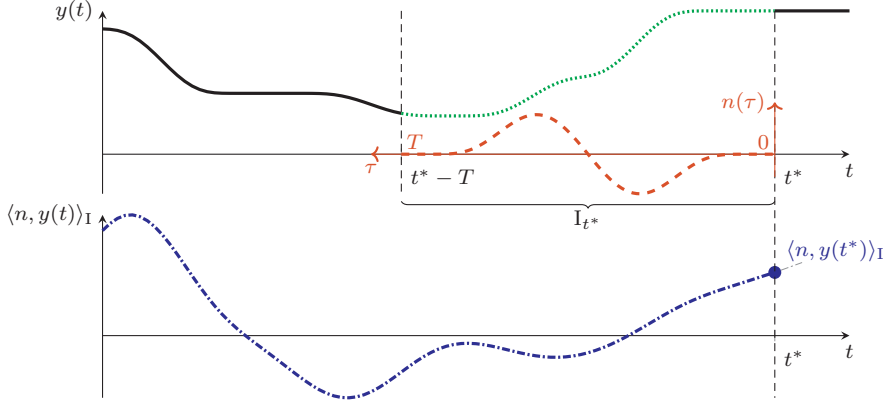
Figure 2.3: Integral transformation $\langle n, y(t)\rangle_I$ (──·──) of a signal $y(t) \in \mathbb{R}$ (───) with the evaluation of the integral transformation visualized at time t^* by $y(t)$, $t \in I_{t^*} = [t^*-T, t^*]$ (········) and the integral kernel $n(\tau) \in \mathbb{R}$ (‑ ‑ ‑) depicted in an additional τ-coordinate system.

yields

$$
\langle m, \partial_z x(t)\rangle_{\Omega,I} = \langle m, \mathcal{A}[x](t)\rangle_{\Omega,I} + \langle m, H_1 w(t)\rangle_{\Omega,I} + \langle m, B_1 u(t)\rangle_{\Omega,I}
$$
$$
+ \langle m, G_1 d(t)\rangle_{\Omega,I} + \langle m, E_1 f(t)\rangle_{\Omega,I} \tag{2.20a}
$$
$$
\langle p, K x_B(t)\rangle_I = -\langle p, H_2 w(t)\rangle_I + \langle p, B_2 u(t)\rangle_I + \langle p, G_2 d(t)\rangle_I + \langle p, E_2 f(t)\rangle_I \tag{2.20b}
$$
$$
\langle q_w, \dot{w}(t)\rangle_I = \langle q_w, F w(t)\rangle_I + \langle q_w, L_1 x(t)\rangle_{\Omega,I} + \langle q_w, L_B x_B(t)\rangle_I + \langle q_w, B_3 u(t)\rangle_I
$$
$$
+ \langle q_w, G_3 d(t)\rangle_I + \langle q_w, E_3 f(t)\rangle_I \tag{2.20c}
$$
$$
\langle n, y(t)\rangle_I = \langle n, C_1 x(t)\rangle_{\Omega,I} + \langle n, C_B x_B(t)\rangle_I + \langle n, C_4 w(t)\rangle_I
$$
$$
+ \langle n, G_4 d(t)\rangle_I + \langle n, E_4 f(t)\rangle_I \tag{2.20d}
$$

with $x_B(t) = \mathrm{col}\,(x(0,t),\, x(1,t))$, $L_B = [\,L_2\ \ L_3\,]$ and $C_B = [\,C_2\ \ C_3\,]$. Note that

$$
\langle q_w, \int_0^1 L_1(z) x(z,t)\mathrm{d}t\rangle_I = \langle q_w, L_1 x(t)\rangle_{\Omega,I} \tag{2.21}
$$

is used to obtain (2.20c) and a similar relation for $\langle n, C_1 x(t)\rangle_{\Omega,I}$ in (2.20d). In the following, the temporal and spatial derivatives, the operator $\mathcal{A}$ and also the matrices in (2.20) are shifted to the integral kernels. Use integration by parts with respect to z for the left-hand side in (2.20a) to transfer the spatial derivative to $m(z,\tau)$,

yielding

$$\langle m, \partial_z x(t)\rangle_{\Omega,\mathrm{I}} = \langle m(1), x(1,t)\rangle_{\mathrm{I}} - \langle m(0), x(0,t)\rangle_{\mathrm{I}} - \langle \partial_z m, x(t)\rangle_{\Omega,\mathrm{I}}. \tag{2.22}$$

In order to shift $\mathcal{A}$ to the kernel $m(z,\tau)$, use its representation (2.2) to obtain

$$\langle m, \mathcal{A}[x](t)\rangle_{\Omega,\mathrm{I}} = \sum_{i=0}^{n_A} \langle m, A_i \partial_t^i x(t)\rangle_{\Omega,\mathrm{I}}. \tag{2.23}$$

With $\partial_t^i x(z, t-\tau) = (-1)^i \partial_\tau^i x(z, t-\tau)$ and by transposing of the matrices $A_i(z)$,

$$\langle m, A_i \partial_t^i x(t)\rangle_{\Omega,\mathrm{I}} = (-1)^i \langle A_i^\top m, \partial_\tau^i x(t)\rangle_{\Omega,\mathrm{I}} \tag{2.24}$$

follows for the summands in (2.23). Hence, the derivative operator ∂_τ^i can be shifted to the kernel $m(z,\tau)$ by means of an i-folded integration by parts with respect to τ. The result reads as

$$\langle A_i^\top m, \partial_\tau^i x(t)\rangle_{\Omega,\mathrm{I}} = \sum_{j=0}^{i-1} \left[(-1)^j \langle A_i^\top \partial_\tau^j m(\tau), \partial_\tau^{i-j-1} x(t-\tau)\rangle_\Omega \right]_0^T$$
$$+ (-1)^i \langle A_i^\top \partial_\tau^i m, x(t)\rangle_{\Omega,\mathrm{I}}. \tag{2.25}$$

The still unknown distributed values $\partial_\tau^i x(z, t-\tau)|_{\tau \in \{0,T\}}$, $z \in [0,1]$, $i = 0, \ldots, n_A - 1$ are eliminated by imposing

$$\partial_\tau^i m(z,\tau)|_{\tau \in \{0,T\}} = 0, \quad z \in [0,1], i = 0, 1, \ldots, n_A - 1. \tag{2.26}$$

As a result of (2.24)–(2.26),

$$\langle m, A_i \partial_t^i x(t)\rangle_{\Omega,\mathrm{I}} = \langle A_i^\top \partial_\tau^i m, x(t)\rangle_{\Omega,\mathrm{I}} \tag{2.27}$$

follows. Consequently, (2.23) reads as

$$\langle m, \mathcal{A}[x](t)\rangle_{\Omega,\mathrm{I}} = \langle \mathcal{A}^*[m], x(t)\rangle_{\Omega,\mathrm{I}}, \quad t \geq T \tag{2.28a}$$

with the formal adjoint

$$\mathcal{A}^*[m(z)](\tau) = \sum_{i=0}^{n_A} A_i^\top(z) \partial_\tau^i m(z,\tau). \tag{2.28b}$$

In the term $\langle m, H_1 w(t)\rangle_{\Omega,\mathrm{I}}$ in (2.20a), the matrix $H_1(z)$ can be shifted to the kernel by taking its transpose. Subsequently, the required form is achieved by changing the

order of integration to

$$\langle m, H_1 w(t)\rangle_{\Omega,\mathrm{I}} = \langle H_1^\top m, w(t)\rangle_{\Omega,\mathrm{I}} = \langle\langle H_1, m\rangle_\Omega, w(t)\rangle_\mathrm{I}, \tag{2.29}$$

where $\langle\cdot,\cdot\rangle_\Omega$ represents the integration with respect to $z \in \Omega$. Then, introducing

$$m_B(\tau) = \begin{bmatrix} -m(0,\tau) \\ m(1,\tau) \end{bmatrix} \tag{2.30}$$

and using (2.22), (2.28), as well as the form (2.29) for the remaining terms in (2.20a) leads to

$$\langle m_B, x_B(t)\rangle_\mathrm{I} = \langle \mathcal{A}^*[m] + \partial_z m, x(t)\rangle_{\Omega,\mathrm{I}} + \langle\langle H_1, m\rangle_\Omega, w(t)\rangle_\mathrm{I} + \langle\langle B_1, m\rangle_\Omega, u(t)\rangle_\mathrm{I}$$
$$+ \langle\langle G_1, m\rangle_\Omega, d(t)\rangle_\mathrm{I} + \langle\langle E_1, m\rangle_\Omega, f(t)\rangle_\mathrm{I}. \tag{2.31}$$

In (2.20b) and (2.20d) the related matrices are shifted to the kernels $p(\tau)$ and $n(\tau)$ yielding

$$\langle K^\top p, x_B(t)\rangle_\mathrm{I} = -\langle H_2^\top p, w(t)\rangle_\mathrm{I} + \langle B_2^\top p, u(t)\rangle_\mathrm{I} + \langle G_2^\top p, d(t)\rangle_\mathrm{I}$$
$$+ \langle E_2^\top p, f(t)\rangle_\mathrm{I} \tag{2.32a}$$
$$\langle n, y(t)\rangle_\mathrm{I} = \langle C_1^\top n, x(t)\rangle_{\Omega,\mathrm{I}} + \langle C_B^\top n, x_B\rangle_\mathrm{I} + \langle C_4^\top n, w(t)\rangle_\mathrm{I}$$
$$+ \langle G_4^\top n, d(t)\rangle_\mathrm{I} + \langle E_4^\top n, f(t)\rangle_\mathrm{I}. \tag{2.32b}$$

For (2.20c), use $\dot{w}(t-\tau) = -\mathrm{d}_\tau w(t-\tau)$, apply integration by parts with respect to τ and impose

$$q_w(\tau)|_{\tau \in \{0,T\}} = 0 \tag{2.33}$$

to obtain

$$\langle q_w, \dot{w}(t)\rangle_\mathrm{I} = \langle \dot{q}_w, w(t)\rangle_\mathrm{I}, \tag{2.34}$$

where $\dot{q}_w(\tau) = \mathrm{d}_\tau q_w(\tau)$. Then, by shifting the matrices of the terms in the right-hand side of (2.20c) to the integral kernels

$$\langle \dot{q}_w - F^\top q_w, w(t)\rangle_\mathrm{I} = \langle L_1^\top q_w, x(t)\rangle_{\Omega,\mathrm{I}} + \langle L_B^\top q_w, x_B(t)\rangle_\mathrm{I} + \langle B_3^\top q_w, u(t)\rangle_\mathrm{I}$$
$$+ \langle G_3^\top q_w, d(t)\rangle_\mathrm{I} + \langle E_3^\top q_w, f(t)\rangle_\mathrm{I} \tag{2.35}$$

follows. By setting

$$\partial_z m(z,\tau) + \mathcal{A}^*[m(z)](\tau) - C_1^\top(z)n(\tau) - L_1^\top(z)q_w(\tau) = 0 \tag{2.36}$$

one can insert (2.32b) and (2.35) in (2.31) to eliminate $x(z,t)$, which yields

$$
\begin{aligned}
\langle m_B + C_B^\top n + L_B^\top q_w, x_B(t)\rangle_I &= \langle n, y(t)\rangle_I \\
&+ \langle \dot{q}_w - F^\top q_w - C_4^\top n + \langle H_1, m\rangle_\Omega, w(t)\rangle_I \\
&+ \langle \langle B_1, m\rangle_\Omega - B_3^\top q_w, u(t)\rangle_I \\
&+ \langle \langle G_1, m\rangle_\Omega - G_3^\top q_w - G_4^\top n, d(t)\rangle_I \\
&+ \langle \langle E_1, m\rangle_\Omega - E_3^\top q_w - E_4^\top n, f(t)\rangle_I.
\end{aligned}
\tag{2.37}
$$

In (2.37), the left-hand side is still dependent on the unknown boundary value $x_B(t)$. However, inserting

$$
m_B(\tau) + C_B^\top n(\tau) + L_B^\top q_w(\tau) = K^\top p(\tau)
\tag{2.38}
$$

in (2.37) and replacing the resulting term by (2.32a) leads to

$$
\begin{aligned}
\langle -\langle E_1, m\rangle_\Omega + E_2^\top p + E_3^\top q_w + E_4^\top n, f(t)\rangle_I &= \langle n, y(t)\rangle_I \\
&+ \langle \dot{q}_w - F^\top q_w + \langle H_1, m\rangle_\Omega + H_2^\top p - C_4^\top n, w(t)\rangle_I \\
&+ \langle \langle B_1, m\rangle_\Omega - B_2^\top p - B_3^\top q_w, u(t)\rangle_I \\
&+ \langle \langle G_1, m\rangle_\Omega - G_2^\top p - G_3^\top q_w - G_4^\top n, d(t)\rangle_I.
\end{aligned}
\tag{2.39}
$$

The unknown ODE state $w(t)$ in (2.39) is eliminated by imposing

$$
\dot{q}_w(\tau) - F^\top q_w(\tau) + \langle H_1, m(\tau)\rangle_\Omega + H_2^\top p(\tau) - C_4^\top n(\tau) = 0, \quad \tau \in (0, T).
\tag{2.40}
$$

By inserting (2.40) in (2.39), the expression

$$
\langle m_f, f(t)\rangle_I = \langle n, y(t)\rangle_I + \langle m_u, u(t)\rangle_I + \langle m_d, d(t)\rangle_I
\tag{2.41}
$$

results, in which

$$
m_f(\tau) = -\langle E_1, m(\tau)\rangle_\Omega + E_2^\top p(\tau) + E_3^\top q_w(\tau) + E_4^\top n(\tau)
\tag{2.42a}
$$

$$
m_u(\tau) = \langle B_1, m(\tau)\rangle_\Omega - B_2^\top p(\tau) - B_3^\top q_w(\tau)
\tag{2.42b}
$$

$$
m_d(\tau) = \langle G_1, m(\tau)\rangle_\Omega - G_2^\top p(\tau) - G_3^\top q_w(\tau) - G_4^\top n(\tau)
\tag{2.42c}
$$

with $m_f(\tau) \in \mathbb{R}^{n_f}$, $m_u(\tau) \in \mathbb{R}^{n_u}$ and $m_d(\tau) \in \mathbb{R}^{n_d}$ are utilized.

In the next step, the disturbance $d(t)$ is taken into account. In view of (2.13), the disturbance term in (2.41) reads as

$$
\langle m_d, d(t)\rangle_I = \langle m_{\tilde{d}}, \tilde{d}(t)\rangle_I + \langle m_{\bar{d}}, \bar{d}(t)\rangle_I
\tag{2.43}
$$

with $m_{\tilde{d}}(\tau) = \tilde{G}^\top m_d(\tau)$ and $m_{\bar{d}}(\tau) = \bar{G}^\top m_d(\tau)$. The signal model (2.15) of the disturbance $\tilde{d}(t)$ can be utilized to decouple (2.41) from $\tilde{d}(t)$. Applying the transformation (2.18e) to (2.15a), using integration by parts in view of $\dot{v}_d(t-\tau) = -\mathrm{d}_\tau v_d(t-\tau)$ and imposing

$$q_d(\tau)|_{\tau \in \{0,T\}} = 0, \tag{2.44}$$

leads to

$$\langle \dot{q}_d - S_d^\top q_d, v_d(t) \rangle_{\mathrm{I}} = 0, \tag{2.45}$$

where $\dot{q}_d(\tau) = \mathrm{d}_\tau q_d(\tau)$. The first term in the right-hand side of (2.43) can be expressed in terms of $v_d(t)$ by making use of (2.15b), which yields

$$\langle m_{\tilde{d}}, \tilde{d}(t) \rangle_{\mathrm{I}} = \langle R_d^\top m_{\tilde{d}}, v_d(t) \rangle_{\mathrm{I}}. \tag{2.46}$$

Thus, inserting

$$\dot{q}_d(\tau) - S_d^\top q_d(\tau) = R_d^\top m_{\tilde{d}}(\tau), \quad \tau \in (0, T) \tag{2.47}$$

in (2.45) leads to $\langle m_{\tilde{d}}, \tilde{d}(t) \rangle_{\mathrm{I}} = 0$ in view of (2.46), i.e., (2.41) is independent of $\tilde{d}(t)$ (see (2.43)). Finally, the resulting *input-output expression* reads as

$$\langle m_f, f(t) \rangle_{\mathrm{I}} = \langle n, y(t) \rangle_{\mathrm{I}} + \langle m_u, u(t) \rangle_{\mathrm{I}} + \langle m_{\bar{d}}, \bar{d}(t) \rangle_{\mathrm{I}}, \quad t \geq T. \tag{2.48}$$

This expression depends only on the known measurement $y(t)$, the known input $u(t)$, the fault $f(t)$ and the unknown disturbances $\bar{d}(t)$. For (2.48) to hold, the integral kernels must satisfy (2.26), (2.33), (2.36), (2.38), (2.40), (2.44) and (2.47), which are summarized in the following lemma.

Lemma 2.1 (Fault detection kernel equations). Let $\tilde{d}(t)$ be described by
(2.15) and the integral kernels $m(z, \tau)$, $p(\tau)$, $q_w(\tau)$, $q_d(\tau)$ and $n(\tau)$ be a
solution of the *fault detection kernel equation*

$$\partial_z m(z, \tau) = -\mathcal{A}^*[m(z)](\tau) + L_1^\top(z)q_w(\tau) + C_1^\top(z)n(\tau) \quad \text{(2.49a)}$$

$$K^\top p(\tau) = m_B(\tau) + C_B^\top n(\tau) + L_B^\top q_w(\tau) \quad \text{(2.49b)}$$

$$\dot{q}_w(\tau) = F^\top q_w(\tau) - \langle H_1, m(\tau)\rangle_\Omega - H_2^\top p(\tau) + C_4^\top n(\tau) \quad \text{(2.49c)}$$

$$\dot{q}_d(\tau) = S_d^\top q_d(\tau) + R_d^\top m_{\tilde{d}}(\tau) \quad \text{(2.49d)}$$

$$\partial_\tau^i m(z, \tau)|_{\tau \in \{0, T\}} = 0, \quad z \in [0, 1], i = 0, \dots, n_A - 1 \quad \text{(2.49e)}$$

$$q_w(\tau)|_{\tau \in \{0, T\}} = 0 \quad \text{(2.49f)}$$

$$q_d(\tau)|_{\tau \in \{0, T\}} = 0, \quad \text{(2.49g)}$$

with (2.49a) defined on $(z, \tau) \in (0, 1) \times (0, T)$ and (2.49b)–(2.49d) on $\tau \in (0, T)$. Then, the input-output expression (2.48) holds.

In order to make use of (2.48) for the fault detection, a solution for (2.49) must be
determined. A constructive approach for this is discussed in Section 2.3.4, whereas a
fault detectability condition based on system properties is derived in Section 2.3.4.3.

2.3.3 Residual generator

In view of the input-output expression (2.48),

$$r(t) = \langle n, y(t)\rangle_I + \langle m_u, u(t)\rangle_I, \quad t \geq T \quad \text{(2.50)}$$

is a candidate for the fault detection residual generator, since it only depends on
the known signals $u(t)$ and $y(t)$. It follows from the derivation of (2.48) that $r(t)$ in
(2.50) is already independent of the operating point and the unknown ICs $x_{i,0}(z)$,
$z \in [0, 1]$, $i = 0, \dots, n_A - 1$ as well as w_0. Hence, it remains to prove (2.16). In the
case $\bar{d}(t) \equiv 0$, insert (2.50) in (2.48) to obtain

$$r(t) = \langle m_f, f(t)\rangle_I, \quad t \geq T, \quad \text{(2.51)}$$

which already implies (2.16b). To show that also (2.16a) holds, rewrite (2.51) in
view of $\langle m_f, f(t)\rangle_I = \int_0^T \sum_{i=1}^{n_f} m_f^\top(\tau)e_{i,n_f}f_i(t-\tau)\mathrm{d}\tau$ in the form $r(t) = \sum_{i=1}^{n_f} r_i(t)$

with

$$r_i(t) = \int_0^T m_f^\top(\tau) e_{i,n_f} f_i(t-\tau) \mathrm{d}\tau, \quad t \geq T. \tag{2.52}$$

By continuing the components $e_{i,n_f}^\top m_f(\tau)$ on $\tau > T$ with zeros, i.e., $e_{i,n_f}^\top m_f(\tau) = 0$, $\tau \geq T$, the upper bound of the integration in (2.52) can be replaced by t. Thus, the right-hand side in (2.52) can be regarded as the convolution of $f_i(t)$ with the integral kernel $e_{i,n_f}^\top m_f(\tau)$, i.e.,

$$r_i(t) = \int_0^t m_f^\top(\tau) e_{i,n_f} f_i(t-\tau) \mathrm{d}\tau, \quad t \geq T. \tag{2.53}$$

Provided that $f_i(t) = 0$ for $t < T$, the *Titchmarsh convolution theorem* [85, Theorem VII] states that $r_i(t)$ given in (2.53) is not identically equal to zero on $t \geq T$, if and only if both $e_{i,n_f}^\top m_f(\tau)$, $\tau \geq 0$ and $f_i(t)$, $t \geq T$, are not identically equal to zero. As a result, imposing

$$e_{i,n_f}^\top m_f(\tau) \not\equiv 0, \quad \tau \in (0, T), \ \forall i = 1, \dots, n_f, \tag{2.54}$$

ensures $r(t) \not\equiv 0$, $t \geq T$ for $f_i(t) = 0$, $t < T$ and $f_i(t) \not\equiv 0$, $t \geq T$, while $f_j(t) \equiv 0$, $j \neq i$, in view of (2.51). Under these assumptions, (2.50) satisfies (2.16) and is thus a residual generator for separately occurring faults on $t \geq T$. However, if multiple faults occur simultaneously, $\sum_{i=1}^{n_f} r_i(t)$ does not hold in general. Hence, the specific case $f(t) \not\equiv 0$, so that $\sum_{i=1}^{n_f} r_i(t) \equiv 0$ must be excluded. However, this is non-restrictive since it requires the simultaneous occurrence of multiple faults and additionally specific signals $f_i(t)$ depending on $m_f(\tau)$. These results are summarized in the following theorem.

Theorem 2.1 (Residual generator)
Assume that $\tilde{d}(t)$ is described by a solution of (2.15), $\bar{d}(t) \equiv 0$ holds and let $f(t)$ satisfy $f(t) = 0$, $t < T$, as well as $\langle m_f, f(t) \rangle_{\mathrm{I}} \not\equiv 0$ for $f(t) \not\equiv 0$. If the integral kernels satisfy (2.49) and (2.54), then (2.50) is a residual generator for the system (2.1). A fault is detected if $r(t) \not\equiv 0$, $t \geq T$, with $r(t)$ given by (2.50).

Proof. The proof of Theorem 2.1 is based on the derivation of (2.50). If the integral kernels satisfy (2.49), the residual generator (2.50) has the structure shown in Figure 2.2, consists only of the input and output filters $\langle n, y(t) \rangle_{\mathrm{I}}$ and $\langle m_u, u(t) \rangle_{\mathrm{I}}$ and is

independent of the operating point of the system, the ICs of the system as well as the disturbance $\tilde{d}(t)$. If (2.54) is satisfied, then it is ensured by the Titchmarsh convolution theorem that $r(t)$ is excited solely by the occurrence of a fault $f_i(t)$, i.e., (2.16) holds. When multiple faults are present, which satisfy $\langle m_f, f(t) \rangle_I \not\equiv 0$, (2.16) is satisfied by the same reasoning. Thus, (2.50) is the sought for residual generator. ∎

The residual generator (2.50) ensures only weak detectability (see Definition 1). This is a consequence of taking faults into account that are as general as possible. In order to achieve strong detectability (see Definition 2), further assumptions on the fault must be imposed, which is investigated in Section 2.4.

To discuss the fault detection with respect to the unknown but bounded disturbance $\bar{d}(t) \not\equiv 0$, insert (2.50) in (2.48) to obtain

$$r(t) = \langle m_f, f(t) \rangle_I - \langle m_{\bar{d}}, \bar{d}(t) \rangle_I, \quad t \geq T. \tag{2.55}$$

It follows from (2.55), that the residual is not only affected by the fault $f(t)$ but also by $\bar{d}(t)$. Hence, a threshold must be introduced to distinguish the influence of $f(t)$ and $\bar{d}(t)$ on $r(t)$. To this end, consider the absolute value of the residual error

$$|\langle m_f, f(t) \rangle_I - r(t)| = |\langle m_{\bar{d}}, \bar{d}(t) \rangle_I|, \quad t \geq T \tag{2.56}$$

caused by $\bar{d}(t)$. Use the integral representation of $\langle \cdot, \cdot \rangle_I$ to estimate (2.56) by

$$|\langle m_{\bar{d}}, \bar{d}(t) \rangle_I| \leq \int_0^T |m_{\bar{d}}^\top(\tau)\bar{d}(t-\tau)| \mathrm{d}\tau. \tag{2.57}$$

Introduce the vector of absolute values $|h(t)| = \mathrm{col}(|h_1(t)|, \ldots, |h_\nu(t)|) \in (\mathbb{R}_0^+)^\nu$, $h(t) \in \mathbb{R}^\nu$, the integrand on the right-hand side of (2.57) can be estimated by

$$|m_{\bar{d}}^\top(\tau)\bar{d}(t-\tau)| \leq |m_{\bar{d}}(\tau)|^\top |\bar{d}(t-\tau)|. \tag{2.58}$$

Then, (2.58) is bounded by

$$|m_{\bar{d}}^\top(\tau)\bar{d}(t-\tau)| \leq |m_{\bar{d}}(\tau)|^\top \delta \tag{2.59}$$

in view of (2.14). Since δ is constant, the *fault detection threshold*

$$r_B = \int_0^T |m_{\bar{d}}(\tau)|^\top \mathrm{d}\tau \delta \tag{2.60}$$

can be introduced. It follows from (2.57) and (2.59) that

$$|\langle m_{\bar{d}}, \bar{d}(t)\rangle_{\mathrm{I}}| \leq r_B, \quad t \geq T \tag{2.61}$$

holds. Furthermore, it can be concluded from (2.56) and (2.61) that in the fault free case, i.e., $f(t) \equiv 0$, the residual $r(t)$ satisfies

$$|r(t)| \leq r_B, \quad t \geq T. \tag{2.62}$$

Consequently, if $|r(t)| > r_B$, a fault must be present. The next theorem summarizes this result.

> **Theorem 2.2 (Fault detection)**
> Assume that $\tilde{d}(t)$ is described by a solution of (2.15), $\bar{d}(t)$ satisfies (2.14) and $\langle m_f, f(t)\rangle_{\mathrm{I}} \not\equiv 0$ holds for $f(t) \not\equiv 0$. Let the integral kernels $m(z, \tau)$, $q_w(\tau)$, $q_d(\tau)$ and $n(\tau)$ satisfy (2.49) and (2.54). Then, for the system (2.1), a fault is detected if the threshold r_B is exceeded by the residual signal $r(t)$ given in (2.50) for $t \geq T$, i.e.,
>
> $$|r(t)| > r_B, \quad t \geq T. \tag{2.63}$$

Proof. The proof of Theorem 2.2 is based on the fact that (2.50) is a residual generator for the case $\bar{d}(t) \equiv 0$ (see Theorem 2.1). Then, it follows from the residual error (2.56) and the estimate (2.61) that a fault can be detected by (2.63). ∎

The first time instant at which the threshold value in the sense of (2.63) is exceeded, is called the *fault detection time* $\hat{t}$, which is an estimate for the fault occurrence time t_f, i.e., $\hat{t} \geq t_f$. Note that if a disturbance $\bar{d}(t)$ is present, missed detections are possible if the excitation of the residual generator by the occurrence of a fault is not sufficient. Hence, attention should be paid in the design of the residual generator to keep the threshold sufficiently small compared to the excitation of the residual generator for expected fault signals. Details on this trade-off design are discussed for the simulation example in Section 2.3.5. However, (2.63) ensures that no false alarms occur.

2.3.4 Solution of the fault detection kernel equations

2.3.4.1 Fault detection kernel equations

A systematic approach for the computation of the integral kernels that satisfy (2.49) and (2.54) can be derived by considering (2.49) as an ODE-PDE system. For this, take into account that (2.49a) is a system of n_x first-order PDEs with respect to z. The corresponding n_x BCs result from (2.49b). In view of (2.3), n_x conditions for the $2n_x$ boundary values $m_B(\tau)$ can be satisfied by a suitable choice of $p(\tau)$ in (2.49b). Thus, the remaining n_x conditions are independent of $p(\tau)$ and these are the required BCs. The latter can be determined by making use of the left annihilator $(K^\top)^\perp \in \mathbb{R}^{n_x \times 2n_x}$ of $K^\top$, which satisfies $(K^\top)^\perp K^\top = 0$ and $\operatorname{rank}(K^\top)^\perp = n_x$. Applying this annihilator to (2.49b) yields with

$$(K^\top)^\perp \left(m_B(\tau) + C_B^\top n(\tau) + L_B^\top q_w(\tau) \right) = 0 \tag{2.64}$$

the n_x BCs for (2.49a). Furthermore, with (2.64) being satisfied, (2.49b) is uniquely solvable for $p(\tau)$ because of (2.3), i.e., $p(\tau)$ is given by

$$p(\tau) = (K^\top)^\dagger \left(m_B(\tau) + C_B^\top n(\tau) + L_B^\top q_w(\tau) \right) \tag{2.65}$$

in terms of $m_B(\tau)$, $q_w(\tau)$ and $n(\tau)$. In (2.65), $(K^\top)^\dagger$ is the Moore-Penrose generalized inverse, which can be computed with

$$(K^\top)^\dagger = (K K^\top)^{-1} K \tag{2.66}$$

in view of (2.3) (see, e.g., [11, Proposition 6.1.5 and Theorem 2.6.1, ix)]). From this, a matrix $\tilde{K} = I - K^\top (K^\top)^\dagger \in \mathbb{R}^{2n_x \times 2n_x}$ satisfying $\tilde{K} K^\top = 0$ and $\operatorname{rank} \tilde{K} = n_x$ (see, e.g., [11, Proposition 6.1.6., xix)]) is deduced. Consequently, $(K^\top)^\perp$ with required $\operatorname{rank}(K^\top)^\perp = n_x$ results from choosing the n_x linear independent rows of $\tilde{K}$.

The result (2.65) allows to eliminate $p(\tau)$ in (2.49c) and (2.49d). Insert (2.65) in (2.49c) to obtain

$$\dot{q}_w(\tau) = \left(F^\top - H_2^\top (K^\top)^\dagger L_B^\top \right) q_w(\tau) - \langle H_1, m(\tau) \rangle_\Omega - H_2^\top (K^\top)^\dagger m_B(\tau)$$
$$+ \left(C_4^\top - H_2^\top (K^\top)^\dagger C_B^\top \right) n(\tau). \tag{2.67}$$

To rewrite (2.49d), insert $m_{\tilde{d}}(\tau) = \tilde{G}^\top m_d(\tau)$ where $p(\tau)$ in $m_d(\tau)$ given in (2.42c) is replaced by (2.65) to obtain

$$\dot{q}_d(\tau) = S_d^\top q_d(\tau) - R_d^\top \tilde{G}^\top (G_2^\top (K^\top)^\dagger L_B^\top + G_3^\top) q_w(\tau) + R_d^\top \tilde{G}^\top \langle G_1, m(\tau) \rangle_\Omega$$
$$- R_d^\top \tilde{G}^\top G_2^\top (K^\top)^\dagger m_B(\tau) - R_d^\top \tilde{G}^\top (G_2^\top (K^\top)^\dagger C_B^\top + G_4^\top) n(\tau). \tag{2.68}$$

As a result, the *fault detection kernel equations* are represented by the ODE-PDE system with the PDE

$$\partial_z m(z, \tau) = -\mathcal{A}^*[m(z)](\tau) + \bar{L}_1(z)q(\tau) + C_1^\top(z)n(\tau) \tag{2.69a}$$

defined on $(z, \tau) \in (0, 1) \times (0, T)$ following from (2.49a), the BCs

$$\bar{K}_0 m(0, \tau) + \bar{K}_1 m(1, \tau) + \bar{L}_2 q(\tau) = \bar{C}_2 n(\tau), \qquad \tau \in (0, T) \tag{2.69b}$$

resulting from (2.64) with (2.30) and the ODE

$$\dot{q}(\tau) = F_e q(\tau) + \int_0^1 \bar{H}_1(z)m(z, \tau)\mathrm{d}z + \bar{H}_2 m(0, \tau) + \bar{H}_3 m(1, \tau) + \bar{C}_3 n(\tau), \tag{2.69c}$$

defined on $\tau \in (0, T)$ where $q(\tau) = \mathrm{col}\,(q_w(\tau),\, q_d(\tau)) \in \mathbb{R}^{n_q}$ with $n_q = n_w + n_{vd}$ summarizes (2.67) and (2.68). The matrix in (2.69a) is $\bar{L}_1(z) = \mathrm{col}\,(L_1^\top(z),\, 0^\top)$. The matrices in (2.69b) result from (2.64) with $m_B(\tau) = \mathrm{col}\,(-m(0, \tau),\, m(1, \tau))$ to

$$\begin{bmatrix} -\bar{K}_0 & \bar{K}_1 \end{bmatrix} = (K^\top)^\perp \tag{2.70a}$$

$$\bar{L}_2 = (K^\top)^\perp \begin{bmatrix} L_B^\top & 0 \end{bmatrix} \tag{2.70b}$$

$$\bar{C}_2 = -(K^\top)^\perp C_B^\top \tag{2.70c}$$

where $\bar{K}_0, \bar{K}_1 \in \mathbb{R}^{n_x \times n_x}$ and $\bar{L}_2 \in \mathbb{R}^{n_x \times n_q}$. The matrices in (2.69c) follow from (2.67) as well as (2.68) and read as

$$F_e = \begin{bmatrix} F^\top - H_2^\top (K^\top)^\dagger L_B^\top & 0 \\ -R_d^\top \bar{G}^\top \left(G_2^\top (K^\top)^\dagger L_B^\top + G_3^\top \right) q_w(\tau) & S_d^\top \end{bmatrix} \tag{2.71a}$$

$$\bar{H}_1(z) = \begin{bmatrix} -H_1^\top(z) \\ R_d^\top \tilde{G}^\top G_1^\top(z) \end{bmatrix} \tag{2.71b}$$

$$\begin{bmatrix} -\bar{H}_2 & \bar{H}_3 \end{bmatrix} = \begin{bmatrix} -H_2^\top \left(K^\top \right)^\dagger \\ -R_d^\top \tilde{G}^\top G_2^\top \left(K^\top \right)^\dagger \end{bmatrix} \tag{2.71c}$$

$$\bar{C}_3 = \begin{bmatrix} C_4^\top - H_2^\top (K^\top)^\dagger C_B^\top \\ -R_d^\top \tilde{G}^\top \left(G_2^\top (K^\top)^\dagger C_B^\top + G_4^\top \right) \end{bmatrix} \tag{2.71d}$$

where $\bar{H}_2, \bar{H}_3 \in \mathbb{R}^{n_q \times n_x}$. For convenience, the fault detection kernel equations are summarized in the following lemma.

Lemma 2.2 (Fault detection kernel equations as ODE-PDE system)**.** Let $\tilde{d}(t)$ be described by (2.15) and the integral kernels $m(z, \tau)$, $q(\tau)$ and $n(\tau)$ be a solution of the *fault detection kernel equation*

$$\partial_z m(z, \tau) = -\mathcal{A}^*[m(z)](\tau) + \bar{L}_1(z)q(\tau) + C_1^\top(z)n(\tau) \tag{2.72a}$$

$$\bar{K}_0 m(0, \tau) + \bar{K}_1 m(1, \tau) + \bar{L}_2 q(\tau) = \bar{C}_2 n(\tau), \tag{2.72b}$$

$$\dot{q}(\tau) = F_e q(\tau) + \int_0^1 \bar{H}_1(z)m(z, \tau)\mathrm{d}z + \bar{H}_2 m(0, \tau)$$

$$+ \bar{H}_3 m(1, \tau) + \bar{C}_3 n(\tau), \tag{2.72c}$$

and

$$\partial_\tau^i m(z, \tau)|_{\tau \in \{0, T\}} = 0, \quad z \in [0, 1], i = 0, \dots, n_A - 1 \tag{2.73a}$$

$$q(\tau)|_{\tau \in \{0, T\}} = 0 \tag{2.73b}$$

with (2.72a) defined on $(z, \tau) \in (0, 1) \times (0, T)$ and (2.72b)–(2.72c) on $\tau \in (0, T)$. The matrices in (2.72) are specified in (2.70) and (2.71). Then, the input-output expression (2.48) holds.

The initial and end conditions (2.73) follow from (2.49e)–(2.49g). It follows that (2.72) is a PDE-ODE system subject to the initial and end values (2.73) as well as an input $n(\tau)$, which is a degree of freedom. Note that this two-point initial-boundary-value problem is equivalent to (2.49) such that any integral kernels that are a solution of (2.72) subject to (2.73) yield the input-output expression (2.48) in accordance with Lemma 2.1. By the consideration of the additional algebraic constraint (2.54) in this transition problem, it is ensured that (2.52) is a residual generator in view of Theorem 2.1.

To solve this two-point initial-boundary-value problem, a suitable input $n(\tau)$ must be determined so that $m(z, \tau)$ and $q(\tau)$ realize the transition subject to (2.54) from the initial point to the end point given in (2.73) in finite time T. By embedding the initial and end values (2.73) into setpoints, which is achieved by additionally requiring

$$\partial_\tau^{n_A} m(z, \tau)|_{\tau \in \{0, T\}} = 0, \quad z \in [0, 1] \tag{2.74a}$$

$$\mathrm{d}_\tau q(\tau)|_{\tau \in \{0, T\}} = 0, \tag{2.74b}$$

the transition problem of the kernel equations is traced back to a setpoint change. The latter can be solved systematically with results from the flatness-based motion

planning, which is a well established method for the motion planning of DPSs (see, e.g., [62, 73, 75, 93]). It is based on the introduction of a parametrizing variable to express the system variables as functions of this so called flat output and its derivatives (see, e.g., [62]). Based on these differential parametrizations, a setpoint change between arbitrary setpoints of the system can be traced back to an algebraic interpolation problem for a reference trajectory for the flat output. For linear systems, the latter can be achieved by solving a linear system of equations, which yields a systematic solution of the in general difficult to solve two-point initial-boundary-value problem. However, since the transition between the specific initial and end points (2.73) can be always achieved, it is not required to show that the parametrizing variable is indeed a flat output. Nevertheless, it must be shown that a transition between the given points can be parametrized, which also satisfies the additional algebraic constraint (2.54). This requirement on the differential expressions for the system variables $m(z,\tau)$, $n(\tau)$ and $q(\tau)$ of the kernel equations system is investigated in Section 2.3.4.3. Before that, the parametrizing variable and the associated differential expressions are introduced in the following section.

2.3.4.2 Determination of the differential expressions

In this section the differential expressions required for the motion planning are derived. In the previous work [102] it was possible to use the results from [75, 93] directly to determine the differential expressions for (2.72). However, the general ODE-PDE coupling occurring in (2.72a) requires an extension of the results [75, 93].

For a systematic derivation of the differential expressions, the *Laplace transform* with the correspondence $h(z,\tau) \circ\!\!-\!\!\bullet \check{h}(z,s) \in \mathbb{C}^\nu$ for $h(z,\tau) \in \mathbb{R}^\nu$ is employed. In the following, the Laplace transformation is applied formally at first. However, a rigorous mathematical justification can be obtained by using operational calculus (see, e.g., [63, 75, 93]).

Use the Laplace correspondences $\partial_\tau^i m(z,\tau) \circ\!\!-\!\!\bullet s^i \check{m}(z,s)$, $i = 0, \dots, n_A$, in view of the homogeneous ICs (see (2.73)) as well as $q(\tau) \circ\!\!-\!\!\bullet \check{q}(s)$ and $n(\tau) \circ\!\!-\!\!\bullet \check{n}(s)$ to obtain the formal Laplace transform of (2.72a)

$$\partial_z \check{m}(z,s) = -\check{A}^*(z,s)\check{m}(z,s) + \bar{L}_1(z)\check{q}(s) + C_1^\top(z)\check{n}(s) \qquad (2.75a)$$

with $\check{A}^*(z,s) = \sum_{i=0}^{n_A} A_i^\top(z)s^i$ (see (2.28b)). The transformation of the BCs (2.72b) reads as

$$\bar{K}_0 \check{m}(0,s) + \bar{K}_1 \check{m}(1,s) + \bar{L}_2 \check{q}(s) = \bar{C}_2 \check{n}(s). \qquad (2.75b)$$

Regard s in (2.75) as complex parameter, then (2.75) is a boundary-value problem with (2.75a) as ODE with respect to z and the BCs given in (2.75b). Let $\check{\Phi} : \Omega^2 \times \mathbb{C} \to \mathbb{C}^{n_x \times n_x}$ be the *state transition matrix* related to (2.75a), which satisfies

$$\partial_z \check{\Phi}(z, \zeta, s) = -\check{A}^*(z, s)\check{\Phi}(z, \zeta, s), \quad \check{\Phi}(\zeta, \zeta, s) = I, \quad (z, \zeta, s) \in \Omega^2 \times \mathbb{C} \qquad (2.76)$$

(see [75, Assumption 1]). As a result

$$\check{m}(z, s) = \check{\Phi}(z, 0, s)\check{m}(0, s) + \check{\Psi}_L(z, s)\check{q}(s) + \check{\Psi}_C(z, s)\check{n}(s), \quad (z, s) \in \Omega \times \mathbb{C} \quad (2.77)$$

is the general solution of (2.75a), with

$$\check{\Psi}_L(z, s) = \int_0^z \check{\Phi}(z, \zeta, s)\bar{L}_1(\zeta)\mathrm{d}\zeta, \qquad\qquad (z, s) \in \Omega \times \mathbb{C} \qquad\qquad (2.78\text{a})$$

$$\check{\Psi}_C(z, s) = \int_0^z \check{\Phi}(z, \zeta, s)C_1^\top(\zeta)\mathrm{d}\zeta, \qquad\qquad (z, s) \in \Omega \times \mathbb{C} \qquad\qquad (2.78\text{b})$$

(see, e.g., [16, Section 4.5]). For the consideration of the BCs (2.75b), insert (2.77) in (2.75b) yielding

$$\left(\bar{K}_0 + \bar{K}_1\check{\Phi}(1, 0, s)\right)\check{m}(0, s) + \left(\bar{K}_1\check{\Psi}_L(1, s) + \bar{L}_2\right)\check{q}(s)$$
$$= \left(\bar{C}_2 - \bar{K}_1\check{\Psi}_C(1, s)\right)\check{n}(s), \qquad\qquad (2.79)$$

which depends only on the lumped variables $\check{m}(0, s)$, $\check{q}(s)$ and the input $\check{n}(s)$. Apply the formal Laplace transform to (2.72c), which gives

$$(sI - F_e)\,\check{q}(s) = \int_0^1 \bar{H}_1(z)\check{m}(z, s)\mathrm{d}z + \bar{H}_2\check{m}(0, s) + \bar{H}_3\check{m}(1, s) + \bar{C}_3\check{n}(s). \qquad (2.80)$$

This relation can be rewritten in terms of $\check{m}(0, s)$, $\check{q}(s)$ and $\check{n}(s)$, by inserting (2.77)

in (2.80). The result

$$
\left(sI - F_e - \int\limits_0^1 \bar{H}_1(z)\check{\Psi}_L(z,s)\mathrm{d}s - \bar{H}_3\check{\Psi}_L(1,s) \right) \check{q}
$$

$$
- \left(\int\limits_0^1 \bar{H}_1(z)\check{\Phi}(z,0,s)\mathrm{d}z + \bar{H}_2 + \bar{H}_3\check{\Phi}(1,0,s) \right) \check{m}(0,s)
$$

$$
= \left(\int\limits_0^1 \bar{H}_1(z)\check{\Psi}_C(z,s)\mathrm{d}z + \bar{C}_3 + \bar{H}_3\check{\Psi}_C(1,s) \right) \check{n}(s) \tag{2.81}
$$

and (2.79) can be summarized in

$$
\check{\Pi}(s) \begin{bmatrix} \check{m}(0,s) \\ \check{q}(s) \end{bmatrix} = \check{D}(s)\check{n}(s) \tag{2.82}
$$

with

$$
\check{\Pi}(s) = \begin{bmatrix} \check{\Pi}_{11}(s) & \check{\Pi}_{12}(s) \\ \check{\Pi}_{21}(s) & \check{\Pi}_{22}(s) \end{bmatrix}, \quad \check{D}(s) = \begin{bmatrix} \check{D}_1(s) \\ \check{D}_2(s) \end{bmatrix} \tag{2.83}
$$

and

$$
\check{\Pi}_{11}(s) = \bar{K}_0 + \bar{K}_1\check{\Phi}(1,0,s) \tag{2.84a}
$$

$$
\check{\Pi}_{12}(s) = \bar{K}_1\check{\Psi}_L(1,s) + \bar{L}_2 \tag{2.84b}
$$

$$
\check{\Pi}_{21}(s) = - \int\limits_0^1 \bar{H}_1(z)\check{\Phi}(z,0,s)\mathrm{d}z - \bar{H}_2 - \bar{H}_3\check{\Phi}(1,0,s) \tag{2.84c}
$$

$$
\check{\Pi}_{22}(s) = sI - F_e - \int\limits_0^1 \bar{H}_1(z)\check{\Psi}_L(z,s)\mathrm{d}s - \bar{H}_3\check{\Psi}_L(1,s) \tag{2.84d}
$$

$$
\check{D}_1(s) = \bar{C}_2 - \bar{K}_1\check{\Psi}_C(1,s) \tag{2.84e}
$$

$$
\check{D}_2(s) = \int\limits_0^1 \bar{H}_1(z)\check{\Psi}_C(z,s)\mathrm{d}z + \bar{C}_3 + \bar{H}_3\check{\Psi}_C(1,s). \tag{2.84f}
$$

A parametrizing variable $\check{\mu}(s) \in \mathbb{C}^{n_y}$ can be introduced as

$$
\check{n}(s) = \det\check{\Pi}(s)\check{\mu}(s), \tag{2.85a}
$$

which leads to

$$\begin{bmatrix} \check{m}(0,s) \\ \check{q}(s) \end{bmatrix} = \operatorname{adj} \check{\Pi}(s) \check{D}(s) \check{\mu}(s) \tag{2.85b}$$

for (2.82) in view of $\check{\Pi}(s) \operatorname{adj} \check{\Pi}(s) = \det \check{\Pi}(s) I$. With (2.85), $\check{m}(z,s)$ can be expressed in terms of $\check{\mu}(s)$ by inserting (2.85b) and (2.85a) in (2.77), which yields

$$\check{m}(z,s) = \Big(\begin{bmatrix} \check{\Phi}(z,0,s) & \check{\Psi}_L(z,s) \end{bmatrix} \operatorname{adj} \check{\Pi}(s) \check{D}(s) + \check{\Psi}_C(z,s) \det \check{\Pi}(s) \Big) \check{\mu}(s). \tag{2.86}$$

By introducing

$$\check{\varpi}(s) = \det \check{\Pi}(s) \tag{2.87a}$$

$$\check{U}(s) = J_q \operatorname{adj} \check{\Pi}(s) \check{D}(s) \tag{2.87b}$$

$$\check{V}(z,s) = \begin{bmatrix} \check{\Phi}(z,0,s) & \check{\Psi}_L(z,s) \end{bmatrix} \operatorname{adj} \check{\Pi}(s) \check{D}(s) + \check{\Psi}_C(z,s) \det \check{\Pi}(s) \tag{2.87c}$$

with $\check{\varpi}(s) \in \mathbb{C}$, $J_p = \begin{bmatrix} 0 & I \end{bmatrix} \in \mathbb{R}^{n_q \times n_q + n_x}$, $\check{U}(s) \in \mathbb{C}^{n_q \times n_y}$ and $\check{V}(z,s) \in \mathbb{C}^{n_x \times n_y}$, the system variables $\check{m}(z,s)$, $\check{q}(s)$ and $\check{n}(s)$ in (2.85) and (2.86) can be rewritten to

$$\check{m}(z,s) = \check{V}(z,s) \check{\mu}(s) \tag{2.88a}$$

$$\check{q}(s) = \check{U}(s) \check{\mu}(s) \tag{2.88b}$$

$$\check{n}(s) = \check{\varpi}(s) \check{\mu}(s). \tag{2.88c}$$

In order to determine the time domain correspondences for the expressions in (2.88), the operators $\check{V}(z,s)$, $\check{U}(s)$ and $\check{\varpi}(s)$ in (2.88) are developed as formal power series in s. This series expansion can be achieved systematically as shown in [75], by expressing $\check{\Phi}(z,\zeta,s)$, $\check{\Psi}_L(z,s)$ and $\check{\Psi}_C(z,s)$ by the formal power series

$$\check{\Phi}(z,\zeta,s) = \sum_{i=0}^{\infty} \Phi_i(z,\zeta) s^i, \quad z,\zeta \in \Omega, s \in \mathbb{C} \tag{2.89a}$$

$$\check{\Psi}_L(z,s) = \sum_{i=0}^{\infty} \Psi_{L,i}(z) s^i, \quad z \in \Omega, s \in \mathbb{C} \tag{2.89b}$$

$$\check{\Psi}_C(z,s) = \sum_{i=0}^{\infty} \Psi_{C,i}(z) s^i, \quad z \in \Omega, s \in \mathbb{C}. \tag{2.89c}$$

Note that the coefficient matrices $\Phi_i(z,\zeta) \in \mathbb{R}^{n_x \times n_x}$, $\Psi_{L,i}(z) \in \mathbb{R}^{n_x \times n_q}$ and $\Psi_{C,i}(z) \in \mathbb{R}^{n_x \times n_y}$ in (2.89) can be computed numerically by using results from [75, 93] or the recursive algorithm described in Appendix A.5.

Taking into account that term wise addition and the Cauchy product for multiplica-

tion of formal power series results again in a formal power series (see Appendix A.1, Lemma A.1), the operators $\check{V}(z, s)$, $\check{U}(s)$ and $\check{\varpi}(s)$ in (2.87) can be also expressed as the formal power series

$$\check{V}(z, s) = \sum_{i=0}^{\infty} V_i(z)s^i \tag{2.90a}$$

$$\check{U}(s) = \sum_{i=0}^{\infty} U_i s^i \tag{2.90b}$$

$$\check{\varpi}(s) = \sum_{i=0}^{\infty} \varpi_i s^i \tag{2.90c}$$

with $V_i(z) \in \mathbb{R}^{n_x \times n_y}$, $U_i \in \mathbb{R}^{n_q \times n_y}$ and $\varpi_i \in \mathbb{R}$ by inserting (2.89) in the containing matrices of (2.87) (see (2.83) and (2.84)). Using (2.90) in (2.88) allows a simple transform of the system variables $\check{m}(z, s)$, $\check{q}(s)$ and $\check{n}(s)$ into the time domain by applying the formal correspondence $s^i \check{\mu}(s) \bullet\!\!-\!\!\circ d_\tau^i \mu(\tau)$. This yields the *formal differential expressions* in terms of $d_\tau^i \mu(\tau)$, $i \in \mathbb{N}_0$, which are summarized in the following lemma.

Lemma 2.3 (Formal differential expressions). Let $V_i(z)$, $U_i(z)$ and ϖ_i be given by the formal power series (2.90), which are defined by (2.87). Then, the system variables $m(z, \tau)$, $q(\tau)$ and $n(\tau)$ can be parametrized by the differential expressions

$$m(z, \tau) = \sum_{i=0}^{\infty} V_i(z) d_\tau^i \mu(\tau) \tag{2.91a}$$

$$q(\tau) = \sum_{i=0}^{\infty} U_i d_\tau^i \mu(\tau) \tag{2.91b}$$

$$n(\tau) = \sum_{i=0}^{\infty} \varpi_i d_\tau^i \mu(\tau) \tag{2.91c}$$

in terms of the parametrizing variable $\mu(\tau)$ and its derivatives.

To make use of the so far only formal derivation of (2.91), the convergence of the containing series must be ensured by a suitable choice of the parametrizing variable $\mu(\tau)$, which is considered in detail in Section 2.3.4.3.

For the residual generator (2.50), the computation of the threshold (2.60) and the

investigation of fault detectability (see (2.54)), the integral kernels $m_u(\tau)$, $m_{\bar{d}}(\tau)$ and $m_f(\tau)$ are required, which can be also expressed in terms of differential expressions with the parametrizing variable $\mu(\tau)$. To this end, insert (2.65) in (2.92) to eliminate the dependence on $p(t)$, yielding

$$m_f(\tau) = -\langle E_1, m(\tau)\rangle_\Omega + E_2^\top (K^\top)^\dagger m_B(\tau) + \left(E_2^\top (K^\top)^\dagger L_B^\top + E_3^\top\right) J_w q(\tau)$$
$$+ \left(E_2^\top (K^\top)^\dagger C_B^\top + E_4^\top\right) n(\tau) \tag{2.92a}$$

$$m_u(\tau) = \langle B_1, m(\tau)\rangle_\Omega - B_2^\top (K^\top)^\dagger m_B(\tau) - \left(B_2^\top (K^\top)^\dagger L_B^\top + B_3^\top\right) J_w q(\tau) \tag{2.92b}$$

$$m_{\bar{d}}(\tau) = \bar{G}^\top \Big(\langle G_1, m(\tau)\rangle_\Omega - G_2^\top (K^\top)^\dagger m_B(\tau) - \left(G_2^\top (K^\top)^\dagger L_B^\top + G_3^\top\right) J_w q(\tau)$$
$$- \left(G_2^\top (K^\top)^\dagger C_B^\top + G_4^\top\right) n(\tau)\Big) \tag{2.92c}$$

with $J_w = [I, 0] \in \mathbb{R}^{n_w \times n_q}$. Then, (2.91) can be inserted in (2.42) to obtain

$$m_f(\tau) = \sum_{i=0}^\infty X_i \mathrm{d}_\tau^i \mu(\tau) \tag{2.93a}$$

$$m_u(\tau) = \sum_{i=0}^\infty X_{u,i} \mathrm{d}_\tau^i \mu(\tau) \tag{2.93b}$$

$$m_{\bar{d}}(\tau) = \sum_{i=0}^\infty X_{\bar{d},i} \mathrm{d}_\tau^i \mu(\tau) \tag{2.93c}$$

where $X_i \in \mathbb{R}^{n_f \times n_y}$, $X_{u,i} \in \mathbb{R}^{n_u \times n_y}$ and $X_{d,i} \in \mathbb{R}^{n_d \times n_y}$ read as

$$X_i = -\langle E_1, V_i\rangle_\Omega + E_2^\top (K^\top)^\dagger \begin{bmatrix} -V_i(0) \\ V_i(1) \end{bmatrix} + \left(E_2^\top (K^\top)^\dagger L_B^\top + E_3^\top\right) J_w U_i$$
$$+ \left(E_2^\top (K^\top)^\dagger C_B^\top + E_4^\top\right) \varpi_i \tag{2.94a}$$

$$X_{u,i} = \langle B_1, V_i\rangle_\Omega - B_2^\top (K^\top)^\dagger \begin{bmatrix} -V_i(0) \\ V_i(1) \end{bmatrix} - \left(B_2^\top (K^\top)^\dagger L_B^\top + B_3^\top\right) J_w U_i \tag{2.94b}$$

$$X_{\bar{d},i} = \bar{G}^\top \Big(\langle G_1, V_i\rangle_\Omega - G_2^\top (K^\top)^\dagger \begin{bmatrix} -V_i(0) \\ V_i(1) \end{bmatrix} - \left(G_2^\top (K^\top)^\dagger L_B^\top + G_3^\top\right) J_w U_i$$
$$- \left(G_2^\top (K^\top)^\dagger C_B^\top + G_4^\top\right) \varpi_i\Big). \tag{2.94c}$$

2.3.4.3 Fault detectability condition

With the differential expressions (2.91), the fault detection kernel equations (2.72), (2.73) and (2.54) can be solved by the planning of a suitable *reference trajectory*

$\mu^\star \in (C^\infty(\mathrm{I}))^{n_y}$ for the parametrizing variable $\mu(\tau)$. On the one hand, this reference trajectory must ensure the convergence of the series in the so far formal differential expressions (2.91) and on the other hand, it must be ensured that the required nontrivial setpoint change can be parametrized by these differential expressions in terms of $\mu^\star(\tau)$. If both can be achieved, then the two-point initial-boundary-value problem of the fault detection kernel equations can be reformulated into an algebraic interpolation problem. With the latter a reference trajectory $\mu^\star(\tau)$ can be determined that yields a solution for the fault detection kernel equations by the evaluation of the differential expressions. Thus, the residual generator (2.50) exists and the faults can be detected.

In view of (2.91), it can be verified that the initial and end condition (2.73) are satisfied if $\mu^\star(\tau)$ holds

$$\mathrm{d}_\tau^i \mu^\star(\tau)|_{\tau \in \{0, T\}} = 0, \quad i \in \mathbb{N}_0. \tag{2.95}$$

However, the only analytic function satisfying (2.95) on an open neighborhood is the zero function. Since a nontrivial setpoint change is required so that the additional constraint (2.54) can be satisfied, $\mu^\star(\tau)$ has to be locally non-analytic. A suitable function class with this property are the *Gevrey functions*, which are specified in the following definition.

> **Definition 3 (Gevrey functions [72, Definition 1.4.1]).** Let $\mathbb{G}^\alpha(\mathrm{I})$ be the class of Gevrey functions of order α in I. The function $\vartheta(\tau)$ is in $\mathbb{G}^\alpha(\mathrm{I})$ if $\vartheta \in C^\infty(\mathrm{I})$ and for every compact subset $\tilde{\mathrm{I}}$ of I there exists $h \in \mathbb{R}^+$ such that
>
> $$|\mathrm{d}_\tau^i \vartheta(\tau)| \le h^{i+1}(i!)^\alpha \tag{2.96}$$
>
> holds for all $i \in \mathbb{N}^+$ and $\tau \in \tilde{\mathrm{I}}$.

Taking into account that $\mathbb{G}^1(\mathrm{I})$ is the space of analytic functions on I (see [72]), $\mu^\star(\tau)$ must be chosen as Gevrey function of order $\alpha > 1$ to be non analytic. A suitable Gevrey function, satisfying the requirement (2.95) is

$$\vartheta(\tau) = \begin{cases} \dfrac{\exp\left(-\left(\left(1-\frac{\tau}{T}\right)\frac{\tau}{T}\right)^{-\sigma}\right)}{\int_0^T \exp\left(-\left(\left(1-\frac{\zeta}{T}\right)\frac{\zeta}{T}\right)^{-\sigma}\right)\mathrm{d}\zeta} & : \tau \in (0, T) \\ 0 & : \text{otherwise,} \end{cases} \tag{2.97}$$

which is a Gevrey function of order $\alpha = 1 + \mathrm{1}/\sigma$ (see, e.g., [60, Lemma 1]). It is illustrated in Figure 2.4 for $T = 1.75$ and $\alpha = 1.999$.
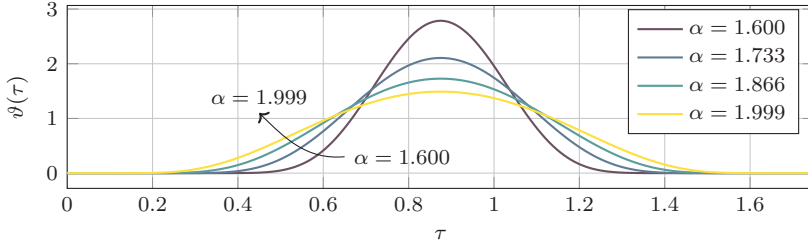
Figure 2.4: Function (2.97) for different values of σ with corresponding Gevrey orders $\alpha \in \{1.6, 1.733, 1.866, 1.999\}$ and $T = 1.75$.

Based on the bounded growth of the derivatives of Gevrey functions (see (2.96)), requirements on the reference trajectory $\mu^\star(\tau)$ can be determined to ensure the convergence of the differential expressions (2.91). For this it is required to determine the order of the power series (2.90) associated with the series in (2.91). The order of formal power series is related to properties of entire functions and can be found in [75, Definition 1] or Appendix A.1 Definition 4. The convergence of such series is shown, e.g., in [93, Satz 5.4] and stated in the following theorem.

Theorem 2.3 (Convergence of formal power series)
Let the formal power series

$$\breve{a}(s) = \sum_{i=0}^{\infty} a_i s^i \tag{2.98}$$

with $a_i \in \mathbb{R}$ be of order ϱ with $0 < \varrho < 1$. If $\varphi(\tau) \in \mathbb{R}$ is a Gevrey function of order $\alpha < 1/\varrho$ on $\tau \in \mathrm{I}$, then the corresponding series

$$a(\tau) = \sum_{i=0}^{\infty} a_i \mathrm{d}_\tau^i \varphi(\tau) \tag{2.99}$$

is locally uniform absolute convergent.

The proof of this theorem is based on the bounded growth of the derivatives of Gevrey functions and shown in the proof of [93, Satz 5.4].

Thus, in view of Theorem 2.3, the series (2.91) are locally uniform absolute convergent, if the formal power series (2.90) is of order $0 < \varrho < 1$ and the reference trajectory $\mu^\star \in \mathbb{G}(\mathrm{I})$ with $\alpha < \frac{1}{\varrho}$ holds. Nevertheless, the order of the power series (2.90) must

be determined. For this, it is utilized that formal power series of order ϱ form a commutative ring, i.e., the addition and multiplication of formal power series of order ϱ result again in a formal power series of the same order (see [93, Hilfssatz 5.3] respectively Appendix A.1, Lemma A.1). Consequently, it suffices to determine the order of the power series representations for $\check{\Phi}(z, \zeta, s)$, $\check{\Psi}_L(z, s)$ and $\check{\Psi}_C(z, s)$ in (2.89). As shown in [93], this can be achieved by an analysis of the structure of $\check{A}^*(z, s)$ as stated in the following lemma.

Lemma 2.4 (Order of the power series (2.89) [93, Satz 5.5])**.** Assume that $\check{A}^*(z, s) = \sum_{i=0}^{n_A} A_i^\top(z)s^i$ has the structure

$$\check{A}^*(z, s) =$$
$$\begin{bmatrix} \check{a}_{11}(z, s) & \check{a}_{12}(z, s) & 0 & \dots & 0 \\ \vdots & & \ddots & & \vdots \\ \check{a}_{n_x-2\,1}(z, s) & \check{a}_{n_x-2\,2}(z, s) & \dots & \check{a}_{n_x-2\,n_x-1}(z, s) & 0 \\ \check{a}_{n_x-1\,1}(z, s) & \check{a}_{n_x-1\,2}(z, s) & \dots & \check{a}_{n_x-1\,n_x-1}(z, s) & \check{a}_{n_x-1\,n_x}(z, s) \\ \check{a}_{n_x\,1}(z, s) & \check{a}_{n_x\,2}(z, s) & \dots & \check{a}_{n_x\,n_x-1}(z, s) & \check{a}_{n_x\,n_x}(z, s) \end{bmatrix}$$
$$(2.100)$$

with the polynomial components

$$\check{a}_{ij}(z, s) = \sum_{k=0}^{n_{a,ij}} a_{ij,k}(z)s^k \tag{2.101}$$

of degree $\deg \check{a}_{ij}(z, s) = n_{a,ij}$ and $a_{ij,k} \in C[0, 1]$ for $i, j = 1, \dots, n_x$, $k = 1, \dots, n_{a,ij}$, which satisfy the inequality

$$\max_{z \in \Omega} \frac{\deg \check{a}_{ij}(z, s)}{\varrho} \le i - j + 1, \tag{2.102}$$

for $i, j = 1, \dots, n_x$, with $i \ge j - 1$ and some $\varrho \in \mathbb{R}$ satisfying $0 < \varrho < 1$ independent of i and j. Then, the components of $\check{\Phi}(z, \zeta, s)$, $\check{\Psi}_L(z, s)$ and $\check{\Psi}_C(z, s)$ are power series of order ϱ.

Note that the required structure of $\check{A}^*(z, s)$ in Lemma 2.4 relies on the choice of the system variable $x(z, t)$. If $\check{A}^*(z, s)$ does not have the required structure (2.100), a different choice of the system variable may lead to a suitable form. Moreover, the structure of $\check{A}^*(z, s)$ in this lemma is not restrictive. In the following example it is shown that the operator $\check{A}^*(z, s)$ related to the parabolic system in the Example 2.1 satisfies this condition.

Example 2.2 *(Order of the power series for* $\check{\Phi}(z,\zeta,s)$ *related to the formal adjoint system operator of the Example 2.1).*
The formal adjoint system operator $\check{A}^*(z,s)$ related to Example 2.1 has the representation

$$\check{A}^*(z,s) = \begin{bmatrix} \frac{-\mathrm{d}_z\alpha(z)}{\alpha(z)} & 1 \\ -\frac{\beta(z)}{\alpha(z)} + \frac{1}{\alpha(z)}s & 0 \end{bmatrix}, \tag{2.103}$$

see (2.6) and (2.28b). In view of (2.103), $\check{A}^*(z,s)$ satisfies the structure given in (2.100) and with

$$\deg \check{a}_{ij}(z,s) = \begin{cases} 1 & : i = 2, j = 1 \\ 0 & : \text{otherwise} \end{cases} \tag{2.104}$$

the inequality (2.102) yields $\frac{1}{\varrho} \leq 2$. Hence, $\check{\Phi}(z,\zeta,s)$ is a formal power series of order $\varrho = \frac{1}{2}$.   ◁

The same can be shown for further parabolic and biharmonic PDE systems by an appropriate choice of the state $x(z,t)$ (see, e.g., [99, 102]). Although Lemma 2.4 is only sufficient, it provides a straightforward verifiable condition for the determination of the order of the formal power series (2.90) for a large class of DPSs.

Finally, the fault detectability condition (2.54) (see Theorem 2.1) must be taken into account in the planning of a suitable reference trajectory $\mu^\star(\tau)$. This is stated in the following theorem.

Theorem 2.4 (Fault detectability)
Let

$$\exists j \in \mathbb{N}_0 \text{ so that } e_{i,n_f}^\top X_j \neq 0^\top, \quad \forall i = 1, \ldots, n_f, \tag{2.105}$$

hold with X_j given in (2.94a) and assume, $\tilde{d}(t)$ is described by (2.15) and $\bar{d}(t) \equiv 0$. Then, for the system (2.1), a fault $f_i(t) = e_{i,n_f}^\top f(t)$ is detectable in the sense of Theorem 2.1. If the system is subject to $\bar{d}(t) \not\equiv 0$ satisfying (2.14), then the fault $f_i(t)$ is detectable according to Theorem 2.2.

Proof. The result of Theorem 2.4 is proven by showing that there exists a reference trajectory $\mu^\star(\tau)$, which parametrizes the fault detection kernels $m^\star(z,\tau)$, $q^\star(\tau)$ and $n^\star(\tau)$ so that they solve (2.72) subject to (2.73) and (2.54). Note that if (2.72)

subject to (2.73) is satisfied, also (2.49) holds, which is the requirement of Theorem 2.1 and Theorem 2.2.

If $\mu^\star \in (\mathbb{G}^\alpha(\mathrm{I}))^{n_y}$, $1 < \alpha < {}^1/_\varrho$ satisfies (2.95), the resulting $m^\star(z,\tau)$, $q^\star(\tau)$ and $n^\star(\tau)$ from (2.91) are solutions of (2.72) subject to (2.73). A possible choice for $\mu^\star(\tau)$ satisfying these requirements is (2.97). Thus, it remains to prove that (2.54) can be satisfied. Express the reference trajectory $m_f^\star(\tau)$ assigned to $m_f(\tau)$ in terms of $\mu^\star(\tau)$ resulting from (2.93a) by

$$m_f^\star(\tau) = \sum_{j=0}^\infty X_j \mathrm{d}_\tau^j \mu^\star(\tau). \tag{2.106}$$

Take (2.106) component-wise into account, i.e., for each $e_{i,n_f}^\top m_f^\star(\tau)$ and $e_{k,n_y}^\top \mu^\star(\tau)$. Consider the ith component of $m_f^\star(\tau)$ in the form

$$e_{i,n_f}^\top m_f^\star(\tau) = \sum_{k=1}^{n_y} m_{f,ik}^\star(\tau). \tag{2.107}$$

In (2.107), the terms

$$m_{f,ik}^\star(\tau) = \sum_{j=0}^\infty \chi_{ik}^j \mathrm{d}_\tau^j \mu_k^\star(\tau), \quad i = 1, \dots, n_f, \ k = 1, \dots, n_y, \tag{2.108}$$

are ordered with respect to the kth component $\mu_k^\star(\tau)$ of $\mu^\star(\tau)$, where $\chi_{ik}^j \in \mathbb{R}$ are the components of

$$X_j = \begin{bmatrix} \chi_{11}^j & \cdots & \chi_{1n_y}^j \\ \vdots & \ddots & \vdots \\ \chi_{n_f 1}^j & \cdots & \chi_{n_f n_y}^j \end{bmatrix}, \tag{2.109}$$

which satisfy $\chi_{ik}^j \neq 0$ for some $j \in \mathbb{N}_0$ in view of (2.105). Consider the case $m_{f,ik}^\star(\tau) \equiv 0$, $\forall k = 1, \dots, n_y$, so that (2.108) reads as

$$\sum_{j=0}^\infty \chi_{ik}^j \mathrm{d}_\tau^j \mu_k^\star(\tau) \equiv 0, \quad i = 1, \dots, n_f, \ k = 1, \dots, n_y. \tag{2.110}$$

Then, (2.110) is a homogeneous differential equation with respect to $\mu_k^\star(\tau)$. The only solution satisfying (2.110) with the ICs $\mathrm{d}_\tau^j \mu_k^\star(\tau)|_{\tau=0} = 0$, $j \in \mathbb{N}_0$, is the trivial solution $\mu_k^\star(\tau) \equiv 0$. Consequently, any $\mu_k^\star(\tau) \not\equiv 0$ satisfying (2.95) yields $m_{f,ik}^\star(\tau) \not\equiv 0$, if $\chi_{ik}^j \neq 0$ holds for some $j \in \mathbb{N}_0$. Moreover, $\sum_{k=0}^{n_y} m_{f,ik}^\star(\tau) \equiv 0$ with

$m^\star_{f,ik}(\tau) \not\equiv 0$, can always be omitted by a suitable choice of $\mu^\star_k(\tau)$. Hence, under assumption (2.105), a nontrivial reference trajectory $\mu^\star \in (\mathbb{G}^\alpha(\mathrm{I}))^{n_y}$, $1 < \alpha < 1/\varrho$, satisfying (2.95) exists so that the parametrized fault detection kernels $m^\star(z,\tau)$, $q^\star(\tau)$ and $n^\star(\tau)$ resulting from (2.91) are solutions of (2.72) subject to (2.73) and (2.54). ∎

Note that the condition (2.105) depends only on the coefficient matrices X_j, $j \in \mathbb{N}_0$, of the differential expression (2.93a). In view of the derivation of X_j in Section 2.3.4.2, it follows that X_j depends only on parameters of the original system (2.1) and the signal model (2.15) of the disturbance $\tilde{d}(t)$. Hence, (2.105) is a system property that can be verified a priori.

2.3.4.4 Systematic approach for the planning of the reference trajectory

If Theorem 2.4 holds, then it remains to choose a suitable reference trajectory $\mu^\star(\tau)$. In the following, an algorithm is proposed, which allows to specify the stationary gain of the residual generator with respect to constant faults and to reduce the influence of the disturbance $\bar{d}(t)$ on the residual signal. This allows to balance the residual signal to the expected magnitudes of faults. Although this approach assumes constant faults for the design of the residual generator, it is shown in Section 2.3.5, that this approach leads also for time-varying faults to good results.

For the case of a constant fault $f_i(t) = const.$, $i = 1, \ldots, n_f$, $t \geq 0$, (2.52) reads as

$$r(t) = \bar{m}_f^\top f, \quad t \geq T \tag{2.111}$$

where

$$\bar{m}_f = \int_0^T m_f^\star(\tau)\mathrm{d}\tau \tag{2.112}$$

is regarded as the *stationary gain* for constant faults. Since

$$\bar{m}_{f,i} \neq 0, \quad \forall i = 1, \ldots, n_f, \tag{2.113}$$

for the components $\bar{m}_{f,i}$ of $\bar{m}_f$ ensures the fault detectability condition (2.54), the reference trajectory planning can be traced back to the determination of a $\bar{m}_f$ satisfying (2.113). To express (2.112) in terms of $\mu^\star(\tau)$ insert (2.106) in (2.112),

yielding

$$\bar{m}_f = \sum_{i=0}^{\infty} X_i \int_0^T \mathrm{d}_\tau^i \mu^\star(\tau) \mathrm{d}\tau \qquad (2.114)$$

after changing the order of the integration and summation. The latter is allowed because the uniform convergence of the series (2.93a) is ensured by $\mu^\star \in (\mathbb{G}^\alpha(\mathrm{I}))^{n_y}$, $1 < \alpha < {}^1/_\varrho$. Let $\mu^\star(\tau)$ satisfy the initial and end conditions specified in (2.95). Then, the evaluation of the integrals in (2.114) gives

$$\int_0^T \mathrm{d}_\tau^i \mu^\star(\tau) \mathrm{d}\tau = \left[\mathrm{d}_\tau^{i-1} \mu^\star(\tau) \right]_0^T = 0, \quad i > 0. \qquad (2.115)$$

With (2.115), (2.112) reads as

$$\bar{m}_f = X_0 \int_0^T \mu^\star(\tau) \mathrm{d}\tau. \qquad (2.116)$$

In order to introduce degrees of freedom in the parametrizing variable $\mu^\star(\tau)$, impose

$$\mu^\star(\tau) = \sum_{i=1}^{n_\mu} \vartheta(\tau) \theta_i(\tau) \eta_i \qquad (2.117)$$

with $\eta_i \in \mathbb{R}^{n_y}$, $i = 1, \ldots, n_\mu$, $\theta_1 = 1$ and linear independent functions $\theta_i \in C^\infty(\mathrm{I})$, $i = 2, \ldots, n_\mu$, $\vartheta \in \mathbb{G}^\alpha(\mathrm{I})$, $1 < \alpha < {}^1/_\varrho$,

$$\mathrm{d}_\tau^i \vartheta(\tau)|_{\tau \in \{0,T\}} = 0, \quad i \in \mathbb{N}_0 \qquad (2.118)$$

and

$$\int_0^T \vartheta(\tau) \mathrm{d}\tau = 1. \qquad (2.119)$$

In (2.117), $\vartheta(\tau)$ ensures the convergence of the series (2.91) as well as the required initial and end conditions (2.95). The degrees of freedom η_i will be used to ensure (2.116) as well as to make the residual generator less sensitive to the disturbance $\bar{d}(t)$.

Rewrite (2.117) into the form

$$\mu^\star(\tau) = \theta(\tau)\eta \tag{2.120}$$

with $\theta(\tau) = \vartheta(\tau)[\theta_1(\tau)\cdots\theta_{n_\mu}(\tau)]\otimes I_{n_y}$, where I_{n_y} is the identity matrix of dimension n_y and $\eta = \mathrm{col}\left(\eta_1,\ldots,\eta_{n_\mu}\right)$. Therein, $A\otimes B$ is the *Kronecker product*, i.e., $A\otimes B = [a_{ij}]\otimes B = [a_{ij}B]$ for matrices $A\in\mathbb{R}^{m\times n}$ and $B\in\mathbb{R}^{p\times q}$ of arbitrary dimension (see, e.g., [11, Def. 7.1.2]). Inserting (2.120) in (2.116) and introducing $\Theta = \int_0^T \theta(\tau)\mathrm{d}\tau$ yields

$$\bar{m}_f = X_0\Theta\eta. \tag{2.121}$$

In general, $X_0\Theta \in \mathbb{R}^{n_f\times n_y n_\mu}$ is non-square, thus a compatible $\bar{m}_f \in \mathcal{R}(X_0)$ must be chosen, where $\mathcal{R}(X_0)$ is the range of X_0. Note that $\mathcal{R}(X_0) = \mathcal{R}(X_0\Theta)$ follows form $\theta_1 = 1$ and [11, Proposition 2.6.3.]. Then, (2.121) has the solution

$$\eta = (X_0\Theta)^\dagger\bar{m}_f + \left(I - (X_0\Theta)^\dagger X_0\Theta\right)\bar{m}_f^*, \tag{2.122}$$

where $(X_0\Theta)^\dagger$ is the Moore-Penrose generalized inverse of $X_0\Theta$, which can be computed by a singular value decomposition as described, e.g., in [11, Section 6.1]. If $\mathrm{rank}\left(I - (X_0\Theta)^\dagger X_0\Theta\right) > 0$ holds, $\bar{m}_f^* \in \mathbb{R}^{n_y n_\mu}$ in (2.122) is a degree of freedom, which will be used to minimize the influence of the disturbance $\bar{d}(t)$. In view of (2.122), the fault detectability can be ensured by specifying an $\bar{m}_f$ satisfying

$$e_{i,n_f}^\top \bar{m}_f \neq 0, \quad \forall i = 1,\ldots,n_f, \text{ so that } \bar{m}_f \in \mathcal{R}(X_0). \tag{2.123}$$

This is possible if

$$e_{i,n_f}^\top X_0 \neq 0 \tag{2.124}$$

holds, which is in accordance with the results of Theorem 2.4.

If $\mathrm{rank}\left(I - (X_0\Theta)^\dagger X_0\Theta\right) > 0$ holds, there exist remaining degrees of freedom $\bar{m}_f^*$, which can be used to reduce the influence of $\bar{d}(t)$ on the residual signal $r(t)$. By regarding the threshold value r_B as a measure for the influence of the disturbance $\bar{d}(t)$ on the residual signal $r(t)$, $\bar{m}_f^*$ should be chosen to reduce r_B. In view of (2.60), express $m_{\bar{d}}(\tau)$ in terms of $\bar{m}_f^*$ by inserting (2.117) with (2.122) in (2.93c) after the substitutions $\mu(\tau) \to \mu^\star(\tau)$ and $m_{\bar{d}}(\tau) \to m_{\bar{d}}^\star(\tau)$ to obtain

$$m_{\bar{d}}^\star(\tau) = \bar{\theta}_0(\tau) + \bar{\theta}_1(\tau)\bar{m}_f^* \tag{2.125}$$

with

$$\bar{\theta}_0(\tau) = \sum_{i=0}^{\infty} X_{\bar{d},i} \mathrm{d}_\tau^i \theta(\tau) \left(X_0\Theta\right)^\dagger \bar{m}_f \tag{2.126a}$$

$$\bar{\theta}_1(\tau) = \sum_{i=0}^{\infty} X_{\bar{d},i} \mathrm{d}_\tau^i \theta(\tau) \left(I - (X_0\Theta)^\dagger X_0\Theta\right). \tag{2.126b}$$

Thus, the desired threshold value becomes

$$r_B = \int_0^T |\bar{\theta}_0(\tau) + \bar{\theta}_1(\tau)\bar{m}_f^*|^\top \mathrm{d}\tau \delta \tag{2.127}$$

by inserting (2.125) in (2.60). Since r_B is an upper bound for the effect of the disturbance $\bar{d}(t)$ on the residual signal $r(t)$, the threshold r_B should be chosen to

$$r_B = \min_{\bar{m}_f^* \in \mathbb{R}^{n_y n_\mu}} \int_0^T |\bar{\theta}_0(\tau) + \bar{\theta}_1(\tau)\bar{m}_f^*|^\top \mathrm{d}\tau \delta. \tag{2.128}$$

By (2.122) and the particular choice of $\vartheta(\tau)$, it is ensured that the resulting reference trajectory $\mu^\star(\tau)$ from (2.120) leads to integral kernels $m^\star(z,\tau)$, $q^\star(\tau)$ and $n^\star(\tau)$ (see (2.91)) that are solutions of (2.72) subject to (2.73) and (2.54) for any $\bar{m}_f^* \in \mathbb{R}^{n_y n_\mu}$. Thus, (2.128) can be solved numerically.

2.3.5 Fault detection for an Euler-Bernoulli beam

For the illustration of the presented fault detection approach, the cantilever beam with a load at its tip depicted in Figure 2.5 is considered. The system setup is inspired by the real-world setup treated in [79] to demonstrate the applicability of the approach. A similar setup has been considered in the previous work [101] for fault diagnosis. However, multiple inputs, outputs, disturbances and faults are added to show the generality of the presented approach. The simulation of the beam and the fault detection are implemented in MATLAB 2020a and are available in [108].

By assuming an Euler-Bernoulli beam with viscous external damping, the well-known equation of motion for the deflection $v(z,t) \in \mathbb{R}$ reads as

$$\mu_b(z)\partial_t^2 v(z,t) + \rho(z)\partial_t v(z,t) + \partial_z^2(\lambda_b(z)\partial_z^2 v(z,t))$$
$$= b_1(z)(1 + \Delta f_1(t))u_1(t) + g_1(z)(\tilde{d}(t) + \bar{d}_1(t)) + e_1(z)f_2(t) \tag{2.129a}$$
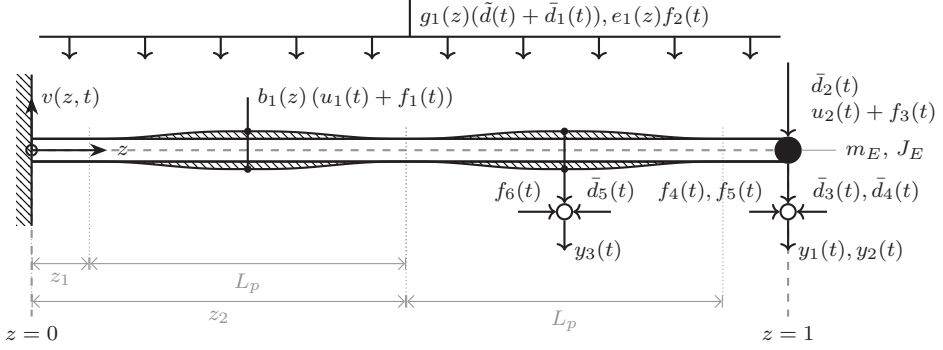
Figure 2.5: Schematic of the cantilever beam with a tip load and patches
mounted on opposite sides of the beam for the actuation as well
as a measurement described in (2.129).

and is defined on $(z,t) \in (0,1) \times \mathbb{R}^+$. The BCs of the cantilever beam with a tip
load are

$$v(0,t) = \partial_z v(0,t) = 0, \qquad\qquad\qquad\qquad t > 0 \qquad\qquad (2.129\text{b})$$

$$\partial_z^2 v(1,t) = -J_E \partial_t^2 \partial_z v(1,t) + g_2 \bar{d}_2(t), \qquad t > 0 \qquad\qquad (2.129\text{c})$$

$$\partial_z^3 v(1,t) = m_E \partial_t^2 v(1,t) + b_2(u_2(t) + f_3(t)), \qquad t > 0 \qquad\qquad (2.129\text{d})$$

and the available measurements $y(t) = \mathrm{col}\,(y_1(t),\, y_2(t),\, y_3(t)) \in \mathbb{R}^3$ are given by

$$y(t) = \begin{bmatrix} (1 + \Delta f_4(t))c_1 v(1,t) + \bar{d}_3(t) \\ c_2 \partial_z v(1,t) + \bar{d}_4(t) + f_5(t) \\ \int_0^1 c_3(z)\partial_z^2 v(z,t)\mathrm{d}z + \bar{d}_5(t) + f_6(t) \end{bmatrix}, \qquad t \geq 0. \qquad (2.129\text{e})$$

The beam is actuated by two asymmetrically controlled piezoelectric patches mounted
on the opposite surfaces of the beam and a force acting on the tip load. The
influence of the input $u_1(t) \in \mathbb{R}$ on the system is modeled by the spatial characteristic
$b_1(z) = b_0 \partial_z^2 h_1(z) \in \mathbb{R}$ with $h_1 \in C^2[0,1]$ and the input $u_2(t) \in \mathbb{R}$ has the gain $b_2 \in \mathbb{R}$.
The deflection and bending at the tip of the beam are available by measurements
$y_1(t), y_2(t) \in \mathbb{R}$. Additionally, $y_3(t) \in \mathbb{R}$ is the output of an attached strain gauge,
which has the spatial characteristic $c_3(z) = c_0 h_2(z) \in \mathbb{R}$, $h_2 \in C^2[0,1]$. The system
parameters are $\mu_b(z) = \mu_c + \mu_p(h_1(z) + h_2(z)) \in \mathbb{R}$, $\rho(z) = \rho_c + \rho_p(h_1(z) + h_2(z)) \in \mathbb{R}$,
$\lambda_b(z) = \lambda_c + \lambda_p(h_1(z) + h_2(z)) \in \mathbb{R}$, where the component with index c reflects the
parameters of the carrier layer and the components with index p the parameters of
the attached patches as described in [79] as well as parameters of the additionally
added strain gauge. The spatial characteristics $h_1(z)$ and $h_2(z)$ are described by

Table 2.1: Normalized model parameters for the cantilever beam.

Value	Parameter	Value	Parameter
μ_c	52.00×10^{-3}	μ_p	88.20×10^{-3}
ρ_c	139.50×10^{-3}	ρ_p	560×10^{-3}
λ_c	1.72	λ_p	5.60
J_E	44.34×10^{-9}	m_E	843.24×10^{-6}
b_0	1.21×10^{-3}	b_2	200×10^{-6}
g_1	1.12×10^{-3}	g_2	1×10^{-3}
c_0	2.74×10^3	c_1, c_2	1.00×10^3
e_{z0}	561.19×10^{-6}	e_{z1}	1.68×10^{-3}
d_h	197.04×10^{-3}	L_p	418.72×10^{-3}
z_1	76.35×10^{-3}		
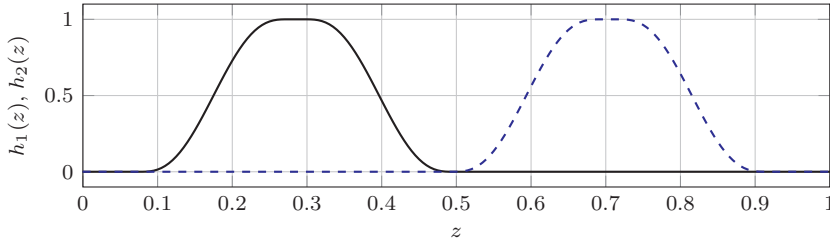
Figure 2.6: Spatial characteristics $h_1(z)$ (——) and $h_2(z)$ (- - -) as piecewise defined polynomials of order 5.

$h_1(z) = \bar{h}(z - z_1)$ and $h_2(z) = \bar{h}(z - z_2)$, $z_2 = z_1 + L_p$ with the piecewise defined function

$$\bar{h}(z) = \begin{cases} 0 & : z \leq 0 \\ h_s(z) & : 0 < z < d_h \\ 1 & : d_h \leq z \leq L_p - d_h \\ 1 - h_s(z - L_p + d) & : L_p - d_h < z < L_p \\ 0 & : z \geq L_p, \end{cases} \qquad (2.130)$$

and are shown in Figure 2.6. In (2.130), $h_s(z) \in \mathbb{R}$, $z \in [0, d_h]$ is a polynomial of order 5 satisfying $\partial_z^i h_s(z)|_{z=0} = 0$, $i = 0, \dots, 2$, $h_s(d_h) = 1$ and $\partial_z^i h_s(z)|_{z=d_h} = 0$, $i = 1, 2$, so that $h_i(z)$, $i = 1, 2$, has the required smoothness. All system parameters are normalized to the length $L_c = 0.41$m of the beam so that $z \in (0, 1)$ holds and are assembled in Table 2.1. Furthermore, the disturbance $\tilde{d}(t) \in \mathbb{R}$ is acting in-domain, whereas the signal form of $\tilde{d}(t) = d_1^0 \sin(3t + \phi_d)$ is known but the parameters d_1^0, $\phi_d \in \mathbb{R}$ are unknown. Hence, $\tilde{d}(t)$ can be described by a signal model specified by

known

$$S_d = \begin{bmatrix} 0 & -3 \\ 3 & 0 \end{bmatrix}, \qquad\qquad R_d = \begin{bmatrix} 0 & 1 \end{bmatrix} \qquad (2.131)$$

and the unknown IC $v_d^0 \in \mathbb{R}^2$. The disturbances $\bar{d}_i(t)$, $i = 1, \ldots, 5$, are bounded by $|\bar{d}_i(t)| \leq \delta_i$, with known upper bounds $\delta_1 = 2$ and $\delta_i = 0.10$, $i = 2, \ldots, 5$. The input $u_1(t)$ is subject to the multiplicative fault $\Delta f_1(t) \in \mathbb{R}$, which is rewritten as additive fault $f_1(t) = u_1(t)\Delta f_1(t)$. With $f_2(t) \in \mathbb{R}$, an additive process fault, acting in-domain with known spatial characteristic $e_1(z) = e_{z0} + e_{z2}z^2 \in \mathbb{R}$ is taken into account. The fault $f_3(t) \in \mathbb{R}$ is an additive actuator fault, affecting $u_2(t)$. The measurement $y_1(t)$ is subject to a multiplicative fault $\Delta f_4(t) \in \mathbb{R}$, which is rewritten as additive fault $f_4(t) = \Delta f_4(t)c_1v(1,t)$. The measurements $y_2(t)$ and $y_3(t)$ are subject to the faults $f_5(t) \in \mathbb{R}$ and $f_6(t) \in \mathbb{R}$, which are additive sensor faults.

In order to use the described fault detection approach, at first, (2.129) must be rewritten into a system of the form (2.1). To this end, introduce

$$x(z,t) = \mathrm{col}\left(\partial_z^3 v(z,t), \, \partial_z^2 v(z,t), \, \partial_z v(z,t), \, v(z,t)\right) \qquad (2.132)$$

so that the defining matrices of the operator $\mathcal{A}$ (see (2.1a)) are given by

$$A_0(z) = \begin{bmatrix} -2\frac{\mathrm{d}_z \lambda_b(z)}{\lambda_b(z)} & -\frac{\mathrm{d}_z^2 \lambda_b(z)}{\lambda_b(z)} & 0 & 0 \\ 1 & 0 & 0 & 0 \\ 0 & 1 & 0 & 0 \\ 0 & 0 & 1 & 0 \end{bmatrix}, \qquad (2.133)$$

$A_1(z) = -\frac{\rho(z)}{\lambda_b(z)}e_{1,4}\,e_{4,4}^\top$ and $A_2(z) = -\frac{\mu_b(z)}{\lambda_b(z)}e_{1,4}\,e_{4,4}^\top$. Moreover, $B_1(z) = \frac{b_1(z)}{\lambda_b(z)}e_{1,4}e_{1,2}^\top$ and $G_1(z) = g_1 e_{1,4}\,e_{1,5}^\top$ result. For the dynamic BCs (2.129b)–(2.129d), the ODE states

$$w(t) = \mathrm{col}\left(\partial_t\partial_z v(1,t), \, \partial_z v(1,t), \, \partial_t v(1,t), \, v(1,t)\right) \qquad (2.134)$$

are introduced. With these, the boundary matrices for (2.1b) are

$$K_0 = \begin{bmatrix} 0 & 0 & 1 & 0 \\ 0 & 0 & 0 & 1 \\ 0 & 0 & 0 & 0 \\ 0 & 0 & 0 & 0 \end{bmatrix}, K_1 = \begin{bmatrix} 0 & 0 & 0 & 0 \\ 0 & 0 & 0 & 0 \\ 0 & 0 & 1 & 0 \\ 0 & 0 & 0 & 1 \end{bmatrix} \text{ and } H_2 = \begin{bmatrix} 0 & 0 & 0 & 0 \\ 0 & 0 & 0 & 0 \\ 0 & -1 & 0 & 0 \\ 0 & 0 & 0 & -1 \end{bmatrix}. \quad (2.135a)$$

With (2.134), the matrices for the ODE (2.1c) read as

$$F = \begin{bmatrix} 0 & 0 & 0 & 0 \\ 1 & 0 & 0 & 0 \\ 0 & 0 & 0 & 0 \\ 0 & 0 & 1 & 0 \end{bmatrix}, \qquad L_3 = \begin{bmatrix} 0 & -\frac{1}{J_E} & 0 & 0 \\ 0 & 0 & 0 & 0 \\ \frac{1}{m_E} & 0 & 0 & 0 \\ 0 & 0 & 0 & 0 \end{bmatrix}, \qquad (2.136)$$

$B_3 = -\frac{b_2}{m_E} e_{3,4}\, e_{2,2}^\top$, $G_3 = \frac{g_2}{J_E} e_{1,4}\, e_{2,5}^\top$ and for the output equation (2.1d), $C_1(z) = c_3(z) e_{3,3}\, e_{2,4}^\top$,

$$C_3 = \begin{bmatrix} 0 & 0 & 0 & c_1 \\ 0 & 0 & c_2 & 0 \\ 0 & 0 & 0 & 0 \end{bmatrix}, \qquad (2.137)$$

as well as $G_4 = I_3$. The matrices to consider the components $\bar{d}(t) = \mathrm{col}(\bar{d}_1(t), \bar{d}_2(t), \bar{d}_3(t))$ and $\tilde{d}(t)$ of the disturbance $d(t)$ (see (2.13)) read as $\bar{G} = e_{1,5}$ and $\tilde{G} = I$. The fault input matrices are $E_1(z) = \frac{b_1(z)}{\lambda_b(z)} e_{1,4} e_{1,6}^\top + \frac{e_1(z)}{\lambda_b(z)} e_{1,4} e_{2,6}^\top$, $E_3 = -\frac{b_2}{m_E} e_{3,4}\, e_{3,6}^\top$ and $E_4 = [0\ I] \in \mathbb{R}^{3 \times 6}$.

The computation of the differential expressions (2.91) and (2.93) is implemented with the help of the toolbox [109] that simplifies the implementation of time and space dependent functions and operators in MATLAB. For the coefficient matrices $V_i(z)$, U_i and ϖ_i of the differential parametrization, it is required to compute $\Phi_i(z, \zeta)$, $\Psi_{L,i}(z)$ and $\Psi_{C,i}(z)$, which is done with the recursive algorithm proposed in Appendix A.5 on a discrete grid with 801 points for the spatial domain and the containing integral terms are computed with the compound trapezoidal rule. Then,

$$X_0 = \begin{bmatrix} 8.01 \times 10^{09} & 1.12 \times 10^{10} & 0 \\ 1.69 \times 10^{10} & 2.16 \times 10^{10} & 2.28 \times 10^{09} \\ 9.71 \times 10^{09} & 1.36 \times 10^{10} & 2.58 \times 10^{09} \\ 2.41 \times 10^{11} & 0 & 0 \\ 0 & 2.41 \times 10^{11} & 0 \\ 0 & 0 & 2.41 \times 10^{11} \end{bmatrix} \qquad (2.138)$$

results by evaluating (2.94a) for $i = 0$ to verify the fault detectability in view of (2.105). With (2.138), the requirement (2.124) for the application of the approach in Section 2.3.4.4 for the planning of the reference trajectory $\mu^\star(\tau)$ is satisfied. Hence, it is used to obtain the following results. In the simulation, faults with the expected magnitudes $f_{ex} = \mathrm{col}\,(41.82, 28.50, 30, 2.65, 16.51, 1.50)$ are assumed. To balance the residual generator stationary gain $\bar{m}_f$ with respect to to f_{ex}, $\bar{m}_f$ should be close to $\bar{\bar{m}}_f = \mathrm{col}(f_{ex,1}^{-1}, \ldots, f_{ex,n_f}^{-1})$ where $f_{ex,i} = e_{i,n_f}^\top f_{ex}$, $i = 1, \ldots, n_f$. Additionally, $\bar{m}_f \in \mathcal{R}(X_0)$ must hold, which is required to solve (2.121). Both requirements can

be achieved by

$$\bar{m}_f = X_0 X_0^\dagger \bar{\bar{m}}_f, \tag{2.139}$$

since (2.139) minimizes $\|\bar{m}_f - \bar{\bar{m}}_f\|_2$ and ensures that $\bar{m}_f \in \mathcal{R}(X_0)$ holds (see [11, Fact 9.15.4]), where $\|\cdot\|_2$ is the Euclidean norm. From the resulting

$$\bar{m}_f = \begin{bmatrix} 0.0154 & 0.0383 & 0.0258 & 0.378 & 0.0611 & 0.667 \end{bmatrix}^\top, \tag{2.140}$$

it is verified by (2.123) that the resulting reference trajectory $\mu^\star(\tau)$ will lead to an integral kernel $m_f^\star(\tau)$ that satisfies the detectability condition (2.54).

As linear independent functions $\theta_i(\tau)$ in (2.117), the first five basis functions of a Fourier series, i.e., $\theta_1(\tau) = 1$, $\theta_2(\tau) = \sin(\frac{\pi\tau}{T})$, $\theta_3(\tau) = \cos(\frac{\pi\tau}{T})$, $\theta_4(\tau) = \sin(\frac{2\pi\tau}{T})$ and $\theta_5(\tau) = \cos(\frac{2\pi\tau}{T})$ are chosen, whereas $n_\mu = 5$ is determined so that an increase would not lead to a relevant improvement of the resulting residual generator.

To choose an appropriate $\vartheta(\tau)$ in (2.117) the upper bound $1/\varrho$ of the Gevrey order α for $\mu^\star(\tau)$ must be determined. According to Lemma 2.4,

$$\check{A}^*(z,s) = \begin{bmatrix} \frac{-2\mathrm{d}_z \lambda_b(z)}{\lambda_b(z)} & 1 & 0 & 0 \\ \frac{-\mathrm{d}_z^2 \lambda_b(z)}{\lambda_b(z)} & 0 & 1 & 0 \\ 0 & 0 & 0 & 1 \\ \frac{-\rho(z)}{\lambda_b(z)}s - \frac{\mu_b(z)}{\lambda_b(z)}s^2 & 0 & 0 & 0 \end{bmatrix} \tag{2.141}$$

satisfies the required structure in (2.100). With (2.141), it follows from (2.102), that the corresponding $\check{\Phi}(z,\zeta,s)$, $\check{\Psi}_L(z,s)$ and $\check{\Psi}_C(z,s)$ are formal power series of order $\varrho = 1/2$. Thus, $\mu^\star(\tau)$ must be a Gevrey function of order $1 < \alpha < 2$. Hence, the Gevrey function specified in (2.97) is used for $\vartheta(\tau)$, since it ensures the requirements (2.118), (2.119) and thus the convergence of the series (2.91) and (2.93) for $1 < \alpha < 2$.

The evaluation of the differential expressions requires to compute $\mathrm{d}_\tau^i(\theta_j(\tau)\vartheta(\tau))$, $i > 0$, $j = 1, \ldots, n_\mu$, (see (2.120)), for which the product rule is applied so that only the derivatives $\mathrm{d}_\tau^i \theta_j(\tau)$ and $\mathrm{d}_\tau^i \vartheta(\tau)$ are required. The latter are computed with the _Symbolic Math Toolbox_ in MATLAB and are then numerically evaluated.

For the residual generator and the threshold r_B, the integral kernels $m_u^\star(\tau)$, $n^\star(\tau)$ and $m_d^\star(\tau)$ must be determined. Since $\alpha < 2$ ensures the convergence of the series in the differential expressions, the integral kernels $m_u^\star(\tau)$, $n^\star(\tau)$ can be computed by a

truncation of the defining series (2.91c), (2.93b) and (2.93c). To be specific,

$$n_{n_s}^\star(\tau) = \sum_{i=0}^{n_s} \varpi_i \mathrm{d}_\tau^i \mu^\star(\tau) \tag{2.142a}$$

$$m_{u,n_s}^\star(\tau) = \sum_{i=0}^{n_s} X_{u,i} \mathrm{d}_\tau^i \mu^\star(\tau) \tag{2.142b}$$

$$m_{\bar{d},n_s}^\star(\tau) = \sum_{i=0}^{n_s} X_{\bar{d},i} \mathrm{d}_\tau^i \mu^\star(\tau) \tag{2.142c}$$

are used as approximations for $m_u^\star(\tau)$, $n^\star(\tau)$ and $m_{\bar{d}}^\star(\tau)$, whereas $n_s = 12$ is determined, so that the relative increment of the last term is less than 10^{-6}, i.e., $\frac{\|\varpi_{n_s} \mathrm{d}_\tau^{n_s} \mu^\star\|_{\mathrm{I},\infty}}{\|n_{n_s}^\star\|_{\mathrm{I},\infty}} < 10^{-6}$ holds for (2.142a) and corresponding expressions for (2.142b) as well as (2.142c). At this, $\|h\|_{\mathrm{I},\infty} = \sup_{\tau \in \mathrm{I}} |h(\tau)|$, $h(\tau) \in \mathbb{R}^\nu$, $\nu \in \mathbb{N}$ is utilized.

The minimization problem (2.128) for the determination of $\bar{m}_f^*$ is solved using the `fminsearch` function from MATLAB, with zero as initial point. Although, this ensures a local minimum only, it leads to suitable results. With the resulting $\bar{m}_f^*$, η can be computed with (2.122) to obtain the required reference trajectory $\mu^\star(\tau)$ from (2.120) for the computation of the integral kernels.

The remaining design parameters are α and T. In order to investigate their influence on the residual generator, the threshold value r_B given in (2.60) and a *normalized detection delay* Δ_f are used. The latter is introduced as a measure for the time from the occurrence of a *normalized fault* $h_f(t)$ to its detection, i.e., Δ_f is quantified by the earliest time where $|\langle m_f, h_f(t) \rangle_{\mathrm{I}}| > r_B$, $t \geq 0$, occurs. For the components of $h_f(\tau)$, the step functions $h_{f,i}(t) = 0$, $t < 0$, $i = 1, \ldots, n_f$, and $h_{f,i}(t) = f_{ex,i}$, $t \geq 0$, are used. Due to (2.121), the integral kernels calculated for different T and α have the same $\bar{m}_f$ (see (2.140)), so their thresholds r_B and normalized detection delays Δ_f can be compared. The result in Figure 2.7 shows that α should be close to the upper bound 2, since this leads to a low threshold as well as a low Δ_f. However, a compromise is required for T. On the one hand, an increase in T leads to a low threshold value r_B, which allows to detect faults of small magnitude and reduces missed detections. On the other hand, an increase in T would increase the fault detection delay Δ_f, which is indicated by Δ_f in Figure 2.7. Choosing $\alpha = 1.999$ and $T = 1.40$, an acceptable threshold $r_B = 0.24$ and a small $\Delta_f = 0.11$ are obtained. The resulting integral kernels $n(\tau)$ and $m_u(\tau)$ required for the residual generator are depicted in Figure 2.8.

At first, the result in Theorem 2.1, i.e., the fault detection for the case $\bar{d}(t) \equiv 0$, is verified by a simulation. The input signal $u(t)$ is a continuous signal taking randomly
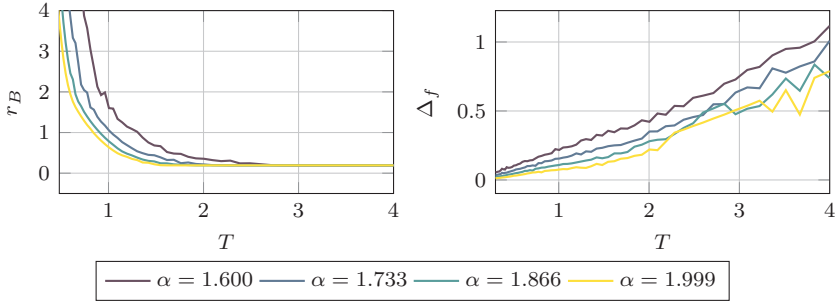
Figure 2.7: Fault detection threshold r_B (see (2.60)) and normalized detection delay Δ_f for different moving horizon lengths T and Gevrey orders α.
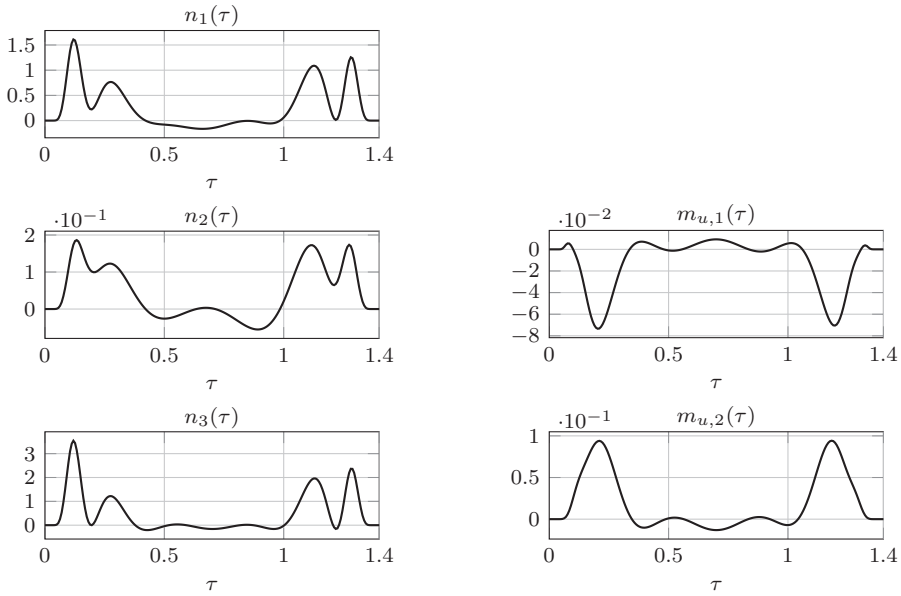
(a) Components $n_i(\tau)$, $i = 1, 2, 3$, of the integral kernel $n(\tau)$.

(b) Components $m_{u,1}(\tau)$ and $m_{u,2}(\tau)$ of the integral kernel $m_u(\tau)$.

Figure 2.8: Integral kernels $n(\tau)$ and $m_u(\tau)$ of the input and output filters of the residual generator (2.50) computed with moving horizon length $T = 1.40$, Gevrey order $\alpha = 1.999$ and $n_\mu = 5$ basis functions for the parametrization of $\mu^\star(\tau)$.
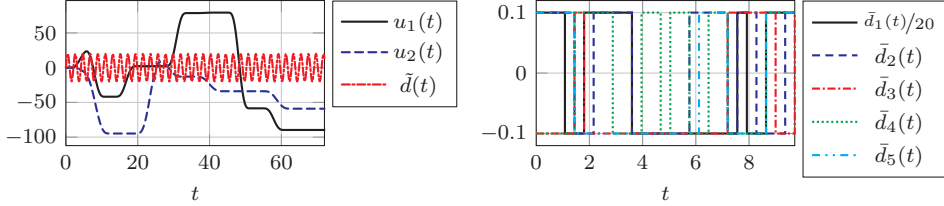
(a) Input $u(t)$ and disturbance $\tilde{d}(t)$ used in the simulation.

(b) Short extract on $0 \leq t \leq 9$ of the bounded disturbance $\bar{d}(t)$ in the simulation.

Figure 2.9: Excitation signals for the simulation of the cantilever beam.
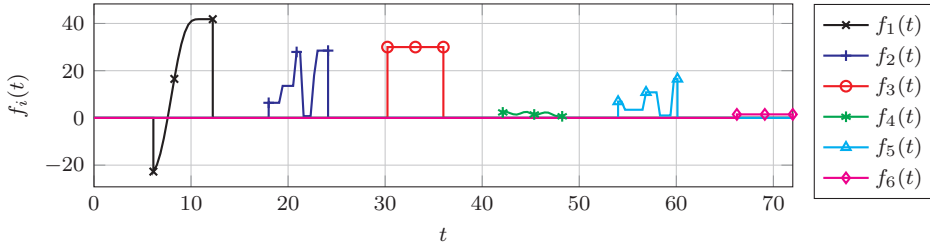
Figure 2.10: Fault scenarios for the fault detection with successively occurring multiplicative actuator fault $\Delta f_i(t)$ leading to the additive fault signal $f_1(t)$, the time-varying additive process fault $f_2(t)$, the constant additive actuator fault $f_3(t)$, the multiplicative sensor fault $\Delta f_4(t)$ leading to the additive fault signal $f_4(t)$, the time-varying additive sensor fault $f_5(t)$ and the constant additive sensor fault $f_6(t)$.

values between ± 100 and the disturbance component $\tilde{d}(t)$ is the solution of the signal model (2.131) with the IC $v_d^0 = \mathrm{col}\,(20, 0)$. Both are depicted in Figure 2.9a. In the simulation, a fault $f_i(t)$, $i = 1, \ldots, 6$, is only present for $t \in \mathrm{I}_f^i = [t_i, t_i + 6]$, where $t_1 = 6$, $t_i = t_{i-1} + 12$, $i = 2, \ldots, 6$. At this, $\Delta f_i(t)$, $t \in \mathrm{I}_f^i$, $i = 1, 4$, and $f_i(t)$, $t \in \mathrm{I}_f^i$, $i = 3, 6$, are constant values, whereas $f_i(t)$, $t \in \mathrm{I}_f^i$, $i = 2, 5$, are signals taking values randomly from a uniform distribution in the intervals $[0, 30]$ respectively $[0, 20]$ yielding the fault signals shown in Figure 2.10.

For the simulation of the faulty beam in MATLAB, a finite-dimensional state-space system of order 56 is derived by the Galerkin approximation of the beam with tip load described in [79]. The simulation of the obtained finite-dimensional model of the beam is performed by the `lsim` function of MATLAB with zero ICs and a sampled time with the step size 5×10^{-3}. The numerical evaluation of the residual generator (2.50) requires a discrete-time approximation of the containing integral expressions. Under the assumption that the input signal $u(t)$ and measurement $y(t)$ are available at equally spaced discrete-time samples, the integral expressions in the residual generator (2.50) can be represented as FIR filters in discrete-time. A detailed discussion about the representation of the integral expressions as FIR filters can be found in [48], where similar expressions are used for the algebraic derivative estimation. Based on the results in [48], the compound midpoint rule (see, e.g., [51]) is used to approximate the integral expressions and to derive the FIR filters. In terms of a quasi-continuous implementation, the step size 5×10^{-3} used in the simulation was also used for the approximation of the integral expressions. Thus, FIR filters of order 281 result, which are evaluated using the MATLAB function `filter` and assuming $u(t) = 0$ and $y(t) = 0$ for $t < 0$. For $0 \leq t < T$, the residual signal in Figure 2.11 has an initialization interval due to the unknown ICs of the beam and the ODE signal model of the disturbance $\tilde{d}(t)$. At the occurrence of a fault $f_i(t)$ at t_i, the residual is excited and indicates the presence of a fault. Because of the particular choice of $\mu^\star(\tau)$, the residual signal is balanced although the faults have different amplitudes and effects on the system. Note that since the residual generator considers the signals on the moving horizon $\mathrm{I}_t = [t - T, t]$, it requires the time $T = 1.40$ after a fault has disappeared until the residual returns to zero.

In a second simulation, the disturbances $\bar{d}_i(t)$, $i = 1, \ldots, 5$, are chosen as the signals shown in Figure 2.9b. The signals are changing their values at random time instants from one bound to the other. It is explicitly chosen so that it has a high influence on the residual signal. The second simulation, performed with the input and disturbance signals shown in Figure 2.9 and the faults shown in Figure 2.10, yields the residual signal in Figure 2.12. After the initialization interval $0 \leq t < T$, the residual signal is bounded by $\pm r_B$ until the occurrence of $f_1(t)$. The occurrence of the fault $f_i(t)$, $i = 1, \ldots, 6$, excites the residual generator, so that the threshold value is exceeded by the residual signal shortly after the occurrence of the fault. However, the detection
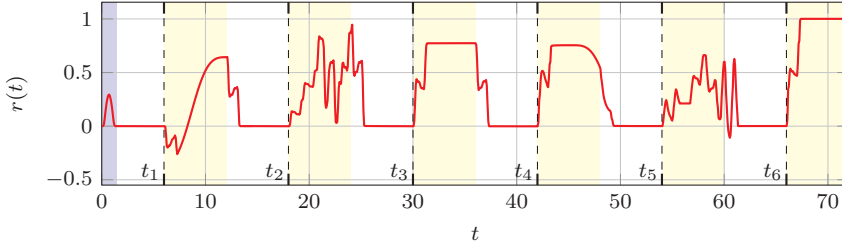
Figure 2.11: Residual signal $r(t)$ (——) for the detection of the faults $f_i(t)$, $i = 1, \ldots, 6$, (▢) from Figure 2.10 with the initialization interval $t < T$ (▨) assuming $\bar{d}(t) \equiv 0$.
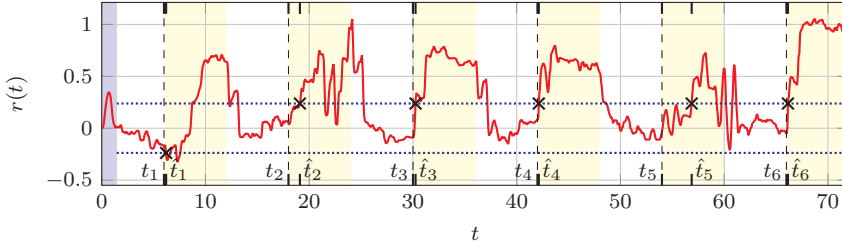
Figure 2.12: Residual signal $r(t)$ (——) and the threshold value $\pm r_B$ (┄┄┄) for the detection of the faults $f_i(t)$, $i = 1, \ldots, 6$, from Figure 2.10, the presence of the faults indicated by (▢), the fault detection (✗) at $\hat{t}_i$ and the initialization interval $t < T$ (▨) in the presence of a disturbance $\bar{d}(t)$.

delay $\hat{\Delta}_i = \hat{t}_i - t_i$ shown in Table 2.2 is dependent on the magnitude and the signal form of the faults. Thus, an increasing fault as, e.g., $f_2(t)$ or a certain signal form as of $f_5(t)$ can lead to a longer detection delay, but the faults $f_i(t)$, $i = 1, 3, 5$, are detected very fast. This demonstrates that the proposed approach for the fault detection is applicable for a complex system setup and a broad class of fault types as well as signals. It allows the detection despite the excitation of the beam by the input, the disturbance $\tilde{d}(t)$ modeled by an ODE as well as the bounded disturbances $\bar{d}_i(t)$, $i = 1, \ldots, 5$.

Table 2.2: Detection delays of the fault detection for the cantilever beam
subject to the bounded disturbance $\bar{d}(t)$.

i	1	2	3	4	5	6
$\hat{\Delta}_i$	0.21	1.10	0.25	0.13	2.87	0.14

2.3.6 Concluding remarks

This section presented the fault detection for a DPS with parabolic or biharmonic
PDE and general ODE-PDE couplings. A residual generator with simple to im-
plement integral expressions is derived. The fault detection is decoupled from
disturbances with known signal form that can be described by the solution of an
ODE. If the system is subject to a disturbance that is only bounded with a known
bound, a threshold was introduced to achieve secured fault detection without false
alarms. The required integral kernels for the residual generator were derived by a
trajectory planning for an ODE-PDE system, which was solved by employing results
from the flatness-based trajectory planning. Based on the differential expressions for
the trajectory planning, a simple to evaluate fault detectability condition is derived,
that can be verified using only system parameters. With the example of a cantilever
beam with a load at the free end, the influence of the remaining degrees of freedom
is shown and the theoretical results are verified by simulations.

2.4 Fault diagnosis

In many applications, not only the detection of faults but their diagnosis, i.e., the
fault detection, isolation and identification, is relevant. To solve this challenging
problem, the fault $f(t)$ is reconstructed by an input-output expression depending
solely on known signals $u(t)$ and $y(t)$. It allows a strong fault detection in sense of
Definition 2 and the fault isolation as well as the fault identification in finite time.
The fault diagnosis can be decoupled from disturbances described by the solution of
a signal model (see (2.15)). However, if also bounded disturbances $\bar{d}(t)$ are present,
then a threshold must be introduced to ensure the fault detection and isolation.
Moreover, the fault can be estimated with bounded estimation error. For the case
$\bar{d}(t) \equiv 0$, an explicit expression is derived for each component $f_i(t)$, $i = 1, \ldots, n_f$,
of $f(t)$ based on the input-output equation (2.48), which is shown in the following
section. Subsequently, the fault diagnosis kernel equations are established in Section
2.4.3, which are solved by a trajectory planning to derive the required integral kernels
for the fault diagnosis. The theoretical results are demonstrated in a simulation for

an Euler-Bernoulli beam in Section 2.4.4.

2.4.1 Problem formulation

Whereas the focus of the residual generator introduced in the previous section is the detection of faults under less restrictive assumptions, the focus of the fault diagnosis approach described in this section is on the identification, respectively estimation of the fault. In order to solve this more challenging task, it is assumed that the fault $f(t)$ is described by a solution of the ODE signal model

$$\dot{v}_f(t) = S_f v_f(t), \qquad\qquad t > 0 \qquad\qquad (2.143\text{a})$$
$$f(t) = R_f v_f(t), \qquad\qquad t \geq 0 \qquad\qquad (2.143\text{b})$$

with the state $v_f(t) \in \mathbb{R}^{n_{vf}}$, the known matrices $S_f \in \mathbb{R}^{n_{vf} \times n_{vf}}$, $R_f \in \mathbb{R}^{n_f \times n_{vf}}$ and unknown ICs $v_f(t_i) = v_f^i \in \mathbb{R}^{n_{vf}}$, $i \in \mathbb{N}^+$, $t_0 = 0$. The matrix S_f is not required to be diagonalizable and it is assumed that the spectrum of S_f satisfies $\sigma(S_f) \subset \mathrm{j}\mathbb{R}$ as well as that the pair (R_f, S_f) is observable (see, e.g., [16, Definition 6.01]). Furthermore, the spectra of S_f and S_d must not be disjoint, i.e., $\sigma(S_f) \cap \sigma(S_d) = \emptyset$ must not hold. The modeling of faults by (2.143) provides a systematic approach for a large signal class, including frequently occurring fault signals described by polynomials and trigonometric functions or combinations thereof. However, this restricts the fault diagnosis to additive faults, since most multiplicative faults cannot be rewritten into the additive form and satisfy (2.143). Nevertheless, (2.143) is a common assumption in the fault diagnosis literature for LPS (see, e.g., [28, Section 14.4]) and covers many relevant fault scenarios.

The occurrence of a fault is modeled by a change of the unknown IC $v_f(t_i) = v_f^i$ at unknown time t_i. This gives rise to piecewise defined signals for $f(t)$, $t \in (t_i, t_{i+1})$, given by piecewise solutions of (2.143) that are uniquely determined by v_f^i. The time intervals between changes of the faults are assumed to be uniformly lower bounded, i.e., $t_{i+1} - t_i > \Delta t > T$ must hold. For an illustration, the modeling of a drifting fault is described in the following example.

Example 2.3 *(ODE signal model for a drifting fault).*
Consider a drifting fault described by the piecewise function

$$f(t) = \begin{cases} 0 & : 0 \leq t < t_1 \\ a_0 + a_1 t & : t \geq t_1, \end{cases} \qquad\qquad (2.144)$$

which occurs at $t_1 > \Delta t$ and is specified by the coefficients $a_0, a_1 \in \mathbb{R}$. The

corresponding signal model reads as

$$S_f = \begin{bmatrix} 0 & 1 \\ 0 & 0 \end{bmatrix} \qquad \text{and} \qquad R_f = \begin{bmatrix} 1 & 0 \end{bmatrix}, \tag{2.145a}$$

from which $f(t) = \begin{bmatrix} 1 & t - t_i \end{bmatrix} v_f^i$ follows. To model (2.144), the ICs are $v_f^0 = 0$ at $t_0 = 0$ and $v_f^1 = \mathrm{col}\,(a_0 + a_1 t_1, a_1)$. $\qquad\qquad\qquad\qquad\qquad\qquad\qquad\qquad \triangleleft$

The following fault diagnosis problems are solved for (2.1), (2.15), $\bar{d}(t) \equiv 0$ and (2.143):

1. *fault detection:* detection of the occurrence of a fault $f(t)$,

2. *fault isolation:* independent detection of each fault $f_i(t)$, $i = 1, \ldots, n_f$, and

3. *fault identification:* determination of $f(t)$.

If a disturbance $\bar{d}(t) \not\equiv 0$ is present, a threshold is introduced to achieve the fault detection and isolation. Since fault identification is not possible any more in this case, *fault estimation*, i.e, the estimation of the fault $f(t)$ with bounded estimation error is investigated.

2.4.2 Fault diagnosis equation

The derivation of the input-output expression, on which the fault diagnosis is based on, is similar to the derivation of the input-output equation (2.48) used for the residual generator in Section 2.3.2. In contrast to the pure fault detection discussed in Section 2.3, the fault isolation and identification require an input-output expression for each fault $f_i(t)$, $i = 1, \ldots, n_f$. These are established by the application of the transformations (2.18) using n_f different kernels $m_i(z, \tau) \in \mathbb{R}^{n_x}$, $q_i(\tau) \in \mathbb{R}^{n_w}$ and $n_i(\tau) \in \mathbb{R}^{n_y}$, $i = 1, \ldots, n_f$. According to the derivation for (2.48), n_f input-output expressions are established by the substitutions $m(z, \tau) \to m_i(z, \tau)$, $p(\tau) \to p_i(\tau) \in \mathbb{R}^{n_x}$, $q_w(\tau) \to q_{w,i}(\tau) \in \mathbb{R}^{n_w}$, $q_d(\tau) \to q_{d,i}(\tau) \in \mathbb{R}^{n_{vd}}$ and $n(\tau) \to n_i(\tau)$, $i = 1, \ldots, n_f$, which requires that $m_i(z, \tau)$, $q_i(\tau) = \mathrm{col}\,(q_{w,i}(\tau), q_{d,i}(\tau))$ and $n_i(\tau)$ satisfy (2.72) and (2.73). The resulting input-output expressions become

$$\langle m_{f,i}, f(t) \rangle_{\mathrm{I}} = \langle n_i, y(t) \rangle_{\mathrm{I}} + \langle m_{u,i}, u(t) \rangle_{\mathrm{I}} + \langle m_{\bar{d},i}, \bar{d}(t) \rangle_{\mathrm{I}}, \quad t \geq T \tag{2.146}$$

for $i = 1, \ldots, n_f$, where the substitutions $m_f(\tau) \to m_{f,i}(\tau) \in \mathbb{R}^{n_f}$, $m_u(\tau) \to m_{u,i}(\tau) \in \mathbb{R}^{n_u}$, $m_{\bar{d}}(\tau) \to m_{\bar{d},i}(\tau) \in \mathbb{R}^{n_{\bar{d}}}$ are used in view of (2.92).

2.4.2.1 Fault identification

At first, the fault identification problem is solved for the case $\bar{d}(t) \equiv 0$. Under latter assumption an identification equation for each fault $f_i(t)$, $i = 1, \ldots, n_f$, can be derived from (2.146). By inserting (2.143) in (2.146) and assuming $\bar{d}(t) \equiv 0$,

$$\langle R_f^\top m_{f,i}, v_f(t) \rangle_I = \langle n_i, y(t) \rangle_I + \langle m_{u,i}, u(t) \rangle_I \tag{2.147}$$

is obtained. In order to derive an expression for the fault $f_i(t)$ from (2.147), a transformation for the signal model of the fault (2.143)

$$\mathcal{Q}_{f,i}[v_f](t) = \langle q_{f,i}, v_f(t) \rangle_I, \tag{2.148}$$

with the integral kernel $q_{f,i}(\tau) \in \mathbb{R}^{n_{vf}}$ is introduced. The application of (2.148) to (2.143a) leads to

$$\langle q_{f,i}, \dot{v}_f(t) \rangle_I = \langle q_{f,i}, S_f v_f(t) \rangle_I. \tag{2.149}$$

Let the fault $f(t)$ occur at t_j, $j \in \mathbb{N}_0$, i.e., the fault signal $f(t)$, $t \in (t_j, t_{j+1})$, is a solution of (2.143) on $t \in (t_j, t_{j+1})$ uniquely determined by the unknown IC $v_f(t_i) = v_f^j \in \mathbb{R}^{n_{vf}}$. Thus, for $t \in I_j = [t_j + T, t_{j+1})$, the substitution $\dot{v}_f(t - \tau)$ by $-\partial_\tau v_f(t - \tau)$ and application of integration by parts to (2.149) results in

$$\langle \dot{q}_{f,i} - S_f^\top q_{f,i}, v_f(t) \rangle_I = q_{f,i}^\top(T) v_f(t - T) - q_{f,i}^\top(0) v_f(t), \quad t \in I_j. \tag{2.150}$$

Given (2.143b), (2.150) can be solved for $f_i(t) = e_{i,n_f}^\top R_f v_f(t)$ using

$$q_{f,i}^\top(0) = -e_{i,n_f}^\top R_f \quad \text{and} \quad q_{f,i}^\top(T) = 0. \tag{2.151}$$

With (2.151) and (2.143b) in (2.150)

$$f(t) = \langle \dot{q}_{f,i} - S_f^\top q_{f,i}, v_f(t) \rangle_I, \quad t \in I_j \tag{2.152}$$

is obtained. Imposing

$$\dot{q}_{f,i}(\tau) - S_f^\top q_{f,i}(\tau) = R_f^\top m_{f,i}(\tau), \quad \tau \in I \tag{2.153}$$

allows to insert (2.152) in (2.147). This leads to

$$f_i(t) = \langle n_i, y(t) \rangle_I + \langle m_{u,i}, u(t) \rangle_I, \quad t \in I_j. \tag{2.154}$$

Since (2.154) depends only on $u(t)$ and $y(t)$, the fault $f_i(t)$ can be determined by an input-output expression depending only on known signals. The identification

equation (2.154) can be summarized for $i = 1, \ldots, n_f$, to

$$f(t) = \langle N, y(t) \rangle_I + \langle M_u, u(t) \rangle_I, \quad t \in I_j \tag{2.155}$$

by introducing

$$N(\tau) = [\, n_1(\tau) \;\; \cdots \;\; n_{n_f}(\tau) \,] \in \mathbb{R}^{n_y \times n_f} \tag{2.156a}$$

$$M_u(\tau) = [\, m_{u,1}(\tau) \;\; \cdots \;\; m_{u,n_f}(\tau) \,] \in \mathbb{R}^{n_u \times n_f}. \tag{2.156b}$$

Since the fault identification equation (2.155) only holds on $t \in I_j = [t_j + T, t_{j+1})$, but t_j is not known, the *fault diagnosis residual generator* candidate

$$\hat{f}(t) = \langle N, y(t) \rangle_I + \langle M_u, u(t) \rangle_I, \quad t \geq T \tag{2.157}$$

for the *fault diagnosis residual signal* $\hat{f}(t) \in \mathbb{R}^{n_f}$ is introduced. For $f(t) \equiv 0$, $\hat{f}(t) \equiv 0$ holds on $t \geq T$ and $\hat{f}(t) = f(t)$, $t \in I_j$, implies $\hat{f}(t) \not\equiv 0$ on $t \geq T$ for $f(t) \not\equiv 0$. This holds for $\tilde{d}(t)$ given by (2.15), any IC of the system and any input $u(t)$. Thus, (2.157) is a residual generator and $\hat{f}(t)$ is a residual signal. To be precise, $\hat{f}(t) = f(t)$, $t \in I_j$, implies strong fault detectability in sense of Definition 2. However, $\hat{f}(t) = f(t)$, $t \in I_j$, implies also that the fault $f(t)$ can be identified by this residual signal. Thus, (2.157) is not only a residual generator but also suitable for the fault identification. To represent this fact in contrast to the residual signal $r(t)$ (see (2.50)), which allows exclusively a detection of the fault, the new symbol $\hat{f}(t)$ is introduced. This fault identification result is summarized in the following theorem.

> **Theorem 2.5 (Fault identification)**
> Let $\bar{d} \equiv 0$ hold, $\tilde{d}(t)$ be described by a solution of the signal model (2.15) and $f(t)$ be described by a piecewise defined solution of the signal model (2.143). Let the integral kernels $m_i(z, \tau)$, $q_i(\tau)$, $n_i(\tau)$ and $q_{f,i}(\tau)$, $i = 1, \ldots, n_f$, satisfy the kernel equations (2.72), (2.73), (2.151) and (2.153). Then, the fault $f(t)$ occurring at t_j, $j \in \mathbb{N}_0$, is identified by $\hat{f}(t)$ given in (2.157) for $t \in I_j = [t_j + T, t_{j+1})$.

The proof of Theorem 2.5 follows from the derivation of (2.157) and that $\hat{f}(t) = f(t)$ holds for $t \in I_j$, $j \in \mathbb{N}_0$.

Note that the fault occurring at t_j, $j \in \mathbb{N}_0$ is identified at $t = t_j + T$ in finite time. Moreover, the identified fault signals already allow the fault isolation.

2.4.2.2 Fault detection, isolation and estimation

In the presence of an unknown but bounded disturbance $\bar{d}(t) \not\equiv 0$, a threshold is introduced to ensure the fault detection and fault isolation as well as to derive an upper bound for the fault estimation error. Following the previously described approach to obtain (2.154) while additionally taking $\bar{d}(t)$ into account, yields

$$f_i(t) = \langle n_i, y(t) \rangle_{\mathrm{I}} + \langle m_{u,i}, u(t) \rangle_{\mathrm{I}} + \langle m_{\bar{d},i}, \bar{d}(t) \rangle_{\mathrm{I}}, \quad t \in \mathrm{I}_j. \tag{2.158}$$

This can be separated into the known part

$$\tilde{f}_i(t) = \langle n_i, y(t) \rangle_{\mathrm{I}} + \langle m_{u,i}, u(t) \rangle_{\mathrm{I}}, \quad t \in \mathrm{I}_j \tag{2.159}$$

and the unknown part

$$\bar{f}_i(t) = \langle m_{\bar{d},i}, \bar{d}(t) \rangle_{\mathrm{I}}. \tag{2.160}$$

Thus, the absolute value of the estimation error for each fault $f_i(t)$ caused by $\bar{d}(t)$ is given by

$$|f_i(t) - \tilde{f}_i(t)| = |\bar{f}_i(t)|, \quad i = 1, \ldots, n_f, \quad t \in \mathrm{I}_j \tag{2.161}$$

and

$$\bar{f}_i(t) = \langle m_{\bar{d},i}, \bar{d}(t) \rangle_{\mathrm{I}}. \tag{2.162}$$

Similar to the derivation of the threshold $r_{B,i}$ (see (2.57)–(2.61)), an upper bound

$$f_{B,i} = \int_0^T |m_{\bar{d},i}(\tau)|^\top \mathrm{d}\tau \delta, \quad i = 1, \ldots, n_f, \tag{2.163}$$

satisfying

$$|\bar{f}_i(t)| \leq f_{B,i} \tag{2.164}$$

results as the upper bound for the fault estimation error. In order to achieve fault diagnosis without knowing the fault occurrence time t_j, the fault diagnosis residual (2.157) is used. In view of (2.161) and (2.164) the components $\hat{f}_i(t)$ of the fault diagnosis residual $\hat{f}(t)$ are bounded by $|\hat{f}_i(t)| \leq f_{B,i}$ for $f(t) \equiv 0$, $t \geq T$, $i = 1, \ldots, n_f$. As a conclusion, $|\hat{f}_i(t)| > f_{B,i}$ for $t \geq T$ necessarily indicates the presence of a fault. This is summarized in the following theorem.

Theorem 2.6 (Strong fault detection)
Let the integral kernels $m_i(z, \tau)$, $q_i(\tau)$, $n_i(\tau)$ and $q_{f,i}(\tau)$, $i = 1, \ldots, n_f$, satisfy
(2.72), (2.73), (2.151) and (2.153). Assume that $\tilde{d}(t)$ is described by a solution
of the signal model (2.15) and $\bar{d}(t)$ is bounded according to (2.14). Then, a
fault $f(t)$ is detected for the system (2.1) if a threshold $f_{B,i}$, $i = 1, \ldots, n_f$,
given in (2.163) is exceeded by some component $\hat{f}_i(t)$ of $\hat{f}(t)$ in (2.157), i.e.,

$$\exists i \in \{1, \ldots, n_f\} \text{ so that } |\hat{f}_i(t)| > f_{B,i}, \quad t \geq T. \qquad (2.165)$$

For a fault that occurs at t_j, $\hat{f}_i(t) = \tilde{f}_i(t)$ holds for $t \in \mathrm{I}_j$, thus the strong fault
detection in sense of Definition 2 is achieved. The fault detection time $\hat{t}_j$, $j \in \mathbb{N}_0$, is
the first time instance a threshold value $f_{B,i}$ is exceeded by $\hat{f}_i(t)$ (see (2.165)).

After the transient interval, i.e., $t \geq t_j + T$, only the residual signal $\hat{f}_i(t)$ corresponding
to the present fault $f_i(t)$, but no other residual signal $\hat{f}_k(t)$, $k \neq i$ exceeds its threshold
value $f_{B,k}$, i.e., $|\hat{f}_k(t)| \leq f_{B,k}$, $k \neq i$, on $t \in \mathrm{I}_j = [t_j + T, t_{j+1})$. Thus, the exceeding
of the corresponding threshold $|\hat{f}_i(t)| > f_{B,i}$ for $t \in \mathrm{I}_j$, indicates that the ith fault is
present, i.e., fault isolation is achieved. However, since only $\hat{t}_j > t_j$ is known, the
fault can be isolated for $t \geq \hat{t}_j + T$, which is the result of the next theorem.

Theorem 2.7 (Fault isolation)
Let the integral kernels $m_i(z, \tau)$, $q_i(\tau)$, $n_i(\tau)$ and $q_{f,i}(\tau)$, $i = 1, \ldots, n_f$, satisfy
(2.72), (2.73), (2.151) and (2.153). Assume that $\tilde{d}(t)$ is described by a solution
of the signal model (2.15), $\bar{d}(t)$ is bounded according to (2.14) and $f(t)$ is
piecewise described by solutions of the signal model (2.143). Then, the fault
$f_i(t)$, $i \in \{1, \ldots, n_f\}$, occurring at t_j, $j \in \mathbb{N}_0$, is detected for the system (2.1)
if the threshold $f_{B,i}$ given in (2.163) is exceeded by the ith component $\hat{f}_i(t)$
of $\hat{f}(t)$ in (2.157) for $t \geq \hat{t}_j + T$, i.e.,

$$|\hat{f}_i(t)| > f_{B,i}, \quad t \geq \hat{t}_j + T. \qquad (2.166)$$

Moreover, for $t \in \mathrm{I}_j$, $\hat{f}_i(t) = \tilde{f}_i(t)$ holds. Thus it follows from (2.161), that a fault
$f_i(t)$ is bounded by

$$\hat{f}_i(t) - f_{B,i} \leq f_i(t) \leq \hat{f}_i(t) + f_{B,i}, \quad t \in \mathrm{I}_j. \qquad (2.167)$$

Consequently, the isolated faults can be estimated, which is the result of the next
theorem.

Theorem 2.8 (Fault estimation)
Let the integral kernels $m_i(z, \tau)$, $q_i(\tau)$, $n_i(\tau)$ and $q_{f,i}(\tau)$, $i = 1, \ldots, n_f$, satisfy (2.72), (2.73), (2.151) and (2.153). Assume that $\tilde{d}(t)$ is described by a solution of the signal model (2.15), $\bar{d}(t)$ is bounded according to (2.14) and $f(t)$ is piecewise described by solutions of the signal model (2.143). Then, for the system (2.1) the estimate $\hat{f}_i(t)$ of a fault $f_i(t)$, $i = 1, \ldots, n_f$, occurring at t_j, $j \in \mathbb{N}_0$, is bounded by

$$f_i(t) - f_{B,i} \leq \hat{f}_i(t) \leq f_i(t) + f_{B,i}, \quad t \in [\hat{t}_j + T, t_{j+1}) \tag{2.168}$$

with $\hat{f}_i(t)$ as ith component of $\hat{f}(t)$ obtained from the residual generator (2.157) and $f_{B,i}$ given by (2.163).

The proofs of the Theorems 2.6, 2.7 and 2.8 follow from (2.161) and the estimate (2.164), since $\hat{f}(t) = \tilde{f}(t)$ holds for $t \in \mathrm{I}_j$.

2.4.3 Solution of the fault diagnosis kernel equations

In order to use the residual generator (2.157) for the fault diagnosis, the integral kernels $m_i(z, \tau)$, $q_i(\tau)$ and $n_i(\tau)$, $i = 1, \ldots, n_f$, must satisfy (2.72) and (2.73) as well as $q_{f,i}(\tau)$ must satisfy (2.151) and (2.153). In the following the design of these kernels is traced back to the trajectory planning problem for the ODE-PDE system given by (2.72) and (2.153) with the initial and end points given by (2.73) and (2.151), which can be solved using results from the flatness-based trajectory planning.

In contrast to the fault detection kernel equations, the newly introduced transformation (2.148) leads to an additional ODE subsystem with nonhomogeneous ICs (see (2.151)). Since the latter generally do not correspond to setpoints, it can no longer be traced back to a setpoint change. Thus, the solution of the kernel equations becomes more challenging.

2.4.3.1 Fault identification kernel equations

Use the substitutions $m(z, \tau) \to m_i(z, \tau)$, $q(\tau) \to q_i(\tau)$ and $n(\tau) \to n_i(\tau)$ in (2.72) respectively (2.73), then the n_f *fault diagnosis kernel equations* are obtained, which are summarized in the following lemma.

Lemma 2.5 (Fault diagnosis kernel equations)**.** Let $\tilde{d}(t)$ be described by (2.15), the fault $f(t)$ be described by (2.143) and the integral kernels $m_i(z, \tau)$, $q_i(\tau)$, $q_{f,i}(\tau)$ and $n_i(\tau)$ be a solution of the *fault diagnosis kernel equations*, which are given by the PDE

$$\partial_z m_i(z, \tau) = -\mathcal{A}^*[m_i(z)](\tau) + \bar{L}_1(z)q_i(\tau) + C_1^\top(z)n_i(\tau) \qquad (2.169a)$$

defined on $(z, \tau) \in (0, 1) \times (0, T)$, the BCs

$$\bar{K}_0 m_i(0, \tau) + \bar{K}_1 m_i(1, \tau) + \bar{L}_2 q_i(\tau) = \bar{C}_2 n_i(\tau), \quad \tau \in (0, T), \qquad (2.169b)$$

the ODEs

$$\dot{q}_i(\tau) = F_e q_i(\tau) + \int_0^1 \bar{H}_1(z)m_i(z, \tau)\mathrm{d}z + \bar{H}_2 m_i(0, \tau) + \bar{H}_3 m_i(1, \tau)$$

$$+ \bar{C}_3 n(\tau) \qquad\qquad\qquad\qquad \tau \in (0, T) \quad (2.169c)$$

$$\dot{q}_{f,i}(\tau) = S_f^\top q_{f,i}(\tau) + R_f^\top m_{f,i}(\tau), \qquad\qquad\qquad \tau \in (0, T) \quad (2.169d)$$

and the initial-end conditions

$$\partial_\tau^j m_i(z, \tau)|_{\tau=0} = 0, \qquad\qquad \partial_\tau^j m_i(z, \tau)|_{\tau=T} = 0 \qquad (2.170a)$$

$$q_i(0) = 0, \qquad\qquad\qquad\qquad q_i(T) = 0 \qquad (2.170b)$$

$$q_{f,i}(0) = -R_f^\top e_{i,n_f}, \qquad\qquad\qquad q_{f,i}(T) = 0 \qquad (2.170c)$$

for $i = 1, \ldots, n_f$, where (2.170a) is defined on $z \in [0, 1]$ for $j = 0, \ldots, n_A - 1$. Then, the fault diagnosis residual generator (2.157) holds.

Each system (2.169) is a cascade of an ODE-PDE subsystem and an ODE subsystem, as depicted in Figure 2.13, which are subject to the initial and end conditions (2.170). Note that the n_f kernel equations that must be solved for the fault diagnosis differ only in the distinct ICs given in (2.170c). Moreover, each system (2.169) has the input $n_i(\tau)$ as a degree of freedom. Similar to the fault detection kernel equations in Lemma 2.1, the fault diagnosis kernel equations described in Lemma 2.5 are a two-point initial-boundary-value problem that can be solved by the determination of an input $n_i(\tau)$ that realizes the specified transition for $m_i(z, \tau)$, $q_i(\tau)$ and $q_{f,i}(\tau)$. In contrast to the fault detection kernel equations, no additional algebraic constraint must be considered, but the IC (2.170c) for the ODE (2.169d) is in general not a setpoint. In particular for sinusoidal faults, the IC corresponds to a nonequilibrium point, as shown in the following example.
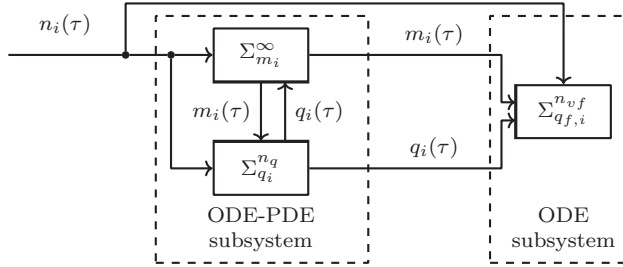
Figure 2.13: Structure of the fault diagnosis kernel equations, composed of the ODE-PDE subsystem including the PDE $(\Sigma_{m_i}^{\infty})$ described by (2.169a), (2.169b) and the ODE $(\Sigma_{q_i}^{n_q})$ described by (2.169c) as well as the ODE subsystem $(\Sigma_{q_{f,i}}^{n_{vf}})$ described by (2.169d).

Example 2.4 *(Nonequilibrium ICs of the kernel equations ODE).*
Assume a sinusoidal fault, i.e., $f(t) = f_1^0 \sin(3t + \phi_f)$, with unknown parameters $f_1^0 \in \mathbb{R}$ and $\phi_f \in \mathbb{R}$. This signal form can be described a signal model (2.143) with

$$S_f = \begin{bmatrix} 0 & -3 \\ 3 & 0 \end{bmatrix} \qquad \text{and} \qquad R_f = \begin{bmatrix} 0 & 1 \end{bmatrix}, \tag{2.171}$$

and the unknown IC $v_f^0 \in \mathbb{R}^2$. Because S_f has full rank, the evaluation of the setpoint requirement $\dot{q}_{f,i}(\tau)|_{\tau=\tau_0} = 0$ yields solely the homogeneous setpoint $q_{f,i}^s = 0$ for (2.170c) with $m_{f,i}(\tau_0) = 0$. Thus, the IC $q_{f,i}(0) = -\mathrm{col}\,(0, 1)$ is not a setpoint of (2.170c). ◁

Consequently, the solution of the fault diagnosis kernel equations cannot be traced back to a setpoint change for the ODE-PDE system (2.169), which requires the solution of a more sophisticated feedforward control problem. In the sense of the flatness-based trajectory planning, similar to Section 2.3.4, a differential expression in terms of a parametrizing variable for the kernel equations system (2.169) is determined in the following section. Based on this parametrization a solution for the fault diagnosis kernel equations can be computed by a reformulation of the transition problem into an interpolation problem for the parametrizing variable. Note that also for this transition problem it is not necessary to verify that the parametrizing variable is indeed a flat output, since it is sufficient if the specific transition from the ICs to the end values specified in (2.170) can be parametrized. Whether this parametrization is possible is checked in Section 2.4.3.3.

2.4.3.2 Determination of the differential expression for the ODE-PDE-ODE cascade system

Since the ODE-PDE subsystem for each integral kernel $m_i(z,\tau)$ and $q_i(\tau)$ of the kernel equations (2.169a)–(2.169c) is equal to the kernel equation of the fault detection problem (2.72), the differential expressions (2.91) can be used. Introducing the substitution $\mu(\tau) \to \mu_i(\tau)$, the differential expressions for the ODE-PDE subsystem read as

$$m_i(z,\tau) = \sum_{j=0}^{\infty} V_j(z) \mathrm{d}_\tau^j \mu_i(\tau) \tag{2.172a}$$

$$q_i(\tau) = \sum_{j=0}^{\infty} U_j \mathrm{d}_\tau^j \mu_i(\tau) \tag{2.172b}$$

$$n_i(\tau) = \sum_{j=0}^{\infty} \varpi_j \mathrm{d}_\tau^j \mu_i(\tau) \tag{2.172c}$$

with $i = 1, \ldots, n_f$. Thus, it remains to determine a differential expression for $q_{f,i}(\tau)$ and a common parametrizing variable. For this, the formal Laplace transform $q_{f,i}(\tau) \circ\!\!-\!\!\bullet \check{q}_{f,i}(s)$ and $\dot{q}_{f,i}(\tau) \circ\!\!-\!\!\bullet s\check{q}_{f,i}(s)$ is used. Note that the latter transform must be regarded formally since the nonhomogeneous ICs $q_{f,i}(0) = -R_f^\top e_{i,n_f}$ (see (2.170c)) are not considered explicitly in the following derivation of the differential expressions. However, this simplification is justified by a time reversal shown in the Appendix A.2. As a result of the formal Laplace transform of (2.169d),

$$\left(sI - S_f^\top\right) \check{q}_{f,i}(s) = R_f^\top \check{m}_{f,i}(s) \tag{2.173}$$

follows. In order to express (2.173) in terms of $\check{\mu}_i(s)$, apply the substitution $\mu(\tau) \to \mu_i(\tau)$ as well as $m_f(z,\tau) \to m_{f,i}(z,\tau)$ and a formal Laplace transform in (2.93a) to obtain

$$\check{m}_{f,i}(s) = \check{X}(s)\check{\mu}_i(s) \tag{2.174}$$

where $\check{X}(s) = \sum_{j=0}^{\infty} X_j s^j$. With (2.174) in (2.173), the latter is expressed in terms of $\check{\mu}_i(s)$, which reads as

$$\left(sI - S_f^\top\right) \check{q}_{f,i}(s) = R_f^\top \check{X}(s)\check{\mu}_i(s). \tag{2.175}$$

By introducing the common parametrizing variable $\check{\varphi}_i(s) \in \mathbb{C}^{n_y}$, $i = 1, \ldots, n_f$, with

$$\check{\mu}_i(s) = \det\left(sI - S_f^\top\right) \check{\varphi}_i(s), \tag{2.176}$$

(2.175) can be solved for

$$\check{q}_{f,i}(s) = \mathrm{adj}\left(sI - S_f^\top\right) R_f^\top \check{X}(s)\check{\varphi}_i(s), \tag{2.177}$$

when using $\mathrm{adj}(sI - S_f^\top)(sI - S_f^\top) = I \det(sI - S_f^\top)$. In order to derive a simple time correspondence for $\check{q}_{f,i}(s)$, utilize

$$\mathrm{adj}\left(sI - S_f^\top\right) = \sum_{j=0}^{n_{vf}-1} S_j s^j \tag{2.178}$$

with $S_j \in \mathbb{R}^{n_{vf} \times n_{vf}}$ and the Cauchy product to rewrite the operator (2.177) as the formal power series

$$\mathrm{adj}\left(sI - S_f^\top\right) R_f^\top \check{X}(s) = \sum_{j=0}^\infty W_j s^j \tag{2.179}$$

with $W_j \in \mathbb{R}^{n_{vf} \times n_y}$, $j \in \mathbb{N}_0$. Then, insert (2.179) in (2.177) to obtain

$$\check{q}_{f,i}(s) = \sum_{j=0}^\infty W_j s^j \check{\varphi}_i(s), \quad i = 1, \ldots, n_f. \tag{2.180}$$

To parametrize $\check{\mu}_i(s)$ with the new parametrizing variable $\check{\varphi}_i(s)$, use

$$\det\left(sI - S_f^\top\right) = \sum_{j=0}^{n_{vf}} a_j s^j \tag{2.181}$$

where $a_j \in \mathbb{R}$ and $a_{n_{vf}} = 1$. Hence, (2.176) reads as

$$\check{\mu}_i(s) = \sum_{j=0}^{n_{vf}} a_j s^j \check{\varphi}_i(s), \quad i = 1, \ldots, n_f. \tag{2.182}$$

Also the integral kernels $\check{m}_i(z,s)$, $\check{q}_i(s)$ and $\check{n}_i(s)$ can be expressed in terms of $\varphi(\tau)$, by inserting (2.182) in (2.172), which yields

$$\check{m}_i(z,s) = \sum_{j=0}^\infty \bar{V}_j(z)s^j \check{\varphi}_i(s) \tag{2.183a}$$

$$\check{q}_i(s) = \sum_{j=0}^\infty \bar{U}_j s^j \check{\varphi}_i(s) \tag{2.183b}$$

$$\check{n}_i(s) = \sum_{j=0}^{\infty} \bar{\varpi}_j s^j \check{\varphi}_i(s) \tag{2.183c}$$

where the coefficients $\bar{V}_i(z) \in \mathbb{R}^{n_f \times n_y}$, $\bar{U}_i \in \mathbb{R}^{n_{ve} \times n_y}$ and $\bar{\varpi}_i \in \mathbb{R}$ can be computed with the Cauchy product. Using the formal correspondence $s^j \check{\varphi}_i(s) \bullet\!\!-\!\!\circ \mathrm{d}_\tau^j \varphi_i(\tau)$ in (2.180) and (2.183), the differential expressions for the system variables of the fault diagnosis kernel equations are obtained, which are summarized in the following lemma.

Lemma 2.6 (Formal differential expressions for the fault diagnosis integral kernels). Let W_j, $\bar{V}_j(z)$, $\bar{U}_j$ and $\bar{\varpi}_j$, $j \in \mathbb{N}_0$, be given by the formal power series (2.180) and (2.183). Then, the system variables $q_{f,i}(\tau)$, $m_i(z, \tau)$, $q_i(\tau)$ and $n_i(\tau)$ can be parametrized by the formal differential expressions

$$q_{f,i}(\tau) = \sum_{j=0}^{\infty} W_j \mathrm{d}_\tau^j \varphi_i(\tau) \tag{2.184a}$$

$$m_i(z, \tau) = \sum_{j=0}^{\infty} \bar{V}_j(z) \mathrm{d}_\tau^j \varphi_i(\tau) \tag{2.184b}$$

$$q_i(\tau) = \sum_{j=0}^{\infty} \bar{U}_j \mathrm{d}_\tau^j \varphi_i(\tau) \tag{2.184c}$$

$$n_i(\tau) = \sum_{j=0}^{\infty} \bar{\varpi}_j \mathrm{d}_\tau^j \varphi_i(\tau) \tag{2.184d}$$

in terms of the parametrizing variable $\varphi_i(\tau)$ and its derivatives.

Note that for the design of the residual generator and the computation of the threshold, also the integral kernels $m_{u,i}(\tau)$, $m_{f,i}(\tau)$ and $m_{\bar{d},i}(\tau)$ are required. These can be computed by inserting the time domain correspondence of (2.182)

$$\mu_i(\tau) = \sum_{j=0}^{n_{vf}} a_j \mathrm{d}_\tau^j \varphi_i(\tau), \tag{2.185}$$

in (2.93) after the substitution $\mu(\tau) \to \mu_i(\tau)$, $m_u(\tau) \to m_{u,i}(\tau)$, $m_f(\tau) \to m_{f,i}(\tau)$

and $m_{\bar{d}}(\tau) \to m_{\bar{d},i}(\tau)$ to obtain

$$m_{u,i}(\tau) = \sum_{j=0}^{\infty} \bar{X}_{u,j} \mathrm{d}_\tau^j \varphi_i(\tau) \tag{2.186a}$$

$$m_{f,i}(\tau) = \sum_{j=0}^{\infty} \bar{X}_{f,j} \mathrm{d}_\tau^j \varphi_i(\tau) \tag{2.186b}$$

$$m_{\bar{d},i}(\tau) = \sum_{j=0}^{\infty} \bar{X}_{\bar{d},j} \mathrm{d}_\tau^j \varphi_i(\tau) \tag{2.186c}$$

with $\bar{X}_{u,j} \in \mathbb{R}^{n_u \times n_y}$, $\bar{X}_{f,j} \in \mathbb{R}^{n_f \times n_y}$ and $\bar{X}_{\bar{d},j} \in \mathbb{R}^{n_{\bar{d}} \times n_y}$.

2.4.3.3 Reference trajectory planning

With the differential expressions (2.184) the system variables $m_i(z,\tau)$, $q_i(\tau)$, $q_{f,i}(\tau)$ and $n_i(\tau)$ of the kernel equations (2.169) can be parameterized by $\varphi_i(\tau)$ and its derivatives. Thus, the fault diagnosis kernel equations (2.169) subject to (2.170) can be solved by the planning of a suitable reference trajectory $\varphi_i^\star(\tau) \in \mathbb{R}^{n_y}$ assigned to $\varphi_i(\tau)$. In contrast to the planning of a reference trajectory for the fault detection case, the planning of the reference trajectory is more involved because of the nonvanishing IC (2.170c). However, exploiting the cascade structure of (2.169) (see Figure 2.13), the ODE-PDE subsystem (2.169a)–(2.169c) and the ODE subsystem (2.169d) can be taken into account sequentially. To be specific, trajectory planning for the ODE-PDE subsystem (2.169a)–(2.169c) can be embedded into a setpoint change by imposing the additional requirement

$$\partial_\tau^{n_A} m_i(z,\tau)|_{\tau \in \{0,T\}} = 0, z \in [0,1] \tag{2.187a}$$

$$\mathrm{d}_\tau q_i(\tau)|_{\tau \in \{0,T\}} = 0. \tag{2.187b}$$

Thus, the solution for this subsystem can be traced backed to a simple algebraic interpolation problem for the reference trajectory $\mu_i^\star(\tau)$ assigned to $\mu_i(\tau)$. Taking the resulting requirements on $\mu_i^\star(\tau)$ into account, the planning of the reference trajectory $\varphi_i^\star(\tau)$ can be traced back to the solution of a feedforward control problem of an ODE with additional constraints.

In a first step, the ODE-PDE subsystem (2.169a)–(2.169c) subject to (2.170a)–(2.170b) and (2.187) is regarded. The differential expressions for this subsystem are given by (2.172), in terms of the parametrizing variable $\mu_i(\tau)$. For each $i = 1, \ldots, n_f$, it is equal to (2.72) subject to (2.73) and (2.74). Hence, the results from Section 2.3.4.3 apply to derive requirements on a reference trajectory $\mu_i^\star(\tau)$ assigned to $\mu_i(\tau)$,

where the usual substitutions $\mu(\tau) \to \mu_i(\tau)$, $m(z,\tau) \to m_i(z,\tau)$, $q(\tau) \to q_i(\tau)$ and $n(\tau) \to n_i(\tau)$ are used. To be specific, if $\mu_i^\star \in (\mathbb{G}^\alpha(\mathrm{I}))^{n_y}$, $1 < \alpha < {}^1/_\varrho$ holds with ϱ as order of the formal power series (2.172), which can be determined by results of Lemma 2.4, then the locally uniform absolute convergence of the series (2.172) is ensured in view of Theorem 2.3. Moreover, it can be verified by (2.172) that the initial-end conditions (2.170a) and (2.170b) of this ODE-PDE subsystem are satisfied if

$$\mathrm{d}_\tau^j \mu_i^\star(\tau)|_{\tau \in \{0,T\}} = 0, \quad i = 1, \ldots, n_f, j \in \mathbb{N}_0 \tag{2.188}$$

holds. The parametrizing variable $\mu_i(\tau)$ of the ODE-PDE subsystem (2.169a)–(2.169c) and the parametrizing variable $\varphi(\tau)$ for the fault diagnosis kernel equations (see Lemma 2.6), are related by (2.185). Thus, in view of the cascade structure (see Figure 2.13), $\varphi_i^\star(\tau)$ must be planned so that the resulting $\mu_i^\star(\tau)$ from (2.185) satisfies the stated requirements. Additionally, $\varphi_i^\star(\tau)$ must be planned so that the resulting $q_{f,i}(\tau)$ from (2.184a) realizes the transition described by (2.170c). For the latter, insert (2.184a) in (2.170c) to obtain

$$\sum_{j=0}^{\infty} W_j \mathrm{d}_\tau^j \varphi_i^\star(\tau)|_{\tau=0} = -R_f^\top e_{i,n_f} \tag{2.189a}$$

$$\sum_{j=0}^{\infty} W_j \mathrm{d}_\tau^j \varphi_i^\star(\tau)|_{\tau=T} = 0 \tag{2.189b}$$

for $i = 1, \ldots, n_f$. Because of the nonvanishing right-hand side in (2.189a), a trivial choice $\mathrm{d}_\tau^j \varphi_i^\star(\tau)|_{\tau=0} = 0$, $j \in \mathbb{N}_0$, is not possible. A systematic approach for the planning of $\varphi_i^\star(\tau)$ results from regarding (2.185) as the ODE

$$\mathrm{d}_\tau^{n_{vf}} \varphi_i^\star(\tau) = - \sum_{j=0}^{n_{vf}-1} a_j \mathrm{d}_\tau^j \varphi_i^\star(\tau) + \mu_i^\star(\tau), \quad \tau \in (0,T) \tag{2.190}$$

where $\mu_i^\star(\tau)$ is considered as the fictional input to be determined. Thus, $\varphi_i^\star(\tau)$ can be computed as a solution of a feedforward control problem for the ODE (2.190) subject to the additional constraints that $\mu_i^\star(\tau)$ must satisfy (2.188) and $\mu_i^\star \in (\mathbb{G}^\alpha(\mathrm{I}))^{n_y}$, $1 < \alpha < {}^1/_\varrho$ must hold. For a systematic solution, rewrite (2.190) in the form of a state-space system

$$\dot{\xi}_i(\tau) = A_\varphi \xi_i(\tau) + B_\varphi \mu_i^\star(\tau), \qquad \tau \in (0,T) \tag{2.191a}$$

$$\varphi_i^\star(\tau) = C_\varphi \xi_i(\tau), \qquad \tau \in \mathrm{I} \tag{2.191b}$$

with the state

$$\xi_i(\tau) = \begin{bmatrix} \xi_{i,1}(\tau) \\ \xi_{i,2}(\tau) \\ \vdots \\ \xi_{i,n_{vf}}(\tau) \end{bmatrix} = \begin{bmatrix} \varphi_i^\star(\tau) \\ \mathrm{d}_\tau \varphi_i^\star(\tau) \\ \vdots \\ \mathrm{d}_\tau^{n_{vf}-1} \varphi_i^\star(\tau) \end{bmatrix} \in \mathbb{R}^{n_\xi}, \quad i = 1, \ldots, n_f, \qquad (2.192)$$

where $\xi_{i,j}(\tau) = \mathrm{d}_\tau^{j-1}\varphi_i^\star(\tau) \in \mathbb{R}^{n_y}$, $j = 1, \ldots, n_{vf}$, and $n_\xi = n_y n_{vf}$. The matrices in (2.191) are $A_\varphi = A_c \otimes I_{n_y}$ with identity matrix $I_{n_y} \in \mathbb{R}^{n_y \times n_y}$ and

$$A_c = \begin{bmatrix} 0 & 1 & \ldots & 0 \\ \vdots & & \ddots & \\ 0 & 0 & \ldots & 1 \\ -a_0 & -a_1 & \ldots & -a_{n_{vf}-1} \end{bmatrix}, \qquad (2.193)$$

$B_\varphi = e_{n_{vf},n_{vf}} \otimes I_{n_y}$ as well as $C_\varphi = e_{1,n_{vf}}^\top \otimes I_{n_y}$. Hence, $\varphi_i^\star(\tau)$ results from the planning of $\mu_i^\star(\tau)$ realizing a suitable transition for (2.191). For this finite-time transition, the initial and end conditions $\xi_i(0) = \xi_i^0 \in \mathbb{R}^{n_\xi}$ and $\xi_i(T) = \xi_i^T \in \mathbb{R}^{n_\xi}$ of (2.191) must be compatible with the initial and end conditions $\mathrm{d}_\tau^j \varphi_i^\star(\tau)|_{\tau \in \{0,T\}}$, $j = 0, \ldots, n_{vf} - 1$, (see (2.192)), i.e., (2.189) must be expressed in terms of ξ_i^0 respectively ξ_i^T. To this end, the time derivatives of (2.191b) are taken into account in view of (2.191a), yielding

$$\mathrm{d}_\tau^j \varphi_i^\star(\tau) = C_\varphi A_\varphi^j \xi(\tau) + C_\varphi \sum_{k=0}^{j-1} A_\varphi^{j-k-1} B_\varphi \mathrm{d}_\tau^k \mu_i^\star(\tau), \quad i = 1, \ldots, n_f, j \in \mathbb{N}_0, \ (2.194)$$

which is proven in Appendix A.3 by induction. Evaluating (2.194) at $\tau \in \{0, T\}$ leads to

$$\mathrm{d}_\tau^j \varphi_i^\star(\tau)|_{\tau=0} = C_\varphi A_\varphi^j \xi_i^0 \qquad (2.195\text{a})$$

$$\mathrm{d}_\tau^j \varphi_i^\star(\tau)|_{\tau=T} = C_\varphi A_\varphi^j \xi_i^T \qquad (2.195\text{b})$$

in view of (2.188). As a result, the required initial and end conditions (2.189) can be expressed in terms of ξ_i^0 and ξ_i^T by inserting (2.195) in (2.189), which yields

$$\Upsilon \xi_i^0 = -R_f^\top e_{i,n_f} \qquad (2.196\text{a})$$

$$\Upsilon \xi_i^T = 0, \qquad (2.196\text{b})$$

with

$$\Upsilon = \sum_{j=0}^{\infty} W_j C_\varphi A_\varphi^j. \tag{2.197}$$

In the Corollary A.1 in Appendix A.4, it is shown that the series in (2.197) is absolutely convergent so that $\Upsilon \in \mathbb{R}^{n_{vf} \times n_\xi}$ exists. Consequently, imposing

$$\xi_i^T = 0 \tag{2.198}$$

satisfies (2.196b). If

$$\operatorname{rank} \Upsilon = \operatorname{rank} \begin{bmatrix} \Upsilon & -R_f^\top e_{i,n_f} \end{bmatrix} \tag{2.199}$$

holds, the linear system of equations (2.196a) has a solution

$$\xi_i^0 = -\Upsilon^\dagger R_f^\top e_{i,n_f} - \left(I - \Upsilon^\dagger \Upsilon\right) \xi_i^*, \tag{2.200}$$

where $\Upsilon^\dagger$ is the Moore-Penrose generalized inverse of Υ (for details see, e.g., [11, Prop. 6.1.7]) and $\xi_i^* \in \mathbb{R}^{n_\xi}$ is a degree of freedom that will be considered later. According to (2.200) and (2.198), the reference trajectory $\varphi_i^\star(\tau)$ results from the planning of a $\mu_i^\star(\tau)$ realizing the transition

$$\xi_i(0) = \xi_i^0 \qquad\qquad \rightarrow \qquad\qquad \xi_i(T) = 0 \tag{2.201}$$

for the ODE system (2.191) under the additional constraints (2.188) and $\mu_i^\star \in (\mathbb{G}^\alpha(\mathrm{I}))^{n_y}$, $1 < \alpha < 1/\varrho$. In general, the transition problem (2.201) for the system (2.191) can be solved by the approach described in [16, Chapter 6.2, Eq. (6.7)], which is based on the Controllability Gramian. However, to consider the additional constraints on $\mu_i^\star(\tau)$, a modification of this approach is required. To this end, introduce the *weighted Controllability Gramian*

$$W_\vartheta = \int_0^T \Phi_\varphi(T,\tau) B_\varphi B_\varphi^\top \Phi_\varphi^\top(T,\tau) \vartheta(\tau) \mathrm{d}\tau \tag{2.202}$$

where $\Phi_\varphi(\tau_1,\tau_2) = \mathrm{e}^{A_\varphi(\tau_1-\tau_2)}$, $(\tau_1,\tau_2) \in \mathrm{I}^2$ is the state transition matrix for (2.191a) (see, e.g., [16, Section 4.1]) and $\vartheta(\tau) \in \mathbb{R}$ is a degree of freedom used to satisfy the additional constraints. With (2.202), a reference trajectory $\mu_i^\star(\tau)$, which leads to a $\xi_i(\tau)$ satisfying (2.201) results from

$$\mu_i^\star(\tau) = -B_\varphi^\top \Phi_\varphi^\top(T,\tau) W_\vartheta^{-1} \Phi_\varphi(T,0) \xi_i^0 \vartheta(\tau). \tag{2.203}$$

The existence of the inverse of W_ϑ is shown in the following lemma.

Lemma 2.7. Let $\vartheta(\tau) > 0$ hold for $\tau \in (0, T)$. Then, W_ϑ^{-1} exists.

Proof. It follows from the differential parametrizations (2.185) and (2.192) for $\mu_i^\star(\tau)$ and $\xi_i(\tau)$ as well as the output equation (2.191b) and $\dim \mu_i^\star(\tau) = \dim \varphi_i^\star(\tau)$, that $\varphi_i^\star(\tau)$ is a flat output for (2.191a), which implies controllability of (A_φ, B_φ) (see, e.g., [82, Sec. 3.2.2]). Thus, the Controllability Gramian

$$W_c = \int_0^T \Phi_\varphi(T, \tau) B_\varphi B_\varphi^\top \Phi_\varphi^\top(T, \tau) \mathrm{d}\tau, \tag{2.204}$$

is positive definite (see [11, Theorem 12.6.18]), i.e.,

$$c^\top W_c c = \int_0^T \|B_\varphi^\top \Phi_\varphi^\top(T, \tau) c\|_2^2 \mathrm{d}\tau > 0 \tag{2.205}$$

holds for $c \in \mathbb{R}^{n_\xi}$, $c \neq 0$, since $\|B_\varphi^\top \Phi_\varphi^\top(T, \tau) c\|_2^2$ is nonnegative and not identical to zero on $\tau \in (0, T)$, where $\|\cdot\|_2$ represents the Euclidean norm. Consequently, for $\vartheta(\tau) > 0$, $\tau \in (0, T)$,

$$c^\top W_\vartheta c = \int_0^T \|B_\varphi^\top \Phi_\varphi^\top(T, \tau) c\|_2^2 \vartheta(\tau) \mathrm{d}\tau > 0, \quad c \in \mathbb{R}^{n_\xi}, c \neq 0, \tag{2.206}$$

holds, since $\|B_\varphi^\top \Phi_\varphi^\top(T, \tau) c\|_2^2 \vartheta(\tau)$ is nonnegative and not identical to zero on $\tau \in (0, T)$. As a result, W_ϑ is positive definite if $\vartheta(\tau) > 0$, $\tau \in (0, T)$, which proves Lemma 2.7. ∎

In order to show that (2.203) leads to a solution of (2.191a) satisfying the initial and end condition (2.201), consider the general solution

$$\xi_i(\tau) = \Phi_\varphi(\tau, 0) \xi_i^0 + \int_0^\tau \Phi_\varphi(\tau, \zeta) B_\varphi \mu_i^\star(\zeta) \mathrm{d}\zeta \tag{2.207}$$

of the LTI system (2.191a) (see, e.g., [16]). Inserting (2.203) in (2.207) yields

$$\xi_i(\tau) = \Phi_\varphi(\tau,0)\xi_i^0 - \int_0^\tau \Phi_\varphi(\tau,\zeta)B_\varphi B_\varphi^\top \Phi_\varphi^\top(T,\zeta)\vartheta(\zeta)\mathrm{d}\zeta W_\vartheta^{-1}\Phi_\varphi(T,0)\xi_i^0. \quad (2.208)$$

Thus, the IC $\xi_i(0) = \xi_i^0$ is verified by evaluation of (2.208) at $\tau = 0$, since $\Phi_\varphi(0,0) = I$. Use (2.202) in (2.208) to verify also the end condition $\xi_i(T) = \xi_i^T = 0$ (see (2.201)).

The remaining requirement (2.188) on $\mu_i^\star(\tau)$ is satisfied by imposing

$$\mathrm{d}_\tau^j \vartheta(\tau)|_{\tau \in \{0,T\}} = 0, \quad j \in \mathbb{N}_0. \quad (2.209)$$

With (2.209), the feedforward control problem for the ODE (2.190) subject to (2.201) so that $\mu_i^\star(\tau)$ satisfies (2.188) and $\mu_i^\star \in (\mathbb{G}^\alpha(\mathrm{I}))^{n_y}$, $1 < \alpha < {}^1\!/\!_\varrho$ holds has been solved. Consequently, a solution for the fault diagnosis kernel equations (2.169) and (2.170) has been derived, which is summarized in the following Lemma.

> **Lemma 2.8** (Solution for the fault diagnosis kernel equations)**.** Let $\vartheta \in \mathbb{G}^\alpha(\mathrm{I})$ satisfy (2.209) and $1 < \alpha < {}^1\!/\!_\varrho$ with ϱ given by (2.102) in Lemma 2.4 hold. If (2.199) holds, then there exists a C^∞-solution for the fault diagnosis kernel equations (2.169) and (2.170).

Proof. To make use of the differential expressions (2.184) for the computation of the integral kernels $m_i(z,\tau)$, $q_i(\tau)$ and $q_{f,i}(\tau)$, the reference trajectory $\varphi_i^\star(\tau)$ must be chosen so that the series in (2.184) are absolute convergent. The latter is achieved in view of [93, Satz 5.4], if $\varphi_i^\star \in (\mathbb{G}^\alpha(\mathrm{I}))^{n_y}$, $1 < \alpha < {}^1\!/\!_\varrho$ with $0 < \varrho < 1$ holds, where ϱ is the order of the power series in (2.183) (see Lemma 2.4). To verify $\varphi_i^\star \in (\mathbb{G}^\alpha(\mathrm{I}))^{n_y}$, at first the corresponding $\mu_i^\star(\tau)$ given by (2.203) is regarded, since $\varphi_i^\star(\tau)$ depends on $\mu_i^\star(\tau)$ (see (2.194)). In (2.203), the time dependent term $\Phi_\varphi^\top(T,\tau)$ is an analytic function in I, i.e., $\Phi_\varphi^\top(T,\cdot) \in (\mathbb{G}^1(\mathrm{I}))^{n_\xi \times n_\xi}$ holds (see [72, Section 1.4.]). Moreover, $\vartheta(\tau)$ satisfies $\vartheta \in (\mathbb{G}^\alpha(\mathrm{I}))^{n_\xi}$ by definition. Since $\mathbb{G}^1(\mathrm{I}) \subset \mathbb{G}^\alpha(\mathrm{I})$ and $\mathbb{G}^\alpha(\mathrm{I})$ is a vector space and a ring with respect to the arithmetic product of functions (see [72, Proposition 1.4.5]), $\mu_i^\star \in (\mathbb{G}^\alpha(\mathrm{I}))^{n_y}$ follows. Then, in view of (2.207), it follows from [72, Proposition 1.4.5], that $\xi_i(\tau)$ is also a Gevrey function of order α and thus $\varphi^\star \in (\mathbb{G}^\alpha(\mathrm{I}))^{n_y}$ holds in the light of (2.191b). Hence, the series in (2.184) are absolutely convergent for $1 < \alpha < {}^1\!/\!_\varrho$, where ϱ can be determined by results of Lemma 2.4. To be specific, by using $\varphi_i^\star(\tau)$ resulting from (2.191b) as parametrizing variable in the differential expressions in (2.184), the resulting integral kernels $m_i^\star(z,\tau)$, $q_i^\star(\tau)$ and $q_{f,i}^\star(\tau)$ are a solution of the ODE-PDE system (2.169). If $\vartheta(\tau)$ satisfies (2.209), then the initial and end conditions (2.170a) as well as (2.170b)

hold in view of (2.172) and (2.203). Moreover, if (2.199) holds, then ξ_i^0 can be determined by (2.200), so that the initial and end condition given in (2.170c) hold in view of (2.189) and (2.195)–(2.197). Thus, a C^∞-solution for the fault diagnosis kernel equations has been constructed. ∎

A suitable choice for $\vartheta(\tau)$ is, e.g., the Gevrey function given in (2.97), since it satisfies the initial and end conditions (2.209) as well as $\vartheta(\tau) > 0$, $\tau \in (0, T)$. The existence of a solution for the fault diagnosis kernel equations implies the identifiability of the fault, which is summarized in the following theorem.

Theorem 2.9 (Identifiability condition)
Assume that the disturbance $\tilde{d}(t)$ is described by (2.15), $\bar{d}(t) \equiv 0$ holds and the fault $f(t)$ is described by (2.143). If

$$\operatorname{rank} \Upsilon = \operatorname{rank} \begin{bmatrix} \Upsilon & -R_f^\top e_{i,n_f} \end{bmatrix} \qquad (2.210)$$

(see (2.199)) with Υ given in (2.197) is satisfied for $i \in \{1, \dots, n_f\}$, then for the system (2.1) the fault $f_i(t)$ is identifiable by (2.154) (see Theorem 2.5).

Proof. The proof of this theorem is based on the solvability of the fault diagnosis kernel equations. According to Lemma 2.8, the kernel equations (2.169) and (2.170) have a C^∞-solution if (2.199) holds and $\vartheta(\tau)$ is chosen so that it satisfies $\vartheta \in \mathbb{G}^\alpha(\mathrm{I})$, $1 < \alpha < 1/\varrho$, as well as (2.209). Hence, the required kernels $N(\tau)$ and $M_u(\tau)$ for the fault diagnosis residual generator (2.157) can be computed and thus the fault $f(t)$ can be identified in view of Theorem 2.5. ∎

For the case $\bar{d}(t) \not\equiv 0$, also fault detection, isolation and estimation (see Theorems 2.6, 2.7 and 2.8) are ensured if (2.199) holds.

The condition (2.199) depends on R_f and Υ. Since, R_f is a property of the signal model of the fault (see (2.143b)) and the matrices defining Υ are only dependent on system parameters (see (2.197) and preceding definitions of the matrices), (2.199) is only dependent on parameters of the system (2.1) and the signal models (2.15) as well as (2.143). Hence, (2.199) is a system property and can be checked a priori. However, since (2.199) is dependent on the proposed approach for the computation of a suitable reference trajectory $\varphi_i^\star(\tau)$, it is a sufficient condition.

The degree of freedom ξ_i^* introduced in (2.200) can be used to make the resulting residual generator less sensitive to $\bar{d}(t)$. As a measure for the sensitivity of the

residual signal with respect to $\bar{d}(t)$, the threshold $f_{B,i}$ given in (2.163) is used. In order to express $f_{B,i}$ in terms of ξ_i^*, at first $m_{\bar{d},i}^\star(\tau)$ is regarded. Use the substitution $m_{\bar{d}}(\tau) \to m_{\bar{d},i}^\star(\tau)$ as well as $\mu(\tau) \to \mu_i^\star(\tau)$ in (2.93c) and insert (2.203) with (2.200) to obtain

$$m_{\bar{d},i}^\star(\tau) = \theta_{0,i}(\tau) + \theta_1(\tau)\xi_i^* \tag{2.211}$$

where

$$\theta_{0,i}(\tau) = \sum_{j=0}^\infty X_{\bar{d},j} B_\varphi^\top \mathrm{d}_\tau^j \left(\Phi_\varphi^\top(T,\tau)\vartheta(\tau) \right) W_\vartheta^{-1} \Phi_\varphi(T,0)\Upsilon^\dagger R_f e_{i,n_f} \tag{2.212a}$$

$$\theta_1(\tau) = \sum_{j=0}^\infty X_{\bar{d},j} B_\varphi^\top \mathrm{d}_\tau^j \left(\Phi_\varphi^\top(T,\tau)\vartheta(\tau) \right) W_\vartheta^{-1} \Phi_\varphi(T,0) \left(I - \Upsilon^\dagger\Upsilon \right). \tag{2.212b}$$

Thus, $f_{B,i}$ can be expressed in terms of ξ_i^*, by inserting (2.211) in (2.163), which leads to

$$f_{B,i} = \int_0^T |\theta_{0,i}(\tau) + \theta_1(\tau)\xi_i^*|^\top \mathrm{d}\tau\delta. \tag{2.213}$$

Hence, ξ_i^* should be chosen so that

$$f_{B,i} = \min_{\xi_i^* \in \mathbb{R}^{n_\xi}} \int_0^T |\theta_{0,i}(\tau) + \theta_1(\tau)\xi_i^*|^\top \mathrm{d}\tau\delta \tag{2.214}$$

results. In general, (2.214) must be solved numerically. However, since fault identifiability is ensured for any $\xi_i^* \in \mathbb{R}^{n_\xi}$ if the requirements in Theorem 2.9 hold, also suboptimal results for (2.214) might be sufficient for the sensitivity of the residual generator with respect to the bounded disturbances.

2.4.4 Fault diagnosis for an Euler-Bernoulli beam

The fault diagnosis results are demonstrated with a simulation example for a cantilever beam with a tip load. The simulation and fault diagnosis is implemented in MATLAB utilizing the toolbox [109], which simplifies the implementation of the time and space dependent matrices and operators. The source code is available under [108].

To allow a comparison of the fault detection and fault diagnosis results, this example

system for the fault diagnosis is similar to the fault detection example system introduced in Section 2.3.5. However, the fault signals for the fault diagnosis must be solutions of the signal models (2.143). Thus, the fault scenarios were adapted accordingly. Apart from that, the example systems are consistent. The system description of the beam for the demonstration of the fault diagnosis reads as

$$\mu_b(z)\partial_t^2 v(z,t) + \rho(z)\partial_t v(z,t) + \partial_z^2(\lambda_b(z)\partial_z^2 v(z,t))$$
$$= b_1(z)u_1(t) + g_1(\tilde{d}_1(t) + \bar{d}_1(t)) + e_1(z)f_1(t), \quad (z,t) \in (0,1) \times \mathbb{R}^+, \quad (2.215a)$$

subject to the BCs

$$v(0,t) = \partial_z v(0,t) = 0, \qquad\qquad t > 0 \qquad (2.215b)$$
$$\partial_z^2 v(1,t) = -J_E\partial_t^2\partial_z v(1,t) + g_2\bar{d}_2(t), \qquad\qquad t > 0 \qquad (2.215c)$$
$$\partial_z^3 v(1,t) = m_E\partial_t^2 v(1,t) + b_2(u_2(t) + f_2(t)), \qquad\qquad t > 0 \qquad (2.215d)$$

and the available measurements are

$$y(t) = \begin{bmatrix} c_1 v(1,t) + \bar{d}_3(t) \\ c_2\partial_z v(1,t) + \bar{d}_4(t) + f_3(t) \\ \int_0^1 c_3(z)\partial_z^2 v(z,t)\mathrm{d}z + \bar{d}_5(t) + f_4(t) \end{bmatrix} \in \mathbb{R}^3, \qquad t \geq 0. \qquad (2.215e)$$

The system parameters are described in Section 2.3.5 and the corresponding numerical values are specified in Table 2.1. In order to bring the system (2.215) in the required form (2.1) for the fault diagnosis, $x(z,t)$ as in (2.132) is introduced. Except the fault input matrices $E_1(z)$, E_3, E_4, which are $E_1(z) = \frac{e_1(z)}{\lambda_b(z)}e_{1,4}e_{1,4}^\top$, $E_3 = -\frac{b_2}{m_E}e_{3,4}\,e_{2,4}^\top$ and

$$E_4 = \begin{bmatrix} 0 & 0 & 0 & 0 \\ 0 & 0 & 1 & 0 \\ 0 & 0 & 0 & 1 \end{bmatrix}, \qquad (2.216)$$

the same system matrices as described in Section 2.3.5 result. The disturbances are the same as in Section 2.3.5, i.e., $\tilde{d}_1(t)$ has a sinusoidal signal form described by the signal model (2.15) with the matrices (2.131) and $\bar{d}_i(t)$, $i = 1,\ldots,5$, are bounded disturbances with the same bounds as specified in Section 2.3.5.

The faults $f_i(t)$ occur successively at unknown time instants $t_i > T$, which implies $f_i(t) = 0$ for $t < t_i$. The fault $f_1(t)$ is assumed to be piecewise constant, i.e., it is a solution of the signal model given by $S_{f1} = 0$, $r_{f1} = 1$, with the state $v_{f,1}(t) \in \mathbb{R}$ and the IC $v_{f,1}^0 = 0$ for $0 \leq t < t_1$ as well as the unknown IC $v_{f,1}(t_1) = v_{f,1}^1$ for $t \geq t_1$. The faults $f_2(t)$ and $f_4(t)$ have sinusoidal forms $f_i(t) = f_i^0 \sin(\omega_i t + \phi_{f,i})$, $i = 2, 4$, with the unknown parameters f_i^0, $\phi_{f,i} \in \mathbb{R}$ and known parameter $\omega_2 = 8$ as well as $\omega_4 = 1$. These fault signals are modeled by the solution of a state space

system described by

$$S_{f,i} = \begin{bmatrix} 0 & -\omega_i \\ \omega_i & 0 \end{bmatrix}, \qquad\qquad r_{f,i}^\top = \begin{bmatrix} 0 & 1 \end{bmatrix}, \quad i = 2, 4, \qquad (2.217)$$

with the state $v_{f,i}(t) \in \mathbb{R}^2$ and IC $v_{f,i}(0) = 0$ for $0 \le t < t_i$ as well as the unknown IC $v_{f,i}(t_i) = v_{f,i}^i$ for $t \ge t_i$, $i = 2, 4$. The fault $f_3(t)$ is ramplike, i.e., $f_3(t) = f_3^0 + f_3^1 t$ for $t \ge t_3$ with unknown coefficients $f_3^0, f_3^1 \in \mathbb{R}$. Thus, $f_3(t)$ is described by a signal model specified by

$$S_{f,3} = \begin{bmatrix} 0 & 1 \\ 0 & 0 \end{bmatrix}, \qquad\qquad r_{f,3}^\top = \begin{bmatrix} 1 & 0 \end{bmatrix} \qquad (2.218)$$

with the state $v_{f,3}(t) \in \mathbb{R}^2$, the IC $v_{f,3}(0) = 0$ for $0 \le t < t_3$ and the unknown IC $v_{f,3}(t_3) = v_{f,3}^3$ for $t \ge t_3$. The matrices of the common signal model for all faults are given by $S_f = \operatorname{diag}(S_{f,1}, \ldots, S_{f,4})$ and $R_f = \operatorname{diag}(r_{f,1}^\top, \ldots, r_{f,4}^\top)$. Note that this setup requires the identification of four faults that are decoupled from $\tilde{d}(t)$ using only three measurements

For the implementation of the residual generator (2.157), the coefficient matrices of the differential expressions (2.186) and (2.184d) must be computed, which requires the matrices $\Phi_i(z, \zeta)$, $\Psi_{L,i}(z)$ and $\Psi_{C,i}(z)$. The latter are determined by the algorithm proposed in Appendix A.5, where the needed transition matrix $\bar{\Phi}(z, \zeta)$ (see (A.31)) is derived from the numerical solution of its defining ODE (A.27) and the integrals in (A.31) are evaluated by means of a compound trapezoidal rule. Subsequently, the identifiability condition (2.199) can be verified by computing the singular values $\bar{\sigma}(\Upsilon)$ of Υ given in (2.197), which are

$$\bar{\sigma}(\Upsilon) \in \{ 22.1, 21.9, 13.7, 13.7, 1.54, 1.04, 0.123 \} \times 10^{12}. \qquad (2.219)$$

According to [11, Theorem 5.6.3.], (2.219) shows that Υ has full row rank, i.e., rank $\Upsilon = 7$ and thus (2.199) holds for all $i = 1, \ldots, n_f$. Consequently, the approach described in Section 2.4.3.3 can be used for the planning of $\varphi_i^\star(\tau)$. According to $\check{A}^*(z, s)$ given in (2.141) and Lemma 2.4, $\check{\Phi}(z, \zeta, s)$, $\check{\Psi}_L(z, s)$ and $\check{\Psi}_C(z, s)$ are formal power series of order $\varrho = 1/2$. Thus, by choosing $\vartheta(\tau)$ (see (2.203)) as the Gevrey function (2.97) with $1 < \alpha < 2$ ensures a solution of the fault diagnosis kernel equations according to Lemma 2.8, since it satisfies $\vartheta(\tau) > 0$, $\tau \in (0, T)$ and (2.188).

To make the residual generator less sensitive with respect to the influence of $\bar{d}(t)$, the available degree of freedom ξ_i^* (see (2.200)) has to be determined as the argument solving (2.214). The latter is solved numerically with the `fminsearch` function from MATLAB, which uses the Nelder–Mead method to find at least a local minimum. For this example, it appeared convenient to choose the initial point of the numerical

optimization so that $S_{\bar{d}} = \|W_{\bar{d}} m_{\bar{d},i}\|_{\mathrm{I},2}^2$ is minimized, where $\|\cdot\|_{\mathrm{I},2}$ denotes the L_2-norm on the domain I and $W_{\bar{d}} = \mathrm{diag}\left(\delta_1, \ldots, \delta_{n_{\bar{d}}}\right)$ is used. Since $\min_{\xi_i^* \in \mathbb{R}^{n_\xi}} S_{\bar{d}}$ yields an unconstrained quadratic program in terms of ξ_i^* (see (2.211)), it can be solved, e.g, by the result [11, Fact 8.14.15]. With ξ_i^* determined, ξ_i^0 can be computed by (2.200) and thus $\mu_i^\star(\tau)$ by (2.203). To obtain $\varphi_i^\star(\tau)$ and its derivatives, (2.194) can be used which depends on $\mathrm{d}_\tau^j \mu_i^\star(\tau)$ and thus on $\mathrm{d}_\tau^j(\Phi_\varphi^\top(T, \tau)\vartheta(\tau))$, $j \in \mathbb{N}_0$. The latter can be computed using the product rule and symbolic computations of $\partial_\tau^j \Phi_\varphi^\top(T, \tau)$ as well as $\mathrm{d}_\tau^j \vartheta(\tau)$. With this, the reference trajectory $\varphi_i^\star(\tau)$ results from evaluating (2.194). The required integral kernels $n_i(\tau)$ and $m_{u,i}(\tau)$ as components of the fault diagnosis residual generator (2.155) can be computed with the differential expressions (2.184d) and (2.186a). For their evaluation, the series in (2.184d) and (2.186a) are truncated when the relative increment of the last term is less than 10^{-9}, which is achieved after $n_s = 12$ terms.

Suitable α and T must be determined to obtain acceptable thresholds $f_{B,i}$ and detection delays for the fault estimation. As a measure for the detection delays of the residual generator, the normalized detection delay $\Delta_{f,i}$ is utilized. The latter is the first time instant where a threshold $f_{B,i}$, $i = 1, \ldots, n_f$, is exceeded by $|\langle M_f, h_{f,i}(t)\rangle_{\mathrm{I}}|$, $h_{f,i}(t) \in \mathbb{R}^{n_f}$, $t \geq 0$. At this, $M_f(\tau) = \begin{bmatrix} m_{f,1}(\tau) & \cdots & m_{f,n_f}(\tau) \end{bmatrix}$ is used, where $m_{f,i}(\tau)$ is given by (2.186b) and the test signal $h_{f,i}(t)$ is chosen as

$$e_{j,n_f}^\top h_{f,i}(t) = \begin{cases} f_j(t) & : i = j \\ 0 & : \text{otherwise,} \end{cases} \qquad i, j = 1, \ldots, n_f, \qquad (2.220)$$

with $f_j(t) = r_{f,j}^\top v_{f,j}(t)$, $j = 1, \ldots, n_f$, as the solution of the corresponding signal model given by $S_{f,j}$ and $r_{f,j}$ subject to the ICs

$$v_{f,1}(0) = 10, \qquad v_{f,2}(0) = \begin{bmatrix} 100 \\ 0 \end{bmatrix}, \qquad v_{f,3}(0) = \begin{bmatrix} 3 \\ 1 \end{bmatrix}, \qquad v_{f,4}(0) = \begin{bmatrix} 50 \\ 0 \end{bmatrix}. \qquad (2.221)$$

The results for $f_{B,i}$ and $\Delta_{f,i}$ computed for several α and T are shown in Figure 2.14. According to these results, α should be close to the upper bound 2, since this reduces the threshold values as well as the detection delays. A small threshold value offers both, the detection of faults with small magnitude (see results of Theorem 2.6) and the fault estimation with small estimation errors (see results of Theorem 2.8). For the choice of T, a compromise has to be made. The fault detection delay shown in Figure 2.14b indicates that a small T leads to an earlier detection. Another reason for a small T, is that the fault isolation and identification are only possible after $t_i + T$, $i \in \mathbb{N}_0$, (see results of Theorem 2.5). Nevertheless, according to the results in Figure 2.14a, this would increase the thresholds. Consequently, T must be chosen in dependence on the magnitudes of faults that are required to be detected and permissible fault detection, isolation and identification delays. In the following,
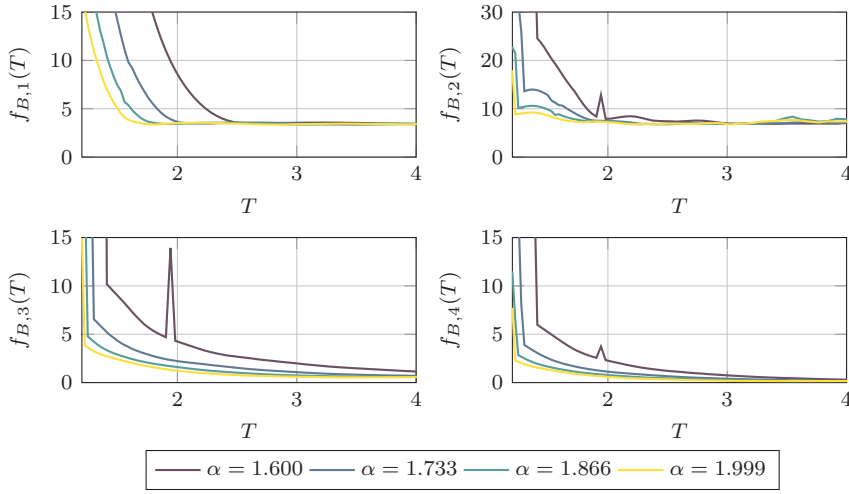
(a) Fault detection threshold $f_{B,i}$, $i = 1, \ldots, 4$, (see (2.163)) in dependence on the moving horizon length T for different Gevrey orders α.
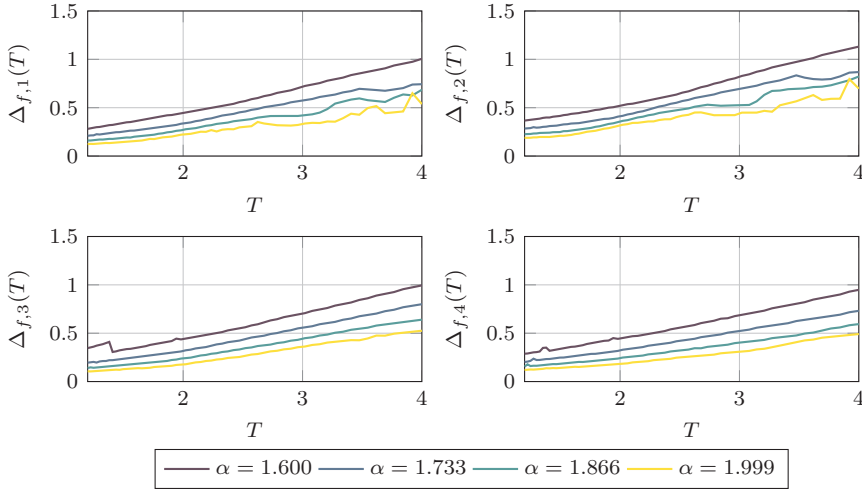
(b) Normalized fault detection delay $\Delta_{f,i}$, $i = 1, \ldots, 4$, in dependence on the moving horizon length T for different Gevrey orders α.

Figure 2.14: Parameter study results to investigate the influence of the Gevrey order α and the moving horizon length T on the threshold $f_{B,i}$, $i = 1, \ldots, 4$, (see (2.163)) and the normalized detection delay $\Delta_{f,i}$ of the fault diagnosis residual generator.

$\alpha = 1.9999$ and $T = 1.75$ is chosen, yielding the thresholds $f_{B,1} = 3.40$, $f_{B,2} = 7.27$, $f_{B,3} = 1.69$ and $f_{B,4} = 0.88$ as well as integral kernels $N(\tau)$ and $M_u(\tau)$ shown in Figure 2.15, which are used for the following fault diagnosis.

The simulation of the faulty beam is performed in MATLAB using a finite-dimensional model determined by the Galerkin approximation described in [79] resulting in a finite-dimensional state space system of order 56, which is simulated with the MATLAB `lsim` command using a step size of 5×10^{-3}. The fault diagnosis residual generator (2.157) is implemented as FIR filters using the compound midpoint rule for the time-discretization of the integral expressions. In the sense of a quasi-continuous implementation, the same step size is used for the discretization of the integral expressions as is used for the simulation. This leads to FIR filters of order 351. At first, the fault identification case, i.e., $\bar{d}(t) \equiv 0$ is regarded. For this the input signals, shown in Figure 2.9 and the fault signals shown in Figure 2.16, which result from the ICs

$$v_{f,1}^1 = 10, \qquad v_{f,2}^2 = \begin{bmatrix} 14 \\ 0 \end{bmatrix}, \qquad v_{f,3}^3 = \begin{bmatrix} 0 \\ -0.50 \end{bmatrix}, \qquad v_{f,4}^4 = \begin{bmatrix} 1.10 \\ 0.40 \end{bmatrix} \qquad (2.222)$$

are used for the simulation of the beam. The simulation results in Figure 2.16 show that the residual signal is excited by the unknown ICs of the system and the signal model of the disturbance $\tilde{d}(t)$ in the initialization interval $0 \leq t \leq T$ only. Subsequently, all residual signals $\hat{f}_i(t)$ are zero until the first fault $f_1(t)$ occurs at t_1. At t_1, the changing IC of the signal model of the fault $f_1(t)$ leads to an excitation of all residual signals in $t \in (t_1, t_1 + T)$. The same applies to the occurrence of the other faults, which shows the coupling of the residual signals in the intervals $(t_i, t_i + T)$, $i = 1, \ldots, 4$. Nevertheless, without an explicit consideration in the residual generator design, the coupling of the residual signals is not very strong and even negligible for $\hat{f}_1(t)$ with respect to $f_i(t)$, $i = 3, 4$, since the occurrence of $f_3(t)$ and $f_4(t)$ does not or only very little excite the residual signal $\hat{f}_1(t)$. However, for $t \in I_j = [t_j + T, t_{j+1})$, $\hat{f}(t) = f(t)$ can be verified.

In a second simulation, fault diagnosis is investigated subject to the influence of the bounded disturbance $\bar{d}(t)$. This includes the fault detection, isolation and estimation. Thereby, the bounded disturbance $\bar{d}(t)$ is chosen as the signal shown in Figure 2.9b. Otherwise, the same input $u(t)$, disturbance $\tilde{d}(t)$ as well as fault $f(t)$ are taken as the signals shown in Figure 2.9a. Using the same integral kernels as computed for the fault identification case, the results in Figure 2.17 are obtained. Until the occurrence of $f_1(t)$ at $t_1 = 6$, all residual signals are bounded by the threshold values. The fault $f_1(t)$ is detected at $\hat{t}_1 = 6.34$ because the residual signal $\hat{f}_1(t)$ exceeds the threshold value $f_{B,1}$ (see Theorem 2.6). In accordance with the result of Theorem 2.7, for $t \in (t_1 + T, t_2)$, only $\hat{f}_1(t)$ exceeds the threshold value $f_{B,1}$ and $\hat{f}_i(t)$, $i = 2, 3, 4$, remain bounded by $f_{B,i}$. Thus, $f_1(t)$ is isolated at $t_1^\circ = 8.09$ and estimated for
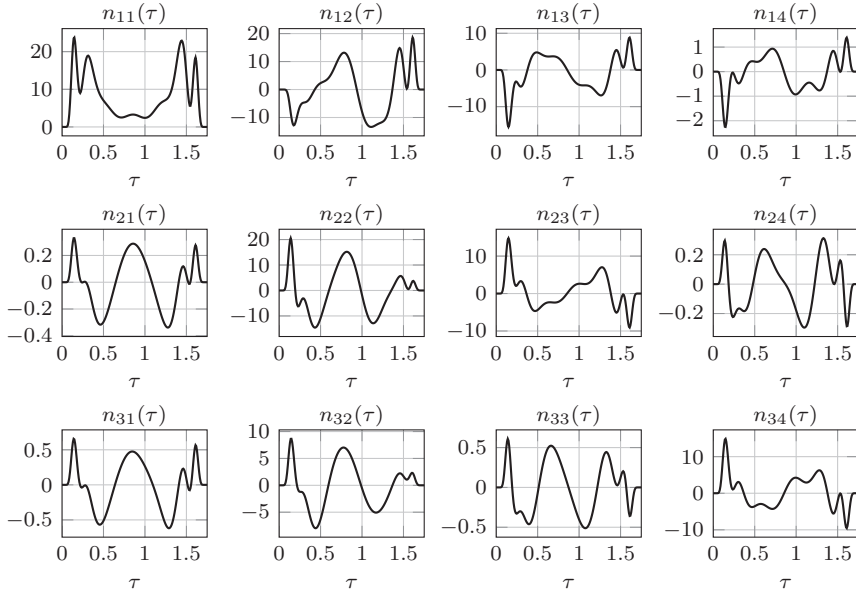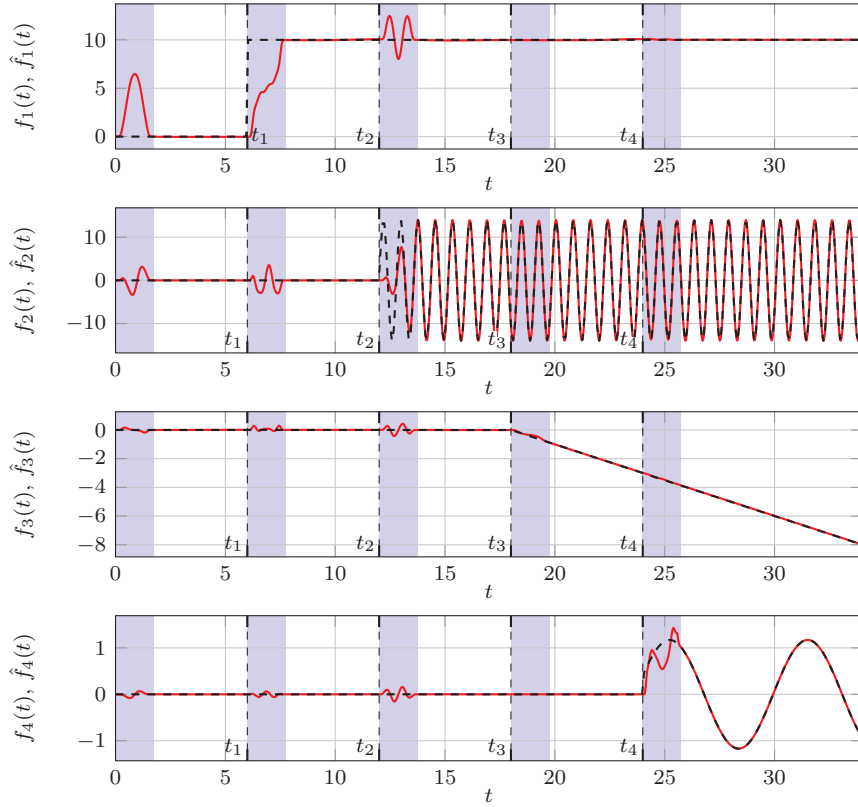
(a) The components $n_{ij}(\tau)$, $i = 1, 2, 3$, $j = 1, \ldots, 4$, of the integral kernel $N(\tau)$.
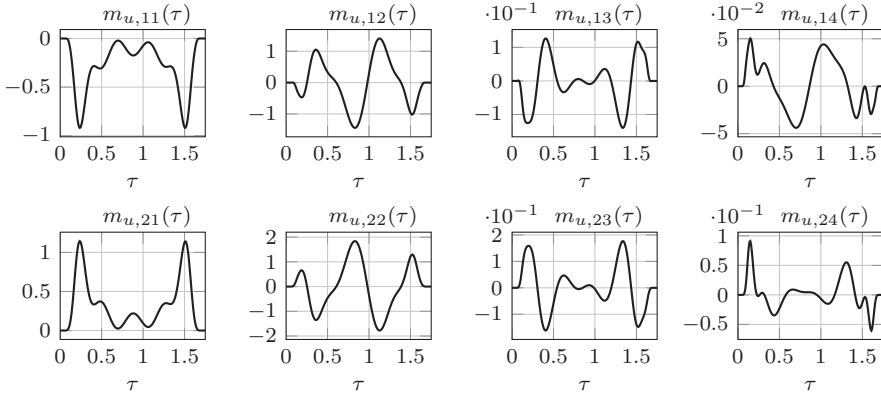
(b) The components $m_{u,ij}$, $i = 1, 2$, $j = 1, \ldots, 4$, of the integral kernel $M_u(\tau)$.

Figure 2.15: The components of the integral kernels $N(\tau)$ and $M_u(\tau)$ computed with moving horizon length $T = 1.75$ and $\vartheta(\tau)$ as Gevrey function (2.97) of order $\alpha = 1.9999$.

Figure 2.16: Fault isolation and identification results $\hat{f}_i(t)$, $i = 1, \ldots, 4$, (——) for the fault $f_i(t)$ (- - -) without bounded disturbance, i.e., $\bar{d}(t) \equiv 0$, the initialization interval $0 \le t < T$ (▨) and the transient intervals $t_i < t < t_i + T$ (▨) after the occurrence of a fault.
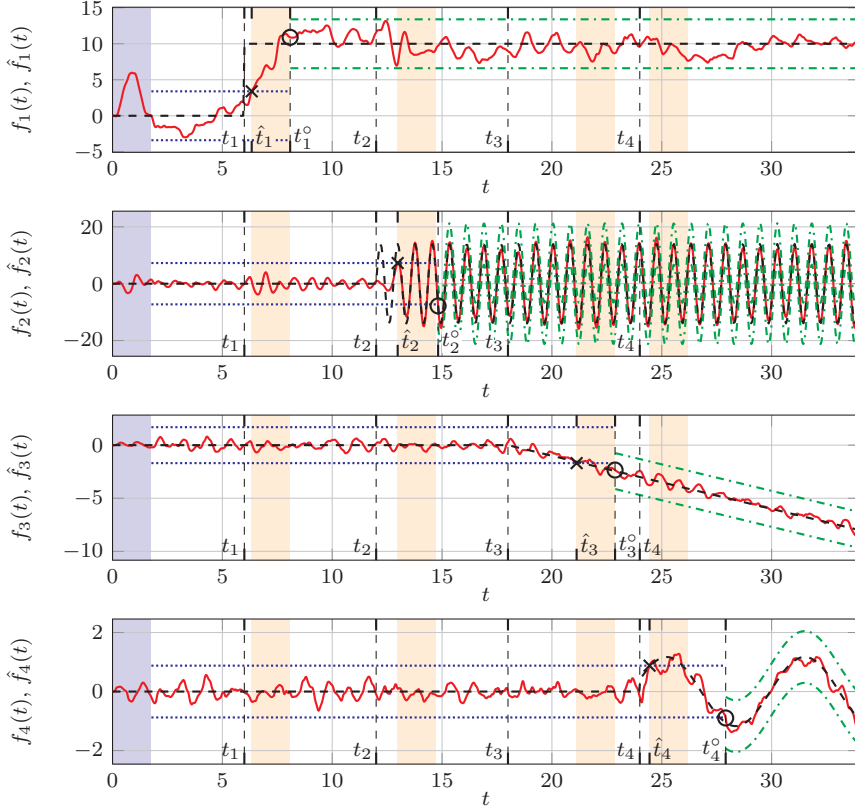
Figure 2.17: Fault diagnosis residual signal $\hat{f}_i(t)$, $i = 1, \ldots, 4$, (——) in the presence of the bounded disturbance $\bar{d}(t)$ depicted in Figure 2.9b for the fault $f_i(t)$ (- - -), the thresholds $\pm f_{B,i}$ (⋯⋯), the bounds of the fault estimation error $f(t) \pm f_{B,i}$ (-·-·-), the initialization interval $0 \leq t < T$ (▢), the detection (✕) of a fault $f_i(t)$ at time $\hat{t}_i$, the isolation delay interval $\hat{t}_i \leq t < \hat{t}_i + T$ (▢) and the isolation (◯) at time t_i°, which is also the beginning of the fault estimation.

$t \in (\hat{t}_1 + T, t_2)$ by $\hat{f}_1(t)$ (see Theorem 2.8). A second fault is detected by the exceed of $f_{B,2}$ at $\hat{t}_2 = 12.98$. Since for $t_2^\circ = \hat{t}_2 + T$, $\hat{f}_i(t_2^\circ) > f_{B,i}$, $i = 1, 2$, holds, $\hat{f}_i(t)$, $i = 3, 4$, are bounded by $f_{B,i}$ and $f_1(t)$ has been isolated before, the second fault must be $f_2(t)$. Similarly, $f_3(t)$, is detected at $\hat{t}_3 = 21.13$ and isolated at $t_3^\circ = 22.88$. At $\hat{t}_4 = 24.45$, a fourth fault is detected. However, the fault $f_4(t)$ can be isolated and thus also estimated not before $t_4^\circ = 27.91$, because of the signal form of $f_4(t)$, the residual signal $\hat{f}_4(t)$ at first remains within the bounds $\pm f_{B,4}$ until t_4°. The results show, that the signals of all faults can be estimated with known estimation error.

2.4.5 Concluding remarks

In this section, the fault diagnosis for parabolic and biharmonic ODE-PDE systems subject to disturbances is presented for additive actuator, process and sensor faults. If the fault and the disturbance have a signal form that can be described by a finite-dimensional signal model, fault detection, isolation and identification is achieved. When an additional unknown but bounded disturbance is present, fault detection, isolation and estimation with bounded estimation error is possible. The fault diagnosis residual generator is derived by the application of integral transforms, whereas the integral kernels must be a solution of an initial-end value problem for an ODE-PDE system. The latter is solved using flatness-based trajectory planning methods, whereas a new approach for the reference trajectory planning is introduced utilizing the cascade structure of the system. This yields a fault identifiability condition that depends solely on system properties and can be checked a priori. Within the simulation example, the remaining degrees of freedom in the residual generator design are discussed and the theoretical results are demonstrated.

The simulation results show that some residual signals have no coupling in the transient interval. Since this has the advantage, that an earlier fault isolation and a more precise estimation is possible as well if further faults occur, the design of residual generators that are explicitly decoupled in the transient interval should be investigated in future work. Moreover, the dependence of the threshold values on T shown in Figure 2.14a indicates that the fault diagnosis could be further improved by not selecting the same detection window length T for all residual generators, but rather by adjusting it to the associated fault.

Chapter 3

Heterodirectional hyperbolic ODE-PDE systems

When the dynamics of a technical system is based on wave propagation, transport processes or time-delays, it can be modeled by a hyperbolic PDE. If such a technical system has dynamic boundary conditions or is otherwise coupled to a process that can be modeled with lumped parameters, then a hyperbolic ODE-PDE system is obtained. Many of these models can be represented by heterodirectional hyperbolic ODE-PDE systems, which consist of ODEs coupled with transport PDEs. The latter propagate in both the negative and positive direction of the spatial coordinate. This system class includes, e.g., models for coupled string networks (see [59, Section 6.2]), networks of open channels and transmission lines (see [10, Section 1]). Since more and more advanced control methods become available for this system class (see, e.g., [10]), systematic fault diagnosis methods are necessary for a safe operation of the resulting control systems.

3.1 System description

Consider the *faulty general linear heterodirectional hyperbolic ODE-PDE system*

$$\partial_z x(z,t) = \Gamma(z)\partial_t x(z,t) + A(z)x(z,t) + A_0(z)x^-(0,t) + \int_0^z D(z,\zeta)x(\zeta,t)\mathrm{d}\zeta$$

$$+ H_1(z)w(t) + B_1(z)u(t) + E_1(z)f(t) + G_1(z)d(t) \tag{3.1a}$$

$$x^+(0,t) = K_0 x^-(0,t) + H_2 w(t) + B_2 u(t) + E_2 f(t) + G_2 d(t), \quad t > 0 \tag{3.1b}$$

$$x^-(1,t) = K_1 x^+(1,t) + B_3 u(t) + E_3 f(t) + G_3 d(t), \quad\quad\quad t > 0 \tag{3.1c}$$

$$\dot{w}(t) = F w(t) + L_2 x^-(0,t) + B_4 u(t) + E_4 f(t) + G_4 d(t), \quad t > 0 \tag{3.1d}$$

$$y(t) = C_0 x^-(0,t) + C_1 w(t) + E_5 f(t) + G_5 d(t), \quad\quad\quad t \geq 0 \tag{3.1e}$$

with (3.1a) defined on $(z,t) \in (0,1) \times \mathbb{R}^+$, the distributed system variable $x(z,t) = \mathrm{col}\,(x^-(z,t),\, x^+(z,t)) \in \mathbb{R}^{n_x}$, the lumped state $w(t) \in \mathbb{R}^{n_w}$, the input $u(t) \in \mathbb{R}^{n_u}$, the output $y(t) \in \mathbb{R}^{n_-}$, the fault $f(t) \in \mathbb{R}^{n_f}$ and the disturbance $d(t) \in \mathbb{R}^{n_d}$. From these signals, only the input $u(t)$ and the measurement $y(t)$ are assumed to be known. The system consists of n_x coupled *transport PDEs* (3.1a) and an ODE (3.1d). The transport behavior of the distributed system variable $x(z,t)$ in (3.1a) is specified by $\Gamma(z) = \mathrm{diag}(\gamma_1(z),\dots,\gamma_{n_x}(z)) \in \mathbb{R}^{n_x \times n_x}$ where $\gamma_i \in C^1[0,1]$, $\gamma_i(z) \neq 0$, $z \in [0,1]$, $i = 1,\dots,n_x$, is assumed. Different from the usual representation for general linear heterodirectional hyperbolic ODE-PDE systems (see, e.g., [40]), the PDE (3.1a) is solved for $\partial_z x(z,t)$. Consequently, the distributed nonvanishing transport velocities are given by $\lambda_i(z) = \frac{1}{\gamma_i(z)}$, $i = 1,\dots,n_x$. Without loss of generality, it is assumed that $x(z,t)$ is ordered, so that the transport velocities $\lambda_i(z)$ are sorted in descending order, i.e.,

$$\overline{\lambda}_- \geq \lambda_1(z) > \lambda_2(z) > \cdots > \lambda_{n_-}(z) \geq \underline{\lambda}_- > 0 \tag{3.2a}$$

$$0 \geq \overline{\lambda}_+ > \lambda_{n_-+1}(z) > \lambda_{n_-+2}(z) > \cdots > \lambda_{n_x}(z) \geq \underline{\lambda}_+ \tag{3.2b}$$

with positive and negative constants $\overline{\lambda}_-, \underline{\lambda}_- \in \mathbb{R}^+$ and $\overline{\lambda}_+, \underline{\lambda}_+ \in \mathbb{R}^-$. Thus, $x(z,t)$ has n_- components

$$x^-(z,t) = J_- x(z,t) \in \mathbb{R}^{n_-} \tag{3.3a}$$

propagating in negative direction of the spatial coordinate and $n_+ = n_x - n_-$ components

$$x^+(z,t) = J_+ x(z,t) \in \mathbb{R}^{n_+} \tag{3.3b}$$

propagating in positive direction of the spatial coordinate, with

$$J_- = \begin{bmatrix} I & 0 \end{bmatrix} \in \mathbb{R}^{n_- \times n_x} \tag{3.3c}$$

$$J_+ = \begin{bmatrix} 0 & I \end{bmatrix} \in \mathbb{R}^{n_+ \times n_x}. \tag{3.3d}$$

Note that (3.3) implies

$$x(z,t) = J_+^\top x^+(z,t) + J_-^\top x^-(z,t). \tag{3.4}$$

Consequently, the PDE subsystem (3.1a)–(3.1c) is a system of n_- and n_+ transport PDEs propagating in opposite directions and is thus according to, e.g., [40], a *heterodirectional hyperbolic system*. Furthermore, the entries of $A(z) = [a_{ij}(z)] \in \mathbb{R}^{n_x \times n_x}$ satisfy $a_{ij} \in C^1[0,1]$, $i,j = 1,\ldots,n_x$, and $a_{ii}(z) = 0$, $z \in [0,1]$, $\forall i = 1,\ldots,n_x$. The latter means no loss of generality, as this form can always be achieved by a change of coordinates (see, e.g., [41, Section 3] and the example in Section 3.2.4). The remaining matrices for the local and the integral term in (3.1a) are $A_0 \in (C^1[0,1])^{n_x \times n_+}$ as well as $D \in (C^1([0,1]^2))^{n_x \times n_x}$. In (3.1b) and (3.1c), the coupling is specified by $K_0 \in \mathbb{R}^{n_+ \times n_-}$ and $K_1 \in \mathbb{R}^{n_- \times n_+}$. The dynamics of the ODE (3.1d) is characterized by $F \in \mathbb{R}^{n_w \times n_w}$, the coupling of the ODE subsystem (3.1d) with the PDE subsystem (3.1a)–(3.1c) is described via $L_2 \in \mathbb{R}^{n_w \times n_-}$, $H_1 \in (L_2(0,1))^{n_x \times n_w}$ as well as $H_2 \in \mathbb{R}^{n_+ \times n_w}$ and the effect of $w(t)$ on the output $y(t)$ via $C_1 \in \mathbb{R}^{n_- \times n_w}$. The influence of the input $u(t)$, the fault $f(t)$ and the disturbance $d(t)$ on (3.1) are defined by $B_1 \in (L_2(0,1))^{n_x \times n_u}$, $E_1 \in (L_2(0,1))^{n_x \times n_f}$, $G_1 \in (L_2(0,1))^{n_x \times n_d}$ and the real valued matrices B_i, $i = 2,3,4$, E_j as well as G_j, $j = 2,3,4,5$, of appropriate dimensions. The output matrix $C_0 \in \mathbb{R}^{n_- \times n_-}$ satisfies

$$\operatorname{rank} C_0 = n_-. \tag{3.5}$$

All system matrices are assumed to be known. The ICs $x(z,0) \in \mathbb{R}^{n_x}$, $z \in [0,1]$ of (3.1a) and $w(0) \in \mathbb{R}^{n_w}$ of (3.1d) are unknown but assumed to be compatible with the BCs (3.1b) and (3.1c), so that (3.1) is well-posed (see, e.g., [10]).

Note that many physical systems of interest can be described by (3.1) (see, e.g., [10, 19, 59]). In particular, coupled wave equations, which occur in many applications (see, e.g., [47, 68, 76, 87–89]), can be mapped into the form (3.1) by introducing *Riemann coordinates* as it is shown in the following example.

Example 3.1.

Consider the faulty wave equation

$$\partial_t^2 v(z,t) = c^2 \partial_z^2 v(z,t) + g_1^\top(z)d(t), \qquad (z,t) \in (0,1) \times \mathbb{R}^+ \qquad (3.6a)$$

$$\rho_0 \partial_t^2 v(0,t) = \partial_z v(0,t) + g_2^\top d(t), \qquad\qquad t > 0 \qquad (3.6b)$$

$$\partial_z v(1,t) = u(t) + f_1(t), \qquad\qquad t > 0 \qquad (3.6c)$$

$$y(t) = \partial_z v(0,t) + f_2(t), \qquad\qquad t \geq 0 \qquad (3.6d)$$

with the distributed variable $v(z,t) \in \mathbb{R}$, the IC $v(z,0) = v_0 \in \mathbb{R}$, the input $u(t) \in \mathbb{R}$, the measurement $y(t) \in \mathbb{R}$, the disturbance $d(t) \in \mathbb{R}^2$ and the faults $f_1(t)$, $f_2(t) \in \mathbb{R}$. The parameters c, $\rho_0 \in \mathbb{R}^+$ and $g_1 \in (C[0,1])^2$, $g_2 \in \mathbb{R}^2$ are known. To bring (3.6) into the required form (3.1), introduce the Riemann coordinates

$$x^-(z,t) = \partial_t v(z,t) + c\partial_z v(z,t) \qquad (3.7a)$$

$$x^+(z,t) = \partial_t v(z,t) - c\partial_z v(z,t) \qquad (3.7b)$$

(see, e.g., [19, Section 7.3]). The inverse of this transformation is given by

$$\partial_t v(z,t) = \frac{1}{2}\left(x^-(z,t) + x^+(z,t)\right) \qquad (3.8a)$$

$$\partial_z v(z,t) = \frac{1}{2c}\left(x^-(z,t) - x^+(z,t)\right). \qquad (3.8b)$$

By taking the derivative of (3.7) with respect to time, i.e.,

$$\partial_t x^-(z,t) = \partial_t^2 v(z,t) + c\partial_t\partial_z v(z,t) \qquad (3.9a)$$

$$\partial_t x^+(z,t) = \partial_t^2 v(z,t) - c\partial_t\partial_z v(z,t), \qquad (3.9b)$$

and the derivative with respect to space, i.e.,

$$\partial_z x^-(z,t) = \partial_z\partial_t v(z,t) + c\partial_z^2 v(z,t) \qquad (3.10a)$$

$$\partial_z x^+(z,t) = \partial_z\partial_t v(z,t) - c\partial_z^2 v(z,t), \qquad (3.10b)$$

the wave equation (3.6a) can be mapped into the form

$$\partial_t x(z,t) = \begin{bmatrix} c & 0 \\ 0 & -c \end{bmatrix} \partial_z x(z,t) + \begin{bmatrix} g_1(z) \\ g_1(z) \end{bmatrix} d_1(t) \qquad (3.11a)$$

by inserting (3.6a) in (3.9) and replacing the terms $\partial_z\partial_t v(z,t)$ with the expressions given in (3.10). Finally, solve (3.11a) with respect to $\partial_z x(z,t)$, which yields the heterodirectional PDE in the form of (3.1a) specified by the matrices $\Gamma = \mathrm{diag}\left(\frac{1}{c}, -\frac{1}{c}\right)$ and $G_1(z) = \mathrm{col}\left(g_1^\top(z), g_1^\top(z)\right)$. To map (3.6b) into the required form (3.1b),

introduce the ODE state $w(t) = \partial_t v(0, t)$, which yields the ODE

$$\dot{w}(t) = \frac{1}{\rho_0} \partial_z v(0, t) + \frac{1}{\rho_0} g_2^\top d(t). \qquad (3.12)$$

Insert (3.8a) in $w(t) = \partial_t v(0, t)$ to obtain

$$x^+(0, t) = -x^-(0, t) + 2w(t) \qquad (3.13)$$

and thus the nonzero matrices in (3.1b) read as $K_0 = -1$ as well as $H_2 = 2$. For the BC at $z = 1$, insert (3.8b) in (3.6c), which yields

$$x^-(1, t) = x^+(1, t) + \frac{1}{2c} u(t) + \frac{1}{2c} f_1(t). \qquad (3.14)$$

By introducing $f(t) = \mathrm{col}\,(f_1(t), f_2(t))$, the nonzero matrices in (3.1c) read as $K_1 = 1$, $B_3 = \frac{1}{2c}$ and $E_3 = \left[\,\frac{1}{2c}\ 0\,\right]$. To map the ODE (3.12) into the required form, insert (3.14) solved for $x^+(1, t)$ in (3.8b) and the result in (3.12), which leads to

$$\dot{w}(t) = -\frac{1}{c\rho_0} w(t) + \frac{1}{c\rho_0} x^-(0, t) + \frac{1}{\rho_0} g_2^\top d(t) \qquad (3.15)$$

in the required form of (3.1d). Finally, (3.6d) is mapped into the form (3.1e) by evaluating (3.8b) at $z = 0$ and inserting (3.13), which yields

$$y(t) = \frac{1}{c} x^-(0, t) - \frac{1}{c} w(t) + E_5 f(t) \qquad (3.16)$$

with $E_5 = \left[\,0\ e_2\,\right]$. ◁

More details about this transformation can be found in [19, Section 7.3] or, e.g., [24], in which the introduction of Riemann coordinates is shown for a more complex wave-ode equation or in the example in Section 3.2.4. The local term $A_0(z)x^-(0, t)$ is, e.g., considered in the backstepping controller design literature for first-order hyperbolic PDEs (see, e.g., [52, Section 9.1] or [14]) occurs also in a linearized model of a plug flow reactor described in [96]. Moreover, this term also occurs, if the non-actuated BC of a wave equation is not of Dirichlet type and a backstepping transformation is used before mapping the wave equation into a system of first order hyperbolic PDEs. Note that the restriction of the output $y(t)$ to the form (3.1e) and the restricted coupling of the distributed system variable $x(z, t)$ into the ODE (see (3.1d)) are not a general limitation of the proposed fault diagnosis method. Both restrictions are only made to facilitate the solution of the kernel equations by a backstepping transformation, which yields explicit expressions to compute a solution of the kernel equations. Despite these limitations, as mentioned before, models of relevant applications can be represented by (3.1). Moreover, note that in dependence

of the input matrices B_2 and B_3, for systems with a non-dynamic BC at $z = 1$, collocated system setups can already be considered. If more general measurements and ODE-PDE couplings have to be taken into account, then a fault diagnosis or detection residual generator can still be derived by a similar derivation as shown in the following. However, the solution of the kernel equations may require to use, e.g., the trajectory planning method described in [93, Section 7]. The abstract system description in the form (3.1) yields a systematic approach to fault detection for a large class of systems. For a simpler introduction to the proposed method, the interested reader is referred to [103]. In this paper, a comparable approach for a vibrating string is derived directly from the wave equation.

As shown in the following, the special form of (3.1a) solved for $\partial_z x(z, t)$ is well suited to solve the considered fault detection and diagnosis problems. With the setup (3.1) additive actuator, process and sensor faults as described in Section 2.2 can be taken into account. For the fault detection, also multiplicative faults can be considered by rewriting them as additive faults, as shown in Section 2.2. According to (2.13), the disturbance $d(t)$ is assumed to be composed of the absolutely bounded part $\bar{d}(t)$, which satisfies (2.14) and the component $\tilde{d}(t)$ is assumed to be described by a solution of the signal model (2.15).

3.2 Fault detection

For systems of the form (3.1), the fault detection problem is solved by using a residual generator as described in Section 2.3.1. Similar to Section 2.3.2 and Section 2.3.3, the residual generator is derived by the application of integral transformations. These are used to determine an input-output expression in Section 3.2.1 from which the fault detection residual generator for heterodirectional hyperbolic ODE-PDE systems (3.1) is derived in Section 3.2.2. After solving the resulting kernel equations in Section 3.2.3, the theoretical results are applied to a simulation of a real-world motivated application example in Section 3.2.4.

3.2.1 Determination of the input-output expression

Consider the integral transformation for the PDE (3.1a)

$$\mathcal{M}[h](t) = \langle m, h(t) \rangle_{\Omega, \mathrm{I}}, \quad h(z, t) \in \mathbb{R}^{n_x}, \tag{3.17a}$$

for the ODE (3.1d)

$$\mathcal{Q}_w[h](t) = \langle q_w, h(t)\rangle_I, \quad h(t) \in \mathbb{R}^{n_w}, \tag{3.17b}$$

for the signal model (2.15)

$$\mathcal{Q}_d[h](t) = \langle q_d, h(t)\rangle_I, \quad h(t) \in \mathbb{R}^{n_{vd}} \tag{3.17c}$$

and for the output equation (3.1e)

$$\mathcal{N}[h](t) = \langle n, h(t)\rangle_I, \quad h(t) \in \mathbb{R}^{n_-} \tag{3.17d}$$

with the integral kernels $m(z,\tau) \in \mathbb{R}^{n_x}$, $q_w(\tau) \in \mathbb{R}^{n_w}$, $q_d(\tau) \in \mathbb{R}^{n_{vd}}$ and $n(\tau) \in \mathbb{R}^{n_-}$ on $z \in \Omega = [0,1]$ and $\tau \in I = [0,T]$. In contrast to the integral transformations (2.18) used for parabolic and biharmonic PDE systems, the length of the moving horizon T has to satisfy $0 < T_0 < T$. The lower bound T_0 results from the transport behavior of the heterodirectional hyperbolic PDE system (3.1a) and it depends on the longest transportation time in the positive and negative spatial direction

$$\tilde{\tau}^- = \tilde{\tau}_{n_-} \tag{3.18a}$$

$$\tilde{\tau}^+ = |\tilde{\tau}_{n_-+1}|, \tag{3.18b}$$

where

$$\tilde{\tau}_i = \int_0^1 \gamma_i(z)\mathrm{d}z, \quad i = 1, \dots, n_x \tag{3.19}$$

is used. To be specific, T_0 is given by $T_0 = \tilde{\tau}^+ + \tilde{\tau}^-$.

The integral kernels $m(z,\tau)$, $q_w(\tau)$, $q_d(\tau)$ and $n(\tau)$ of the transformations (3.17) are determined similarly to the approach shown in Section 2.3.2 so that the *input-output expression*

$$\langle m_f, f(t)\rangle_I = \langle n, y(t)\rangle_I + \langle m_u, u(t)\rangle_I + \langle m_{\bar{d}}, \bar{d}(t)\rangle_I \tag{3.20}$$

depending only on $f(t)$, $y(t)$, $u(t)$ and $\bar{d}(t)$ results. The integral kernels $m_f(\tau)$,

$m_u(\tau)$ and $m_{\bar{d}}(\tau)$ used in (3.20) are defined by

$$m_f(\tau) = -\langle E_1, m(\tau)\rangle_\Omega - E_2^\top m^+(0,\tau) + E_3^\top m^-(1,\tau)$$
$$- E_4^\top q_w(\tau) + E_5^\top n(\tau) \tag{3.21a}$$
$$m_u(\tau) = \langle B_1, m(\tau)\rangle_\Omega + B_2^\top m^+(0,\tau) - B_3^\top m^-(1,\tau) + B_4^\top q_w(\tau) \tag{3.21b}$$
$$m_{\bar{d}}(\tau) = \bar{G}^\top \left(\langle G_1, m(\tau)\rangle_\Omega + G_2^\top m^+(0,\tau) - G_3^\top m^-(1,\tau) \right.$$
$$\left. + G_4^\top q_w(\tau) - G_5^\top n(\tau) \right), \tag{3.21c}$$

where $m^+(z,\tau) = J_+ m(z,\tau)$, $m^-(z,\tau) = J_- m(z,\tau)$ and $\langle \cdot, m(\tau)\rangle_\Omega$ denotes the integration with respect to z on Ω. For (3.20) and (3.21) to hold, the integral kernels $m(z,\tau)$, $q_w(\tau)$ and $q_d(\tau)$ must satisfy the *fault detection kernel equations* for heterodirectional hyperbolic ODE-PDE systems, which are summarized in the following lemma.

Lemma 3.1 (Fault detection kernel equations for heterodirectional hyperbolic ODE-PDE systems)**.** Let $\tilde{d}(t)$ be described by (2.15) and the integral kernels $m(z,\tau)$, $q_w(\tau)$ and $q_d(\tau)$ satisfy the *fault detection kernel equations*

$$\partial_z m(z,\tau) = -\Gamma(z)\partial_\tau m(z,\tau) - A^\top(z)m(z,\tau) - \mathcal{D}^*[m(\tau)](z) \tag{3.22a}$$

$$m^-(0,\tau) = -K_0^\top m^+(0,\tau) - \langle A_0, m(\tau)\rangle_\Omega - L_2^\top q_w(\tau) + C_0^\top n(\tau) \tag{3.22b}$$

$$m^+(1,\tau) = -K_1^\top m^-(1,\tau) \tag{3.22c}$$

$$\dot{q}_w(\tau) = F^\top q_w(\tau) + \langle H_1, m(\tau)\rangle_\Omega + H_2^\top m^+(0,\tau) - C_1^\top n(\tau) \tag{3.22d}$$

$$\dot{q}_d(\tau) = S_d^\top q_d(\tau) + R_d^\top \tilde{G}^\top \left(\langle G_1, m(\tau)\rangle_\Omega + G_2^\top m^+(0,\tau)\right.$$
$$\left. -G_3^\top m^-(1,\tau) + G_4^\top q_w(\tau) - G_5^\top n(\tau)\right), \tag{3.22e}$$

subject to the initial and end conditions

$$m(z,\tau)|_{\tau\in\{0,T\}} = 0, \qquad z \in \Omega \tag{3.23a}$$

$$q_w(\tau)|_{\tau\in\{0,T\}} = 0 \tag{3.23b}$$

$$q_d(\tau)|_{\tau\in\{0,T\}} = 0, \tag{3.23c}$$

with (3.22a) defined on $(z,\tau) \in (0,1) \times (0,T)$, (3.22b)–(3.22e) defined on $\tau \in (0,T)$ and $\mathcal{D}^*[m(\tau)](z)$ in (3.22a) is specified by

$$\mathcal{D}^*[m(\tau)](z) = \int_z^1 D^\top(\zeta,z)m(\zeta,\tau)\mathrm{d}\zeta, \quad (z,\tau) \in (0,1) \times (0,T). \tag{3.24}$$

Then, the input-output expression (3.20) holds.

The derivation of (3.20) and (3.21) in view of (3.22) and (3.23) is shown in Appendix A.7 and follows the same reasoning as in the case of parabolic and biharmonic ODE-PDE systems (see Section 2.3.2). At first, the integral transformations (3.17) are applied to the corresponding system equation in (3.1). Subsequently, the operators and matrices are shifted to the integral kernels. By eliminating all terms that contain unknown system variables except the disturbance $\bar{d}(t)$, the kernel equations (3.22) subject to (3.23) are derived and (3.20) is established.

3.2.2 Residual generator

At first, consider the case $\bar{d}(t) \equiv 0$. With the same argument as for the derivation of Theorem 2.1, the fault detection residual generator for heterodirectional hyperbolic ODE-PDE systems is introduced in the following theorem.

Theorem 3.1 (Residual generator)

Assume that $\tilde{d}(t)$ is described by a solution of (2.15), $\bar{d}(t) \equiv 0$ holds and let $f(t)$ satisfy $f(t) = 0$, $t < T$, as well as $\langle m_f, f(t) \rangle_{\mathrm{I}} \not\equiv 0$ for $f(t) \not\equiv 0$. If the integral kernels $m(z, \tau)$, $q_w(\tau)$, $q_d(\tau)$ and $n(\tau)$ are solutions of the kernel equations (3.22) and (3.23) as well as $m_f(\tau)$ given in (3.21a) satisfies (2.54), then

$$r(t) = \langle n, y(t) \rangle_{\mathrm{I}} + \langle m_u, u(t) \rangle_{\mathrm{I}}, \quad t \geq T \tag{3.25}$$

is a residual generator for the system (3.1). A fault is detected if $r(t) \not\equiv 0$, $t \geq T$, occurs.

The proof of this theorem follows the reasoning in the proof of Theorem 2.1.

For the case $\bar{d}(t) \not\equiv 0$, the influence of $\bar{d}(t)$ on the residual $r(t)$ can be estimated after inserting (3.25) in (3.20). Then, the fault detection threshold r_B is given by (2.60) as the upper bound for the absolute value of the residual error in (2.56). By the same reasoning as for Theorem 2.2, the fault detection for heterodirectional hyperbolic ODE-PDE systems subject to a bounded disturbance $\bar{d}(t)$ is obtained and summarized in the following theorem.

Theorem 3.2 (Fault detection)

Assume that $\tilde{d}(t)$ is described by a solution of (2.15) and let $f(t)$ satisfy $f(t) = 0$, $t < T$, as well as $\langle m_f, f(t) \rangle_{\mathrm{I}} \not\equiv 0$ for $f(t) \not\equiv 0$. Let the integral kernels $m(z, \tau)$, $q_w(\tau)$, $q_d(\tau)$ and $n(\tau)$ satisfy (3.22) subject to (3.23) and $m_f(\tau)$ given by (3.21a) satisfy (2.54). Then, for the system (3.1) a fault is detected if the threshold r_B is exceeded by the residual signal $r(t)$ for $t \geq T$, i.e.,

$$|r(t)| > r_B, \quad t \geq T, \tag{3.26}$$

with r_B and $r(t)$ given in (2.60) respectively (3.25).

The proof of this theorem is similar to the proof of Theorem 2.2.

3.2.3 Solution of the fault detection kernel equations

With (3.22) and (3.23), the fault detection kernel equation consists of a heterodi-rectional hyperbolic ODE-PDE system subject to initial and end conditions. In (3.22), $n(\tau)$ is freely assignable and is thus interpreted as an input. Consequently, the solution of the fault detection kernel equations amounts to solve a feedforward control problem. To be specific, the input $n(\tau)$ must be determined such that it drives the integral kernels $m(z, \tau)$, $q_w(\tau)$ and $q_d(\tau)$ from the initial to the end point given in (3.23) in finite time. Similar to the solution of the kernel equations corresponding to the parabolic or biharmonic ODE-PDE systems (see Section 2.3.4), this trajectory planning problem can be solved by using results from the flatness-based trajectory planning. With the introduction of a parametrizing variable $\varphi(\tau)$, the integral kernels $m(z, \tau)$, $q_w(\tau)$, $q_d(\tau)$ and $n(\tau)$ can be expressed in terms of a differential expression. Thus, the kernel equations two-point initial-boundary-value problem can be also traced back to an algebraic interpolation problem for a reference trajectory of the parametrizing variable. In contrast to the case with parabolic or biharmonic PDEs in Section 2.3.4.2, the differential expressions for hyperbolic ODE-PDE systems involve derivatives of the parametrizing variable $\varphi(\tau)$ only up to a finite order but distributed delays and predictions of the latter. Note that for the solution of the kernel equations specified in Lemma 3.1, it is not required to verify that the parametrizing variable is indeed a flat output. However, it must be shown that a solution for the specific transition (3.23) could be parametrized in terms of $\varphi(\tau)$, which is considered in Section 3.2.3.4. In general, results from [93, Section 7] can be used to introduce such a parametrizing variable and compute the differential expressions by the method of characteristics and a fixpoint iteration. However, for systems of the form (3.22), the derivation of the differential expressions can be significantly facilitated by making use of a backstepping transformation which is, e.g., described in [41]. This transformation is used to map the ODE-PDE system of the integral kernel equations (3.22) into a target system with PDE-ODE cascade structure for which the differential expressions can be explicitly specified. Based on these expressions, an easily evaluable fault detectability condition is derived. Moreover, because of the target systems cascade structure, a subsequent trajectory planning for the PDE and the ODE subsystem becomes possible. Hence, the transition problem for the PDE subsystem is significantly facilitated, since the initial and end conditions for the PDE subsystem can be embedded into a setpoint. Thus, the solution of the kernel equations (3.22) and (3.23) can be traced back to a nontrivial setpoint change for the PDE subsystem in combination with a transition problem for an ODE subsystem. Therefore, the derivation of the differential expressions using a backstepping transformation is described below.

3.2.3.1 Backstepping transformation

The following backstepping transformation is based on a result from [41], where heterodirectional ODE-PDE systems of the form (3.1) are considered. However, because of the use of the formal adjoint in the derivation of the residual generator, a kernel equation with transport PDEs that propagate in reversed direction of the spatial coordinate compared to [41] and an input $n(\tau)$ on the opposite BC is obtained. Thus, a spatial reversal $\bar{z} = 1 - z$ is applied to (3.22), which restores the propagation direction of the transport processes and the position of the boundary input so that the assumed form in [41] is derived. The resulting system variables defined for $\bar{z}$ are denoted by adding an overline, e.g., $\bar{\Gamma}(\bar{z}) = \Gamma(1 - \bar{z})$ with the diagonal components $\bar{\gamma}_i(\bar{z}) = \gamma_i(1 - \bar{z})$, $i = 1, \ldots, n_x$. Furthermore, use $\int_0^{\bar{z}} \bar{D}^\top(\zeta, \bar{z}) \bar{m}(\zeta, \tau) \mathrm{d}\zeta$ for the term $\mathcal{D}^*[m(\tau)](z)$. With this spatial reversal,

$$\partial_z \bar{m}(\bar{z}, \tau) = \bar{\Gamma}(\bar{z}) \partial_\tau \bar{m}(\bar{z}, \tau) + \bar{A}^\top(\bar{z}) \bar{m}(\bar{z}, \tau) + \int_0^{\bar{z}} \bar{D}^\top(\zeta, \bar{z}) \bar{m}(\zeta, \tau) \mathrm{d}\zeta \tag{3.27a}$$

$$\bar{m}^+(0, \tau) = -K_1^\top \bar{m}^-(0, \tau) \tag{3.27b}$$

$$\bar{m}^-(1, \tau) = -K_0^\top \bar{m}^+(1, \tau) - \int_0^1 \bar{A}_0^\top(\zeta) \bar{m}(\zeta, \tau) \mathrm{d}\zeta - L_2^\top J_w q(\tau) + C_0^\top n(\tau) \tag{3.27c}$$

$$\dot{q}(\tau) = \bar{F} q(\tau) + \int_0^1 \bar{B}_1(\zeta) \bar{m}(\zeta, \tau) \mathrm{d}\zeta + \bar{B}_2 \bar{m}^-(0, \tau) + \bar{B}_3 \bar{m}^+(1, \tau)$$
$$+ \bar{B}_4 n(\tau) \tag{3.27d}$$

is obtained, where (3.27a) is defined on $(\bar{z}, \tau) \in (0, 1) \times (0, T)$, (3.27b)–(3.27d) are defined on $\tau \in (0, T)$, $q(\tau) = \mathrm{col}\,(q_w(\tau), q_d(\tau)) \in \mathbb{R}^{n_q}$, $n_q = n_w + n_{vd}$ and $J_w = [\,I \ 0\,] \in \mathbb{R}^{n_w \times n_q}$ so that $q_w(\tau) = J_w q(\tau)$. The matrices in (3.27d) result from aggregating (3.22d) and (3.22e) and read as

$$\bar{F} = \begin{bmatrix} F^\top & 0 \\ R_d^\top \tilde{G}^\top G_4^\top & S_d^\top \end{bmatrix}, \quad \bar{B}_1(\bar{z}) = \begin{bmatrix} \bar{H}_1^\top(\bar{z}) \\ R_d^\top \tilde{G}^\top \bar{G}_1^\top(\bar{z}) \end{bmatrix}, \quad \bar{B}_2 = \begin{bmatrix} 0 \\ -R_d^\top \tilde{G}^\top G_3^\top \end{bmatrix},$$
$$\bar{B}_3 = \begin{bmatrix} H_2^\top \\ R_d^\top \tilde{G}^\top G_2^\top \end{bmatrix}, \qquad \bar{B}_4 = \begin{bmatrix} -C_1^\top \\ -R_d^\top \tilde{G}^\top G_5^\top \end{bmatrix}. \tag{3.28}$$

The initial and end conditions following from (3.23) are

$$\bar{m}(\bar{z}, \tau)|_{\tau \in \{0, T\}} = 0, \quad \bar{z} \in \Omega \tag{3.29a}$$

$$q(\tau)|_{\tau \in \{0, T\}} = 0. \tag{3.29b}$$

For notational convenience, the substitution $\bar{z} \to z$ is used in the following.

With the spatial reversal, results from [41] can be used to map (3.27) into a system of cascade structure. To this end, the invertible *backstepping transformation*

$$\tilde{m}(z,\tau) = \bar{m}(z,\tau) - \int_0^z \bar{K}(z,\zeta)\bar{m}(\zeta,\tau)\mathrm{d}\zeta = \mathcal{T}[\bar{m}(\tau)](z) \tag{3.30}$$

with the *backstepping kernel* $\bar{K}(z,\zeta) \in \mathbb{R}^{n_x \times n_x}$ is utilized. The corresponding *inverse backstepping transformation*

$$\bar{m}(z,\tau) = \tilde{m}(z,\tau) + \int_0^z \bar{K}_I(z,\zeta)\tilde{m}(\zeta,\tau)\mathrm{d}\zeta = \mathcal{T}^{-1}[\tilde{m}(\tau)](z) \tag{3.31}$$

with $\bar{K}_I(z,\zeta) \in \mathbb{R}^{n_x \times n_x}$ (see [41, Section 2.3]) can be computed based on the reciprocity relation as shown in [25]. For a general introduction to the backstepping transformation see the textbook [52]. The backstepping kernel $\bar{K}(z,\zeta)$ in (3.30) is determined to map (3.27) into the *target system*

$$\partial_z \tilde{m}(z,\tau) = \bar{\Gamma}(z)\partial_\tau \tilde{m}(z,\tau) + \tilde{P}_0(z)\tilde{m}^-(0,\tau), \quad (z,\tau) \in (0,1) \times (0,T) \tag{3.32a}$$

$$\tilde{m}^+(0,\tau) = -K_1^\top \tilde{m}^-(0,\tau), \qquad\qquad \tau \in (0,T) \tag{3.32b}$$

$$\tilde{m}^-(1,\tau) = \tilde{n}(\tau), \qquad\qquad \tau \in (0,T) \tag{3.32c}$$

$$\dot{q}(\tau) = \tilde{F}q(\tau) + \int_0^1 \tilde{B}_1(\zeta)\tilde{m}(\zeta,\tau)\mathrm{d}\zeta + \tilde{B}_2\tilde{m}^-(0,\tau) + \tilde{B}_3\tilde{m}(1,\tau) \tag{3.32d}$$

with (3.32d) defined on $\tau \in (0,T)$. The matrices in (3.32d) result from utilizing the inverse backstepping transformation (3.31). To be specific, (3.27c) is solved for $n(\tau)$ and the result is inserted in (3.27d). Note that the required matrix $(C_0^\top)^{-1}$ exists because of (3.5). After inserting (3.31) in (3.27d) and changing the order of integration, (3.32d) follows with the matrices

$$\tilde{F} = \bar{F} + \bar{B}_4 \left(C_0^\top\right)^{-1} L_2^\top J_w \tag{3.33a}$$

$$\tilde{B}_1(z) = \bar{B}_1(z) + \int_z^1 \bar{B}_1(\zeta)\bar{K}_I(\zeta,z)\mathrm{d}\zeta + \bar{B}_3 J_+ \bar{K}_I(1,z)$$

$$+ \bar{B}_4 \left(C_0^\top\right)^{-1} \left((\bar{A}_0^\top(z) + J_- + K_0^\top J_+)\bar{K}_I(1,z) + \int_z^1 \bar{A}_0^\top(\zeta)\bar{K}_I(\zeta,z)\mathrm{d}\zeta\right) \tag{3.33b}$$

$$\bar{B}_2 = \bar{B}_2 \tag{3.33c}$$

$$\tilde{B}_3 = \bar{B}_3 J_+ + \bar{B}_4 \left(C_0^\top\right)^{-1} (J_- + K_0^\top J_+). \tag{3.33d}$$

To preserve an input for the target system (3.32), the new boundary input $\tilde{n}(\tau) \in \mathbb{R}^{n_-}$ in (3.32c) is introduced instead of choosing a homogeneous BC as in [41]. To this end, insert (3.30) in (3.32c) and utilize (3.27c) to obtain

$$\tilde{n}(\tau) = C_0^\top n(\tau) - K_0^\top \bar{m}^+(1,\tau) - L_2^\top J_w q(\tau)$$

$$- \int_0^1 \left(\bar{A}_0^\top(\zeta) + J_- \bar{K}(1,\zeta)\right) \bar{m}(\zeta,\tau)\mathrm{d}\zeta. \tag{3.34}$$

The matrices $\tilde{P}_0(z) \in \mathbb{R}^{n_x \times n_-}$ in (3.32a) will be specified in detail below (see (3.35b)).

To map (3.27) into the target system (3.32), solve (3.32a) for $\partial_\tau \tilde{m}(z,\tau)$. The latter is set equal to the derivative of (3.30) with respect to τ in which the resulting $\partial_\tau \bar{m}(z,\tau)$ in the integral term is replaced by the PDE (3.27a) solved for $\partial_\tau \bar{m}(z,\tau)$. After the application of integration by parts, a change of the order of integration, the usage of $\bar{m}(0,\tau) = J_+^\top \bar{m}^+(0,\tau) + J_-^\top \bar{m}^-(0,\tau)$ and (3.27b), the *backstepping kernel equations*

$$\Lambda(z)\partial_z \bar{K}(z,\zeta) + \partial_\zeta(\bar{K}(z,\zeta)\Lambda(\zeta)) = -\bar{K}(z,\zeta)\Lambda(z)\bar{A}^\top(z) + \Lambda(z)\bar{D}^\top(\zeta,z)$$

$$- \int_\zeta^z \bar{K}(z,\bar{\zeta})\Lambda(\bar{\zeta})\bar{D}^\top(\zeta,\bar{\zeta})\mathrm{d}\bar{\zeta} \tag{3.35a}$$

$$\bar{K}(z,0)\Lambda(0)(J_-^\top - J_+^\top K_1^\top) = -\Lambda(z)\tilde{P}_0(z) \tag{3.35b}$$

$$\Lambda(z)\bar{K}(z,z) - \bar{K}(z,z)\Lambda(z) = \Lambda(z)\bar{A}^\top(z), \tag{3.35c}$$

are derived by a comparison of coefficients (see, e.g., [41]). The PDE (3.35a) is defined on $0 < \zeta < z < 1$ and $\Lambda(z) = \bar{\Gamma}^{-1}(z)$ exists due to (3.2). The matrix $\tilde{P}_0(z)$ in (3.35b) has the form

$$\tilde{P}_0(z) = \begin{bmatrix} \tilde{P}_1(z) \\ \tilde{P}_2(z) \end{bmatrix}, \tag{3.36a}$$

and is composed of $\tilde{P}_2(z) \in \mathbb{R}^{n_+ \times n_-}$ as well as the *strictly lower triangular matrix*

$\tilde{P}_1(z) \in \mathbb{R}^{n_- \times n_-}$, i.e.,

$$\tilde{P}_1(z) = \begin{bmatrix} 0 & \cdots & \cdots & 0 \\ \tilde{p}_{1,2\,1}(z) & \ddots & \ddots & \vdots \\ \vdots & \ddots & \ddots & \vdots \\ \tilde{p}_{1,n_-\,1}(z) & \cdots & \tilde{p}_{1,n_-\,n_--1}(z) & 0 \end{bmatrix}. \tag{3.36b}$$

The zero entries of the upper triangular part in (3.36b), are BCs for the PDE (3.35a) of the backstepping kernel equations in view of (3.35b). Moreover, the resulting form of $\tilde{P}_0(z)$ yields a cascade structure of the transport processes in the target system (3.32), which was used in [41] to achieve the stability of the target system. Although this is not necessary for the derivation of the differential expressions, it is retained for consistency with [41]. Note that in order to ensure the well-posedness of (3.35), artificial BCs must be added, which is described in detail in [41, Section 2.2]. Then, both the components of $\tilde{P}_2(z)$ and the strictly lower triangular part of $\tilde{P}_1(z)$ result from the solution of the backstepping kernel equations (3.35) and are thus given by (3.35b). The backstepping kernel equations (3.35) have been investigated in [41, Section 2.2] without the integral term. Since, the latter term does not change the result in [41], it can be shown by [41, Theorem A.1.] that (3.35) has a piecewise C^1-solution.

Since the ODE-PDE system (3.32) is a cascade of the PDE subsystem (3.32a)–(3.32c) and the ODE subsystem (3.32d), the differential expression for the PDE subsystem can be determined independently of the ODE subsystem. Moreover, the in-domain couplings $\bar{A}^\top(z)\bar{m}(z)$ and $\bar{D}^\top(\zeta, z)\bar{m}(\zeta)$ appearing in (3.27a) are removed by the backstepping transformation. Thus, the resulting PDE subsystem is a cascade of the transport processes in negative and positive direction of the spatial coordinate, as depicted in Figure 3.1. This inherent cascade structure significantly simplifies the determination of a differential expression in terms of the parametrizing variable $\tilde{m}^-(0, \tau)$ for the PDE subsystem (3.32a)–(3.32c). Note that because of the strictly lower triangular form of the coupling matrix $\tilde{P}_1(z)$ (see (3.36a)) of the boundary value $\tilde{m}^-(0, \tau)$ into the distributed variable $\tilde{m}^-(z, \tau)$, also the transport process in negative transport direction exhibits a cascade structure.

3.2.3.2 Differential expression for the PDE subsystem

To derive the corresponding differential expressions for the PDE subsystem, it is convenient to use the formal Laplace transform, i.e., the correspondence $h(z, \tau) \circ\!\!-\!\!\bullet \check{h}(z, s) \in \mathbb{C}^\nu$ for $h(z, \tau) \in \mathbb{R}^\nu$ is used. For a rigorous mathematical justification of the following see, e.g., [75, 95].
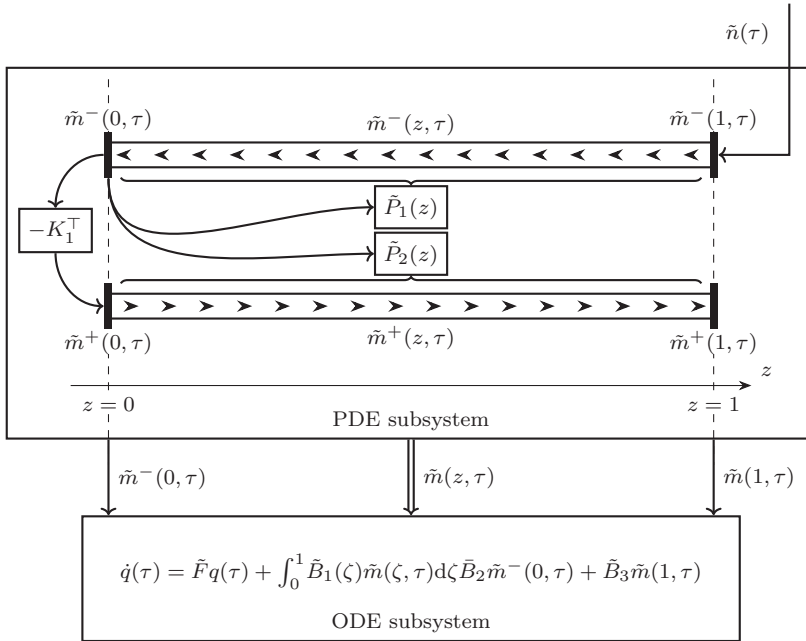
Figure 3.1: Cascade structure of the target system (3.32) with the PDE subsystem (3.32a)–(3.32c) and the ODE subsystem (3.32d), whereas also the inherent cascade structure of the transport processes in negative and positive spatial direction of the PDE subsystem is illustrated.

Apply the Laplace transform to (3.32a) and (3.32b) to obtain the initial value problem

$$\partial_z \check{\tilde{m}}(z,s) = s\bar{\Gamma}(z)\check{\tilde{m}}(z,s) + \tilde{P}_0(z)\check{\tilde{m}}^-(0,s), \qquad z \in (0,1), s \in \mathbb{C} \qquad (3.37a)$$

$$\check{\tilde{m}}(0,s) = V\check{\tilde{m}}^-(0,s), \qquad\qquad\qquad s \in \mathbb{C}, \qquad (3.37b)$$

where $V = (J_-^\top - J_+^\top K_1^\top)$ in view of $\check{\tilde{m}}(0,s) = J_-^\top \check{\tilde{m}}^-(0,s) + J_+^\top \check{\tilde{m}}^+(0,s)$ is used. By regarding (3.37a) as an ODE with respect to z, its general solution is given by

$$\check{\tilde{m}}(z,s) = \check{\Phi}(z,0,s)V\check{\tilde{m}}^-(0,s) + \int_0^z \check{\Phi}(z,\zeta,s)\tilde{P}_0(\zeta)\mathrm{d}\zeta \check{\tilde{m}}^-(0,s) \qquad (3.38)$$

with the state transition matrix $\check{\Phi} : \Omega^2 \times \mathbb{C} \to \mathbb{C}^{n_x \times n_x}$ satisfying

$$\partial_z \check{\Phi}(z,\zeta,s) = s\bar{\Gamma}(z)\check{\Phi}(z,\zeta,s), \quad \check{\Phi}(\zeta,\zeta,s) = I, \quad (z,\zeta,s) \in \Omega^2 \times \mathbb{C} \qquad (3.39)$$

(see [75, Assumption 1]). Due to the diagonal form of $\bar{\Gamma}(z)$, the latter can be explicitly determined as

$$\check{\Phi}(z,\zeta,s) = \mathrm{diag}\left(\exp\left(s\bar{\tau}_1(z,\zeta)\right),\ldots,\exp\left(s\bar{\tau}_{n_x}(z,\zeta)\right)\right) \qquad (3.40a)$$

with

$$\bar{\tau}_i(z,\zeta) = \int_\zeta^z \bar{\gamma}_i(\sigma)\mathrm{d}\sigma, \quad (z,\zeta) \in \Omega^2, \quad i = 1,\ldots,n_x, \qquad (3.40b)$$

where $\bar{\gamma}_i(z)$ are the diagonal components of $\bar{\Gamma}(z)$. Thus, in view of (3.32c) and (3.38), the kernels $\check{\tilde{m}}(z,s)$ and $\check{\tilde{n}}(s)$ can be represented by

$$\check{\tilde{m}}(z,s) = \check{\Psi}(z,s)\check{\tilde{m}}^-(0,s), \quad z \in \Omega \qquad (3.41a)$$

$$\check{\tilde{n}}(s) = J_- \check{\Psi}(1,s)\check{\tilde{m}}^-(0,s) \qquad (3.41b)$$

with

$$\check{\Psi}(z,s) = \check{\Phi}(z,0,s)V + \int_0^z \check{\Phi}(z,\zeta,s)\tilde{P}_0(\zeta)\mathrm{d}\zeta. \qquad (3.42)$$

To make use of the previous formal computations, (3.41) must be mapped into the time domain. Consider (3.42) rowwise, i.e., $\check{\Psi}_i^\top(z,s) = e_{i,n_x}^\top \check{\Psi}(z,s)$, $i = 1,\ldots,n_x$, in (3.42). Due to the diagonal form of $\check{\Phi}^\top(z,\zeta,s)$ (see (3.40a)), its ith row is

$e_{i,n_x}^\top \check{\Phi}(z,\zeta,s) = e_{i,n_x}^\top \exp\left(s\bar{\tau}_i(z,\zeta)\right)$, which yields

$$\check{\Psi}_i^\top(z,s) = e_{i,n_x}^\top V \exp\left(s\bar{\tau}_i(z,0)\right) + \int_0^z e_{i,n_x}^\top \tilde{P}_0(\zeta) \exp\left(s\bar{\tau}_i(z,\zeta)\right) \mathrm{d}\zeta. \tag{3.43}$$

By utilizing the correspondences $\check{h}(s) \bullet\!\!-\!\!\circ h(\tau) \in \mathbb{R}^{n_-}$ and $\check{h}(s)\exp\left(s\bar{\tau}_i(z,\zeta)\right) \bullet\!\!-\!\!\circ h(\tau + \bar{\tau}_i(z,\zeta))$ for $\check{h}(s) \in \mathbb{C}^{n_-}$, the time domain representation of $\check{\Psi}_i^\top(z,s)\check{h}(s)$ reads as

$$\Psi_i^\top[h](z,\tau) = e_{i,n_x}^\top V h(\tau + \bar{\tau}_i(z,0)) + \int_0^z e_{i,n_x}^\top \tilde{P}_0(\zeta) h(\tau + \bar{\tau}_i(z,\zeta)) \mathrm{d}\zeta \tag{3.44}$$

in view of (3.43). Thus, the time domain correspondence for $\check{\Psi}(z,s)\check{h}(s)$ is given by

$$\Psi[h](z,\tau) = \mathrm{col}\left(\Psi_1^\top[h](z,\tau), \ldots, \Psi_{n_x}^\top[h](z,\tau)\right) \tag{3.45}$$

and finally

$$\tilde{m}(z,\tau) = \Psi\left[\tilde{m}^-(0)\right](z,\tau) \tag{3.46a}$$

$$\tilde{n}(\tau) = J_- \Psi\left[\tilde{m}^-(0)\right](1,\tau) \tag{3.46b}$$

result as the time domain correspondence of (3.41). In the light of (3.46), $\tilde{m}(z,\tau)$ and $\tilde{n}(\tau)$ can be parameterized in terms of $\tilde{m}^-(0,\tau)$, which is the parametrizing variable for the PDE subsystem. In contrast to the formal differential expressions in the form of series that result for parabolic or biharmonic systems (see Section 2.3.4.2), distributed delays and predictions (see (3.44)) have to be evaluated. Based on (3.46), the differential expression for the cascade system (3.32) can readily be constructed.

3.2.3.3 Differential expression for the cascade system

Applying the formal Laplace transform $h(\tau) \circ\!\!-\!\!\bullet \check{h}(s)$ and $\mathrm{d}_\tau h(\tau) \circ\!\!-\!\!\bullet s\check{h}(s)$ to (3.32d) yields

$$\left(sI - \tilde{F}\right)\check{q}(s) = \int_0^1 \tilde{B}_1(\zeta)\check{\tilde{m}}(\zeta,s)\mathrm{d}\zeta + \bar{B}_2\check{\tilde{m}}^-(0,s) + \tilde{B}_3\check{\tilde{m}}(1,s), \tag{3.47}$$

where (3.41a) can be inserted to obtain

$$\left(sI - \tilde{F}\right)\check{q}(s) = \left(\int\limits_0^1 \tilde{B}_1(\zeta)\check{\Psi}(\zeta, s)\mathrm{d}\zeta + \bar{B}_2 + \tilde{B}_3\check{\Psi}(1, s)\right)\check{\tilde{m}}^-(0, s). \qquad (3.48)$$

In view of $\mathrm{adj}(sI - \tilde{F})(sI - \tilde{F}) = \det(sI - \tilde{F})I$, both $\check{q}(s)$ and $\check{\tilde{m}}^-(0, s)$ can be expressed by

$$\check{q}(s) = \mathrm{adj}\left(sI - \tilde{F}\right)\left(\int\limits_0^1 \tilde{B}_1(\zeta)\check{\Psi}(\zeta, s)\mathrm{d}\zeta + \bar{B}_2 + \tilde{B}_3\check{\Psi}(1, s)\right)\check{\varphi}(s) \qquad (3.49\mathrm{a})$$

$$\check{\tilde{m}}^-(0, s) = \det\left(sI - \tilde{F}\right)\check{\varphi}(s) \qquad (3.49\mathrm{b})$$

in terms of the parametrizing variable $\check{\varphi}(s) \in \mathbb{C}^{n_-}$. To determine the time domain correspondences for $\check{q}(s)$, use

$$\mathrm{adj}(sI - \tilde{F}) = \sum_{i=0}^{n_q-1} \tilde{F}_i s^i \qquad (3.50)$$

with $\tilde{F}_i \in \mathbb{R}^{n_q \times n_q}$ and $s^i\check{\Psi}(z, s)\check{h}(s) \bullet\!\!-\!\!\circ \Psi[\mathrm{d}_\tau^i h](z, \tau)$, which yields the differential expression

$$q(\tau) = \sum_{i=0}^{n_q-1} \tilde{F}_i\left(\int\limits_0^1 \tilde{B}_1(\zeta)\Psi\left[\mathrm{d}_\tau^i\varphi\right](\zeta, \tau)\mathrm{d}\zeta + \bar{B}_2\mathrm{d}_\tau^i\varphi(\tau) + \tilde{B}_3\Psi\left[\mathrm{d}_\tau^i\varphi\right](1, \tau)\right) \qquad (3.51)$$

in terms of derivatives as well as distributed delays and predictions of the parametrizing variable $\varphi(\tau)$. It remains to parametrize $\tilde{m}(z, \tau)$ and $\tilde{n}(\tau)$ in terms of $\varphi(\tau)$, its derivatives and distributed time-shifts thereof. Use

$$\det\left(sI - \tilde{F}\right) = \sum_{i=0}^{n_q} a_i s^i \qquad (3.52)$$

with $a_i \in \mathbb{R}$ and $a_{n_q} = 1$ in (3.49b) to obtain the differential parametrization

$$\tilde{m}^-(0, \tau) = \sum_{i=0}^{n_q} a_i\mathrm{d}_\tau^i\varphi(\tau). \qquad (3.53)$$

Consequently, the differential expressions for $\tilde{m}(z, \tau)$ and $\tilde{n}(\tau)$ follow from inserting (3.53) in (3.46). Thus, the differential expressions for the fault detection kernel equation are summarized in the following lemma.

Lemma 3.2 (Differential expressions for the fault detection kernel equations)**.**
Let $\Psi[\cdot](z,\tau)$ be given by (3.45) and a_i be defined by (3.52). Then, the
integral kernels $q(\tau)$, $\tilde{m}(z,\tau)$ and $\tilde{n}(\tau)$ can be parametrized by the differential
expressions

$$q(\tau) = \sum_{i=0}^{n_q-1} \tilde{F}_i \left(\int_0^1 \tilde{B}_1(\zeta)\Psi\left[\mathrm{d}_\tau^i\varphi\right](\zeta,\tau)\mathrm{d}\zeta + \bar{B}_2\mathrm{d}_\tau^i\varphi(\tau) + \tilde{B}_3\Psi\left[\mathrm{d}_\tau^i\varphi\right](1,\tau) \right)$$
(3.54a)

$$\tilde{m}(z,\tau) = \sum_{i=0}^{n_q} a_i\Psi\left[\mathrm{d}_\tau^i\varphi\right](z,\tau)$$
(3.54b)

$$\tilde{n}(\tau) = J_- \sum_{i=0}^{n_q} a_i\Psi\left[\mathrm{d}_\tau^i\varphi\right](1,\tau)$$
(3.54c)

in terms of the parametrizing variable $\varphi(\tau)$.

With (3.54), $\tilde{m}(z,\tau)$ $\tilde{n}(\tau)$ and $q(\tau)$ can be expressed by distributed delays and
predictions as well as derivatives up to the order n_q of $\varphi(\tau)$. Therefore, (3.54) can
be used as a differential expression for the ODE-PDE system of the fault detection
kernel equations (3.32) in backstepping coordinates. In contrast to the formal
differential parametrizations for parabolic or biharmonic systems (see Lemma 2.3),
only a finite number of derivatives of the parametrizing variable $\varphi(\tau)$ is required
and no convergence conditions need to be considered in the planning of a reference
trajectory $\varphi^\star(\tau)$. Conversely, the distributed delays and predictions result in a lower
bound for the transition time.

Note that for a solution of the kernel equations, the flatness of the target system
(3.32) is not necessarily required, since only the specific transition (3.29) must be
parametrized. In contrast, however, to derive the integral kernels for a residual
generator (see Theorem 3.25), it must be ensured that the additional constraint
(2.54) can be satisfied. Thus, a condition is introduced in the following to ensure
that a solution of the kernel equations given in Lemma 3.1 can be parameterized in
terms of $\varphi(\tau)$ by the differential expressions specified in Lemma 3.2.

3.2.3.4 Fault detectability condition

Based on the differential expressions (3.54) a solution of (3.32) can be determined
by the planning of a reference trajectory $\varphi^\star(\tau)$ assigned to $\varphi(\tau)$. The reference

trajectories $\tilde{m}^\star(z,\tau)$ and $q^\star(\tau)$ assigned to the integral kernels $\tilde{m}(z,\tau)$ and $q(\tau)$ must satisfy the initial and end condition (3.29b) as well as

$$\tilde{m}(z,\tau)|_{\tau\in\{0,T\}} = 0, \quad z \in \Omega. \tag{3.55}$$

The latter results from mapping (3.29a) into backstepping coordinates via (3.30) and is the initial and end condition for the distributed system variable $\tilde{m}(z,\tau)$ of the ODE-PDE system (3.32) in backstepping coordinates. Additionally, $\varphi^\star(\tau)$ must be determined so that the resulting reference trajectory $m_f^\star(\tau)$ assigned to $m_f(\tau)$ given by (3.21a) satisfies the general detectability condition (2.54). To verify if such a reference trajectory $\varphi^\star(\tau)$ exists, the requirements for the integral kernels, i.e., the initial and end conditions (3.55) and (3.29b) as well as the additional constraint (2.54) are reformulated into requirements on the reference trajectory $\varphi^\star(\tau)$ by utilizing the differential expressions (3.54). To this end, the initial and end conditions (3.55) are embedded into setpoints, so that a nontrivial setpoint change for the PDE subsystem can be planned and a general transition of the ODE subsystem.

To take (3.55) into account, consider (3.54b) rowwise, which yields

$$e_{j,n_x}^\top \tilde{m}^\star(z,\tau) = \sum_{i=0}^{n_q} a_i e_{j,n_x}^\top \left(V \mathrm{d}_\tau^i \varphi^\star(\tau + \bar{\tau}_j(z,0)) + \int_0^z \tilde{P}_0(\zeta) \mathrm{d}_\tau^i \varphi^\star(\tau + \bar{\tau}_j(z,\zeta)) \mathrm{d}\zeta \right) \tag{3.56}$$

for $j = 1, \ldots, n_x$, in view of (3.44) and the substitutions $\varphi(\tau) \to \varphi^\star(\tau)$ and $\tilde{m}(z,\tau) \to \tilde{m}^\star(z,\tau)$. Consequently, (3.55) holds if $\varphi^\star(\tau)$ satisfies $\varphi^\star \in (C^{n_q-1}[-\tilde{\tau}^-, T+\tilde{\tau}^+])^{n_-}$ with $\mathrm{d}_\tau^{n_q}\varphi^\star(\tau)$, $\tau \in [-\tilde{\tau}^-, T+\tilde{\tau}^+]$ existing and

$$\varphi^\star(\tau + \bar{\tau}_j(z,\zeta))|_{\tau\in\{0,T\}} = 0, \quad 0 \leq \zeta \leq z \leq 1, j = 1, \ldots, n_x. \tag{3.57}$$

The latter embeds (3.55) into setpoints and can be achieved by imposing

$$\varphi^\star(\tau) = \begin{cases} 0 & : \tau \in \mathrm{I}_1 = [-\tilde{\tau}^-, \tilde{\tau}^+] \\ \tilde{\varphi}(\tau) & : \tau \in \mathrm{I}_2 = (\tilde{\tau}^+, T-\tilde{\tau}^-) \\ 0 & : \tau \in \mathrm{I}_3 = [T-\tilde{\tau}^-, T+\tilde{\tau}^+], \end{cases} \tag{3.58}$$

where $\tilde{\tau}^+$ and $\tilde{\tau}^-$ are the largest prediction and delay times resulting from the longest transportation time $\tilde{\tau}_{n_-}$ in the negative spatial direction and the longest transportation time $|\tilde{\tau}_{n_-+1}|$ in the positive spatial direction (see (3.2), (3.18) and (3.19)). In (3.58), $\tilde{\varphi}(\tau) \in \mathbb{R}^{n_-}$ is a degree of freedom that must satisfy $\tilde{\varphi} \in (C^{n_q-1}(\tilde{\tau}^+, T-\tilde{\tau}^-))^{n_-}$ with $\mathrm{d}_\tau^{n_q}\tilde{\varphi}(\tau)$ existing and

$$\mathrm{d}_\tau^i \tilde{\varphi}(\tau)|_{\tau\in\{\tilde{\tau}^+, T-\tilde{\tau}^-\}} = 0, \quad i = 0, \ldots, n_q - 1, \tag{3.59}$$

to ensure $\varphi^\star \in (C^{n_q-1}(\mathrm{I}))^{n_-}$ with $\mathrm{d}_\tau^{n_q}\varphi^\star(\tau)$ existing and fulfilling (3.57). To achieve $\varphi^\star(\tau) \not\equiv 0$, the condition $T - \tilde{\tau}^- > \tilde{\tau}^+$ can be inferred directly from (3.58), i.e., the length of the moving horizon T is lower bounded by $T > T_0$ with

$$T_0 = \tilde{\tau}^+ + \tilde{\tau}^-. \tag{3.60}$$

Under the condition (3.58), it follows from (3.54a), that also $q^\star(\tau)$ satisfies the required initial and end conditions (3.29b). Thus, $\tilde{\varphi}(\tau)$, respectively $\varphi^\star(\tau)$ in the light of (3.58), can be determined by an algebraic interpolation problem without the recourse of solving a differential equation, which presented in detail in Section 3.2.3.5.

Nevertheless, the existence of reference trajectories that satisfy the detectability condition (2.54) remains to be verified. To this end, express $m_f(\tau)$ given in (3.21a) in terms of $\varphi(\tau)$, which can be achieved by representing (3.21a) in backstepping coordinates $\tilde{m}(z,\tau)$ and $q(\tau)$. Use the spatial reversal $\bar{z} = 1 - z$ in (3.21a) to obtain

$$m_f(\tau) = -\langle \bar{E}_1, \bar{m}(\tau)\rangle_\Omega - E_2^\top \bar{m}^+(1,\tau) + E_3^\top \bar{m}^-(0,\tau) - E_4^\top q_w(\tau) + E_5^\top n(\tau). \tag{3.61}$$

Subsequently, solve (3.27c) for $n(\tau)$, insert the result in (3.61) and substitute $\bar{m}(z,\tau)$ in the derived expression by the inverse backstepping transformation (3.31) to obtain

$$m_f(\tau) = \int\limits_0^1 \tilde{E}_1(z)\tilde{m}(z,\tau)\mathrm{d}z + E_3^\top \tilde{m}^-(0,\tau) + \tilde{E}_3\tilde{m}(1,\tau) + \tilde{E}_4 q(\tau), \tag{3.62}$$

with the matrices

$$\tilde{E}_1(z) = E_5^\top \left(C_0^\top\right)^{-1} \bar{A}_0^\top(z) - \bar{E}_1^\top(z) + \left(E_5^\top \left(C_0^\top\right)^{-1}\left(J_-^\top + J_+^\top K_0\right)\right.$$
$$\left. - E_2^\top J_+\right)\bar{K}_I(1,z) + \int\limits_z^1 (E_5^\top \left(C_0^\top\right)^{-1}\bar{A}_0^\top(\zeta) - E_1^\top(\zeta))\bar{K}_I(\zeta,z)\mathrm{d}\zeta \tag{3.63a}$$

$$\tilde{E}_3 = -E_2^\top J_+ + E_5^\top \left(C_0^\top\right)^{-1}\left(J_- + K_0^\top J_+\right) \tag{3.63b}$$

$$\tilde{E}_4 = -E_4^\top J_w + E_5^\top \left(C_0^\top\right)^{-1} L_2^\top J_w. \tag{3.63c}$$

Then, $\tilde{m}(z,\tau)$ and $q(\tau)$ can be replaced by (3.54b) and (3.54a), so that (3.63) reads as

$$m_f(\tau) = \sum_{i=0}^{n_q}\left(\int\limits_0^1 X_{1,i}^f(z)\Psi[\mathrm{d}_\tau^i\varphi](z,\tau)\mathrm{d}z + X_{2,i}^f\mathrm{d}_\tau^i\varphi(\tau) + X_{3,i}^f\Psi[\mathrm{d}_\tau^i\varphi](1,\tau)\right) \tag{3.64}$$

with

$$X_{1,i}^f(z) = \tilde{E}_1(z)a_i + \tilde{E}_4\tilde{F}_i\tilde{B}_1(z) \tag{3.65a}$$

$$X_{2,i}^f = E_3^\top a_i + \tilde{E}_4\tilde{F}_i\bar{B}_2 \tag{3.65b}$$

$$X_{3,i}^f = \tilde{E}_3 a_i + \tilde{E}_4\tilde{F}_i\tilde{B}_3 \tag{3.65c}$$

where $\tilde{F}_{n_q} = 0$ is used (see (3.50)). Because of the distributed delays and predictions in $\Psi[\cdot](z,\tau)$, the consideration of the fault detectability condition (2.54) is involved in the time domain. However, by using the Laplace correspondence $\Psi[\mathrm{d}_\tau^i h](z,\tau) \circ\!\!-\!\!\bullet\, s^i\check{\Psi}(z,s)\check{h}(s)$, (2.54) can be investigated independently of a specific reference trajectory $\varphi^\star(\tau)$ for $\varphi(\tau)$. Hence, apply the formal Laplace transform to (3.64) to obtain

$$\check{m}_f(s) = \check{X}(s)\check{\varphi}(s) \tag{3.66}$$

with

$$\check{X}(s) = \sum_{i=0}^{n_q} \left(\int_0^1 X_{1,i}^f(z)\check{\Psi}(z,s)\mathrm{d}z + X_{2,i}^f + X_{3,i}^f\check{\Psi}(1,s) \right) s^i \ \in \mathbb{C}^{n_f \times n_-} \tag{3.67}$$

in view of the $\Psi[\mathrm{d}_\tau^i h](z,\tau) \circ\!\!-\!\!\bullet\, s^i\check{\Psi}(z,s)\check{h}(s)$. Based on (3.66), the fault detectability condition for heterodirectional hyperbolic ODE-PDE systems can be stated in the following theorem.

Theorem 3.3 (Fault detectability)
If

$$e_{i,n_f}^\top \check{X}(s) \not\equiv 0^\top, \quad i \in \{1, \ldots, n_f\} \tag{3.68}$$

holds with $\check{X}(s)$ given in (3.67), then the fault $f_i(t) = e_{i,n_f}^\top f(t)$ is detectable in the sense of Definition 1 for the system (3.1).

Proof. The prove of the fault detectability is based on the existence of a residual generator specified in Theorem 3.1, which requires that the integral kernels $m(z,\tau)$, $q_w(\tau)$, $q_d(\tau)$ and $n(\tau)$ are solutions of the kernel equations (3.22) and (3.23) as well as $m_f(\tau)$ given in (3.21a) satisfies (2.54). Because of the bounded invertibility of the backstepping transformation (3.30) (see, e.g., [41]), the imposed requirements on the integral kernels $m(z,\tau)$, $q_w(\tau)$, $q_d(\tau)$ and $n(\tau)$ are satisfied if the integral kernels in backstepping coordinates $\tilde{m}(\tau)$, $q(\tau)$ and $\tilde{n}(\tau)$ are solutions of the ODE-PDE system

(3.32) subject to the initial and end conditions (3.29b) and (3.55) as well as $m_f(\tau)$.

If the reference trajectory $\varphi^\star(\tau)$ takes into account the initial and end values (3.57) as well as $\varphi^\star \in (C^{n_q-1}[-\tilde\tau^-, T + \tilde\tau^+])^{n_-}$ with $\mathrm{d}_\tau^{n_q}\varphi^\star(\tau)$ existing, then the reference trajectories $\tilde m^\star(z, \tau)$, $q^\star(\tau)$ and $\tilde n^\star(\tau)$ derived from the differential expressions (3.54) are piecewise C-solutions of the fault detection kernel equations in backstepping coordinates (3.32) subject to (3.29b) and (3.55). Moreover, for $T > T_0$, with T_0 given in (3.60), (3.58) implies that there exists a $\varphi^\star(\tau) \not\equiv 0$ so that the resulting integral kernels are solutions of the kernel equations. It follows from the uniqueness of the Laplace transform (see, e.g., [92, Theorem 6.3]), that $\varphi^\star(\tau) \not\equiv 0$ implies $\check\varphi^\star(s) \not\equiv 0$. Since $\check\varphi^\star(s)$ and $\check X(s)$ are analytic functions (see, e.g., [92, Theorem 5a]) and (3.68) ensures $e_{i,n_f}^\top \check X(s) \not\equiv 0^\top$, there exists a $e_{i,n_f}^\top \check m_f^\star(s) \not\equiv 0^\top$ in view of (3.66) and the substitutions $\check\varphi(s) \to \check\varphi^\star(s)$ as well as $\check m_f(s) \to \check m_f^\star(s)$. According to the uniqueness of the Laplace transform, $e_{i,n_f}^\top \check m_f^\star(s) \not\equiv 0^\top$ implies $e_{i,n_f}^\top m_f^\star(\tau) \not\equiv 0^\top$, i.e., the detectability condition (2.54) can be satisfied. Thus, for the faults $f_i(t)$, $i = 1, \ldots, n_f$, for which (3.68) holds, a residual generator exists in accordance with Theorem 3.3. In view of Definition 1, this implies the detectability of the faults. ∎

Note that Theorem 3.3 implies also that if the system is subject to $\bar d(t) \not\equiv 0$ satisfying (2.14), then the fault $f_i(t)$ is detectable by results of Theorem 3.2.

The condition (3.68) depends on $\check X(s)$ given in (3.67) and is dependent on the terms $X_{j,i}^f$, $j = 1, 2, 3$, and $i = 0, \ldots, n_q$, described in (3.65). According to the derivation of the matrices in the terms in (3.65), $\check X(s)$ only depends on system parameters. Hence, (3.68) is a property of the system that can be checked a priori. Moreover, in view of (3.62), $m_f(\tau)$ can be regarded as an output of the target system (3.32). Thus, the fault detectability condition (2.54) can be satisfied if there is an input $\tilde n(\tau)$ of (3.32) which affects $m_f(\tau)$.

3.2.3.5 Systematic approach for the planning of the reference trajectory

The results of Section 3.2.3.4 show that if (3.68) holds, the reference trajectory $\varphi^\star(\tau)$ can be determined by a simple solution of an algebraic interpolation problem. However, for a successful fault detection, it is also necessary that the residual generator has a balanced response to the excitation of faults of different magnitudes and is insensitive to disturbances. In the following, these objectives are used to compute the reference trajectory $\varphi^\star(\tau)$.

For the reference trajectory planning of $\varphi^\star(\tau)$ in view of (3.58), impose

$$\tilde{\varphi}(\tau) = \sum_{i=1}^{n_\varphi} \theta_i(\tau)\eta_i, \quad \tau \in I_2 \tag{3.69}$$

with known linear independent functions $\theta_i \in C^{n_q-1}(I_2)$ and $d_\tau^{n_q}\theta_i(\tau)$ existing as well as the coefficients $\eta_i \in \mathbb{R}^{n_y}$ to be determined. From (3.69),

$$\varphi^\star(\tau) = \theta(\tau)\eta, \quad \tau \in [-\tilde{\tau}^-, T + \tilde{\tau}^+] \tag{3.70}$$

with

$$\theta(\tau) = \begin{cases} 0 & : \tau \in I_1 = [-\tilde{\tau}^-, \tilde{\tau}^+] \\ \tilde{\theta}(\tau) & : \tau \in I_2 = (\tilde{\tau}^+, T - \tilde{\tau}^-) \\ 0 & : \tau \in I_3 = [T - \tilde{\tau}^-, T + \tilde{\tau}^+], \end{cases} \tag{3.71}$$

follows, where $\tilde{\theta}(\tau) = [\theta_1(\tau) \cdots \theta_{n_\varphi}(\tau)] \otimes I_{n_y}$ and $\eta = \mathrm{col}\left(\eta_1, \ldots, \eta_{n_\varphi}\right)$ are introduced. To ensure (3.59) impose that η is a solution of

$$\bar{\Theta}\eta = 0, \tag{3.72}$$

with $\bar{\Theta} = \mathrm{col}\left(\bar{\Theta}_1, \bar{\Theta}_2\right) \in \mathbb{R}^{2n_y n_q \times n_y n_\varphi}$ and

$$e_{i,n_q}^\top \bar{\Theta}_1 = d_\tau^{i-1}\tilde{\theta}(\tau)\big|_{\tau=\tilde{\tau}^+}, \qquad e_{i,n_q}^\top \bar{\Theta}_2 = d_\tau^{i-1}\tilde{\theta}(\tau)\big|_{\tau=T-\tilde{\tau}^-}, \tag{3.73}$$

for $i = 1, \ldots, n_q$. However, a nontrivial reference trajectory $\varphi^\star(\tau) \not\equiv 0$ for (3.72) must be determined, which is possible only if the null space of $\bar{\Theta}$ denoted by $\mathcal{K}(\bar{\Theta})$ is nonempty, i.e., $\dim \mathcal{K}(\bar{\Theta}) > 0$ holds. This requirement can be achieved by choosing a sufficient number n_φ of linear independent functions $\theta_i(\tau)$. To make this more specific, an example for polynomial $\tilde{\theta}(\tau)$ is given in the following.

Example 3.2 *(Polynomial basis functions for $\tilde{\theta}(\tau)$).*
Impose the monomials $\theta_i(\tau) = \frac{(\tau - \tilde{\tau}^+)^{i-1}}{(i-1)!}$ for $\theta_i(\tau)$ in (3.69). Then, the computation of $\bar{\Theta}$ shows that $\mathrm{rank}\,\bar{\Theta} = 2n_y n_q$ holds for $n_\varphi > 2n_q$ and thus $\dim \mathcal{K}(\bar{\Theta}) = n_y n_\varphi - \mathrm{rank}\,\bar{\Theta} = n_y(n_\varphi - 2n_q) > 0$ is ensured. ◁

If $\dim \mathcal{K}(\bar{\Theta}) = \bar{n}_\Theta > 0$ holds, then a right annihilator $\bar{\Theta}^\perp \in \mathbb{R}^{n_y n_\varphi \times \bar{n}_\Theta}$ exists, which satisfies $\bar{\Theta}\bar{\Theta}^\perp = 0$. It can be computed by selecting the linear independent rows of $I - \bar{\Theta}^\dagger\bar{\Theta}$, where $\bar{\Theta}^\dagger$ is the Moore-Penrose generalized inverse of $\bar{\Theta}$. Thus, a nontrivial solution, i.e., $\eta \neq 0$, can be computed by

$$\eta = \bar{\Theta}^\perp \eta^* \tag{3.74}$$

with $\eta^* \in \mathbb{R}^{\bar{n}_\Theta}$ and $\eta^* \notin \mathcal{K}(\bar{\Theta}^\perp)$. Because of (3.72), any coefficient vector η determined by (3.74) ensures (3.59) and thus the resulting reference trajectory $\varphi^\star(\tau)$ determined by (3.70) ensures (3.57) and satisfies $\varphi^\star \in (C^{n_q-1}[-\tilde{\tau}^-, T+\tilde{\tau}^+])^{n_-}$ with $\mathrm{d}_\tau^{n_q} \varphi^\star(\tau)$ existing. Moreover, the degrees of freedom η^* can be used to ensure the detectability condition (2.54) and to make the residual generator less sensitive with respect to the bounded disturbance $\bar{d}(t)$.

In Section 2.3.4.4 it was shown how to derive a residual generator with a prescribed stationary gain. For the case that the required condition (2.113) is not satisfied, an extension of the approach in Section 2.3.4.4 is proposed. Instead of prescribing the response to constant faults as shown in Section 2.3.4.4, the response of the residual generator to specific time-varying fault signals will be regarded in the sequel. Consider the design form of the residual generator (3.25)

$$r(t) = \int_0^T m_f^\top(\tau) f(t-\tau) \mathrm{d}\tau \tag{3.75}$$

(see (2.51)) in terms of the fault $f(t)$. Let $f^\star(t) \in \mathbb{R}^{n_f}$, $t \in [0, T]$ be an expected signal for the fault $f(t)$. Then, the response of (3.75) at time $t = T$ to the ith component $f_i^\star(t)$ of $f^\star(t)$, i.e.,

$$\bar{r}_i = \int_0^T m_f^\top(\tau) e_{i,n_f} f_i^\star(T-\tau) \mathrm{d}\tau, \quad i = 1, \ldots, n_f, \tag{3.76}$$

serves as a measure for the influence of the expected fault signal $f_i^\star(t)$ on the residual signal $r(t)$. To be specific, the detectability condition (2.54) can be satisfied if the expected fault signals $f_i^\star(t)$ are such that

$$\bar{r}_i \neq 0, \quad i = 1, \ldots, n_f, \tag{3.77}$$

can be achieved. Summarizing (3.76) for $i = 1, \ldots, n_f$,

$$\bar{r} = \int_0^T F^\star(\tau) m_f(\tau) \mathrm{d}\tau \tag{3.78}$$

with $\bar{r} = \mathrm{col}\left(\bar{r}_1, \ldots, \bar{r}_{n_f}\right)$ and $F^\star(\tau) = \mathrm{diag}(f_1^\star(T-\tau), \ldots, f_{n_f}^\star(T-\tau))$ results. To determine η^* so that $\bar{r}$ given by (3.78) satisfies (3.77), insert (3.70) in (3.64) after substituting $\varphi(\tau) \to \varphi^\star(\tau)$ and $m_f(\tau) \to m_f^\star(\tau)$ to obtain

$$m_f^\star(\tau) = \Theta_f(\tau) \eta^* \tag{3.79}$$

with

$$\Theta_f(\tau) = \sum_{i=0}^{n_q} \left(\int_0^1 X_{1,i}^f(z) \Psi[\mathrm{d}_\tau^i \Theta](z,\tau) \mathrm{d}z + X_{2,i}^f \mathrm{d}_\tau^i \Theta(\tau) + X_{3,i}^f \Psi[\mathrm{d}_\tau^i \Theta](1,\tau) \right) \bar{\Theta}^\perp \tag{3.80}$$

in view of (3.74). By using (3.79) in (3.78), the linear system of equations

$$\bar{r} = \bar{\Theta}_f \eta^* \tag{3.81}$$

with

$$\bar{\Theta}_f = \int_0^T F^\star(\tau) \Theta_f(\tau) \mathrm{d}\tau, \tag{3.82}$$

is derived for the determination of η^*. For $\bar{r} \in \mathcal{R}(\bar{\Theta}_f)$, where $\mathcal{R}(\bar{\Theta}_f)$ is the range of $\bar{\Theta}_f$, (3.81) has the solution

$$\eta^* = \bar{\Theta}_f^\dagger \bar{r} + (I - \bar{\Theta}_f^\dagger \bar{\Theta}_f) \bar{r}^*. \tag{3.83}$$

Consequently, choosing $\bar{r} \in \mathcal{R}(\bar{\Theta}_f)$ which satisfies also (3.77), it is ensured that the resulting $m_f^\star(\tau)$ from (3.79) with η^* given by (3.83) satisfies the detectability condition (2.54). A suitable $\bar{r}$ exists, if $F^\star(\tau)$ is such that the resulting $\bar{\Theta}_f$ from (3.82) holds

$$e_{i,n_f}^\top \bar{\Theta}_f \neq 0. \tag{3.84}$$

Moreover, if $\mathrm{rank}\,(I - \bar{\Theta}_f^\dagger \bar{\Theta}_f) > 0$ holds, then the degrees of freedom $\bar{r}^* \in \mathbb{R}^{\bar{n}_\Theta}$ can be used to make the residual generator less sensitive with respect to the unknown but bounded disturbance $\bar{d}(t)$. Consider the threshold value r_B as a measure for the influence of $\bar{d}(t)$ on $r(t)$. To express r_B in dependence of $\bar{r}^*$, at first express $m_{\bar{d}}^\star(\tau)$ in terms of $\varphi^\star(\tau)$ (see (2.60)). As shown in Appendix A.8,

$$m_{\bar{d}}^\star(\tau) = \Theta_{\bar{d}}(\tau) \eta^* \tag{3.85}$$

can be derived by a similar derivation as used for (3.79). Then, insert (3.83) in (3.85) to obtain

$$m_{\bar{d}}^\star(\tau) = \bar{\Theta}_0(\tau) + \bar{\Theta}_1(\tau) \bar{r}^* \tag{3.86}$$

with

$$\bar{\Theta}_0(\tau) = \Theta_{\bar{d}}(\tau)\bar{\Theta}_f^\dagger \bar{r} \tag{3.87a}$$

$$\bar{\Theta}_1(\tau) = \Theta_{\bar{d}}(\tau)(I - \bar{\Theta}_f^\dagger \bar{\Theta}_f). \tag{3.87b}$$

Thus, the threshold value can be computed by

$$r_B = \int\limits_0^T \left|\bar{\theta}_0(\tau) + \bar{\theta}_1(\tau)\bar{r}^*\right|^\top \mathrm{d}\tau\delta, \tag{3.88}$$

whereas $\bar{r}^*$ should be determined by

$$r_B = \min_{\bar{r}^* \in \mathcal{K}(\bar{\Theta}_f)} \int\limits_0^T |\bar{\theta}_0(\tau) + \bar{\theta}_1(\tau)\bar{r}^*|^\top \mathrm{d}\tau\delta. \tag{3.89}$$

With $\bar{r}^*$ resulting from (3.89) and a suitable $\bar{r}$ that satisfies (3.77), a reference trajectory $\varphi^\star(\tau)$ can be computed with (3.70) such that the integral kernels following from (3.54) satisfy the requirements for a residual generator given in Theorem 3.1. In addition, the residual signal $r(t)$ is made less sensitive to the unknown but bounded disturbances $\bar{d}(t)$ and can be balanced with respect to the expected fault signals $f^\star(t)$.

3.2.4 Fault detection for a cable with a payload immersed in water

To demonstrate the previously presented fault detection approach, it is applied to a model of a cable with an attached payload immersed in water of constant flow. This real-world motivated example system is illustrated in Figure 3.2. Such models are used, e.g., to describe the positioning of a payload at the seabed with deep-sea construction vessels (see, e.g., [13, 87]). The upper end of the cable is attached to a crane on the deep-sea construction vessel and at the lower end the equipment to be positioned is attached. The mathematical modeling of the cable with payload using the extended Hamilton's principle and a linearization of the nonlinear model leads to two coupled wave equations describing the motion of the deflection of the cable and an ODE for the dynamics of the payload. For details see [13, 87] and the references therein. In contrast to the scenario regarded in [87], the length of the cable is considered to be constant, but faults and further disturbances have been added. The following simulations are implemented for MATLAB 2020a and are available in [108].
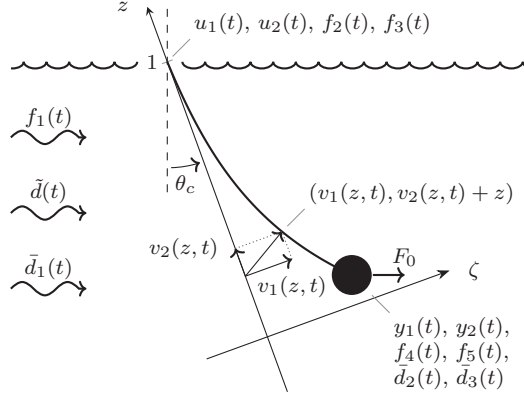
Figure 3.2: Schematic of the cable with an attached payload immersed in water of constant flow F_0, with actuators at $z = 1$ and measurement at $z = 0$ subject to multiple disturbances $\tilde{d}(t)$, $\bar{d}(t)$ and faults $f(t)$ as described by (3.90).

Before the proposed fault detection approach can be applied to the considered model, it must be at first rewritten into the form (3.1). After a normalization of the spatial domain to length 1, the *cable deflection in lateral and longitudinal direction* $v_1(z,t)$ and $v_2(z,t)$ (see Figure 3.2) is described by

$$\partial_t^2 v_1(z,t) = \kappa_1(z)\partial_z^2 v_1(z,t) + \kappa_2(z)\partial_z v_1(z,t) + \kappa_3(z)\partial_z v_2(z,t)$$
$$+ \kappa_4(z)\partial_t v_1(z,t) + \bar{d}_1(t) + e_1(z)f_1(t) \tag{3.90a}$$

$$\partial_t^2 v_2(z,t) = \kappa_5(z)\partial_z^2 v_2(z,t) + \kappa_6(z)\partial_z v_1(z,t) + \kappa_7(z)\partial_t v_2(z,t)$$
$$+ \bar{d}_1(t) + \tilde{d}(t) \tag{3.90b}$$

defined on $(z,t) \in (0,1) \times \mathbb{R}^+$. The consideration of the attached payload leads to the dynamic BC at $z = 0$

$$\ddot{v}_1(0,t) = \kappa_8 \dot{v}_1(0,t) + \kappa_9 \partial_z v_1(0,t) + \kappa_{10} \partial_z v_2(0,t), \qquad t > 0 \tag{3.90c}$$
$$\ddot{v}_2(0,t) = \kappa_{11} \dot{v}_2(0,t) + \kappa_{12} \partial_z v_2(0,t) + \kappa_{13} \partial_z v_1(0,t), \qquad t > 0. \tag{3.90d}$$

At the upper boundary, i.e., $z = 1$, the cable is actuated by the forces $u_i(t) \in \mathbb{R}$, $i = 1, 2$, so that the corresponding BC becomes

$$\partial_z v_1(1,t) = b_1(1 + e_2\Delta f_2(t))u_1(t), \qquad t > 0 \tag{3.90e}$$
$$\partial_z v_2(1,t) = b_2 u_2(t) + e_3 f_3(t), \qquad t > 0. \tag{3.90f}$$

As measurement $y(t) = \mathrm{col}\,(y_1(t), y_2(t)) \in \mathbb{R}^2$ the strain $\partial_z v_2(0,t)$ and the pivot

angle $\partial_z v_1(0,t)$ at the lower end of the cable $z = 0$ are available, which are given by

$$y_1(t) = (1 + \Delta f_4(t))\partial_z v_1(0,t) + \bar{d}_2(t), \qquad t \geq 0 \qquad (3.90\text{g})$$

$$y_2(t) = \partial_z v_2(0,t) + f_5(t) + \bar{d}_3(t), \qquad t \geq 0. \qquad (3.90\text{h})$$

Note that the outputs (3.90g) and (3.90h) differ from those in [87] to simplify the following transformations of the coupled wave equation system (3.90) into a heterodirectional hyperbolic ODE-PDE system of the form (3.1).

Other differences to [87] are the added faults $f_i(t)$, $i = 1, \ldots, 5$, and disturbances $\tilde{d}(t)$ as well as $\bar{d}_j(t)$, $j = 1, 2, 3$. The disturbance $\tilde{d}(t) \in \mathbb{R}$ is acting in-domain with the signal form $\tilde{d}(t) = d_1^0 \sin(5t + \phi_d)$, whereas the particular signal is specified by the unknown parameters $d_1^0, \phi_d \in \mathbb{R}$. Hence, $\tilde{d}(t)$ can be described by the signal model (2.15) with the known matrices

$$S_d = \begin{bmatrix} 0 & -5 \\ 5 & 0 \end{bmatrix}, \qquad R_d = \begin{bmatrix} 0 & 1 \end{bmatrix}, \qquad (3.91)$$

the state $v_d(t) \in \mathbb{R}^2$ and the unknown IC $v_d(0) = v_d^0 \in \mathbb{R}^2$. The further disturbances $\bar{d}_i(t) \in \mathbb{R}$, $i = 1, 2, 3$, are absolutely bounded by $|\bar{d}_i(t)| \leq \delta_i$ with known upper bound $\delta = \mathrm{col}\,(0.03, 0.01, 0.02)$. A fault $f_1(t) \in \mathbb{R}$ is affecting the deflection of the cable in lateral direction via the spatial characteristic $e_1(z) = 1$, which is thus an additive process fault. Additionally, both actuators $u_i(t)$, $i = 1, 2$, can be faulty. The actuator related to $u_1(t)$ is subject to a multiplicative actuator fault described by $e_2 = 10.00 \times 10^3$ and $\Delta f_2(t) \in \mathbb{R}$, which is rewritten as the additive fault $f_2(t) = u_1(t)\Delta f_2(t)$ so that (3.90e) becomes

$$\partial_z v_1(1,t) = b_1 u_1(t) + b_1 e_2 f_2(t), \qquad t > 0. \qquad (3.92)$$

The actuator related to $u_2(t)$ is affected by the additive actuator fault $f_3(t) \in \mathbb{R}$ with $e_3 = 0.37$. Also the measurements are assumed to be potentially faulty, where $y_1(t)$ is subject to the multiplicative sensor fault described by $\Delta f_4(t) \in \mathbb{R}$. This multiplicative fault is rewritten in the form of an additive sensor fault $f_4(t) = \Delta f_4(t)\partial_z v_1(0,t)$, so that (3.90g) can also be described by

$$y_1(t) = \partial_z v_1(0,t) + f_4(t) + \bar{d}_2(t), \qquad t \geq 0. \qquad (3.93)$$

The measurement $y_2(t)$ is subject to the additive sensor fault $f_5(t) \in \mathbb{R}$. According to the modeling in [87], the system parameters $\kappa_i(z)$, $i = 1, ..., 18$, and b_i, $i = 1, 2$,

Table 3.1: Normalized model parameters for the cable with a payload taken from [87].

Parameter	Value	Parameter	Value
L_c	1.21×10^3	A_c	470×10^{-6}
E_c	70.30×10^9	m_c	8.95
M_L	8.00×10^3	V_p	5
g_a	9.80	V_s	2
ρ_w	1.02×10^3	c_u	500×10^{-3}
c_v	300×10^{-3}	c_h	500×10^{-3}
c_w	300×10^{-3}	θ_c	1.40
M_c	2.88×10^3	ρ_c	8.47

are specified in dependence of physical parameters and are given by

$$\kappa_1(z) = \frac{\frac{3}{2}E_cA_c\phi_c^2(z) + T_c(z)}{m_cL_c^2}, \quad \kappa_2(z) = \frac{\frac{1}{L}E_cA_c\frac{\mathrm{d}_z\epsilon_c(z)}{L_c} + \rho g_a}{m_cL_c} \tag{3.94a}$$

$$\kappa_3(z) = -\frac{E_cA_c\mathrm{d}_z\phi_c(z)}{m_cL_c^2}, \qquad \kappa_4 = \frac{c_v}{m_c} \tag{3.94b}$$

$$\kappa_5 = \frac{E_cA_c}{m_cL_c^2}, \qquad \kappa_6(z) = -\frac{E_cA_c\mathrm{d}_z\phi_c(z)}{m_cL_c^2} \tag{3.94c}$$

$$\kappa_7 = -\frac{c_u}{m_c}, \qquad \kappa_8 = -\frac{c_w}{M_L} \tag{3.94d}$$

$$\kappa_9 = \frac{E_cA_c\phi_c^2(0)}{2M_LL}, \qquad \kappa_{10} = -\frac{E_cA_c\phi_c(0)}{M_LL} \tag{3.94e}$$

$$\kappa_{11} = -\frac{c_h}{M_L}, \qquad \kappa_{12} = \frac{E_cA_c}{M_LL} \tag{3.94f}$$

$$\kappa_{13} = -\frac{E_cA_c\phi_c(0)}{2M_LL}, \qquad b_1 = \frac{L}{E_cA_c(\epsilon_c(1) + \frac{1}{2}\phi_c^2(1)) + T_c(1)} \tag{3.94g}$$

$$b_2 = \frac{L}{E_cA_c}, \qquad \phi_c(z) = \arctan\left(\frac{F_0}{\rho g_aL_cz + M_cg_a}\right) - \theta_c \tag{3.94h}$$

$$T_c(z) = \rho_cg_aLz + Mg_a, \qquad F_0 = \frac{\rho_w}{2}V_s^2. \tag{3.94i}$$

The values of the physical parameters in (3.94) are assembled in Table 3.1.

To rewrite the system (3.90) into a first order system of PDEs, the *Riemann*

coordinates

$$\breve{v}_1(z,t) = \partial_t v_1(z,t) + \sqrt{\kappa_1(z)}\partial_z v_1(z,t) \tag{3.95a}$$

$$\breve{v}_2(z,t) = \partial_t v_2(z,t) + \sqrt{\kappa_5(z)}\partial_z v_2(z,t) \tag{3.95b}$$

$$\breve{v}_3(z,t) = \partial_t v_2(z,t) - \sqrt{\kappa_5(z)}\partial_z v_2(z,t) \tag{3.95c}$$

$$\breve{v}_4(z,t) = \partial_t v_1(z,t) - \sqrt{\kappa_1(z)}\partial_z v_1(z,t) \tag{3.95d}$$

are introduced (see, e.g., [19, Section 7.3]). By following the calculations in [87], the wave equations (3.90a) and (3.90b) are mapped into

$$\partial_t \breve{v}(z,t) = \Lambda(z)\partial_z \breve{v}(z,t) + \breve{A}(z)\breve{v}(z) + \breve{E}_1(z)f(t) + \breve{G}_{c,1}(z)d(t) \tag{3.96}$$

with $\Lambda(z) = \mathrm{diag}\left(\sqrt{\kappa_1(z)}, \sqrt{\kappa_5}, -\sqrt{\kappa_5}, -\sqrt{\kappa_1(z)}\right)$ and

$$e_{1,4}^\top \breve{A}(z) = e_{4,4}^\top \breve{A}(z) = \begin{bmatrix} s_1(z) + \frac{\kappa_4}{2} & \frac{\kappa_3(z)}{2\kappa_5} & -\frac{\kappa_3(z)}{2\sqrt{\kappa_5}} & \frac{\kappa_4}{2} - s_1(z) \end{bmatrix} \tag{3.97a}$$

$$e_{2,4}^\top \breve{A}(z) = e_{3,4}^\top \breve{A}(z) = \begin{bmatrix} \frac{\kappa_6(z)}{2\sqrt{\kappa_1(z)}} & \frac{\kappa_7}{2} & \frac{\kappa_7}{2} & -\frac{\kappa_6(z)}{2\sqrt{\kappa_1(z)}} \end{bmatrix} \tag{3.97b}$$

$$s_1(z) = \frac{\kappa_2(z) - \frac{1}{2}\mathrm{d}_z\kappa_1(z)}{2\sqrt{\kappa_1(z)}} \tag{3.97c}$$

$$e_{1,4}^\top \breve{E}_1(z) = e_{4,4}^\top \breve{E}_1 = \begin{bmatrix} 1 & 0 & 0 & 0 & 0 \end{bmatrix} \tag{3.97d}$$

$$e_{2,4}^\top \breve{E}_1(z) = e_{3,4}^\top \breve{E}_1(z) = 0 \tag{3.97e}$$

$$e_{1,4}^\top \breve{G}_{c,1}(z) = e_{4,4}^\top \breve{G}_{c,1}(z) = \begin{bmatrix} 0 & 1 & 0 & 0 \end{bmatrix} \tag{3.97f}$$

$$e_{2,4}^\top \breve{G}_{c,1}(z) = e_{3,4}^\top \breve{G}_{c,1}(z) = \begin{bmatrix} 1 & 1 & 0 & 0 \end{bmatrix}. \tag{3.97g}$$

In (3.96), the faults are summarized to $f(t) = \mathrm{col}\left(f_1(t), \ldots, f_5(t)\right)$ and the disturbances to $d(t) = \mathrm{col}\left(\tilde{d}(t), \bar{d}_1(t), \bar{d}_2(t), \bar{d}_3(t)\right)$. Note that with $\min \sqrt{\kappa_1(z)} = 2.58$ and $\sqrt{\kappa_5} = 1.59$, the transport velocities $\lambda_i(z)$, $i = 1, \ldots, 4$, as the diagonal entries of $\Lambda(z)$ are already sorted in descending order according to (3.2) because of the matched choice of the Riemann coordinates (3.95) in contrast to [87]. Because of $\kappa_1(z) > \kappa_5 > 0$, $J_- = \begin{bmatrix} I_2 & 0 \end{bmatrix}$ and $J_+ = \begin{bmatrix} 0 & I_2 \end{bmatrix}$ follow with the identity matrix $I_2 \in \mathbb{R}^{2\times 2}$ according to (3.2) and (3.3). Regarding the dynamic BCs at $z = 0$, the ODE state

$$w(t) = \mathrm{col}\left(\dot{v}_1(0,t), \dot{v}_2(0,t)\right) \tag{3.98}$$

is introduced so that the boundary dynamics are governed by

$$\dot{w}(t) = Fw(t) + \breve{L}_2 \breve{v}^-(0,t) \tag{3.99}$$

with

$$F = \begin{bmatrix} \kappa_8 - \frac{\kappa_9}{\sqrt{\kappa_1(0)}} & -\frac{\kappa_{10}}{\sqrt{\kappa_5}} \\ -\frac{\kappa_{12}}{\sqrt{\kappa_1(0)}} & \kappa_{11} - \frac{\kappa_{13}}{\sqrt{\kappa_5}} \end{bmatrix}, \qquad \breve{L}_2 = \begin{bmatrix} \frac{\kappa_9}{\sqrt{\kappa_1(0)}} & \frac{\kappa_{10}}{\sqrt{\kappa_5}} \\ \frac{\kappa_{12}}{\sqrt{\kappa_1(0)}} & \frac{\kappa_{13}}{\sqrt{\kappa_5}} \end{bmatrix}. \tag{3.100}$$

In contrast to [87], the ODE state (3.98) shows that a second order ODE system is sufficient to describe the boundary dynamics for the considered setup. In view of (3.99), the BCs at $z = 0$ can be expressed by

$$\breve{v}^+(0, t) = \breve{Q}_0 \breve{v}^-(0, t) + \breve{H}_2 w(t) \tag{3.101}$$

and the corresponding matrices in (3.101) are

$$\breve{Q}_0 = \begin{bmatrix} 0 & -1 \\ -1 & 0 \end{bmatrix} \qquad \text{and} \qquad \breve{H}_2 = \begin{bmatrix} 0 & 2 \\ 2 & 0 \end{bmatrix}. \tag{3.102}$$

At $z = 1$, the BC is

$$\breve{v}^-(1, t) = \breve{Q}_1 \breve{v}^+(1, t) + \breve{B}_3 u(t) + \breve{E}_3 f(t), \tag{3.103}$$

with $u(t) = \mathrm{col}\,(u_1(t),\, u_2(t))$ and the matrices in (3.103) are

$$\breve{Q}_1 = \begin{bmatrix} 0 & 1 \\ 1 & 0 \end{bmatrix}, \qquad\qquad \breve{B}_3 = \begin{bmatrix} 2\sqrt{\kappa_1(1)}b_1 & 0 \\ 0 & 2\sqrt{\kappa_5}b_2 \end{bmatrix} \tag{3.104a}$$

$$\breve{E}_3 = \begin{bmatrix} 0 & 2\sqrt{\kappa_1(1)}e_2 & 0 & 0 & 0 \\ 0 & 0 & 2\sqrt{\kappa_5}e_3 & 0 & 0 \end{bmatrix}. \tag{3.104b}$$

Finally, also the output equations (3.90g) and (3.90h) can be expressed in Riemann coordinates by

$$y(t) = \breve{C}_0 \breve{v}^-(0, t) + C_1 w(t) + E_5 f(t) + G_5 d(t) \tag{3.105}$$

with the matrices $\breve{C}_0 = \mathrm{diag}\left(\frac{1}{2\sqrt{\kappa_1(0)}}, \frac{1}{2\sqrt{\kappa_5}} \right)$, $C_1 = -\breve{C}_0$,

$$E_5 = \begin{bmatrix} 0 & 0 & 0 & 1 & 0 \\ 0 & 0 & 0 & 0 & 1 \end{bmatrix} \qquad \text{and} \qquad G_5 = \begin{bmatrix} 0 & 0 & 1 & 0 \\ 0 & 0 & 0 & 1 \end{bmatrix}. \tag{3.106}$$

To rewrite (3.96) in the required form (3.1), solve (3.96) for $\partial_z \breve{v}(z, t)$ by multiplying (3.96) with $\Gamma(z) = \Lambda^{-1}(z)$. The inverse of $\Lambda(z)$ exists because $\lambda_i(z) \neq 0$, $i = 1, \ldots, 4$,

holds. However, in the resulting PDE

$$\partial_z \breve{v}(z,t) = \Gamma(z)\partial_t \breve{v}(z,t) + \Gamma(z)\breve{A}(z)\breve{v}(z) + \Gamma(z)\breve{E}_1(z)f(t)$$
$$+ \Gamma(z)\breve{G}_{c,1}(z)d(t), \qquad (z,t) \in (0,1) \times \mathbb{R}^+, \qquad (3.107)$$

the main diagonal entries of the matrix $\Gamma(z)\breve{A}(z)$ in (3.107) are not zero as it is required for (3.1) (see (3.97a) and (3.97b)). To obtain a PDE (3.1a) with the matrix $A(z)$ satisfying $e_{i,4}^\top A(z)e_{i,4} = a_{ii}(z) = 0$, $i = 1, \ldots, 4$, the transform

$$x(z,t) = \breve{W}(z)\breve{v}(z,t), \qquad (3.108)$$

with $\breve{W}(z) = \operatorname{diag}(\breve{w}_1(z), \ldots, \breve{w}_4(z))$ and

$$\breve{w}_i(z) = \mathrm{e}^{-\int_0^z \frac{\breve{a}_{ii}(\zeta)}{\lambda_i(\zeta)} \mathrm{d}\zeta}, \quad z \in [0,1], i = 1, \ldots, 4, \qquad (3.109)$$

proposed, e.g., in [41, Section 3], is used. In (3.109), $\breve{a}_{ii}(z) \in \mathbb{R}$, $i = 1, \ldots, 4$, are the main diagonal entries of $\breve{A}(z)$. Since $\breve{W}(z)$ is diagonal and $\breve{w}_i(z) > 0$, $z \in [0,1]$, $i = 1, \ldots, 4$, holds, $\breve{W}^{-1}(z)$ exists and thus (3.108) is invertible for $z \in [0,1]$. With (3.108) applied to (3.107), (3.99), (3.101), (3.103) and (3.105), the governing equations for the model of the cable with a payload immersed in water are finally obtained in the required form (3.1). The matrices of the system (3.1), that have not been introduced before, read as

$$A(z) = \left(\partial_z \breve{W}(z) + \breve{W}(z)\Gamma(z)\breve{A}(z)\right)\breve{W}^{-1}(z) \qquad (3.110a)$$

$$E_1(z) = \breve{W}(z)\Gamma(z)\breve{E}_1(z), \qquad\qquad G_1(z) = \breve{W}(z)\Gamma(z)\breve{G}_1(z) \qquad (3.110b)$$

$$Q_0 = \breve{W}_+(0)\breve{Q}_0\breve{W}_-^{-1}(0), \qquad\qquad H_2 = \breve{W}_+(0)\breve{H}_2 \qquad (3.110c)$$

$$Q_1 = \breve{W}_-(1)\breve{Q}_1\breve{W}_+^{-1}(1), \qquad\qquad B_3 = \breve{W}_-(1)\breve{B}_3 \qquad (3.110d)$$

$$E_3 = \breve{W}_-(1)\breve{E}_3, \qquad\qquad C_0 = \breve{C}_0\breve{W}_-^{-1}(0) \qquad (3.110e)$$

wherein $\breve{W}_+(z) = J_+\breve{W}(z)J_+^\top$ and $\breve{W}_-(z) = J_-\breve{W}(z)J_-^\top$ are used.

To design the fault detection residual generator for the model of the cable with a payload, the fault detection kernel equations (3.22) subject to (3.23) must be solved. For the proposed approach in Section 3.2.3, at first the backstepping kernel equations (3.35) must be solved to compute the backstepping kernel $\bar{K}(z,\zeta)$. To this end, the boundary value problem (3.35) is converted into integral equations with the method of characteristics, which can be solved with the method of successive approximation (see, e.g., [40, Section VI.B.]). To be specific, the integral equations are solved along 301 characteristic lines on a discrete grid of 301 points. The successive approximation is stopped when the maximum pointwise difference between two iterations is less than

1×10^{-6}, which requires 7 steps. With the resulting backstepping kernel $\bar{K}(z, \zeta)$ on an equidistant spaced grid for z and ζ with 301^2 points, the matrices for the fault detection kernel equations in backstepping coordinates (3.32) and also the coefficient matrices $X_{j,i}^f$, $j = 1, \ldots, 3$, and $i = 1, \ldots, n_q$, for the differential parametrization of $m_f(\tau)$ (see (3.64) and (3.65)) can be computed. Since the resulting $\check{X}(s)$ given in (3.67) and shown in Figure 3.3 satisfies (3.68), the detectability of the faults $f_i(t)$, $i = 1, \ldots, 5$, in view of Theorem 3.3 is verified.

To determine a suitable reference trajectory $\varphi^\star(\tau)$ in view of (3.70) for the parametrization of the integral kernels $m^\star(z, \tau)$, $q^\star(\tau)$ and $n^\star(\tau)$, the monomials $\theta_i(\tau) = \frac{(\tau - \tilde{\tau}^+)^{i-1}}{(i-1)!}$, $i = 1, \ldots, n_\varphi$, are convenient. As shown in Example 3.2, rank $\bar{\Theta} = 2n_y n_q = 16$ results, so that for $n_\varphi > 8$, a nontrivial reference trajectory $\varphi^\star(\tau)$ can be determined. Thus, $n_\varphi = 10$ is chosen. However, suitable $f_i^\star(t)$ for (3.78) must be chosen to derive a $\bar{\Theta}_f$ given in (3.82) so that (3.84) holds. Numerical evaluations of (3.82) have shown that $f_i^\star(t) = \frac{1}{2}t^2$, $i = 1, \ldots, 5$, leads to suitable results so that a $\bar{r} = \begin{bmatrix} 0.389 & 1.04 & -0.371 & 2.57 & -1.54 \end{bmatrix} \in \mathcal{R}(\bar{\Theta}_f)$ satisfying (3.77) can be chosen. Thus, the coefficients η in (3.70) can be determined by (3.74), where η^* follows from (3.83) with $\bar{r}^*$ as a solution of (3.89). The latter is solved numerically with the `fminsearch` function from MATLAB and zero as initial point.

The threshold value r_B and the normalized detection delay Δ_f are computed for a polynomial basis function $\tilde{\theta}(\tau)$ of order $n_\varphi = 10$ and several values of the remaining design parameter $T > T_0$. The normalized detection delay Δ_f denotes the first time instant where the threshold r_B is exceeded by $|\langle m_f, h_f(\tau) \rangle_I|$, $h_f(t) = \text{col}(\frac{1}{\bar{r}_1}, \ldots, \frac{1}{\bar{r}_{n_f}})$ with $\bar{r}_i = e_{i,n_f}^\top \bar{r}$. For the lower bound of T, $T_0 = 1.26$ is obtained, which is computed with the longest transportation time in positive and negative spatial direction $\tilde{\tau}^- = \tilde{\tau}^+ = 0.63$ given by (3.18) and (3.19). The result in Figure 3.4 shows that a compromise is required for the moving horizon length T, since the threshold r_B decreases and the detection delay Δ_f increases with increasing T. Thus, $T = 6$ and $n_\varphi = 10$ is chosen, yielding the threshold $r_B = 55.10 \times 10^{-3}$ as well as the integral kernels $n(\tau)$ and $m_u(\tau)$ shown in Figure 3.5, which are computed on a grid with the step size 0.02. Note that a higher order for the polynomial $\tilde{\theta}(\tau)$, i.e., $n_\varphi > 10$ has only minor effects on the threshold value r_B and the normalized detection delay Δ_f but increases the numerical errors significantly.

The simulation of the faulty cable is performed in MATLAB using a finite-dimensional model for (3.90) determined by the spectral method. To be specific, the spatial derivatives in (3.90a) and (3.90b) are approximated by *Chebyshev differentiation matrices* of order 51 (see, e.g, in [86, Section 6]). Based on the resulting finite-dimensional model, (3.90) can be rewritten into a state space system of order 202, which is simulated in MATLAB using the `lsim` function. Since the input signal $u(t)$
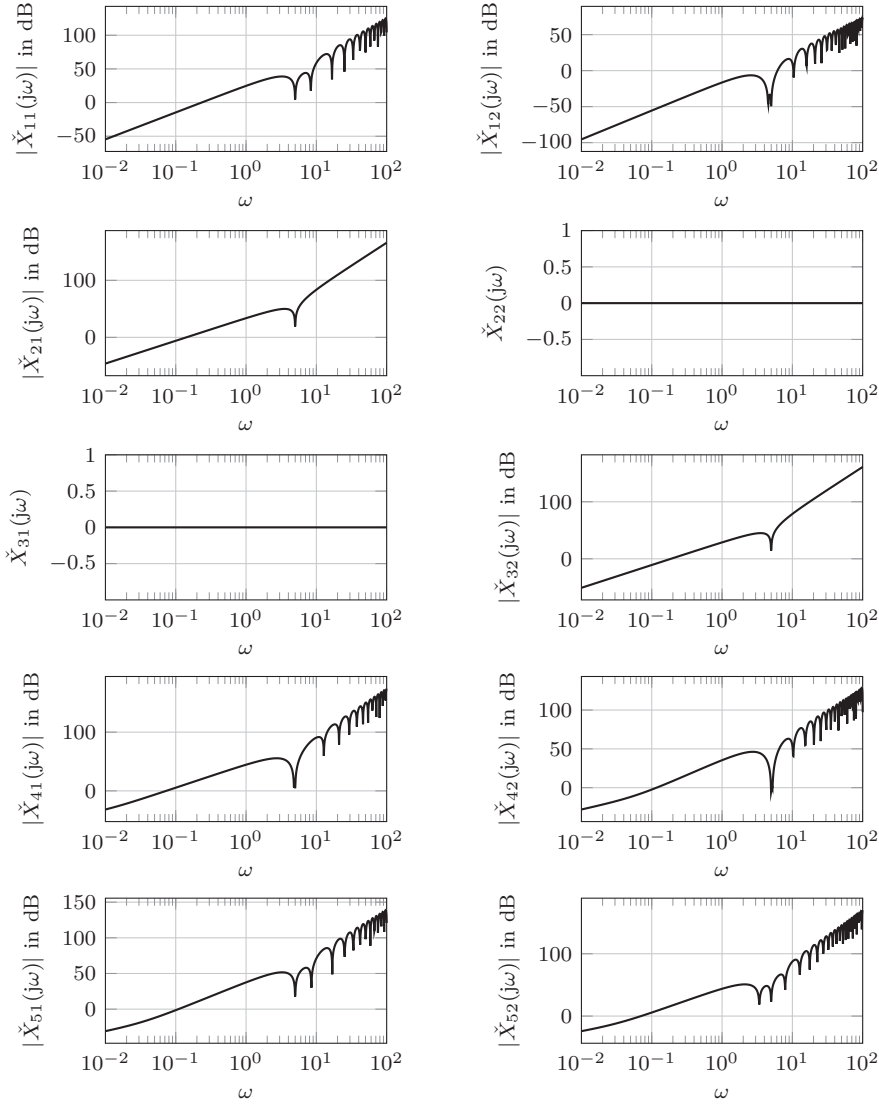
Figure 3.3: The magnitudes of the absolute values of the components $\check{X}_{kl}(s)$, $k = 1, \ldots, 5$, and $l = 1, 2$, of $\check{X}(s)$ for $s = \mathrm{j}\omega$ in dB, except $\check{X}_{22}(\mathrm{j}\omega) = 0$ and $\check{X}_{31}(\mathrm{j}\omega) = 0$.
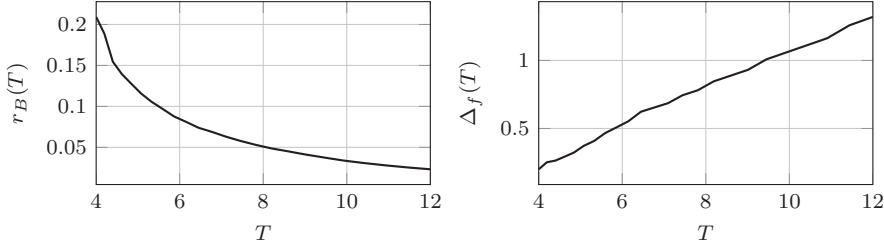
Figure 3.4: Fault detection threshold r_B (see 2.60) and normalized detection delay Δ_f for a polynomial basis function $\tilde{\theta}(\tau)$ of order $n_\varphi = 10$ and different moving horizon lengths T.
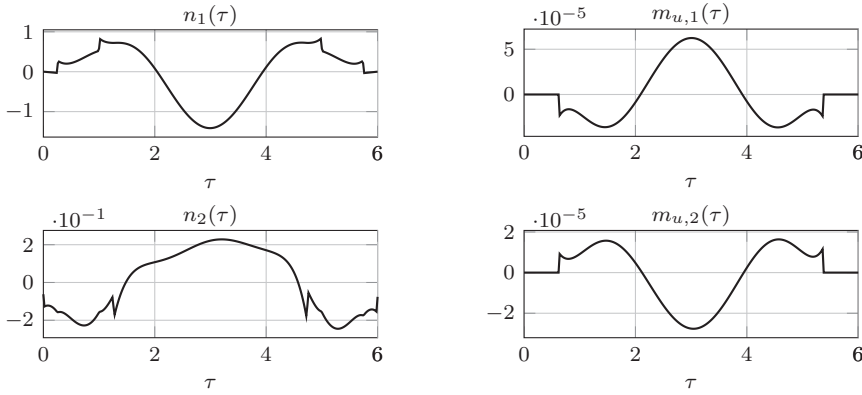
(a) Components $n_1(\tau)$ and $n_2(\tau)$ of the integral kernel $n(\tau)$.

(b) Components $m_{u,1}(\tau)$ and $m_{u,2}(\tau)$ of the integral kernel $m_u(\tau)$.

Figure 3.5: Integral kernels $n(\tau)$ and $m_u(\tau)$ of the input and output filters of the residual generator (2.50) computed with the moving horizon length $T = 6$ and polynomial $\tilde{\theta}(\tau)$ of order $n_\varphi = 10$.
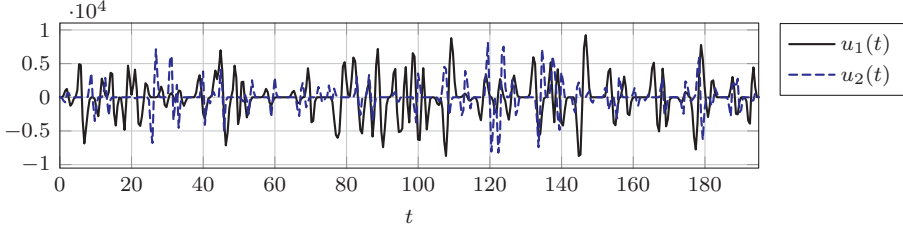
(a) Input signal $u(t)$ used in the simulation.
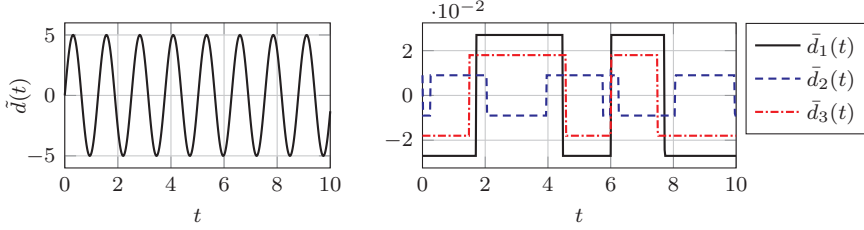
(b) Extract of the disturbance sig-
nal $\tilde{d}(t)$ on $0 \le t \le 10$.

(c) Extract of the unknown but bounded
disturbance signal $\bar{d}(t)$ on $0 \le t \le 10$.

Figure 3.6: Excitation signals $u(t)$, $\tilde{d}(t)$ and $\bar{d}(t)$ used for the simulation of
the faulty cable with a payload immersed in water.

and output signal $y(t)$ from such a simulation are only available at equally spaced
discrete-time samples, the integral expressions of the residual generator (3.25) are
approximated by FIR filters to be applicable in discrete-time. Using the compound
midpoint rule and a step size of 0.02, FIR filters of order 301 are obtained, which
are evaluated in MATLAB by using the `filter` function.

In a first simulation, the results for the fault detection residual generator in Theorem
3.2.2 are verified, i.e., the case $\bar{d}(t) \equiv 0$ is regarded. For a suitable excitation
of the cable, the input signal $u(t)$ is described by bump functions occurring at
random time instants with an amplitude randomly taking values between $\pm 10\,000$
as shown in Figure 3.6a. The sinusoidal disturbance $\tilde{d}(t)$ is the solution of the signal
model (3.91) with the IC $v_d^0 = \mathrm{col}\,(5, 0)$ and is depicted in Figure 3.6b. The faults
$f_i(t)$, $i = 1, \ldots, 5$, occur successively and are only present in the time intervals
$t \in \mathrm{I}_f^i = [t_i, t_i + 20]$, where $t_1 = 15$, $t_i = t_{i-1} + 40$, $i = 2, \ldots, 5$. At this, $\Delta f_i(t)$,
$t \in \mathrm{I}_f^i$, $i = 2, 4$, and $f_5(t)$ are constant values, whereas $f_i(t)$, $t \in \mathrm{I}_f^i$, $i = 1, 3$, are
continuous signals taking values randomly from a uniform distribution between
± 0.70 respectively ± 2. The resulting fault signals used for the simulation are shown
in Figure 3.7. The simulation is preformed with zero ICs and the step size 1×10^{-3}
in time. Imposing $u(t) = 0$ and $y(t) = 0$ for $t < 0$ and sampling the input signal
$u(t)$ and output signal $y(t)$ with the same step size as it is used for the FIR filters,
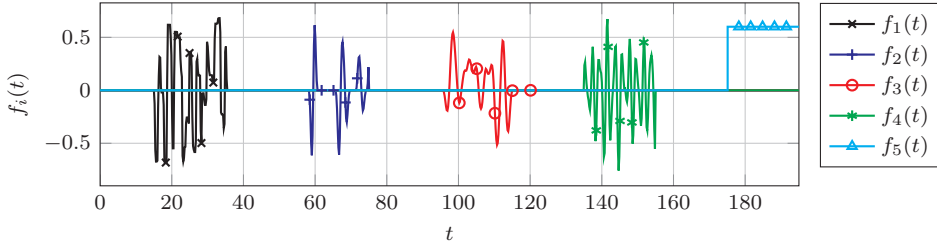
Figure 3.7: Fault scenarios for the fault detection with successively occurring additive process fault $f_1(t)$, the additive fault signal $f_2(t)$ resulting from the multiplicative actuator fault $\Delta f_2(t)$, the additive actuator fault $f_3(t)$, the additive fault signal $f_4(t)$ resulting from the multiplicative sensor fault $\Delta f_4(t)$ and the constant additive sensor fault $f_5(t)$.
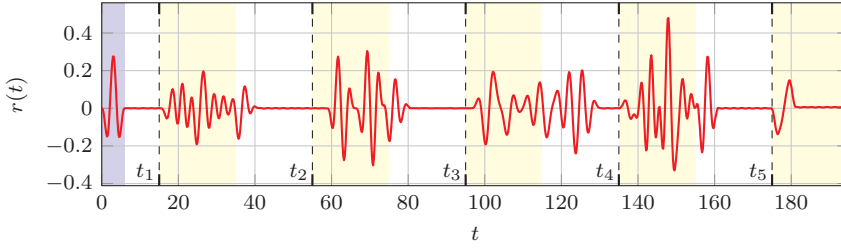
Figure 3.8: Residual signal $r(t)$ (———) for the detection of the faults $f_i(t)$, $i = 1, \ldots, 5$, from Figure 3.7 present in (▢) and the initialization interval $t < T$ (▢) assuming $\bar{d}(t) \equiv 0$.

the residual signal $r(t)$ shown in Figure 3.8 is obtained from the evaluation of the FIR filter representation of the residual generator (3.25). After the initialization interval $0 \le t < T$ and T after a fault was present, the residual signal $r(t)$ in Figure 3.8 remains zero as required. When a fault occurs at t_i, $i = 1, \ldots, 5$, the residual signal $r(t)$ is excited, i.e., $r(t) \not\equiv 0$ holds for $t \in I_f^i$, which indicates the presence of a fault $f_i(t)$ and verifies the results of Theorem 3.1. Note that the response of the residual signal to the occurrence of $f_5(t)$ at t_5 shows that this fault is only weakly detectable since the residual signal $r(t)$ is affected by the occurrence of the fault but returns to zero although the fault $f_5(t)$ is sill present (see Figure 3.7).

To demonstrate the fault detection influenced by a bounded disturbance $\bar{d}(t)$, the signals $\bar{d}_i(t)$ shown in Figure 3.6c are chosen such that the residual signal $r(t)$ will be close to the threshold value r_B at some time instants. With these disturbances $\bar{d}(t)$
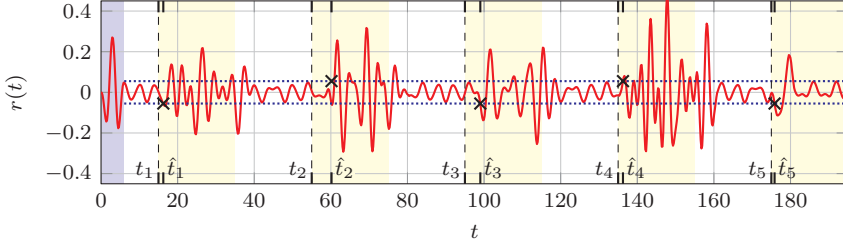
Figure 3.9: Residual signal $r(t)$ (——) and the threshold value $\pm r_B$ (⋯⋯)
for the detection of the faults $f_i(t)$, $i = 1, \ldots, 5$, from Figure 3.7,
the presence of the faults indicated by (▢), the fault detection
(✕) at $\hat{t}_i$ and the initialization interval $t < T$ (▢) in the presence
of a disturbance $\bar{d}(t)$ shown in Figure 3.6c.

Table 3.2: Detection delays of the fault detection for the cable immersed in
water with a payload subject to the bounded disturbance $\bar{d}(t)$.

i	1	2	3	4	5
$\hat{\Delta}_i$	1.26	5.18	4.02	1.26	0.84

and the input signal $u(t)$, disturbance $\tilde{d}(t)$ as well as the faults $f_i(t)$, $i = 1, \ldots, 5$,
shown in Figure 3.6a, 3.6b respectively Figure 3.7, a second simulation for the faulty
cable is performed. Evaluating the FIR filter representation of the residual generator
3.1 with the input $u(t)$ and output signal $y(t)$ derived from this simulation, the
residual signal $r(t)$ shown in Figure 3.9 is obtained. It shows that the residual signal
$r(t)$ is bounded by the threshold valued $\pm r_B$ according to Theorem 3.2 after the
initialization interval until the first fault occurs, i.e., $T \leq t < t_i$, and in the intervals
between the occurrence of two faults, i.e., $t_i + 20 + T < t < t_{i+1}$. If a fault occurs,
the residual signal $r(t)$ is excited and exceeds the threshold value shortly after the
occurrence of the fault. The first time instant when the threshold is exceeded is
denoted by $\hat{t}_i$ and the detection delays $\hat{\Delta}_i = \hat{t}_i - t_i$ given in Table 3.2 indicate that
the detection delay depends on the fault input location, since both faults $f_2(t)$ and
$f_3(t)$ that act on the opposite boundary than the measurement have the longest
detection delays. The specially chosen signal of the disturbance $\bar{d}(t)$ shows that the
threshold value r_B is not conservative but can be reached by the residual signal $r(t)$
if no fault is present for such disturbance signals. Similar to the previous simulation
results (see Figure 3.8), $r(t)$ shown in Figure 3.9 is only affected by the occurrence
of the constant fault $f_5(t)$ and then returns below the threshold. Thus, the weak
detectability is also relevant for the case $\bar{d}(t) \not\equiv 0$. However, the time-varying faults
$f_1(t)$, $i = 1, \ldots, 4$, affect the residual signal as long as they are present. Thus, the
detection of the occurrence of all faults $f_i(t)$, $i = 1, \ldots, 5$, is possible despite the

cable is additionally excited by the control input $u(t)$, the modeled disturbance $\tilde{d}(t)$ as well as the unknown but bounded disturbance $\bar{d}(t)$.

3.3 Fault diagnosis

To solve the fault diagnosis problem, the approach presented in Section 2.4 is transferred to the heterodirectional hyperbolic ODE-PDE systems. For the considered fault diagnosis problem the same assumptions given in Section 2.4.1 on the disturbances $\tilde{d}(t)$ and $\bar{d}(t)$ as well as on the fault $f(t)$ are imposed. To be specific, the fault signal $f(t)$ and the disturbance $\tilde{d}(t)$ are assumed to be described by a solution of the signal model (2.143) respectively (2.15). Hence, additive actuator, sensor and process faults can be taken into account for a large class of fault signals and the fault diagnosis can be decoupled from frequently occurring disturbance signals. The disturbance $\bar{d}(t)$ is assumed to be bounded according to (2.14). For the case $\bar{d}(t) \equiv 0$, the fault diagnosis problem considers the fault detection, isolation and identification. If a bounded but unknown disturbance $\bar{d}(t)$ is present, i.e., $\bar{d}(t) \not\equiv 0$, then the fault detection, isolation and estimation are achieved.

3.3.1 Fault diagnosis equation

For the fault diagnosis of a heterodirectional hyperbolic ODE-PDE system (3.1) that is subject to a fault $f(t) \in \mathbb{R}^{n_f}$, a residual generator is introduced that provides a residual signal $\hat{f}(t) \in \mathbb{R}^{n_f}$ with the components $\hat{f}_i(t) \in \mathbb{R}$ for each fault $f_i(t) = e_{i,n_f}^\top f(t)$. The residual generator is designed so that the residual signal $\hat{f}_i(t)$ reconstructs the fault signal $f_i(t)$ in finite time. Based on the input-output expression (3.20) a residual generator is derived for each fault $f_i(t)$, i.e., n_f integral kernels are introduced by the substitutions $m(z,\tau) \to m_i(z,\tau) \in \mathbb{R}^{n_x}$, $n(\tau) \to n_i(\tau) \in \mathbb{R}^{n_-}$, $q_w(\tau) \to q_{w,i}(\tau) \in \mathbb{R}^{n_w}$, $q_d(\tau) \to q_{d,i}(\tau) \in \mathbb{R}^{n_{vd}}$, $i = 1, \ldots, n_f$. The index i indicates that the integral kernels $m_i(z,\tau)$, $n_i(\tau)$, $q_{w,i}(\tau)$ and $q_{d,i}(\tau)$ correspond to the residual signal $\hat{f}_i(t)$. In addition, by using the substitutions $m_f(\tau) \to m_{f,i}(\tau) \in \mathbb{R}^{n_f}$, $m_u(\tau) \to m_{u,i}(\tau) \in \mathbb{R}^{n_u}$ and $m_{\bar{d}}(\tau) \to m_{\bar{d},i}(\tau) \in \mathbb{R}^{n_{\bar{d}}}$ in (3.21), the input-output expression (3.20) becomes

$$\langle m_{f,i}, f(t) \rangle_{\mathrm{I}} = \langle n_i, y(t) \rangle_{\mathrm{I}} + \langle m_{u,i}, u(t) \rangle_{\mathrm{I}} + \langle m_{\bar{d},i}, \bar{d}(t) \rangle_{\mathrm{I}} \qquad (3.111)$$

if the integral kernels $m_i(z,\tau)$, $n_i(\tau)$, $q_{w,i}(\tau)$ and $q_{d,i}(\tau)$ are solutions of the kernel equations (3.22) subject to (3.23) for $i = 1, \ldots, n_f$.

For the case $\bar{d}(t) \equiv 0$, the application of the transformation (2.148) and derivation as shown in (2.149)–(2.154) leads to the fault diagnosis residual generator candidate (2.157). In view of (3.22) and (3.23) as well as because of (2.151) and (2.153), the integral kernels must be solutions of the *fault diagnosis kernel equations*, which are summarized in the following lemma.

Lemma 3.3 (Fault diagnosis kernel equations). Let $\tilde{d}(t)$ be described by (2.15), the fault $f(t)$ be described by (2.143) and the integral kernels $m_i(z, \tau)$, $q_{w,i}(\tau)$, $q_{d,i}(\tau)$, $q_{f,i}(\tau)$ and $n_i(\tau)$ be a solution of the *fault diagnosis kernel equations*

$$\partial_z m_i(z, \tau) = -\Gamma(z)\partial_\tau m_i(z, \tau) - A^\top(z)m_i(z, \tau) - \mathcal{D}^*[m_i(\tau)](z) \quad (3.112a)$$

$$m_i^-(0, \tau) = -K_0^\top m_i^+(0, \tau) - \langle A_0, m_i(\tau)\rangle_\Omega - L_2^\top q_{w,i}(\tau) + C_0^\top n_i(\tau) \quad (3.112b)$$

$$m_i^+(1, \tau) = -K_1^\top m_i^-(1, \tau) \quad (3.112c)$$

$$\dot{q}_{w,i}(\tau) = F^\top q_{w,i}(\tau) + \langle H_1, m_i(\tau)\rangle_\Omega + H_2^\top m_i^+(0, \tau) - C_1^\top n_i(\tau) \quad (3.112d)$$

$$\dot{q}_{d,i}(\tau) = S_d^\top q_{d,i}(\tau) + R_d^\top \tilde{G}^\top \big(\langle G_1, m_i(\tau)\rangle_\Omega + G_2^\top m_i^+(0, \tau)$$
$$-G_3^\top m_i^-(1, \tau) + G_4^\top q_{w,i}(\tau) - G_5^\top n_i(\tau)\big) \quad (3.112e)$$

$$\dot{q}_{f,i}(\tau) = S_f^\top q_{f,i}(\tau) + R_f^\top \big(-\langle E_1, m_i(\tau)\rangle_\Omega - E_2^\top m_i^+(0, \tau)$$
$$+E_3^\top m_i^-(1, \tau) - E_4^\top q_{w,i}(\tau) + E_5^\top n_i(\tau)\big) \quad (3.112f)$$

subject to the initial and end conditions

$$m_i(z, 0) = 0, \qquad\qquad m_i(z, T) = 0, \qquad z \in \Omega \qquad (3.113a)$$
$$q_{w,i}(0) = 0, \qquad\qquad q_{w,i}(T) = 0 \qquad\qquad\qquad (3.113b)$$
$$q_{d,i}(0) = 0, \qquad\qquad q_{d,i}(T) = 0 \qquad\qquad\qquad (3.113c)$$
$$q_{f,i}(0) = -R_f^\top e_{i,n_f}, \qquad q_{f,i}(T) = 0 \qquad\qquad\qquad (3.113d)$$

for $i = 1, \ldots, n_f$, where (3.112a) is defined on $(z, \tau) \in (0, 1) \times (0, T)$ and (3.112b)–(3.112f) are defined on $\tau \in (0, T)$. Then, (2.157) is a residual generator for the heterodirectional hyperbolic ODE-PDE system.

By the same reasoning as for Theorem 2.5, the fault diagnosis for the case $\bar{d}(t) \equiv 0$ can be established in the following theorem.

Theorem 3.4 (Fault diagnosis residual generator)
Assume that $\bar{d}(t) \equiv 0$ holds, $\tilde{d}(t)$ is described by a solution of the signal model (2.15) and $f(t)$ is described by a piecewise defined solution of the signal model (2.143). If the integral kernels $m_i(z, \tau)$, $q_{w,i}(\tau)$, $q_{d,i}(\tau)$, $q_{f,i}(\tau)$ and $n_i(\tau)$, $i = 1, \ldots, n_f$, satisfy (3.112) and (3.113), then (2.157) is a residual generator for the heterodirectional hyperbolic ODE-PDE system (3.1) with the residual signal $\hat{f}_i(t)$ given in (2.157). A fault $f(t)$ is detected by $\hat{f}(t) \not\equiv 0$, $t \geq T$. Moreover, the fault $f(t)$ occurring at t_j, $j \in \mathbb{N}_0$, is identified by $\hat{f}(t)$ for $t \in \mathrm{I}_j = [t_j + T, t_{j+1})$.

Because of $f(t) = \hat{f}(t)$, $t \in \mathrm{I}_j$, the strong fault detectability in the sense of Definition 2 is achieved by the fault diagnosis residual generator (2.157). For $t = t_j + T$, the fault occurring at t_j is identified in finite time, which also includes the fault isolation. Thus, $\hat{f}(t)$ provides not only strong fault detection, but also fault isolation and identification. Nevertheless, (2.157) is called a residual generator, but the corresponding residual signal is distinguished from the fault detection residual $r(t)$ by the new symbol $\hat{f}(t)$.

If an unknown but bounded disturbance is present, i.e., $\bar{d}(t) \not\equiv 0$, then a threshold must be introduced to ensure the fault detection and isolation. As shown in (2.158)–(2.164), the fault estimation error $\bar{f}_i(t)$ caused by the disturbance $\bar{d}(t)$ is bounded by $|\bar{f}_i(t)| \leq f_{B,i}$ (see (2.164)) with the threshold value $f_{B,i}$ given in (2.163). Thus, using the same reasoning as for Theorem 2.6, the strong fault detection can be derived for the heterodirectional hyperbolic ODE-PDE system (3.1), which is stated in the following theorem.

Theorem 3.5 (Strong fault detection)
Assume that $\tilde{d}(t)$ is described by a solution of the signal model (2.15), $\bar{d}(t)$ satisfies (2.14) and $f(t)$ is described by a piecewise defined solution of the signal model (2.143). Let the integral kernels $m_i(z, \tau)$, $q_{w,i}(\tau)$, $q_{d,i}(\tau)$, $q_{f,i}(\tau)$ and $n_i(\tau)$, $i = 1, \ldots, n_f$, satisfy (3.112) and (3.113). If a threshold $f_{B,i}$, $i = 1, \ldots, n_f$, given in (2.163) is exceeded by some component $\hat{f}_i(t)$ of $\hat{f}(t)$ in (2.157), i.e.,

$$\exists i \in \{1, \ldots, n_f\} \text{ so that } |\hat{f}_i(t)| > f_{B,i}, \quad t \geq T, \qquad (3.114)$$

then a fault $f(t)$ is detected for the system (3.1).

Since $\hat{f}_i(t) = \tilde{f}_i(t)$ holds for $t \in \mathrm{I}_j$, with the fault estimate $\tilde{f}(t)$ given in (2.159), the

strong fault detection in sense of Definition 2 is achieved. The first time instance $\hat{t}_j$, $j \in \mathbb{N}_0$, a threshold value $f_{B,i}$ is exceeded by $\hat{f}_i(t)$ (see (2.165)), is called the *fault detection time*.

After the transient interval, i.e., $t \geq t_j + T$, where t_j is the occurrence time of the fault $f_i(t)$, the residual signals $\hat{f}_k(t)$, $k \neq i$, return to zero or the estimations of their corresponding faults. Thus, the exceed of a threshold $|\hat{f}_i(t)| > f_{B,i}$, $t \geq t_j + T$, indicates that the ith fault is present, i.e., fault isolation is achieved. However, since only $\hat{t}_j > t_j$ is known, the fault can be isolated for $t \geq \hat{t}_j + T$, which is the result of the next theorem.

> **Theorem 3.6 (Fault isolation)**
> Assume that $\tilde{d}(t)$ is described by a solution of the signal model (2.15), $\bar{d}(t)$ satisfies (2.14) and $f(t)$ is described by a piecewise defined solution of the signal model (2.143). Let the integral kernels $m_i(z,\tau)$, $q_i(\tau)$, $n_i(\tau)$ and $q_{f,i}(\tau)$, $i = 1, \ldots, n_f$, satisfy the kernel equations (3.112) and (3.113). If the threshold $f_{B,i}$ given in (2.163), is exceeded by the ith component $\hat{f}_i(t)$ of $\hat{f}(t)$ in (2.157), i.e.,
>
> $$|\hat{f}_i(t)| > f_{B,i}, \quad t \geq \hat{t}_j + T, \tag{3.115}$$
>
> then the fault $f_i(t)$, $i \in \{1, \ldots, n_f\}$, occurring at t_j, $j \in \mathbb{N}_0$, is detected for the system (3.1).

Moreover, for $t \in I_j$, $\hat{f}_i(t) = \tilde{f}_i(t)$ holds. Thus, it follows from (2.161), that the fault signal $f_i(t)$ is bounded by

$$\hat{f}_i(t) - f_{B,i} \leq f_i(t) \leq \hat{f}_i(t) + f_{B,i}, \quad t \in I_j. \tag{3.116}$$

Consequently, the faults can be estimated, which is stated in the next theorem.

Theorem 3.7 (Fault estimation)
Assume that $\tilde{d}(t)$ is described by a solution of the signal model (2.15), $\bar{d}(t)$ satisfies (2.14) and $f(t)$ is described by a piecewise defined solution of the signal model (2.143). Let the integral kernels $m_i(z,\tau)$, $q_i(\tau)$, $n_i(\tau)$ and $q_{f,i}(\tau)$, $i = 1, \ldots, n_f$, satisfy the kernel equations (3.112) and (3.113). Then, for system (3.1) the estimate of a fault $f_i(t)$, $i \in \{1, \ldots, n_f\}$, occurring at t_j, $j \in \mathbb{N}_0$, is bounded by

$$f_i(t) - f_{B,i} \leq \hat{f}_i(t) \leq f_i(t) + f_{B,i}, \quad t \in [\hat{t}_j + T, t_{j+1}) \tag{3.117}$$

with $\hat{f}_i(t)$ as ith component of $\hat{f}(t)$ in (2.157) and $f_{B,i}$ given by (2.163).

The proofs of the Theorems 2.6, 2.7 and 2.8 follow from (2.161) and the estimate (2.164), since $\hat{f}(t) = \tilde{f}(t)$, $t \in I_j$.

3.3.2 Solution of the fault diagnosis kernel equations

The kernel equations for the fault diagnosis (see Lemma 3.3) are a heterodirectional hyperbolic ODE-PDE system (3.112) with n_f distinct initial and end conditions (3.113) as well as a freely assignable input $n_i(\tau)$. Thus, the computation of the ith integral kernels $m_i(z,\tau)$, $q_{w,i}(\tau)$, $q_{d,i}(\tau)$ and $q_{f,i}(\tau)$ amounts to determine a suitable control input $n_i(\tau)$, $i = 1, \ldots, n_f$, that drives the ODE-PDE system in (3.112) in finite time from the ith IC to the end point, both given in (3.113). This two-point initial-boundary-value problem can be solved by using results from the flatness-based trajectory planning. To be specific, a parametrizing variable $\varphi_i(\tau)$ is introduce so that the system variables $m_i(z,\tau)$, $q_{w,i}(\tau)$, $q_{d,i}(\tau)$, $q_{f,i}(\tau)$ and $n_i(\tau)$ can be expressed by differential expressions. The latter allows the reformulation of the two-point initial-boundary-value problem into an interpolation problem for a reference trajectory $\varphi^\star(\tau)$ assigned to this parametrizing variable. With the resulting reference trajectory $\varphi^\star(\tau)$ from the solution of this interpolation problem, the required integral kernels $m_i(z,\tau)$, $q_{w,i}(\tau)$, $q_{d,i}(\tau)$, $q_{f,i}(\tau)$ and $n_i(\tau)$ can be computed by the evaluation of the differential expressions. As already introduced in Section 3.2.3, the determination of the required differential expressions is significantly facilitated by utilizing a backstepping transformation to map the ODE-PDE system in (3.112) into an ODE-PDE cascade system. For the latter, the differential expressions can be explicitly specified.

3.3.2.1 Backstepping transformation

In order to reformulate the ODE-PDE system (3.112) so that the transport directions correspond to the system description in [41], use the spatial reversal $\bar{z} = 1 - z$, where the resulting quantities in the new coordinate $\bar{z}$ are denoted by an overline similar to Section 3.2.3.1. The resulting system reads as

$$\partial_z \bar{m}_i(\bar{z}, \tau) = \bar{\Gamma}(\bar{z}) \partial_\tau \bar{m}_i(\bar{z}, \tau) + \bar{A}^\top(\bar{z}) \bar{m}_i(\bar{z}, \tau) + \int_0^{\bar{z}} \bar{D}^\top(\zeta, \bar{z}) \bar{m}_i(\zeta, \tau) \mathrm{d}\zeta \qquad (3.118a)$$

$$\bar{m}_i^+(0, \tau) = -K_1^\top \bar{m}_i^-(0, \tau) \qquad (3.118b)$$

$$\bar{m}_i^-(1, \tau) = -K_0^\top \bar{m}_i^+(1, \tau) - \int_0^1 \bar{A}_0^\top(\zeta) \bar{m}_i(\zeta, \tau) \mathrm{d}\zeta - L_2^\top J_w q_i(\tau) + C_0^\top n_i(\tau) \, (3.118c)$$

$$\dot{q}_i(\tau) = \bar{F} q_i(\tau) + \int_0^1 \bar{B}_1(\zeta) \bar{m}_i(\zeta, \tau) \mathrm{d}\zeta + \bar{B}_2 \bar{m}_i^-(0, \tau) + \bar{B}_3 \bar{m}_i^+(1, \tau)$$
$$+ \bar{B}_4 n_i(\tau) \qquad (3.118d)$$

where (3.118a) is defined on $(\bar{z}, \tau) \in (0, 1) \times (0, T)$ and (3.27b)–(3.27d) on $\tau \in (0, T)$. In contrast to (3.27d), the ODE state is $q_i(\tau) = \mathrm{col}\,(q_{w,i}(\tau), q_{d,i}(\tau), q_{f,i}(\tau)) \in \mathbb{R}^{n_q}$, $n_q = n_w + n_{vd} + n_{vf}$ and $J_w = [\, I \;\; 0\,] \in \mathbb{R}^{n_w \times n_q}$ so that $q_{w,i}(\tau) = J_w q_i(\tau)$ holds. The matrices in (3.118d) result from aggregating (3.112d)–(3.112f) to

$$\bar{F} = \begin{bmatrix} F^\top & 0 & 0 \\ R_d^\top \tilde{G}^\top G_4^\top & S_d^\top & 0 \\ -R_f^\top E_4^\top & 0 & S_f^\top \end{bmatrix}, \quad \bar{B}_1(\bar{z}) = \begin{bmatrix} \bar{H}_1^\top(\bar{z}) \\ R_d^\top \tilde{G}^\top \bar{G}_1^\top(\bar{z}) \\ -R_f^\top \bar{E}_1^\top \end{bmatrix}, \quad \bar{B}_2 = \begin{bmatrix} 0 \\ -R_d^\top \tilde{G}^\top G_3^\top \\ R_f^\top E_3^\top \end{bmatrix},$$
$$\bar{B}_3 = \begin{bmatrix} H_2^\top \\ R_d^\top \tilde{G}^\top G_2^\top \\ -R_f^\top E_2^\top \end{bmatrix}, \qquad\qquad \bar{B}_4 = \begin{bmatrix} -C_1^\top \\ -R_d^\top \tilde{G}^\top G_5^\top \\ R_f^\top E_5^\top \end{bmatrix}. \qquad (3.119)$$

In accordance with (3.113), the initial and end conditions for (3.118) are

$$\bar{m}_i(\bar{z}, 0) = 0, \qquad\qquad \bar{m}_i(\bar{z}, T) = 0, \quad \bar{z} \in \Omega \qquad (3.120a)$$
$$q_i(0) = q_i^0, \qquad\qquad q_i(T) = 0 \qquad (3.120b)$$

with the inhomogeneous IC

$$q_i^0 = \begin{bmatrix} 0 \\ 0 \\ -R_f^\top e_{i,n_f} \end{bmatrix}. \tag{3.121}$$

For convenience of notation, the substitution $\bar{z} \to z$ is used.

By utilizing the invertible backstepping transformation $\tilde{m}_i(z,\tau) = \mathcal{T}[\bar{m}_i(\tau)](z)$ (see (3.30)), the PDE subsystem (3.118a)–(3.118c) is mapped into the target system

$$\partial_z \tilde{m}_i(z,\tau) = \bar{\Gamma}(z)\partial_\tau \tilde{m}_i(z,\tau) + \tilde{P}_0(z)\tilde{m}_i^-(0,\tau), \quad (z,\tau) \in (0,1) \times (0,T) \tag{3.122a}$$

$$\tilde{m}_i^+(0,\tau) = -K_1^\top \tilde{m}_i^-(0,\tau), \qquad\qquad \tau \in (0,T) \tag{3.122b}$$

$$\tilde{m}_i^-(1,\tau) = \tilde{n}_i(\tau), \qquad\qquad \tau \in (0,T) \tag{3.122c}$$

$$\dot{q}_i(\tau) = \tilde{F}q_i(\tau) + \int_0^1 \tilde{B}_1(\zeta)\tilde{m}_i(\zeta,\tau)\mathrm{d}\zeta + \bar{B}_2\tilde{m}_i^-(0,\tau) + \tilde{B}_3\tilde{m}_i(1,\tau) \tag{3.122d}$$

where (3.122d) is defined on $\tau \in (0,T)$. The backstepping kernel $\bar{K}(z,\zeta)$ is the solution of (3.35) and the new input $\tilde{n}_i(\tau)$ is given by

$$\tilde{n}_i(\tau) = C^\top n_i(\tau) - K_0^\top \bar{m}_i^+(1,\tau) - L_2^\top J_w q_i(\tau)$$

$$- \int_0^1 \left(\bar{A}_0^\top(\zeta) + J_-\bar{K}(1,\zeta)\right)\bar{m}_i(\zeta,\tau)\mathrm{d}\zeta. \tag{3.123}$$

The matrices $\tilde{F}$ and $\tilde{B}_i$, $i = 1, 2, 3$, in (3.122d) result from the application of the inverse backstepping transformation $\bar{m}_i(z,\tau) = \mathcal{T}^{-1}[\tilde{m}_i(\tau)](z)$ (see (3.31)) and are specified in (3.33). Note that for $\bar{F}$ and $\bar{B}_i$, $i = 1, \ldots, 4$, the matrices defined in (3.119) are used.

3.3.2.2 Differential expression for the target system

Since the fault diagnosis target system (3.122) has the same structure as the fault detection target system (3.32), the differential expressions

$$\tilde{m}_i(z,\tau) = \Psi\left[\tilde{m}_i^-(0)\right](z,\tau) \tag{3.124a}$$

$$\tilde{n}_i(\tau) = J_-\Psi\left[\tilde{m}_i^-(0)\right](1,\tau) \tag{3.124b}$$

in terms of $\tilde{m}_i^-(0, \tau)$ are derived from the same derivation as described in Section 3.2.3.2, whereas $\Psi[\cdot](z, \tau)$ in (3.124) is specified by (3.44). Following the derivation in Section 3.2.3.3 a common parametrizing variable $\varphi_i(\tau) \in \mathbb{R}^{n_-}$, $i = 1, \ldots, n_f$, for the PDE and the ODE subsystems can be introduced by

$$\tilde{m}_i^-(0, \tau) = \sum_{j=0}^{n_q} a_j \mathrm{d}_\tau^j \varphi_i(\tau), \quad i = 1, \ldots, n_f. \tag{3.125}$$

Thus, the differential expressions for the ODE-PDE system (3.122) are derived and stated in the following lemma.

Lemma 3.4 (Differential expressions for the fault diagnosis kernel equations)**.**
Let $\Psi[\cdot](z, \tau)$ be given by (3.45) and a_i be defined by (3.52). Then, the integral kernels $\tilde{m}_i(z, \tau)$, $q_i(\tau)$ and $\tilde{n}_i(\tau)$ can be parametrized by the differential expressions

$$\tilde{m}_i(z, \tau) = \sum_{j=0}^{n_q} a_j \Psi\left[\mathrm{d}_\tau^j \varphi_i\right](z, \tau) \tag{3.126a}$$

$$q_i(\tau) = \sum_{j=0}^{n_q-1} \left(\int_0^1 \tilde{F}_j \bar{B}_1(\zeta) \Psi\left[\mathrm{d}_\tau^j \varphi_i\right](\zeta, \tau) \mathrm{d}\zeta \right.$$

$$\left. + \tilde{F}_j \bar{B}_2 \mathrm{d}_\tau^j \varphi_i(\tau) + \tilde{F}_j \bar{B}_3 \Psi\left[\mathrm{d}_\tau^j \varphi_i\right](1, \tau) \right) \tag{3.126b}$$

$$\tilde{n}_i(\tau) = J_- \sum_{j=0}^{n_q} a_j \Psi\left[\mathrm{d}_\tau^j \varphi_i\right](1, \tau) \tag{3.126c}$$

in terms of the parametrizing variable $\varphi_i(\tau)$.

In (3.126), the coefficients a_j, $j = 0, \ldots, n_q$, and the coefficient matrices $\tilde{F}_j$, $j = 0, \ldots, n_q - 1$, are defined in (3.52) respectively (3.50), when $\tilde{F}$ given in (3.122d) is used.

It must be remarked, that the formal Laplace transform $\mathrm{d}_\tau q(\tau) \circ\!\!-\!\!\bullet\, s\check{q}(s)$ is used in the derivation of (3.126c), despite the nonhomogeneous ICs $q(0) \neq 0$. However the resulting differential expressions (3.126) can be justified by a similar verification as shown in Appendix A.2.

3.3.2.3 Reference trajectory planning

To express also the initial and end points of the fault diagnosis kernel equations in the backstepping coordinates, (3.120a) is mapped into

$$\tilde{m}_i(z,\tau)|_{\tau \in \{0,T\}} = 0, \quad z \in \Omega \tag{3.127}$$

using (3.30). Then, the kernels $\tilde{m}_i(z,\tau)$ and $q_i(\tau)$ have to be a solution of the two-point initial-boundary-value problem (3.122) subject to (3.120b) and (3.127). In view of the differential expressions (3.126), the initial and end conditions (3.120b) and (3.127) lead to requirements for the parametrizing variable $\varphi_i(\tau)$. Thus, by the planning of a suitable reference trajectory $\varphi_i^\star(\tau) \in \mathbb{R}^{n-}$ for $\varphi_i(\tau)$ that satisfies these requirements, the kernel equations can be solved. In the light of (3.126), the reference trajectory must satisfy $\varphi_i^\star \in (C^{n_q-1}[-\tilde{\tau}^-, T + \tilde{\tau}^+])^{n-}$ with $\mathrm{d}_\tau^{n_q} \varphi_i^\star(\tau)$ existing.

For a systematic realization of the finite-time transition, the initial and end conditions for the PDE and the ODE states are successively taken into account. At first (3.124a) is used to formulate the conditions on a reference trajectory $\tilde{m}_i^{-\star}(0,\tau)$ for $\tilde{m}_i^-(0,\tau)$ so that $\tilde{m}_i(z,\tau)$ satisfies (3.127). To this end, consider (3.124a) rowwise, which yields

$$e_{j,n_x}^\top \tilde{m}_i^\star(z,\tau) = e_{j,n_x}^\top V \tilde{m}_i^{-\star}(0, \tau + \bar{\tau}_j(z,0)) + \int_0^z e_{j,n_x}^\top \tilde{P}_0(\zeta) \tilde{m}_i^{-\star}(0, \tau + \bar{\tau}_j(z,\zeta)) \mathrm{d}\zeta \tag{3.128}$$

in view of (3.44). Consequently, (3.127) holds if $\tilde{m}_i^{-\star}(0,\tau)$, $i = 1, \ldots, n_f$, satisfies

$$\tilde{m}_i^{-\star}(0, \tau + \bar{\tau}_i(z,\zeta))|_{\tau \in \{0,T\}} = 0 \tag{3.129}$$

for $j = 1, \ldots, n_x$, on $0 \leq \zeta \leq z \leq 1$. In view of the largest prediction time $\tilde{\tau}^+$ and delay time $\tilde{\tau}^-$ (see (3.18) and (3.19)), it follows from (3.129) that the initial and end conditions (3.127) are embedded into setpoints for the PDE subsystem corresponding to $\tilde{m}_i(z,\tau)$, i.e., $\tilde{m}_i^{-\star}(0,\tau)$ is piecewise defined by

$$\tilde{m}_i^{-\star}(0,\tau) = \begin{cases} 0 & : \tau \in \mathrm{I}_1 = [-\tilde{\tau}^-, \tilde{\tau}^+] \\ \mu_i(\tau) & : \tau \in \mathrm{I}_2 = (\tilde{\tau}^+, T - \tilde{\tau}^-) \\ 0 & : \tau \in \mathrm{I}_3 = [T - \tilde{\tau}^-, T + \tilde{\tau}^+], \end{cases} \tag{3.130}$$

where $\mu_i(\tau) \in \mathbb{R}^{n-}$ is a degree of freedom that is considered later. From Figure 3.10, the condition $T - \tilde{\tau}^- > \tilde{\tau}^+$ is directly inferred, i.e., the length of the moving horizon is lower bounded by (3.60).
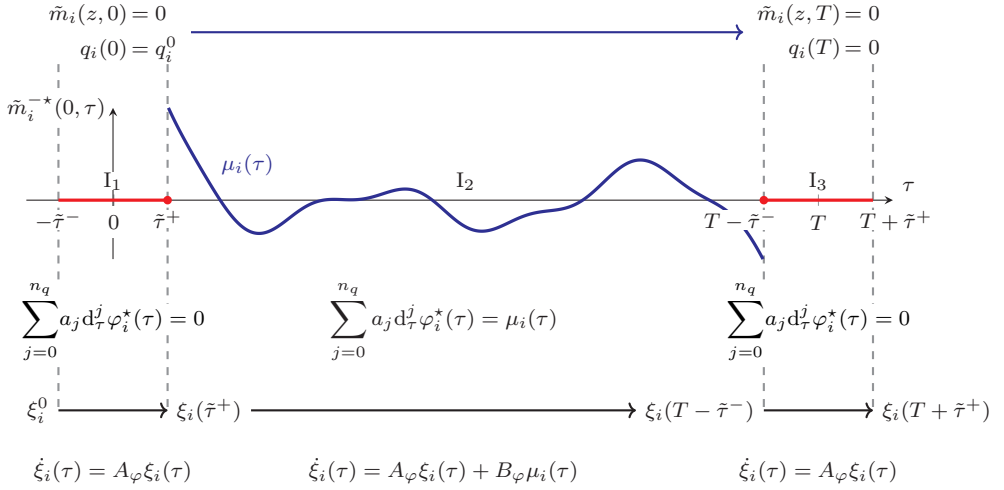
Figure 3.10: Visualization of the reference trajectory planning for $\mu_i(\tau)$ and $\xi_i(\tau)$ on the three time periods I_1, I_2 and I_3.

However, since the IC q_i^0 is inhomogeneous, the trivial condition (3.57) used in Section 3.2.3.4 cannot be used anymore. Thus, to determine $\varphi_i^\star(\tau)$, regard (3.125) as an ODE for $\varphi_i^\star(\tau)$ with $\tilde{m}_i^{-\star}(0,\tau)$ as input. In view of (3.130), $\varphi_i^\star(\tau)$ is piecewise defined and must be a solution of a homogeneous ODE on I_1 and I_3, which is illustrated in Figure 3.10. On I_2, $\varphi_i^\star(\tau)$ is governed by the ODE (3.125) with input $\mu_i(\tau)$ (see (3.130)). Hence, $\varphi_i^\star(\tau)$ on I_1 is uniquely determined by the ICs $\mathrm{d}_\tau^j \varphi_i^\star(\tau)|_{\tau=-\tilde{\tau}^-}$, $j = 0, \ldots, n_q - 1$. On I_2, $\varphi_i^\star(\tau)$ is given by the ICs $\mathrm{d}_\tau^j \varphi_i^\star(\tau)|_{\tau=\tilde{\tau}^+}$, $j = 0, \ldots, n_q - 1$, and the input $\mu_i(\tau)$. For $\tau \in I_3$, $\varphi_i^\star(\tau)$ results from the ICs $\mathrm{d}_\tau^j \varphi_i^\star(\tau)|_{\tau=T-\tilde{\tau}^-}$, $j = 0, \ldots, n_q - 1$. Thus, the ICs for $\mathrm{d}_\tau^j \varphi_i^\star(\tau)$ at $\tau = -\tilde{\tau}^-$ and $\tau = T - \tilde{\tau}^-$ have to be determined so that $\varphi_i^\star(\tau)$ ensures the initial and end condition (3.120b) for $q_i(\tau)$ by evaluating (3.126b) at $\tau = 0$ and $\tau = T$. Then, the input $\mu_i(\tau)$ must be determined so that the resulting $\varphi_i^\star(\tau)$ connects the derived $\varphi_i^\star(\tilde{\tau}^+)$ and $\varphi_i^\star(T - \tilde{\tau}^-)$ as well as satisfies $\varphi_i^\star \in (C^{n_q-1}[-\tilde{\tau}^-, T + \tilde{\tau}^+])^{n_-}$ with $\mathrm{d}_\tau^{n_q} \varphi_i^\star(\tau)$ existing in view of (3.125). To be specific, the derivatives of the reference trajectory $\mathrm{d}_\tau^j \varphi_i^\star(\tau)$, $j = 0, \ldots, n_q - 1$, must be consistent at the interfaces $\tilde{\tau}^+$ and $T - \tilde{\tau}^-$ of the piecewise defined time domain. This planning of a suitable $\varphi_i^\star(\tau)$ can be systematically achieved by introducing the state

$$\xi_i(\tau) = \begin{bmatrix} \xi_{i,1}(\tau) \\ \xi_{i,2}(\tau) \\ \vdots \\ \xi_{i,n_{vf}}(\tau) \end{bmatrix} = \begin{bmatrix} \varphi_i^\star(\tau) \\ \mathrm{d}_\tau \varphi_i^\star(\tau) \\ \vdots \\ \mathrm{d}_\tau^{n_q-1} \varphi_i^\star(\tau) \end{bmatrix} \in \mathbb{R}^{n_\xi}, \quad i = 1, \ldots, n_f, \qquad (3.131)$$

with $n_\xi = n_- n_q$ for (3.125), where $\xi_{i,j}(\tau) = \mathrm{d}_\tau^{j-1} \varphi_i^\star(\tau) \in \mathbb{R}^{n_-}$, $j = 1, \ldots, n_q$. This yields

$$\dot{\xi}_i(\tau) = A_\varphi \xi_i(\tau) + B_\varphi \tilde{m}_i^{-\star}(0, \tau), \qquad \tau \in (-\tilde{\tau}^-, T + \tilde{\tau}^+] \qquad (3.132\text{a})$$

$$\varphi_i^\star(\tau) = C_\varphi \xi_i(\tau), \qquad \tau \in [-\tilde{\tau}^-, T + \tilde{\tau}^+] \qquad (3.132\text{b})$$

for $i = 1, \ldots, n_f$, with the matrices $A_\varphi = A_c \otimes I_{n_-}$,

$$A_c = \begin{bmatrix} 0 & 1 & \ldots & 0 \\ \vdots & & \ddots & \\ 0 & 0 & \ldots & 1 \\ -a_0 & -a_1 & \ldots & -a_{n_{vf}-1} \end{bmatrix}, \qquad (3.133)$$

$B_\varphi = e_{n_{vf}, n_{vf}} \otimes I_{n_-}$ and $C_\varphi = e_{1, n_{vf}}^\top \otimes I_{n_-}$. Then, in view of (3.131), use

$$\mathrm{d}_\tau^j \varphi_i^\star(\tau) = U_j \xi_i(\tau) \qquad (3.134)$$

with $U_j = e_{j+1, n_q}^\top \otimes I_{n_-}$ for $i = 1, \ldots, n_f$, and $j = 0, \ldots, n_q - 1$, to express the reference trajectory $q_i^\star(\tau)$ for $q(\tau)$ given in (3.126b) by

$$q_i^\star(\tau) = \sum_{j=0}^{n_q-1} \left(\int_0^1 \tilde{F}_j \tilde{B}_1(\zeta) \Psi \left[U_j \xi_i \right] (\zeta, \tau) \mathrm{d}\zeta + \tilde{F}_j \bar{B}_2 U_j \xi_i(\tau) + \tilde{F}_j \tilde{B}_3 \Psi \left[U_j \xi_i \right] (1, \tau) \right).$$

$$(3.135)$$

According to (3.130) three cases have to be considered to determine $\tilde{m}_i^{-\star}(0, \tau)$, which are illustrated in Figure 3.10. On the first interval, i.e., $\tau \in \mathrm{I}_1$, (3.132) is autonomous. Thus, $\xi_i(\tau)$ is uniquely defined on $\tau \in \mathrm{I}_1$ by the IC $\xi_i(-\tilde{\tau}^-) = \xi_i^0$. The latter must be determined so that $q_i(\tau)$ resulting from (3.135) satisfies the IC in (3.120b). To this end, use

$$\xi_i(\tau) = \Phi_\varphi(\tau, -\tilde{\tau}^-) \xi_i^0, \quad \tau \in \mathrm{I}_1, \qquad (3.136)$$

with $\Phi_\varphi(\tau, \tau_0) = \exp\left(A_\varphi(\tau - \tau_0) \right)$ in (3.135) and evaluate the result at $\tau = 0$, which yields

$$q_i^\star(0) = \sum_{j=0}^{n_q-1} \left(\int_0^1 \tilde{F}_j \tilde{B}_1(\zeta) \Psi \left[U_j \Phi_\varphi(\cdot, -\tilde{\tau}^-) \xi_i^0 \right] (\zeta, 0) \mathrm{d}\zeta \right.$$

$$\left. + \tilde{F}_j \bar{B}_2 U_j \Phi_\varphi(0, -\tilde{\tau}^-) \xi_i^0 + \tilde{F}_j \tilde{B}_3 \Psi \left[U_j \Phi_\varphi(\cdot, -\tilde{\tau}^-) \xi_i^0 \right] (1, 0) \right). \qquad (3.137)$$

Utilzing $\Psi\left[U_j\Phi_\varphi(\cdot,-\tilde{\tau}^-)\xi_i^0\right](\zeta,0) = \Psi\left[U_j\Phi_\varphi(\cdot,-\tilde{\tau}^-)\right](\zeta,0)\xi_i^0$ in (3.137), the result

$$q_i^0 = \Upsilon\xi_i^0 \tag{3.138}$$

follows with

$$\Upsilon = \sum_{j=0}^{n_q-1}\left(\int_0^1 \tilde{F}_j\tilde{B}_1(\zeta)\Psi\left[U_j\Phi_\varphi(\cdot,-\tilde{\tau}^-)\right](\zeta,0)\mathrm{d}\zeta\right.$$
$$\left. + \tilde{F}_j\bar{B}_2 U_j\Phi_\varphi(0,-\tilde{\tau}^-) + \tilde{F}_j\tilde{B}_3\Psi\left[U_j\Phi_\varphi(\cdot,-\tilde{\tau}^-)\right](1,0)\right). \tag{3.139}$$

If

$$\operatorname{rank}\Upsilon = \operatorname{rank}\left[\Upsilon \quad q_i^0\right], \quad i=1,\ldots,n_f, \tag{3.140}$$

holds, then (3.138) has a solution

$$\xi_i^0 = \Upsilon^\dagger q_i^0 + (I - \Upsilon^\dagger\Upsilon)\xi_i^* \tag{3.141}$$

where $\Upsilon^\dagger$ is the Moore-Penrose generalized inverse of Υ (for details see, e.g., [11, Prop. 6.1.7]) and $\xi_i^* \in \mathbb{R}^{n_\xi}$ is a degree of freedom that will be considered later.

On the third interval, i.e., $\tau \in I_3$, (3.132) is also autonomous due to $\mu_i(\tau) = 0$, $\tau \in I_3$ and thus $\xi_i(\tau)$, $\tau \in I_3$ is specified by $\xi_i(T-\tilde{\tau}^-) = \xi_i^1 \in \mathbb{R}^{n_\xi}$. Obviously, the end condition in (3.120b) is satisfied for the IC $\xi_i^1 = 0$, which implies

$$\xi_i(\tau) = 0, \quad \tau \in I_3 \tag{3.142}$$

in the light of (3.130) and (3.135).

On the remaining interval I_2, $\xi_i(\tau)$ has to satisfy the imposed initial and end conditions

$$\xi_i(\tilde{\tau}^+) = \Phi_\varphi(\tilde{\tau}^+,-\tilde{\tau}^-)\xi_i^0 \tag{3.143a}$$
$$\xi_i(T-\tilde{\tau}^-) = 0, \tag{3.143b}$$

which are implied by (3.136) and (3.142). Provided (A_φ, B_φ) is controllable, there exists an input $\mu_i(\tau)$ on $\tau \in I_2$ for (3.132) such that (3.143) holds. This input takes the form

$$\mu_i(\tau) = -B_\varphi^\top \Phi_\varphi^\top(\tilde{\tau}^+,\tau)W_\varphi^{-1}\xi_i(\tilde{\tau}^+), \quad \tau \in I_2, \tag{3.144}$$

(see [16, Section 6.2]) in which

$$W_\varphi = \int\limits_{\tilde\tau^+}^{T-\tilde\tau^-} \Phi_\varphi(\tilde\tau^+,\tau)B_\varphi B_\varphi^\top \Phi_\varphi^\top(\tilde\tau^+,\tau)\mathrm{d}\tau \tag{3.145}$$

is the *Controllability Gramian* (see, e.g., [16, Theorem 6.1]). The required inverse of W_φ for (3.144) exists if (A_φ, B_φ) is controllable. In view of (3.125), (3.131), $\dim \varphi_i^\star(\tau) = \dim \mu_i^\star(\tau)$ and (3.132b), $\varphi_i^\star(\tau)$ in (3.132b) is a flat output for (3.132a). This flatness property implies the controllability of (A_φ, B_φ) (see, e.g., [82, Sec. 3.2.2]). Thus, by inserting (3.144) in the solution

$$\xi_i(\tau) = \Phi_\varphi(\tau,\tilde\tau^+)\left(\xi_i(\tilde\tau^+) + \int\limits_{\tilde\tau^+}^{\tau} \Phi_\varphi(\tilde\tau^+,\zeta)B_\varphi\mu_i(\zeta)\mathrm{d}\zeta\right), \quad \tau \in \mathrm{I}_2, \tag{3.146}$$

of (3.132a) on I_2, the result

$$\xi_i(\tau) = \Phi_\varphi(\tau,\tilde\tau^+)\left(I - \int\limits_{\tilde\tau^+}^{\tau} \Phi_\varphi(\tilde\tau^+,\zeta)B_\varphi B_\varphi^\top \Phi_\varphi^\top(\tilde\tau^+,\zeta)\mathrm{d}\zeta W_\varphi^{-1}(\tilde\tau^+, T-\tau^-)\right)\xi_i(\tilde\tau^+) \tag{3.147}$$

for $\tau \in \mathrm{I}_2$ is obtained. With (3.147) the initial and end conditions (3.143) can be verified in view of (3.145).

Consequently, a constructive approach for the solution of the fault diagnosis kernel equations (3.112) subject to (3.113) has been found. Furthermore, it leads to the easy verifiable condition (3.140). The results of this section are summarized in the following theorem.

Theorem 3.8 (Identifiability condition)
Let (3.140) hold and assume $T > T_0$. Then, the fault $f_i(t)$, $i = 1, \ldots, n_f$, is identifiable by (2.157).

Proof. The proof of this theorem is based on the solvability of the kernel equations. If $T > T_0$ and (3.140) hold for $i = 1, \ldots, n_f$, then the fault diagnosis kernels in backstepping coordinates (3.122) have a piecewise C-solution satisfying the initial and end conditions (3.120b) and (3.127). It can be concluded from the invertible backstepping transformation and invertible spatial reversal, that this solution satisfies also the fault diagnosis kernel equations (3.112) and (3.113). Hence, the required

kernels $n_i(\tau)$ and $m_{u,i}(\tau)$, $i = 1, \ldots, n_f$, for the fault identification equation (2.157) and the integral kernel $m_{\bar{d},i}(\tau)$ required for the computation of the threshold $f_{B,i}$ (see (2.163)) for the fault detection, isolation and estimation can be computed. Thus, the residual generator (2.157) exists in accordance with Theorem 3.4 and the fault $f_i(t)$ can be diagnosed. ∎

The condition (3.140) depends on q_i^0 and Υ. In view of (3.120b), q_i^0 depends only on R_f, which is a property of the fault signal model. The matrix Υ is given in (3.139) from which it can be seen, that it only depends on system parameters and the signal models for the fault and the disturbance. Hence, (3.140) is a property of the system (3.1), the disturbance signal model (2.15) and the signal model (2.143) of the fault to be identified. Note that if (3.140) holds, then also fault detection, isolation and estimation are ensured (see Theorems 3.5, 3.6 and 3.7).

Finally, the remaining degrees of freedom ξ_i^* in (3.141) can be used to make the residual generator less sensitive to the bounded disturbance $\bar{d}(t)$. Consider $f_{B,i}$ given in (2.163) as a measure for the sensitivity of the residual generator with respect to $\bar{d}(t)$. In view of (2.163), $m_{\bar{d},i}(\tau)$ is expressed in terms of ξ_i^*, for which the result (A.63) is used. With the substitutions $m_{\bar{d}}^\star(\tau) \to m_{\bar{d},i}^\star(\tau)$ and $\varphi^\star(\tau) \to \varphi_i^\star(\tau)$ in (A.63),

$$m_{\bar{d},i}^\star(\tau) = \Psi_{\bar{d}}[\xi_i](\tau) \tag{3.148}$$

is obtained where

$$\Psi_{\bar{d}}[\xi_i](\tau) = \sum_{j=0}^{n_q} \int_0^1 X_{1,j}^{\bar{d}} \Psi[U_j \xi_i](z,\tau) \mathrm{d}z + X_{2,j}^{\bar{d}} U_j \xi_i(\tau) + X_{3,j}^{\bar{d}} \Psi[U_j \xi_i](1,\tau) \tag{3.149}$$

results from inserting (3.134) in (A.63). To obtain $m_{\bar{d},i}^\star(\tau)$ in terms of ξ_i^0, introduce

$$\xi_i(\tau) = \theta_\xi(\tau) \xi_i^0 \tag{3.150}$$

with

$$\theta_\xi(\tau) = \begin{cases} \Phi_\varphi(\tau, -\tilde{\tau}^-)\xi_i^0 & : \tau \in \mathrm{I}_1 \\ \Phi_\xi(\tau)\xi_i^0 & : \tau \in \mathrm{I}_2 \\ 0 & : \tau \in \mathrm{I}_3 \end{cases} \tag{3.151}$$

in the light of (3.136), (3.142) and

$$\Phi_\xi(\tau) = \Phi_\varphi(\tau, \tilde{\tau}^+) \left(I - \int_{\tilde{\tau}^+}^{\tau} \Phi_\varphi(\tilde{\tau}^+, \zeta) B_\varphi B_\varphi^\top \Phi_\varphi^\top(\tilde{\tau}^+, \zeta) \mathrm{d}\zeta W_\varphi^{-1}(\tilde{\tau}^+, T - \tau^-) \right)$$
$$\cdot \Phi_\varphi(\tilde{\tau}^+, -\tilde{\tau}^-)\xi_i^0, \quad \tau \in \mathrm{I}_2. \tag{3.152}$$

The latter results from inserting (3.143a) in (3.147). Thus,

$$m_{\bar{d},i}^\star(\tau) = \Psi_{\bar{d}}\left[\theta_\xi\right](\tau)\xi_i^0 \tag{3.153}$$

follows from (3.150) and (3.151). Finally, (3.153) can be rewritten in the form (2.211) by utilizing (3.141) in (3.153), which yields

$$\theta_{0,i}(\tau) = \Psi_{\bar{d}}\left[\theta_\xi\right](\tau)\Upsilon^\dagger q_i^0 \tag{3.154a}$$
$$\theta_1(\tau) = \Psi_{\bar{d}}\left[\theta_\xi\right](\tau)\left(I - \Upsilon^\dagger \Upsilon\right). \tag{3.154b}$$

With (3.154), the threshold $f_{B,i}$ can be computed by (2.213) and ξ_i^* should be chosen as the solution of the minimization problem (2.214).

3.3.3 Fault diagnosis for the cable immersed in water

In the following, the described fault diagnosis approach for heterodirectional hyperbolic ODE-PDE systems is demonstrated with a simulation of a real-world motivated application example. The simulations are performed in MATLAB 2020a and the code is available at [108]. The example system is a cable with a payload immersed in water with constant flow and is motivated by a real-world system (see [87]). A similar model has already been used for the fault detection in Section 3.2.4. However, to make the fault diagnosis method applicable, the fault setup is adapted so that only additive faults are considered, which are described by the signal model (2.143). The equations of motion for the deflection of the cable in transversal and longitudinal

direction read as

$$\partial_t^2 v_1(z,t) = \kappa_1(z)\partial_z^2 v_1(z,t) + \kappa_2(z)\partial_z v_1(z,t) + \kappa_3(z)\partial_z v_2(z,t)$$
$$+ \kappa_4(z)\partial_t v_1(z,t) + \bar{d}_1(t) + e_1(z)f_1(t) \tag{3.155a}$$

$$\partial_t^2 v_2(z,t) = \kappa_5(z)\partial_z^2 v_2(z,t) + \kappa_6(z)\partial_z v_1(z,t) + \kappa_7(z)\partial_t v_2(z,t)$$
$$+ \bar{d}_1(t) + \tilde{d}(t) \tag{3.155b}$$

$$\ddot{v}_1(0,t) = \kappa_8 \dot{v}_1(0,t) + \kappa_9 \partial_z v_1(0,t) + \kappa_{10}\partial_z v_2(0,t), \qquad t > 0 \tag{3.155c}$$

$$\ddot{v}_2(0,t) = \kappa_{11}\dot{v}_2(0,t) + \kappa_{12}\partial_z v_2(0,t) + \kappa_{13}\partial_z v_1(0,t), \qquad t > 0 \tag{3.155d}$$

$$\partial_z v_1(1,t) = b_1 u_1(t), \qquad t > 0 \tag{3.155e}$$

$$\partial_z v_2(1,t) = b_2 u_2(t) + e_3 f_2(t), \qquad t > 0 \tag{3.155f}$$

$$y_1(t) = \partial_z v_1(0,t) + \bar{d}_2(t), \qquad t \geq 0 \tag{3.155g}$$

$$y_2(t) = \partial_z v_2(0,t) + f_3(t) + \bar{d}_3(t), \qquad t \geq 0 \tag{3.155h}$$

with (3.155a) and (3.155b) defined on $(z,\tau) \in (0,1) \times \mathbb{R}^+$. In (3.155), $v_i(z,t) \in \mathbb{R}$, $i = 1,2$, are the lateral and longitudinal deflection of the cable (see Figure 3.2), the dynamics of the attached payload is described with the dynamic BCs (3.155c) and (3.155d) at $z = 0$, the actuated BCs are (3.155e) as well as (3.155f) and the components $y_i(t)$, $i = 1,2$, of the measurement $y(t)$ are given by (3.155g) and (3.155h). The disturbance $\tilde{d}(t)$ is assumed to be a solution of the finite-dimensional signal model (2.15) specified by the matrices (3.91) and the unknown but bounded disturbances $\bar{d}_i(t)$, $i = 1,2,3$, are absolutely bounded by $|\bar{d}_i(t)| \leq \delta_i$ with known upper bound $\delta = \mathrm{col}\,(0.03, 0.01, 0.02)$. The considered faults $f_i(t)$, $i = 1,2,3$, are a process fault $f_1(t)$, an actuator fault $f_2(t)$ and a sensor fault $f_3(t)$. All faults are assumed to be of sinusoidal form $f_i(t) = f_i^0 \sin(\omega_i t + \phi_{f,i})$, $i = 1,2,3$, with the unknown parameters f_i^0, $\phi_{f,i} \in \mathbb{R}$ and known parameter $\omega_1 = 2$, $\omega_2 = 0.5$ as well as $\omega_3 = 1$. The signal models for the sinusoidal fault signals $f_i(t)$ are

$$\dot{v}_{f,i}(t) = S_{f,i} v_{f,i}(t), \qquad t > 0 \tag{3.156a}$$

$$f_i(t) = r_{f,i}^\top v_{f,i}, \qquad t \geq 0 \tag{3.156b}$$

with the states $v_{f,i}(t) \in \mathbb{R}^2$, $i = 1,2,3$, and the matrices

$$S_{f,i} = \begin{bmatrix} 0 & -\omega_i \\ \omega_i & 0 \end{bmatrix}, \qquad r_{f,i}^\top = \begin{bmatrix} 0 & 1 \end{bmatrix}, \quad i = 1,2,3. \tag{3.156c}$$

It is assumed that the fault $f_i(t)$ is zero until it occurs at $t_i > 0$, i.e., for $t < t_i$, $f_i(t) = 0$ holds. Thus, the fault signal $f_i(t)$ is piecewise described by the solution of the signal model (3.156) and the ICs $v_{f,i}(0) = 0$ on the domain $0 < t < t_i$. For $t > t_i$, the fault signal $f_i(t)$ is specified by the unknown ICs $v_{f,i}(t_i) = v_{f,i}^i \in \mathbb{R}^2$, $v_{f,i}^i \neq 0$. The matrices (3.156c) for $i = 1,2,3$, can be aggregated to the common

signal model (2.143) with $S_f = \text{diag}\,(S_{f,1}, S_{f,2}, S_{f,3})$ and $R_f = \text{diag}(r_{f,1}^\top, r_{f,2}^\top, r_{f,3}^\top)$. Consequently, the fault diagnosis problem amounts to the identification of three faults $f_1(t)$, $f_2(t)$ and $f_3(t)$ in the presence of the disturbance $\tilde{d}(t)$, while only two measurements $y_1(t)$ and $y_2(t)$ are available.

According to Section 3.2.4, system (3.155) can be rewritten as a heterodirectional hyperbolic ODE-PDE system (3.1) by introducing the Riemann coordinates (3.95) and applying the Hopf-Cole-type transformation (3.108). Except the fault input matrices $\breve{E}_1 = e_{4,1}e_{3,1}^\top + e_{4,4}e_{3,1}^\top$, $\breve{E}_3 = 2\sqrt{\kappa_5}e_3 e_{2,2}e_{3,2}^\top$ and $E_5 = e_{2,3}e_{3,3}^\top$, the required matrices for the system in the form (3.1) are already specified in Section 3.2.4.

To compute a solution for the fault diagnosis kernel equations (3.112) subject to (3.113), at first the backstepping kernel $\bar{K}(z,\zeta)$ must be determined as the solution of the backstepping kernel equations (3.35). To this end, the boundary-value problem (3.35) is solved as described in Section 3.2.4. With the resulting ODE-PDE system of the fault diagnosis kernel equations in backstepping coordinates (3.32), all matrices for the evaluation of the fault identifiability condition (3.140) can be computed. The singular values

$$\bar{\sigma}(\Upsilon) \in \{864, 814, 107, 67.3, 32.5, 19.7, 3.11, 1.79, 0.151, 0.0313\} \tag{3.157}$$

of $\Upsilon \in \mathbb{R}^{10 \times 20}$, show that rank $\Upsilon = 10$ holds and thus that the identifiability of all three faults is verified in view of Theorem 3.8. Hence, the required IC ξ_i^0 can be computed with (3.141). By solving (2.214) with the MATLAB function `fminsearch`, where the initial point for the numerical optimization is zero, the reference trajectory $\varphi_i^\star(\tau)$ can be determined as the solution of the auxiliary ODE system (3.132). With $\varphi_i^\star(\tau)$, the integral kernel $q^\star(\tau)$ results from the parametrizing expressions (3.126b). Note that for the integral kernels $\tilde{m}(z, \tau)$ and $\tilde{n}(\tau)$, it is convenient to use the differential expressions (3.124) in dependence of $\tilde{m}_i^{-\star}(0, \tau)$, which can be computed by (3.144) in view of (3.130). The required kernels $n_i(\tau)$ and $m_{u,i}(\tau)$ for the residual generator (2.157) can be derived from solving (3.123) for $n_i(\tau)$ respectively by (3.21b) and the usual substitutions.

From the evaluation of (3.19), the longest transportation time in positive and negative spatial direction $\tilde{\tau}^- = \tilde{\tau}^+ = 0.63$ follow, which yields $T_0 = 1.26$ as lower bound for T. To chose a suitable moving horizon length $T > T_0$, the threshold values $f_{B,i}$ and normalized detection delays $\Delta_{f,i}$ are taken into account. The latter is the first time instant where a threshold $f_{B,i}$, $i = 1, 2, 3$, is exceeded by $|\langle M_f, h_{f,i}(t)\rangle_{\text{I}}|$, $h_{f,i}(t) \in \mathbb{R}^{n_f}$, $t \geq 0$. For the integral kernel $M_f(\tau)$ in this expression, $M_f(\tau) = [\, m_{f,1}(\tau)\ m_{f,2}(\tau)\ m_{f,3}(\tau)\,]$ is used with $m_{f,i}(\tau)$ given by (3.21a) and the

substitution $m_f(\tau) \to m_{f,i}(\tau)$. The test signal $h_{f,i}(t)$ is

$$e_{j,n_f}^\top h_{f,i}(t) = \begin{cases} f_j(t) & : i = j \\ 0 & : \text{otherwise}, \end{cases} \qquad i, j = 1, \ldots, n_f, \tag{3.158}$$

with $f_j(t) = r_{f,j}^\top v_{f,j}(t)$, $j = 1, 2, 3$, as the solution of the corresponding signal model given by $S_{f,j}$ and $r_{f,j}$ subject to the ICs $v_{f,1}(0) = \text{col}\,(5, 2)$, $v_{f,2}(0) = \text{col}\,(5, 2)$ and $v_{f,3}(0) = \text{col}\,(1, 1)$. According to the results shown in Figure 3.11 for different T, a trade-off is required since an increase in T reduces the threshold values $f_{B,i}$ but increases the normalized detection delay $\Delta_{f,i}$. For the following simulation results $T = 8.14$ is chosen yielding the threshold values $f_{B,1} = 0.32$, $f_{B,2} = 0.29$ and $f_{B,2} = 0.29$ as well as the integral kernels $N(\tau)$ and $M_u(\tau)$ depicted in Figure 3.12. To motivate the use of (2.214) for the reference trajectory planning, the threshold values are computed with $\xi_0^* = 0$ for a comparison, i.e., without the use of the remaining degrees of freedom. The resulting thresholds $\bar{f}_B = \text{col}\,(26.56, 8.10, 1.57)$ with $\xi_0^* = 0$ demonstrate the effect of the available degrees of freedom to design a residual generator that is less sensitive with respect to the unknown but bounded disturbance $\bar{d}(t)$.

For the simulation of the faulty cable with a payload immersed in water with constant flow, a finite-dimensional state-space model of order 202 is derived for (3.155) by using the spectral method with Chebyshev differentiation matrices of order 51 as described in [86]. Since the control input signal $u(t)$ and the measurement signal $y(t)$ for the following simulation are only available at equally spaced discrete-time samples, the integral expressions in the residual generator (2.157) are approximated by FIR filters. By using the step size 0.01 for the discrete-time sampling, FIR filters of order 815 result.

To verify the fault diagnosis results in Theorem 3.4 for the case $\bar{d}(t) \equiv 0$, a simulation of the faulty cable with a payload immersed in water is performed in MATLAB. For this simulation an equally spaced discrete-time grid with step size 1×10^{-3}, zero ICs, the input signal $u(t)$ shown in Figure 3.6a, the disturbance $\tilde{d}(t)$ shown in Figure 3.6b, $\bar{d}(t) \equiv 0$ and the fault signals shown in Figure 3.13, which result from the ICs

$$v_{f,1}(t_1) = \begin{bmatrix} 0.50 \\ 0 \end{bmatrix}, \qquad v_{f,2}(t_2) = \begin{bmatrix} 0.50 \\ 0 \end{bmatrix}, \qquad v_{f,3}(t_3) = \begin{bmatrix} 0.15 \\ 0 \end{bmatrix} \tag{3.159}$$

and $t_1 = 20$, $t_2 = 50$, $t_3 = 80$, are used. By evaluating the FIR filter representation of the residual generator (2.157) in discrete-time, imposing $u(t) = 0$ and $y(t) = 0$ for $t < 0$ as well as sampling the input $u(t)$ and the output from the simulation $y(t)$ on a time grid with step size 0.01, the residual signal $\hat{f}(t)$ shown Figure 3.13 is derived. After the initialization interval $0 \le t \le T$ all residual signals $\hat{f}_i(t)$ are zero
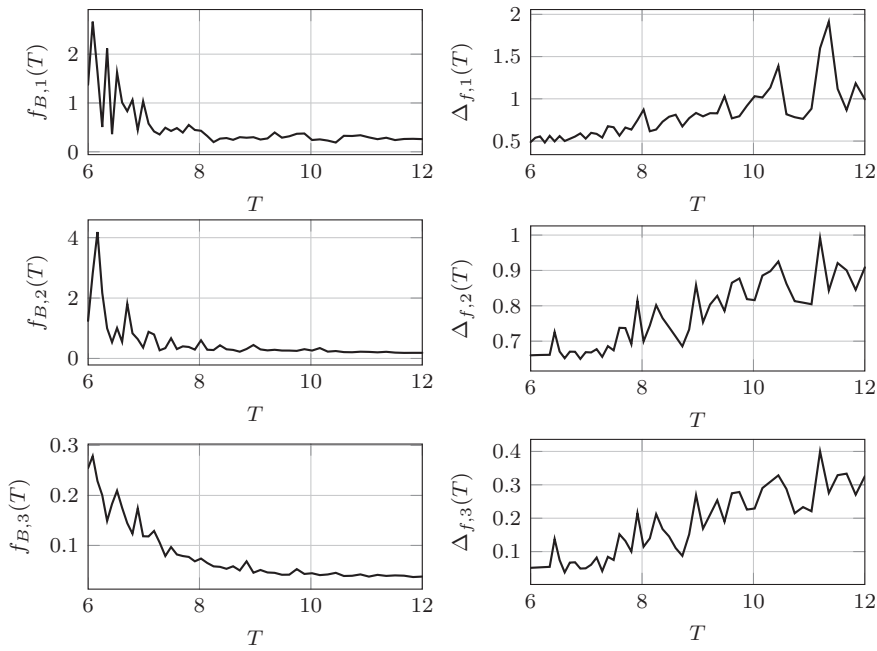
Figure 3.11: Fault detection threshold $f_{B,i}$, $i = 1, 2, 3$, and normalized detection delay $\Delta_{f,i}$ for different moving horizon lengths T.
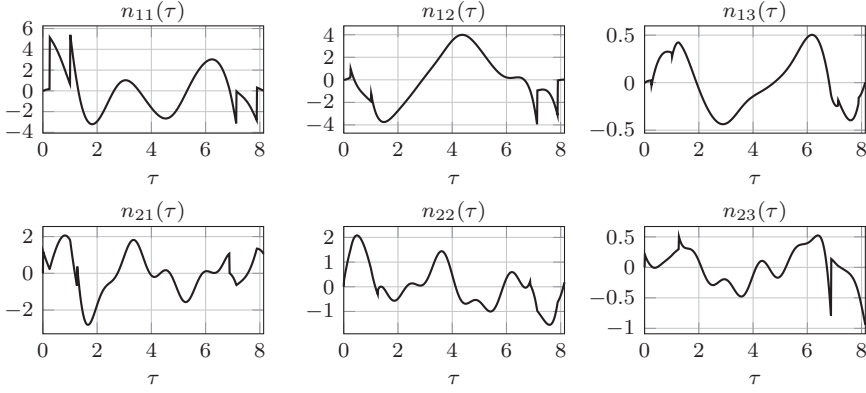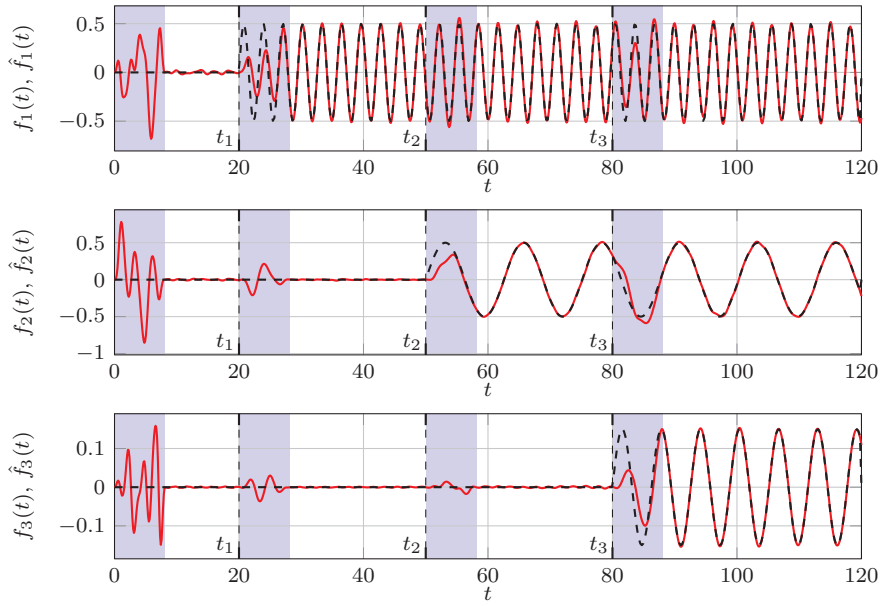
(a) The components $n_{ij}(\tau)$, $i = 1, 2$, $j = 1, 2, 3$, of the integral kernel $N(\tau)$.
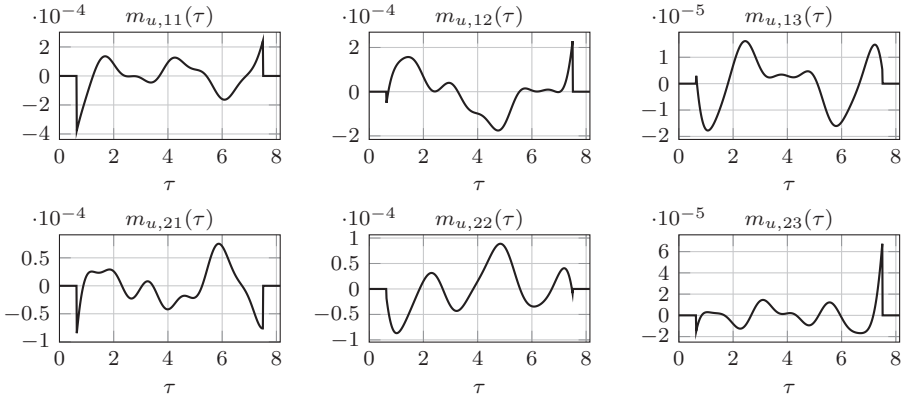
(b) The components $m_{u,ij}(\tau)$, $i = 1, 2$, $j = 1, 2, 3$, of the integral kernel $M_u(\tau)$.

Figure 3.12: The components of the integral kernels $N(\tau)$ and $M_u(\tau)$ of the residual generator (2.157) computed with $T = 8.14$.

Figure 3.13: Fault isolation and identification results $\hat{f}_i(t)$, $i = 1, 2, 3$, (——) for the fault $f_i(t)$ (- - -) without bounded disturbance, i.e., $\bar{d}(t) \equiv 0$, the initialization interval $0 \leq t < T$ (▨) and the transient intervals $t_i < t < t_i + T$ (▨) after the occurrence of a fault.
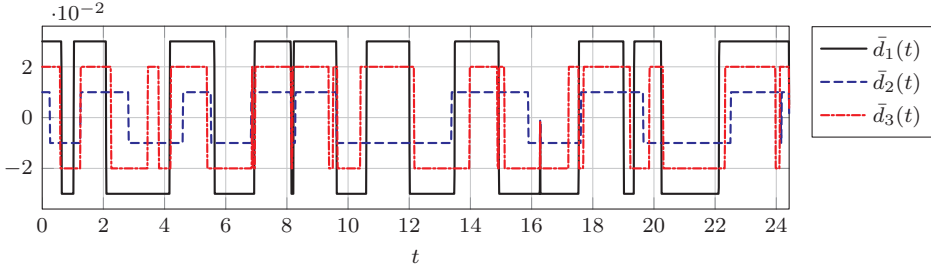
Figure 3.14: Extract of the components $\bar{d}_i(t)$, $i = 1, 2, 3$, of the bounded disturbance $\bar{d}(t)$ on $0 \leq t \leq 24.42$ used for the fault estimation simulation.

until the first fault $f_1(t)$ occurs at $t_1 = 20$, which excites all three residual signals $\hat{f}_i(t)$, $i = 1, 2, 3$. For $t_1 + T < t < t_2$, the fault $f_1(t)$ is identified in finite time by the residual signal $\hat{f}_1(t)$ and both $\hat{f}_i(t)$, $i = 2, 3$, are again zero. Similar results are obtained for the identification of fault $f_2(t)$ and $f_3(t)$.

The fault diagnosis subject to the bounded disturbance $\bar{d}(t)$ is verified by a second simulation, whereas the disturbance $\bar{d}(t)$ shown in Figure 3.14 is explicitly chosen so that the residual signals $\hat{f}_i(t)$ will be close to the threshold values at some time instants. With this disturbance $\bar{d}(t)$, the input signal $u(t)$ shown in Figure 3.6a, the disturbance $\tilde{d}(t)$ shown in Figure 3.6b and the same faults as used for the previous simulation, a simulation for (3.155) is performed. By using the integral kernels shown in Figure 3.12 and the corresponding FIR filters, the residual signals $\hat{f}_i(t)$ presented in Figure 3.15 result. According to Theorem 3.5, the fault $f_1(t)$ is detected at $\hat{t}_1 = 23.55$, since the threshold $f_{B,2}$ is exceeded by the corresponding residual signal $\hat{f}_{B,2}(t)$. The determination of which fault occurred is possible at $t_i^\circ = 31.70$. It follows from Theorem 3.6 that the previously detected fault has to be $f_1(t)$, since the residual signals $\hat{f}_i(t)$, $i = 2, 3$, remain below their threshold values for $t_1 + T \leq t \leq t_2$. At $\hat{t}_2 = 53.77$, the threshold value $f_{B,2}$ is exceeded by $\hat{f}_2(t)$, which indicates the occurrence of a second fault. By $\hat{f}_2(t) > f_{B,2}$ at $t_2^\circ = 63.81$, the second fault must be $f_2(t)$. Finally, $f_3(t)$ is detected at $\hat{t}_3 = 84.27$ and verified by the isolation at $t_3^\circ = 93.20$. After the isolation of a fault, the residual signal $\hat{f}_i(t)$ is an estimate for the corresponding fault $f_i(t)$, since the estimation error is upper bounded by (3.117) as stated in Theorem 3.7.
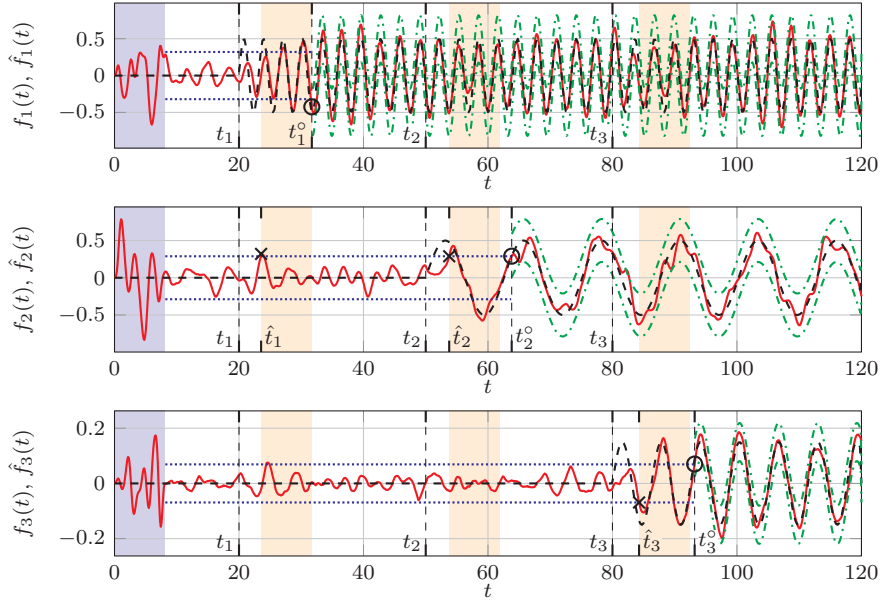
Figure 3.15: Fault diagnosis residual signal $\hat{f}_i(t)$, $i = 1, 2, 3$, (——) in the presence of the bounded disturbance $\bar{d}(t)$ depicted in Figure 3.14 for the fault $f_i(t)$ (- - -), the thresholds $\pm f_{B,i}$ (⋯⋯), the bounds of the fault estimation error $f(t) \pm f_{B,i}$ (-·-·-), the initialization interval $0 \le t < T$ (▨), the detection (✕) of a fault $f_i(t)$ at time $\hat{t}_i$, the isolation delay interval $\hat{t}_i \le t < \hat{t}_i + T$ (▨) and the isolation (◯) at time t_i°, which is also the beginning of the fault estimation.

3.4 Concluding remarks

In this section, it was shown that the fault detection and diagnosis approach developed for parabolic and biharmonic systems in Section 2 can also be applied to heterodirectional hyperbolic ODE-PDE systems. Whereas the derivation of the residual generators for the fault detection and diagnosis follows the same reasoning as for the parabolic and biharmonic ODE-PDE systems, the solution of the kernel equations requires a different approach because of the coupled ODE-PDE system and the distributed delays and predictions of the hyperbolic PDE subsystem. By utilizing a backstepping transformation to map the kernel equations into a target system of cascade structure, a systematic solution for the kernel equations was presented. Note that the use of the backstepping transformation introduces limitations in the possible measurements in the considered system class, since it requires an output equation of the form (3.1e). However, the latter was chosen to simplify the solution of the kernel equations and to derive simple conditions to verify the detectability (see Theorem 3.3) and the identifiability (see Theorem 3.8). By the application of the proposed fault detection and diagnosis approach to a simulation of a cable with payload immersed in water, the effectiveness of the fault detection and diagnosis scheme is demonstrated.

Chapter 4

Concluding remarks and outlook

In the previous Chapters 2 and 3 a fault detection and diagnosis approach was presented, which is based on integral transformations and does not require a system approximation. The separate derivation of the solutions of the fault detection and diagnosis problems for parabolic and biharmonic ODE-PDE systems in Chapter 2 and heterodirectional hyperbolic ODE-PDE systems in Chapter 3 is only due to different system representations, but the general approach is the same. Therefore, this thesis introduces a unified framework for the fault detection and diagnosis for a large system class.

Note that the solution of the kernel equations with flatness-based methods provides an interesting link between the fault diagnosis and flatness-based trajectory planning. Moreover, it is promising for future works to extend the approach also to further system classes, e.g., lumped-parameter and distributed-parameter time-variant systems or also DPS with higher-dimensional spatial domain. To solve the corresponding kernel equations, the flatness-based trajectory planning approaches presented in [62] should be applicable.

Although the consideration of disturbances with known signal form and unknown but bounded disturbances is a first step towards the application of the proposed approach to real-world fault diagnosis problems, further investigations are required. In particular, the influence of model uncertainties should be considered to quantify their effect on the fault diagnosis in order to incorporate them in the threshold value of the residual signal. Moreover, also the consideration of different types of disturbances, e.g., stochastic disturbances or L_2-bounded disturbances in future work will increase the flexibility of the proposed fault detection and diagnosis approaches. According to the assumptions on the disturbances, the sensitivity optimization of the residual generator has to be adapted. A further interesting point for future work is the systematic investigation of the time discretization of the integral expressions in the residual generators. The quasi-continuous implementation of the residual

generator integral expressions in the presented simulation examples leads to FIR filters of high order. However, the results in [48], where similar integral expressions are used for the derivative estimation, suggest that the order of the FIR filters can be considerably reduced. This order reduction can be achieved by a more sophisticated approximation scheme of the integral expression but preserves the simplicity of the FIR filters. For low order approximations of the integral expressions, the approximation error of the time discretization should be considered explicitly in form of a threshold value to make the fault detection and diagnosis results even more reliable.

The simulation results for the fault detection in Section 2.3.5 and Section 3.2.4 show that the fault detection is possible by using only one residual signal. This scalar residual signal is obtained from a residual generator with low computational complexity, but it does not allow fault isolation. Thus, an interesting extension of the proposed fault detection residual generator would be the introduction of a vector valued residual signal, which allows the fault isolation without assumptions on the signal form of the faults.

Appendix A

Proofs, definitions and derivations

A.1 Properties of formal power series

The following definition of formal power series of order ϱ is from [75, Definition 1].

Definition 4 (Formal power series of order ϱ [75, Definition 1]). A formal power series $\sum_{i=0}^{\infty} c_i s^i$, $c_i, s \in \mathbb{C}$ is of order $\varrho > 0$ if for all $\tilde{\varrho} > \varrho$ and all $Z \in \mathbb{R}^+$ the sequence $(c_i Z^i (i!)^{\frac{1}{\tilde{\varrho}}})$ is absolutely bounded.

From this, it follows that for each $\tilde{\varrho} > \varrho$ and $Z \in \mathbb{R}^+$ an upper bound

$$c_{\varrho,Z} = \sup_{i \in \mathbb{N}} |c_i| Z^i (i!)^{\frac{1}{\tilde{\varrho}}} \tag{A.1}$$

with $c_{\varrho,Z} \in \mathbb{R}^+$ exists, so that

$$|c_i| \leq c_{\varrho,Z} (i!)^{-\frac{1}{\tilde{\varrho}}} Z^{-i} \tag{A.2}$$

holds.

The following lemma is taken from [93, 5.3 Hilfssatz], where the proof can be found.

Lemma A.1 ([93, 5.3 Hilfssatz]). A formal power series of order ϱ with term wise sum

$$\hat{c}(s) = \hat{a}(s) + \hat{b}(s) = \sum_{i=0}^{\infty} c_i s^i, \quad c_i = a_i + b_i \tag{A.3}$$

and the *Cauchy product* for multiplication

$$\hat{d}(s) = \hat{a}(s)\hat{b}(s) = \sum_{i=0}^{\infty} d_i s^i, \quad d_i = \sum_{j=0}^{i} a_j b_{j-i} \tag{A.4}$$

form a commutative ring.

It follows from Lemma A.1, that if $\hat{a}(s)$ and $\hat{b}(s)$ are formal power series of order ϱ, also $\hat{c}(s)$ and $\hat{d}(s)$ are formal power series of order ϱ.

A.2 Confirmation of formal Laplace transform in (2.173)

In Section 2.4.3.2 the formal Laplace transform $\dot{q}_{f,i}(\tau) \circ\!\!-\!\!\bullet s\check{q}_{f,i}(s)$ is used. Since the IC of $q_{f,i}(0) = -R_f^\top e_{i,n_f}$ is not zero (see (2.170c)) and is not a steady state of the corresponding system (2.169d), it should be considered in the Laplace transform. However, this makes the calculations far more cumbersome and it is shown in the sequel that the differential expressions derived in Section 2.4.3.2 do not depend on the neglected ICs.

Insert (2.93a) in (2.169d), consider the time reversal $\bar{\tau} = T - \tau$ and introduce $\bar{q}_{f,i}(\bar{\tau}) = q_{f,i}(\tau)$ and $\bar{\mu}_i(\bar{\tau}) = \mu_i(\tau)$, so that

$$-\dot{\bar{q}}_{f,i}(\bar{\tau}) = S_f^\top \bar{q}_{f,i}(\bar{\tau}) + R_f^\top \sum_{j=0}^{\infty} X_j (-1)^j \mathrm{d}_\tau^j \bar{\mu}_i(\bar{\tau}), \quad \bar{\tau} \in (0,T) \tag{A.5}$$

results with the IC $\bar{q}_{f,i}(0) = 0$ following from (2.170c). Applying the Laplace transform $\dot{\bar{q}}_{f,i}(\bar{\tau}) \circ\!\!-\!\!\bullet \check{\bar{q}}_{f,i}(s)$ and using $\check{X}(s) = \sum_{j=0}^{\infty} X_j (-1)^j s^j$, yields

$$\left(-sI - S_f^\top \right) \check{\bar{q}}_{f,i}(s) = R_f^\top \check{X}(s) \check{\bar{\mu}}_i(s). \tag{A.6}$$

Introduce the parametrizing variable $\breve{\bar{\varphi}}_i(s)$, by establishing the expressions

$$\breve{\bar{q}}_{f,i}(s) = \mathrm{adj}\left(-sI - S_f^\top\right) R_f^\top \breve{X}(s)\breve{\bar{\varphi}}_i(s) \tag{A.7a}$$

$$\breve{\bar{\mu}}_i(s) = \det\left(-sI - S_f^\top\right) \breve{\bar{\varphi}}_i(s). \tag{A.7b}$$

With the substitution $s = -\bar{s}$,

$$\det(\bar{s}I - S_f^\top) = \sum_{i=0}^{n_{vf}} a_i \bar{s}^i \tag{A.8}$$

follows in view of (2.181) and a re-substitution $s = -\bar{s}$, yields

$$\det\left(-sI - S_f^\top\right) = \sum_{i=0}^{n_{vf}} (-1)^i a_i s^i. \tag{A.9}$$

Insert (A.9) in (A.7b) and apply the Laplace correspondence $\breve{\bar{\varphi}}_i(s)\,\bullet\!\!-\!\!\circ\,\bar{\varphi}_i(\bar{\tau})$, to obtain

$$\bar{\mu}_i(\bar{\tau}) = \sum_{j=0}^{n_{vf}} (-1)^i a_i \mathrm{d}_{\bar{\tau}}^i \bar{\varphi}_i(\bar{\tau}). \tag{A.10}$$

The time reversal $\tau = T - \bar{\tau}$, shows that (A.10) is equivalent to (2.185) as it is derived in Section 2.4.3.2. To verify the differential expression for $q_{f,i}(\tau)$, consider $\bar{s} = -s$ in $\mathrm{adj}(-sI - S_f^\top)$ and express $\breve{X}(s)$ in (A.7a) with $\breve{X}(\bar{s}) = \sum_{i=0}^\infty X_i \bar{s}^i$. By inserting the result in (A.7a)

$$\breve{\bar{q}}_{f,i}(\bar{s}) = \sum_{j=0}^\infty W_j \bar{s}^j \breve{\bar{\varphi}}_i(\bar{s}) \tag{A.11}$$

is obtained in view of (2.179). After the re-substitution $s = -\bar{s}$ in (A.11), the time domain correspondences

$$\bar{q}_{f,i}(\bar{\tau}) = \sum_{j=0}^\infty W_j (-1)^j \mathrm{d}_{\bar{\tau}}^j \bar{\varphi}_i(\bar{\tau}) \tag{A.12}$$

follows. Finally, the time reversal $\tau = T - \bar{\tau}$ yields (2.184a). Thus, the computation in reverse time with homogeneous ICs leads to the same result as the formal calculation, which verifies that the expressions (2.180) and (2.182) are independent of the ICs. Consequently, the formal application of the Laplace transform can be used to compute the differential expressions.

A.3 Derivation of (2.194)

In the following, the expression (2.194) is proven with induction. The initial case is given directly by (2.191b). The induction step is obtained by taking the time derivatives of (2.191b) and inserting of (2.191a) for the time derivative of $\xi_i(\tau)$. This yields the induction step (2.194). Computing this for $j + 1$,

$$\mathrm{d}_\tau^{j+1}\varphi_i^\star(\tau) = C_\varphi A_\varphi^j \mathrm{d}_\tau \xi(\tau) + C_\varphi \sum_{k=0}^{j-1} A_\varphi^{j-k-1} B_\varphi \mathrm{d}_\tau^{k+1} \mu_i^\star(\tau), \quad i = 1, \ldots, n_f \quad \text{(A.13)}$$

results. Inserting (2.191a) yields

$$\mathrm{d}_\tau^{j+1}\varphi_i^\star(\tau) = C_\varphi A_\varphi^{j+1} \xi(\tau) + C_\varphi A_\varphi^j B_\varphi \mu_i^\star(\tau) + C_\varphi \sum_{k=0}^{j-1} A_\varphi^{j-k-1} B_\varphi \mathrm{d}_\tau^{k+1} \mu_i^\star(\tau). \quad \text{(A.14)}$$

Then, summarizing the terms dependent on $\mu_i^\star(\tau)$ leads to

$$\mathrm{d}_\tau^{j+1}\varphi_i^\star(\tau) = C_\varphi A_\varphi^{j+1} \mathrm{d}_\tau \xi(\tau) + C_\varphi \sum_{k=0}^{j} A_\varphi^{j-k} B_\varphi \mathrm{d}_\tau^{k} \mu_i^\star(\tau), \quad \text{(A.15)}$$

which is equal to $\mathrm{d}_\tau^{j+1}\varphi_i^\star(\tau)$ obtained from (2.194) and completes the inductive step.

A.4 Convergence of the series (2.197)

Corollary A.1. Let the coefficients w_j^{kl}, $k = 1, \ldots, n_{vf}$, $l = 1, \ldots, n_y$ of $W_j \in \mathbb{R}^{n_{vf} \times n_y}$, $j \in \mathbb{N}_0$ be a formal power series of order ϱ. Then, the series defining Υ in (2.197) is absolutely convergent.

Proof. To use the direct comparison test to show the absolute convergence of the series in (2.197), the upper bound

$$\|W_i C_\varphi A_\varphi^i\|_\infty \leq \|C_\varphi\|_1 \|W_i\|_\infty \|A_\varphi\|_1^i \quad \text{(A.16)}$$

for the summands in (2.197) is derived, where $\|H\|_\infty = \max_{i \in \{1,\ldots,n\}, j \in \{1,\ldots,m\}} |h_{ij}|$ for the components $h_{ij} \in \mathbb{R}$ of $H \in \mathbb{R}^{n \times m}$ and $\|H\|_1 = \sum_{i=1}^{n} \sum_{j=1}^{m} |h_{ij}|$. At this, (A.16) results from utilizing that $\|H\|_\infty$ and $\|H\|_1$ are compatible norms and that

$\|H\|_1$ is submultiplicative (for both see [11, Proposition 9.3.5]). Since the coefficients w_j^{kl}, $k = 1, \ldots, n_{vf}$, $l = 1, \ldots, n_y$ of W_j are formal power series of order ϱ, (A.2) gives

$$\|W_i\|_\infty \le c_{\varrho,Z}(i!)^{-\frac{1}{\tilde{\varrho}}} Z^{-i}, \quad i \in \mathbb{N}_0 \tag{A.17}$$

where $c_{\varrho,Z}$ and Z are real valued constants and $\tilde{\varrho} > \rho > 0$. With (A.17) and $a = \frac{\|A_\varphi\|_1}{Z}$, (2.197) is dominated by the formal power series

$$\bar{\Upsilon} = \|C_\varphi\|_1 c_{\varrho,Z} \sum_{i=0}^\infty (i!)^{-\frac{1}{\tilde{\varrho}}} a^i. \tag{A.18}$$

The *Cauchy-Hadamard theorem* states that (A.18) is absolutely convergent, since

$$\varlimsup_{i\to\infty} \left| (i!)^{-\frac{1}{\tilde{\varrho}}} \right|^{\frac{1}{i}} = 0 \tag{A.19}$$

holds, where $\varlimsup_{i\to\infty}$ is the *limit superior*. This can be shown utilizing the estimate $i! \ge (\frac{i}{e})^i e$ with the Euler's number e. The absolute convergence of (A.18) verifies that (2.197) is absolutely convergent. ∎

A.5 Recursive algorithm for the computation of the coefficient matrices in (2.89)

In the following, the presented approach in [75] for the determination of $\Phi_i(z, \zeta)$ in (2.89a) is used to derive explicit expressions for the computation of $\Phi_i(z, \zeta)$, $\Psi_{C,i}(z)$ and $\Psi_{L,i}(z)$ in (2.89).

Since the operator $\check{\Phi}(z, \zeta, s)$ defined as state transition matrix satisfying (2.76) as well as $\check{\Psi}_L(z, s)$ and $\check{\Psi}_C(z, s)$ given in (2.78) must be independent of $\check{m}(0, s)$ and $\check{q}(s)$ as well as $\check{n}(s)$, they can be determined by

$$\partial_z \check{m}(z, s) = -\check{A}^*(z, s)\check{m}(z, s) + \bar{L}_1(z)\check{q} + C_1^\top(z)\check{n} \tag{A.20}$$

with the IC $\check{m}(0, s) = \omega_0^0 \in \mathbb{R}^{n_x}$ and $\check{q} = const. \in \mathbb{R}^{n_q}$ as well as $\check{n} = const. \in \mathbb{R}^{n_y}$ independent of s. As shown in [75], the solution of (A.20) can be described by

$$\check{m}(z, s) = \sum_{i=0}^\infty \omega_i(z) s^i. \tag{A.21}$$

By inserting (A.21) in (A.20) and taking $\check{A}^*(z,s) = \sum_{i=0}^{n_A} A_i^\top(z)s^i$ into account,

$$\sum_{i=0}^{\infty} \partial_z \omega_i(z)s^i = -\sum_{j=0}^{n_A}\sum_{k=0}^{\infty} A_j^\top(z)\omega_k(z)s^{j+k} + \bar{L}_1(z)\check{q} + C_1^\top(z)\check{n} \qquad (A.22)$$

follows. With a change of the order of the summation, the substitution $k \to i-j$ and convention $\omega_i(z) = 0$, $i < 0$, (A.22) can be rewritten into

$$\sum_{i=0}^{\infty} \partial_z \omega_i(z)s^i = -\sum_{i=0}^{\infty}\sum_{j=0}^{n_A} A_j^\top(z)\omega_{i-j}(z)s^i + \bar{L}_1(z)\check{q} + C_1^\top(z)\check{n} \qquad (A.23)$$

(see [75]). A coefficient comparison with respect to s, yields

$$\partial_z \omega_0(z) = -A_0^\top(z)\omega_0(z) + \bar{L}_1(z)\check{q} + C_1^\top(z)\check{n} \qquad (A.24a)$$

$$\partial_z \omega_i(z) = -\sum_{j=0}^{n_A} A_j^\top(z)\omega_{i-j}(z), \quad i > 0, \qquad (A.24b)$$

with the corresponding ICs $\omega_0(0) = \omega_0^0$ and $\omega_i(0) = 0$, $i > 0$, resulting from $\check{m}(0,s) = \omega_0^0$. Consequently, (A.24a) has the general solution

$$\omega_0(z) = \Phi_0(z)\omega_0^0 + \Psi_{L,0}(z)\check{q} + \Psi_{C,0}(z)\check{n} \qquad (A.25)$$

with

$$\Phi_0(z) = \bar{\Phi}(z,0) \qquad (A.26a)$$

$$\Psi_{L,0}(z) = -\int_0^z \bar{\Phi}(z,\zeta)\bar{L}_1(\zeta)\mathrm{d}\zeta \qquad (A.26b)$$

$$\Psi_{C,0}(z) = -\int_0^z \bar{\Phi}(z,\zeta)C_1^\top(\zeta)\mathrm{d}\zeta \qquad (A.26c)$$

and $\bar{\Phi}(z,\zeta)$ as state transition matrix of $\partial_z\omega_0(z) = -A_0^\top(z)\omega_0(z)$ given by the unique solution of

$$\partial_z\bar{\Phi}(z,\zeta) = -A_0^\top(z)\bar{\Phi}(z,\zeta), \quad \bar{\Phi}(z,z) = I, \quad (z,\zeta) \in (0,1)^2 \qquad (A.27)$$

(see, e.g., [16, Definition 4.2]). Rewriting (A.24b) into the form

$$\partial_z\omega_i(z) = A_0^\top(z)\omega_i(z) - \sum_{j=1}^{n_A} A_j^\top(z)\omega_{i-j}(z), \quad i > 0 \qquad (A.28)$$

and taking $\omega_i(0) = 0$, $i > 0$ into account, the solution of (A.24b) reads as

$$\omega_i(z) = -\int_0^z \bar{\Phi}(z,\zeta) \sum_{j=1}^{n_A} A_j^\top(\zeta)\omega_{i-j}(\zeta)\mathrm{d}\zeta. \tag{A.29}$$

With induction, it can be shown that (A.29) can be rewritten into the form

$$\omega_i(z) = \Phi_i(z)\omega_0^0 + \Psi_{L,i}(z)\breve{q} + \Psi_{C,i}(z)\breve{n}, \quad i > 0 \tag{A.30}$$

where the introduced matrices are

$$\Phi_i(z) = -\int_0^z \bar{\Phi}(z,\zeta) \sum_{j=1}^{n_A} A_j^\top(z)\Phi_{i-j}(\zeta)\mathrm{d}\zeta \tag{A.31a}$$

$$\Psi_{L,i}(z) = -\int_0^z \bar{\Phi}(z,\zeta) \sum_{j=1}^{n_A} A_j^\top(z)\Psi_{L,i-j}(\zeta)\mathrm{d}\zeta \tag{A.31b}$$

$$\Psi_{C,i}(z) = -\int_0^z \bar{\Phi}(z,\zeta) \sum_{j=1}^{n_A} A_j^\top(z)\Psi_{C,i-j}(\zeta)\mathrm{d}\zeta \tag{A.31c}$$

for $i > 0$ with the convention $\Phi_j(\zeta) = 0$, $\Psi_{L,j}(\zeta) = 0$ and $\Psi_{C,j}(\zeta) = 0$ for $j < 0$. The initial case $i = 1$ of the induction follows directly from inserting (A.25) in (A.29) for $i = 1$ yielding

$$\omega_1(z) = -\int_0^z \bar{\Phi}(z,\zeta)A_1^\top(\zeta)(\Phi_0(\zeta)\omega_0^0 + \Psi_{L,0}(\zeta)\breve{q} + \Psi_{C,0}(\zeta)\breve{n})\mathrm{d}\zeta, \tag{A.32}$$

which proves (A.31) for $i = 1$. To show the induction step, insert (A.30) in (A.29) to obtain

$$\omega_{i+1} = -\int_0^z \bar{\Phi}(z,\zeta) \sum_{j=1}^{n_A} A_j^\top(\zeta) \left(\Phi_{i+1-j}(\zeta)\omega_0^0 + \Psi_{L,i+1-j}(\zeta)\breve{q} + \Psi_{C,i+1-j}(\zeta)\breve{n}\right)\mathrm{d}\zeta, \tag{A.33}$$

so that (A.31) is verified for $i+1$, after sorting the terms for ω_0^0, $\breve{q}$ and $\breve{n}$. Consequently, the required coefficient matrices can be computed with (A.26) for $i = 0$ and the recursion (A.31) for $i > 0$.

A.6 Approximation of the integral expressions as FIR filters using the compound midpoint rule

As described in Section 2.3.3, the integral expressions of the residual generator can be interpreted as a convolution of a system variable and an integral kernel. Therefore, it is reasonable that a discrete-time realization of these integral expressions with sampled data leads to a convolution sum. An interesting investigation of different numerical quadrature rules for the determination of the convolution sum can be found in [50]. Based on these results, the compound midpoint rule is chosen for the discrete-time realization of the integral expressions in the input and output filters of the residual generators (2.50) respectively (2.157). Below, this approximation is shown for a simple integral expression of the form

$$\langle n, y(t) \rangle_{\mathrm{I}} = \int_0^T n(\tau) y(t - \tau) \mathrm{d}\tau, \quad t \geq T \tag{A.34}$$

with $n(\tau) \in \mathbb{R}$ and $y(t) \in \mathbb{R}$. The compound midpoint rule (see, e.g., [51]) is a simple but efficient numerical quadrature, which leads to a good approximation of the integral expression for a sufficient number of sampling points in the moving horizon $\mathrm{I}_t = [t - T, t]$. Assume an equidistant sampling of $y(t)$ at the sampling points $t_k = kT_s$, $k \in \mathbb{N}$, with the sampling period $T_s \in \mathbb{R}^+$, which satisfies $N_s = T/T_s$ so that $N_s \in \mathbb{N}$ holds. Thus, (A.34) can be represented as a sum of integrals

$$\langle n, y(t) \rangle_{\mathrm{I}} = \sum_{i=0}^{N_s - 1} \int_{iT_s}^{(i+1)T_s} n(\tau) y(t - \tau) \mathrm{d}\tau, \quad t \geq T. \tag{A.35}$$

Assume that T_s is sufficiently small so that the integrand of (A.35) can be assumed to be constant on a period $\tau \in (iT_s, (i+1)T_s)$, i.e.,

$$n(\tau) y(t - \tau) \approx n\left((i + \text{\small 1/2}) T_s\right) y\left(t - (i + \text{\small 1/2}) T_s\right), \quad \tau \in (iT_s, (i+1)T_s) \tag{A.36}$$

holds. Hence, the integrals in (A.35) can be computed as the area of the resulting rectangle, which is given by

$$\int_{iT_s}^{(i+1)T_s} n(\tau) y(t - \tau) \mathrm{d}\tau \approx T_s n\left((i + \text{\small 1/2}) T_s\right) y\left(t - (i + \text{\small 1/2}) T_s\right) \tag{A.37}$$

for $i = 0, \ldots, N_s - 1$. Thus, (A.35) can be approximated by

$$\langle n, y(t) \rangle_\mathrm{I} \approx T_s \sum_{i=0}^{N_s-1} n\left((i + {}^1\!/_2)\, T_s\right) y\left(t - (i + {}^1\!/_2)\, T_s\right), \quad t \geq T. \tag{A.38}$$

To take into account that $y(t)$ is only known at the time steps $y(kT_s)$, $k \in \mathbb{N}$, (A.38) must be evaluated at $t = (k + {}^1\!/_2)\, T_s$, which yields

$$\langle n, y\left((k + {}^1\!/_2)\, T_s\right) \rangle_\mathrm{I} \approx T_s \sum_{i=0}^{N_s-1} \bar{n}_i \bar{y}_{k-i}, \quad k \geq N_s \tag{A.39}$$

with $\bar{n}_i = n\left((i + {}^1\!/_2)\, T_s\right)$ and $\bar{y}_{k-i} = y\left((k - i)T_s\right)$. Thus, the compound midpoint rule approximates the time-continuous integral expression (A.34) by a linear difference equation with constant coefficients and compensates a half sampling period. In view of, e.g, [64, Section 2.4.2], the right-hand side in (A.39) exhibits the form of a FIR filter. The implementation of matrix valued integral kernels and vector valued signals can be achieved component-wise using the above described approach.

A.7 Derivation of the input-output expression (3.20)

Apply (3.17a) to (3.1a) resulting in

$$\begin{aligned}
\langle m, \partial_z x(t) \rangle_{\Omega,\mathrm{I}} = {}& \langle m, \Gamma \partial_t x(t) \rangle_{\Omega,\mathrm{I}} + \langle m, A x(t) \rangle_{\Omega,\mathrm{I}} + \langle m, A_0 x^-(0,t) \rangle_{\Omega,\mathrm{I}} \\
& + \langle m, \mathcal{D}[x(t)] \rangle_{\Omega,\mathrm{I}} + \langle m, H_1 w(t) \rangle_{\Omega,\mathrm{I}} + \langle m, B_1 u(t) \rangle_{\Omega,\mathrm{I}} \\
& + \langle m, E_1 f(t) \rangle_{\Omega,\mathrm{I}} + \langle m, G_1 d(t) \rangle_{\Omega,\mathrm{I}}
\end{aligned} \tag{A.40}$$

with $\mathcal{D}[x(t)](z) = \int_0^z D(z,\zeta) x(\zeta,t) \mathrm{d}\zeta$. In order to eliminate the terms in (A.40) depending on $x(z,t)$, at first apply integration by parts with respect to z for the left-hand-side in (A.40), yielding

$$\langle m, \partial_z x(t) \rangle_{\Omega,\mathrm{I}} = \langle m(1), x(1,t) \rangle_\mathrm{I} - \langle m(0), x(0,t) \rangle_\mathrm{I} - \langle \partial_z m, x(t) \rangle_{\Omega,\mathrm{I}}. \tag{A.41}$$

Similarly, for an integration by parts with respect to τ for the first term in the right-hand-side of (A.40), use $\partial_t x(z, t - \tau) = -\partial_\tau x(z, t - \tau)$. This leads to

$$\begin{aligned}
\langle m, \Gamma \partial_\tau x(t) \rangle_{\Omega,\mathrm{I}} = {}& \langle \Gamma^\top m(T), x(t - T) \rangle_\Omega - \langle \Gamma^\top m(0), x(t) \rangle_\Omega \\
& - \langle \Gamma^\top \partial_\tau m, x(t) \rangle_{\Omega,\mathrm{I}}.
\end{aligned} \tag{A.42}$$

Consequently, the unknown states $x(z,t)$ and $x(z, t - T)$ in the initial and end value terms in (A.42) vanish due to (3.23a). For the integral term in (A.40), changing the order of integration, i.e.,

$$\int_0^1 \int_0^z m^\top(z,\tau) D(z,\zeta) x(\zeta,\tau) \mathrm{d}\zeta \mathrm{d}z = \int_0^1 \left(\int_z^1 D^\top(\zeta,z) m(\zeta,\tau) \mathrm{d}\zeta \right)^\top x(z,\tau) \mathrm{d}z \quad \text{(A.43)}$$

leads to

$$\langle m, \mathcal{D}[x] \rangle_{\Omega,\mathrm{I}} = \langle \mathcal{D}^*[m], x \rangle_{\Omega,\mathrm{I}}, \quad \text{(A.44)}$$

where $\mathcal{D}^*$ (see (3.24)) is the formal adjoint of $\mathcal{D}$. Then, using (A.41), (A.42) with (3.23a), (A.44) in (A.40) and straightforward manipulations to shift the remaining matrices to the other arguments yields

$$\langle -\partial_z m - \Gamma \partial_\tau m - A^\top m - \mathcal{D}^*[m], x(t) \rangle_{\Omega,\mathrm{I}} = \langle m(0), x(0,t) \rangle_\mathrm{I} - \langle m(1), x(1,t) \rangle_\mathrm{I}$$
$$+ \langle \langle A_0, m \rangle_\Omega, x^-(0,t) \rangle_\mathrm{I} + \langle \langle H_1, m \rangle_\Omega, w(t) \rangle_{\Omega,\mathrm{I}} + \langle \langle B_1, m \rangle_\Omega, u(t) \rangle_{\Omega,\mathrm{I}}$$
$$+ \langle \langle E_1, m \rangle_\Omega, f(t) \rangle_{\Omega,\mathrm{I}} + \langle \langle G_1, m \rangle_\Omega, d(t) \rangle_{\Omega,\mathrm{I}}. \quad \text{(A.45)}$$

Hence, (A.45) becomes independent of $x(z,t)$ if (3.22a) holds. The BCs (3.1b) and (3.1c) can be utilized to simplify $x(0,t)$ and $x(1,t)$ in (A.45). In view of (3.4) and the BCs (3.1b) as well as (3.1c) the result

$$x(0,t) = J_+^\top \big(K_0 x^-(0,t) + H_2 w(t) + B_2 u(t)$$
$$+ E_2 f(t) + G_2 d(t) \big) + J_-^\top x^-(0,t) \quad \text{(A.46a)}$$
$$x(1,t) = J_+^\top x^+(1,t) + J_-^\top \big(K_1 x^+(1,t) + B_3 u(t) + E_3 f(t) + G_3 d(t) \big) \quad \text{(A.46b)}$$

is obtained. Consequently, the terms with $x(0,t)$ and $x(1,t)$ in (A.45) become

$$\langle m(0), x(0,t) \rangle_\mathrm{I} = \langle \big(K_0^\top J_+ + J_- \big) m(0), x^-(0,t) \rangle_\mathrm{I} + \langle H_2^\top J_+ m(0), w(t) \rangle_\mathrm{I}$$
$$+ \langle B_2^\top J_+ m(0), u(t) \rangle_\mathrm{I} + \langle E_2^\top J_+ m(0), f(t) \rangle_\mathrm{I} + \langle G_2^\top J_+ m(0), d(t) \rangle_\mathrm{I} \quad \text{(A.47a)}$$

as well as

$$\langle m(1), x(1,t) \rangle_\mathrm{I} = \langle \big(K_1^\top J_- + J_+ \big) m(1), x^+(1,t) \rangle_\mathrm{I} + \langle B_3^\top J_- m(1), u(t) \rangle_\mathrm{I}$$
$$+ \langle E_3^\top J_- m(1), f(t) \rangle_\mathrm{I} + \langle G_3^\top J_- m(1), d(t) \rangle_\mathrm{I}. \quad \text{(A.47b)}$$

Using $m^-(z,\tau) = J_- m(z,\tau)$ and $m^+(z,\tau) = J_+ m(z,\tau)$ as well as inserting (3.22a) and (A.47) in (A.45),

$$
\begin{aligned}
0 = {}& \langle \langle A_0, m \rangle_\Omega + K_0^\top m^+(0) + m^-(0), x^-(0,t) \rangle_\mathrm{I} - \langle K_1^\top m^-(1) + m^+(1), x^+(1,t) \rangle_\mathrm{I} \\
& + \langle \langle H_1, m \rangle_\Omega + H_2^\top m^+(0), w(t) \rangle_{\Omega,\mathrm{I}} \\
& + \langle \langle B_1, m \rangle_\Omega + B_2^\top m^+(0) - B_3^\top m^-(1), u(t) \rangle_\mathrm{I} \\
& + \langle \langle E_1, m \rangle_\Omega + E_2^\top m^+(0) - E_3^\top m^-(1), f(t) \rangle_\mathrm{I} \\
& + \langle \langle G_1, m \rangle_\Omega + G_2^\top m^+(0) - G_3^\top m^-(1), d(t) \rangle_\mathrm{I}
\end{aligned}
\tag{A.48}
$$

results.

The result (A.48) still depends on the lumped state $w(t)$. In order to eliminate it, apply the transformation (3.17b) to (3.1d) and use the substitution $\partial_t w(t-\tau) = -\partial_\tau w(t-\tau)$. This yields

$$
\begin{aligned}
-\langle q_w, \partial_\tau w(t) \rangle_\mathrm{I} = {}& \langle F^\top q_w, w(t) \rangle_\mathrm{I} + \langle L_2^\top q_w, x^-(0,t) \rangle_\mathrm{I} + \langle B_4^\top q_w, u(t) \rangle_\mathrm{I} \\
& + \langle E_4^\top q_w, f(t) \rangle_\mathrm{I} + \langle G_4^\top q_w, d(t) \rangle_\mathrm{I}.
\end{aligned}
\tag{A.49}
$$

For the left-hand side in (A.49), integration by parts leads to

$$
\langle q_w, \partial_\tau w(t) \rangle_\mathrm{I} = -\langle \dot{q}_w, w(t) \rangle_\mathrm{I}
\tag{A.50}
$$

with $\dot{q}_w(\tau) = \partial_\tau q_w(\tau)$ if $q_w(\tau)$ satisfies (3.23b). Then, taking (A.50) in (A.49) into account,

$$
\begin{aligned}
\langle \dot{q}_w - F^\top q_w, w(t) \rangle_\mathrm{I} = {}& \langle L_2^\top q_w, x^-(0,t) \rangle_\mathrm{I} + \langle B_4^\top q_w, u(t) \rangle_\mathrm{I} \\
& + \langle E_4^\top q_w, f(t) \rangle_\mathrm{I} + \langle G_4^\top q_w, d(t) \rangle_\mathrm{I}
\end{aligned}
\tag{A.51}
$$

results. In view of (3.22b), the first term on the right-hand side in (A.48) becomes

$$
\begin{aligned}
\langle \langle A_0, m \rangle_\Omega + K_0^\top m^+(0) &+ m^-(0), x^-(0,t) \rangle_\mathrm{I} \\
&= -\langle L_2^\top q_w, x^-(0,t) \rangle_\mathrm{I} + \langle C_0^\top n, x^-(0,t) \rangle_\mathrm{I}.
\end{aligned}
\tag{A.52}
$$

To incorporate the output equation (3.1e) in (A.52), apply (3.17d) to (3.1e) to obtain

$$
\langle C_0^\top n, x^-(0,t) \rangle_\mathrm{I} = \langle n, y(t) \rangle_\mathrm{I} - \langle E_5^\top n, f(t) \rangle_\mathrm{I} - \langle G_5^\top n, d(t) \rangle_\mathrm{I} - \langle C_1^\top n, w(t) \rangle_\mathrm{I}
\tag{A.53}
$$

after shifting the matrices to the integral kernels and solving for the term dependent

on $x^-(0,t)$. By inserting (A.51) and (A.53) in (A.52),

$$\langle\langle A_0, m\rangle_\Omega + K_0^\top m^+(0) + m^-(0), x^-(0,t)\rangle_I$$
$$= \langle F^\top q_w - \dot{q}_w, w(t)\rangle_I + \langle B_4^\top q_w, u(t)\rangle_I + \langle E_4^\top q_w, f(t)\rangle_I + \langle G_4^\top q_w, d(t)\rangle_I$$
$$+ \langle n, y(t)\rangle_I - \langle E_5^\top n, f(t)\rangle_I - \langle G_5^\top n, d(t)\rangle_I - \langle C_1^\top n, w(t)\rangle_I \qquad (A.54)$$

With (A.54), (A.48) reads as

$$0 = \langle n, y(t)\rangle_I - \langle K_1^\top m^-(1) + m^+(1), x^+(1,t)\rangle_I$$
$$+ \langle\langle H_1, m\rangle_\Omega + H_2^\top m^+(0) + F^\top q_w - \dot{q}_w - C_1^\top n, w(t)\rangle_I$$
$$+ \langle\langle B_1, m\rangle_\Omega + B_2^\top m^+(0) - B_3^\top m^-(1) + B_4^\top q_w, u(t)\rangle_I$$
$$+ \langle\langle E_1, m\rangle_\Omega + E_2^\top m^+(0) - E_3^\top m^-(1) + E_4^\top q_w - E_5^\top n, f(t)\rangle_I$$
$$+ \langle\langle G_1, m\rangle_\Omega + G_2^\top m^+(0) - G_3^\top m^-(1) + G_4^\top q_w - G_5^\top n, d(t)\rangle_I, \qquad (A.55)$$

after sorting the terms according to the system variables $w(t)$, $u(t)$, $f(t)$ and $d(t)$. Hence, (A.55) becomes independent of $w(t)$ if (3.22d) holds (see second line in (A.55)) and independent of $x^+(1,t)$ if (3.22c) holds. Subsequently and by consideration of (3.21a) and (3.21b) in (A.55),

$$0 = \langle n, y(t)\rangle_I + \langle m_u, u(t)\rangle_I - \langle m_f, f(t)\rangle_I + \langle m_d, d(t)\rangle_I \qquad (A.56)$$

follows, in which $m_d(\tau)$ is

$$m_d(\tau) = \langle G_1, m(\tau)\rangle_\Omega + G_2^\top m^+(0,\tau) - G_3^\top m^-(1,\tau) + G_4^\top q_w(\tau) - G_5^\top n(\tau). \quad (A.57)$$

In light of (2.13) and (3.21c),

$$0 = \langle n, y(t)\rangle_I + \langle m_u, u(t)\rangle_I + \langle m_f, f(t)\rangle_I + \langle m_{\bar{d}}, \bar{d}(t)\rangle_I + \langle \tilde{G}^\top m_d, \tilde{d}(t)\rangle_I \qquad (A.58)$$

is obtained. This can be decoupled from the term dependent on $\tilde{d}(t)$ by inserting (2.15b), yielding

$$\langle \tilde{G}^\top m_d, \tilde{d}(t)\rangle_I = \langle R_d^\top \tilde{G}^\top m_d, v_d(t)\rangle_I. \qquad (A.59)$$

Applying (3.17c) to (2.15a), the substitution $\dot{v}_d(t-\tau) = -\mathrm{d}_\tau v_d(t-\tau)$ and integration by parts lead to

$$\langle \dot{q}_d - S_d^\top q_d, v_d(\tau)\rangle_I = 0 \qquad (A.60)$$

with $\dot{q}_d(\tau) = \mathrm{d}_\tau q_d(\tau)$ in view of (3.23c). Thus, $\langle \tilde{G}^\top m_d, \tilde{d}(t)\rangle_I = 0$ results from (3.22e) in view of (A.57). Finally (3.20) is obtained.

A.8 Derivation for (3.85)

To derive $\Theta_{\bar{d}}(\tau)$ in (3.85), the spatial reversal $\bar{z} = 1 - z$ is applied to (3.21c) and $n(\tau)$ following from solving (3.27c) for $n(\tau)$ is inserted. Then, by replacing $\bar{m}(\tau)$ by the inverse backstepping transformation (3.31), $m_{\bar{d}}(\tau)$ can be expressed by

$$m_{\bar{d}}(\tau) = \int_0^T \tilde{\bar{G}}_1(z)\tilde{m}(z,\tau)\mathrm{d}z + \tilde{\bar{G}}_2 \tilde{m}^-(0,\tau) + \tilde{\bar{G}}_3 \tilde{m}(1,\tau) + \tilde{\bar{G}}_4 q(\tau) \qquad \text{(A.61)}$$

with

$$\tilde{\bar{G}}_1(z) = -\bar{G}^\top \left(G_5^\top \left(C_0^\top \right)^{-1} \bar{A}_0^\top(z) - \bar{G}_1^\top(z) + \left(G_5^\top \left(C_0^\top \right)^{-1} \left(J_-^\top + J_+^\top K_0 \right) \right.$$

$$\left. - G_2^\top J_+ \right) \bar{K}(1,z) + \int_z^1 (G_5^\top \left(C_0^\top \right)^{-1} \bar{A}_0^\top(\zeta) - \bar{G}_1^\top(\zeta))\bar{K}_I(\zeta,z)\mathrm{d}\zeta \right) \quad \text{(A.62a)}$$

$$\tilde{\bar{G}}_2 = -\bar{G}^\top G_3^\top \qquad \text{(A.62b)}$$

$$\tilde{\bar{G}}_3 = \bar{G}^\top \left(G_2^\top J_+ - G_5^\top \left(C_0^\top \right)^{-1} \left(J_- + K_0^\top J_+ \right) \right) \qquad \text{(A.62c)}$$

$$\tilde{\bar{G}}_4 = \bar{G}^\top \left(G_4^\top - G_5^\top \left(C_0^\top \right)^{-1} L_2^\top \right) J_w. \qquad \text{(A.62d)}$$

By replacing $\tilde{m}(z,\tau)$, $\tilde{m}^-(0,\tau)$ and $q(\tau)$ in (A.61) with (3.54b), (3.53) and (3.54a),

$$m_{\bar{d}}(\tau) = \sum_{i=0}^{n_q} \int_0^1 X_{1,i}^{\bar{d}}(z)\Psi[\mathrm{d}_\tau^i \varphi](z,\tau)\mathrm{d}z + X_{2,i}^{\bar{d}}\mathrm{d}_\tau^i \varphi(\tau) + X_{3,i}^{\bar{d}}\Psi[\mathrm{d}_\tau^i \varphi](1,\tau) \quad \text{(A.63)}$$

is obtained, where the matrices are given by

$$X_{1,i}^{\bar{d}}(z) = \tilde{\bar{G}}_1(z)a_i + \tilde{\bar{G}}_4 \tilde{F}_i \tilde{B}_1(z) \qquad \text{(A.64a)}$$

$$X_{2,i}^{\bar{d}} = \tilde{\bar{G}}_2 a_i + \tilde{\bar{G}}_4 \tilde{F}_i \bar{B}_2 \qquad \text{(A.64b)}$$

$$X_{3,i}^{\bar{d}} = \tilde{\bar{G}}_3 a_i + \tilde{\bar{G}}_4 \tilde{F}_i \tilde{B}_3 \qquad \text{(A.64c)}$$

and $\tilde{F}_{n_q} = 0$ is used. Finally, insert (3.70) in (A.63) and subsequently (3.74), which yields

$$\Theta_{\bar{d}}(\tau) = \sum_{i=0}^{n_q} \left(\int_0^1 X_{1,i}^{\bar{d}}(z) \Psi[\mathrm{d}_\tau^i \Theta](z,\tau) \mathrm{d}z + X_{2,i}^{\bar{d}} \mathrm{d}_\tau^i \Theta(\tau) + X_{3,i}^{\bar{d}} \Psi[\mathrm{d}_\tau^i \Theta](1,\tau) \right) \bar{\Theta}^\perp.$$

$$(\text{A}.65)$$

Bibliography

[1] O. M. Aamo. "Leak detection, size estimation and localization in pipe flows". In: *IEEE Transactions on Automatic Control* 61 (2015), pp. 246–251 (cit. on p. 3).

[2] A. Aldoghaither, D.-Y. Liu, and T.-M. Laleg-Kirati. "Modulating functions based algorithm for the estimation of the coefficients and differentiation order for a space-fractional advection-dispersion equation". In: *SIAM Journal on Scientific Computing* 37 (2015), A2813–A2839 (cit. on p. 7).

[3] Y. Aoustin, M. Fliess, H. Mounier, P. Rouchon, and J. Rudolph. "Theory and practice in the motion planning and control of a flexible robot arm using Mikusinski operators". In: *Proc. of the Fifth IFAC Symposium on Robot Control*. Vol. 2. 1997, pp. 287–293 (cit. on pp. 2, 5, 11).

[4] A. Armaou and M. A. Demetriou. "Robust detection and accommodation of incipient component and actuator faults in nonlinear distributed processes". In: *American Institute of Chemical Engineers Journal* 54 (2008), pp. 2651–2662 (cit. on p. 3).

[5] S. Asiri and T.-M. Laleg-Kirati. "Modulating functions-based method for parameters and source estimation in one-dimensional partial differential equations". In: *Inverse Problems in Science and Engineering* 25 (2017), pp. 1191–1215 (cit. on p. 8).

[6] B. Atkinson. *Biochemical Reactors*. London: Pion Limited, 1974 (cit. on pp. 2, 11).

[7] M. J. Balas. "Active control of flexible systems". In: *Journal of Optimization Theory and Applications* 25 (1978), pp. 415–436 (cit. on pp. 2, 11).

[8] H. T. Banks, R. C. Smith, and Y. Wang. *Smart Material Structures: Modeling, Estimation and Control*. Chichester: John Wiley & Sons/Masson, 1996 (cit. on pp. 2, 11).

[9] H. Baruh. "Actuator failure detection in the control of distributed systems". In: *Journal of Guidance, Control, and Dynamics* 9 (1986), pp. 181–189 (cit. on p. 2).

[10] G. Bastin and J.-M. Coron. *Stability and Boundary Stabilization of 1-d Hyperbolic Systems*. Basel: Birkhäuser, 2016 (cit. on pp. 2, 89, 91).

[11] D. S. Bernstein. *Matrix Mathematics: Theory, Facts, and Formulas with Application to Linear Systems Theory*. New Jersey: Princeton University Press, 2009 (cit. on pp. 9, 30, 46, 52, 74, 75, 80, 81, 140, 159).

[12] M. Blanke, M. Kinnaert, J. Lunze, and M. Staroswiecki. *Diagnosis and Fault-Tolerant Control*. Berlin: Springer, 2016 (cit. on pp. 2, 18, 19).

[13] M. Böhm, M. Krstic, S. Küchler, and O. Sawodny. "Modeling and boundary control of a hanging cable immersed in water". In: *Journal of Dynamic Systems, Measurement, and Control* 136 (2014). Article 011006 (cit. on p. 116).

[14] F. Bribiesca-Argomedo and M. Krstic. "Backstepping-forwarding control and observation for hyperbolic PDEs with fredholm integrals". In: *IEEE Transactions on Automatic Control* 60 (2015), pp. 2145–2160 (cit. on p. 93).

[15] J. Cai, H. Ferdowsi, and J. Sarangapani. "Model-based fault detection, estimation, and prediction for a class of linear distributed parameter systems". In: *Automatica* 66 (2016), pp. 122–131 (cit. on p. 3).

[16] C.-T. Chen. *Linear System Theory and Design*. New York: Oxford University Press, Inc., 1999 (cit. on pp. 2, 34, 59, 74, 76, 141, 160).

[17] O. B. Cieza, J. C. Tafur, and J. Reger. "Frequency domain modulating functions for continuous-time identification of linear and nonlinear systems". In: *16th Latinamerican Control Conference*. Quintana Roo, Mexico, 2014, pp. 690–695 (cit. on p. 7).

[18] R. F. Curtain and H. Zwart. *An Introduction to Infinite-dimensional Linear Systems Theory*. New York: Springer-Verlag, 2012 (cit. on p. 13).

[19] C. M. Dafermos. *Hyperbolic Conservation Laws in Continuum Physics*. Berlin: Springer-Verlag, 2010 (cit. on pp. 91–93, 120).

[20] M. A. Demetriou. "A model-based fault detection and diagnosis scheme for distributed parameter systems: A learning systems approach". In: *ESAIM: Control, Optimisation and Calculus of Variations* 7 (2002), pp. 43–67 (cit. on p. 3).

[21] M. A. Demetriou and A. Armaou. "Dynamic online nonlinear robust detection and accommodation of incipient component faults for nonlinear dissipative distributed processes". In: *International Journal of Robust and Nonlinear Control* 22 (2012), pp. 3–23 (cit. on p. 3).

[22] M. A. Demetriou, K. Ito, and R. C. Smith. "Adaptive monitoring and accommodation of nonlinear actuator faults in positive real infinite dimensional systems". In: *IEEE Transactions on Automatic Control* 52 (2007), pp. 2332–2338 (cit. on p. 3).

[23] J. Deutscher. "Fault detection for linear distributed-parameter systems using finite-dimensional functional observers". In: *International Journal of Control* 89 (2016), pp. 550–563 (cit. on p. 3).

[24] J. Deutscher and J. Gabriel. "A backstepping approach to output regulation for coupled linear wave–ODE systems". In: *Automatica* 123 (2021). Article 109338 (cit. on p. 93).

[25] J. Deutscher, N. Gehring, and R. Kern. "Output feedback control of general linear heterodirectional hyperbolic PDE-ODE systems with spatially-varying coefficients". In: *International Journal of Control* 92 (2018), pp. 2274–2290 (cit. on p. 101).

[26] S. Dey and S. J. Moura. "Robust fault diagnosis of uncertain one-dimensional wave equations". In: *57th IEEE Conference on Decision and Control*. Miami Beach, Florida, USA, 2018, pp. 2902–2907 (cit. on p. 3).

[27] S. Dey, H. E. Perez, and S. J. Moura. "Robust fault detection of a class of uncertain linear parabolic PDEs". In: *Automatica* 107 (2019), pp. 502–510 (cit. on p. 3).

[28] S. X. Ding. *Model-based Fault Diagnosis Techniques: Design Schemes, Algorithms, and Tools*. Berlin: Springer-Verlag, 2008 (cit. on pp. 2, 15, 16, 59).

[29] V. Duindam, A. Macchelli, S. Stramigioli, and H. Bruyninckx. *Modeling and Control of Complex Physical Systems: The Port-Hamiltonian Approach*. Berlin: Springer-Verlag, 2009 (cit. on p. 2).

[30] S. K. Dwivedy and P. Eberhard. "Dynamic analysis of flexible manipulators, a literature review". In: *Mechanism and Machine Theory* 41 (2006), pp. 749–777 (cit. on p. 2).

[31] M. Eckert, M. Kupper, and S. Hohmann. "Functional fractional calculus for system identification of battery cells". In: *at-Automatisierungstechnik* 62 (2014), pp. 272–281 (cit. on p. 7).

[32] N. H. El-Farra. "Integrated fault detection and fault-tolerant control architectures for distributed processes". In: *Industrial & Engineering Chemistry Research* 45 (2006), pp. 8338–8351 (cit. on p. 2).

[33] Y. Feng, Y. Wang, B.-C. Wang, and H.-X. Li. "Spatial decomposition-based fault detection framework for parabolic-distributed parameter processes". In: *IEEE Transactions on Cybernetics* (2021), pp. 1–9 (cit. on p. 3).

[34] Y. Feng, Y. Wang, J.-W. Wang, H.-X. Li, and S. X. Ding. "Spatio-temporal fault localization for nonlinear spatially distributed processes: a spatial mapping filter-based framework". In: *International Journal of Robust and Nonlinear Control* 31 (2021), pp. 6953–6971 (cit. on p. 3).

[35] N. Gehring, C. Stauch, and J. Rudolph. "Parameter identification, fault detection and localization for an electrical transmission line". In: *European Control Conference*. Ålborg, Denmark, 2016, pp. 2090–2095 (cit. on p. 3).

[36]   L. Ghaffour, M. Noack, J. Reger, and T.-M. Laleg-Kirati. "Non-asymptotic state estimation of linear reaction diffusion equation using modulating functions". In: *21th World Congress of the International Federation of Automatic Control*. Berlin, Germany, 2020, pp. 4196–4201 (cit. on p. 8).

[37]   S. Ghantasala and N. H. El-Farra. "Robust actuator fault isolation and management in constrained uncertain parabolic PDE systems". In: *Automatica* 45 (2009), pp. 2368–2373 (cit. on pp. 2, 3).

[38]   W. B. Gu and C. Y. Wang. "Thermal-electrochemical modeling of battery systems". In: *Journal of The Electrochemical Society* 147 (2000), pp. 2910–2922 (cit. on p. 11).

[39]   H. Hao, S. X. Ding, A. Haghani, and S. Yin. "An observer-based fault detection scheme for distributed parameter systems of hyperbolic type and its application in paper production process". In: *8th IFAC Symposium on Fault Detection, Supervision and Safety for Technical Processes, SAFEPROCESS*. Mexico City, Mexico, 2012, pp. 1047–1052 (cit. on p. 2).

[40]   L. Hu, F. Di Meglio, R. Vazquez, and M. Krstic. "Control of homodirectional and general heterodirectional linear coupled hyperbolic PDEs". In: *IEEE Transactions on Automatic Control* 61 (2016), pp. 3301–3314 (cit. on pp. 90, 91, 122).

[41]   L. Hu, R. Vazquez, F. Di Meglio, and M. Krstic. "Boundary exponential stabilization of 1-dimensional inhomogeneous quasi-linear hyperbolic systems". In: *SIAM Journal on Control and Optimization* 57 (2019), pp. 963–998 (cit. on pp. 7, 91, 99–103, 111, 122, 134).

[42]   R. Isermann. *Fault-Diagnosis Systems: An Introduction from Fault Detection to Fault Tolerance*. Berlin: Springer–Verlag, 2006 (cit. on p. 2).

[43]   R. Isermann and P. Ballé. "Trends in the application of model-based fault detection and diagnosis of technical processes". In: *Control Engineering Practice* 5 (1997), pp. 709–719 (cit. on p. 1).

[44]   H. A. Jakobsen. *Chemical Reactor Modeling*. Cham: Springer International Publishing, 2014 (cit. on pp. 2, 11).

[45]   K. F. Jensen and W. H. Ray. "The bifurcation behavior of tubular reactors". In: *Chemical Engineering Science* 37 (1982), pp. 199–222 (cit. on pp. 2, 11).

[46]   J. Jouffroy and J. Reger. "Finite-time simultaneous parameter and state estimation using modulating functions". In: *IEEE Conference on Control Applications*. Sydney, Australia, 2015, pp. 394–399 (cit. on pp. 8, 20).

[47]   R. M. Kern. "Design and Experimental Validation of Output Feedback Tracking Controllers for a Pneumatic System with Distributed Parameters". PhD thesis. München: Technische Universität München, 2019 (cit. on pp. 2, 91).

[48]   L. Kiltz. "Algebraische Ableitungsschätzer in Theorie und Anwendung". PhD thesis. Saarbrücken: Naturwissenschaftlich-Technische Fakultät der Universität des Saarlandes, 2018 (cit. on pp. 56, 154).

[49]   L. Kiltz, C. Join, M. Mboup, and J. Rudolph. "Fault-tolerant control based on algebraic derivative estimation applied on a magnetically supported plate". In: *Control Engineering Practice* 26 (2014), pp. 107–115 (cit. on pp. 8, 20).

[50]   L. Kiltz, M. Mboup, and J. Rudolph. "Fault diagnosis on a magnetically supported plate". In: *2012 1st International Conference on Systems and Computer Science (ICSCS)*. IEEE. 2012, pp. 1–6 (cit. on p. 162).

[51]   A. R. Krommer and C. W. Ueberhuber. *Computational Integration.* Philadelphia: SIAM, 1998 (cit. on pp. 56, 162).

[52]   M. Krstic and A. Smyshlyaev. *Boundary Control of PDEs: A Course on Backstepping Designs.* Philadelphia: SIAM, 2008 (cit. on pp. 2, 7, 93, 101).

[53]   B. Laroche, P. Martin, and P. Rouchon. "Motion planning for the heat equation". In: *International Journal of Robust and Nonlinear Control* 10 (2000), pp. 629–643 (cit. on p. 6).

[54]   J. Levine. *Analysis and Control of Nonlinear Systems: A Flatness-Based Approach.* Berlin: Springer, 2009 (cit. on p. 6).

[55]   D.-Y. Liu, O. Gibaru, and W. Perruquetti. "Error analysis of Jacobi derivative estimators for noisy signals". In: *Numerical Algorithms* 58 (2011), pp. 53–83 (cit. on p. 8).

[56]   J. Loeb and G. Cahen. "More about process identification". In: *IEEE Transactions on Automatic Control* 10 (1965), pp. 359–361 (cit. on p. 7).

[57]   A. Lomakin and J. Deutscher. "Algebraic fault detection and identification for rigid robots". In: *2020 IEEE International Conference on Robotics and Automation.* Paris, France, 2020, pp. 9352–9358 (cit. on p. 8).

[58]   A. Lomakin and J. Deutscher. "Fault detection and identification for nonlinear MIMO systems using derivative estimation". In: *IFAC-PapersOnLine* 53 (2020), pp. 658–663 (cit. on p. 8).

[59]   Z.-H. Luo, B.-Z. Guo, and Ö. Morgül. *Stability and Stabilization of Infinite Dimensional Systems with Applications.* London: Springer-Verlag, 1999 (cit. on pp. 2, 89, 91).

[60]   A. F. Lynch and J. Rudolph. "Flatness-based boundary control of a class of quasilinear parabolic distributed parameter systems". In: *International Journal of Control* 75 (2002), pp. 1219–1230 (cit. on p. 39).

[61]   M. Mboup, C. Join, and M. Fliess. "Numerical differentiation with annihilators in noisy environment". In: *Numerical Algorithms* 50 (2008), pp. 439–467 (cit. on p. 8).

[62] T. Meurer. *Control of Higher-dimensional PDEs: Flatness and Backstepping Designs*. Berlin: Springer-Verlag, 2012 (cit. on pp. 2, 6, 33, 153).

[63] J. Mikusiński. *Operational Calculus, Vol. 1*. Oxford: Pergamon Press Ltd., 1983 (cit. on p. 33).

[64] A. V. Oppenheim, A. S. Willsky, and S. H. Nawab. *Signals & Systems*. London: Prentice-Hall, 1997 (cit. on p. 163).

[65] A. Othmane, H. Mounier, and J. Rudolph. "Parametrization of algebraic differentiators for disturbance annihilation with an application to the differentiation of quantized signals". In: *24th International Symposium on Mathematical Theory of Networks and Systems*. Cambridge, United Kingdom, 2021, pp. 335–340 (cit. on p. 8).

[66] A. Othmane and J. Rudolph. "Data and computation efficient model-based fault detection for rolling element bearings using numerical differentiation". In: *5th International Conference on Control and Fault-Tolerant Systems*. Saint-Raphaël, France, 2021 (cit. on p. 8).

[67] F. J. Perdreauville and R. E. Goodson. "Identification of systems described by partial differential equations". In: *Journal of Basic Engineering* 88 (1966), pp. 463–468 (cit. on p. 7).

[68] N. Petit and P. Rouchon. "Flatness of heavy chain systems". In: *SIAM Journal on Control and Optimization* 40 (2001), pp. 475–495 (cit. on pp. 2, 91).

[69] G. Pin, B. Chen, and T. Parisini. "Robust deadbeat continuous-time observer design based on modulation integrals". In: *Automatica* 107 (2019), pp. 95–102 (cit. on p. 8).

[70] H. A. Preisig and D. W. T. Rippin. "Theory and application of the modulating function method–I. Review and theory of the method and theory of the spline-type modulating functions". In: *Computers & Chemical Engineering* 17 (1993), pp. 1–16 (cit. on pp. 7, 20).

[71] W. Ray. *Advanced Process Control*. New York, USA: McGraw-Hill, 1981 (cit. on p. 11).

[72] L. Rodino. *Linear Partial Differential Operators in Gevrey Spaces*. Singapore: World Scientific Publishing, 1993 (cit. on pp. 39, 76).

[73] J. Rudolph. *Beiträge zur flachheitsbasierten Folgeregelung linearer und nichtlinearer Systeme endlicher und unendlicher Dimension*. Aachen: Shaker Verlag, 2003 (cit. on pp. 6, 33).

[74] J. Rudolph. *Flatness-Based Control: An Introduction*. Düren: Shaker Verlag, 2021 (cit. on p. 6).

[75] J. Rudolph and F. Woittennek. "Motion planning and open loop control design for linear distributed parameter systems with lumped controls". In: *International Journal of Control* 81 (2008), pp. 457–474 (cit. on pp. 6, 7, 13, 33, 34, 36, 40, 103, 105, 155, 159, 160).

[76] C. Sagert, F. Di Meglio, M. Krstic, and P. Rouchon. "Backstepping and flatness approaches for stabilization of the stick-slip phenomenon for drilling". In: *5th IFAC Symposium on System Structure and Control*. Vol. 46. Grenoble, France, Elsevier BV, 2013, pp. 779–784 (cit. on p. 91).

[77] C. Schmid. *Parameteridentifikation für zeitkontinuierliche Systeme mittels signalmodellgenerierter Modulationsfunktionen*. Berichte aus der Steuerungs- und Regelungstechnik. Aachen: Shaker Verlag, 2011 (cit. on p. 8).

[78] C. Schmid and G. Roppenecker. "Parameteridentifikation für LTI-Systeme mit Hilfe signalmodellgenerierter Modulationsfunktionen". In: *at-Automatisierungstechnik* 59 (2011), pp. 521–528 (cit. on pp. 8, 20).

[79] J. Schröck, T. Meurer, and A. Kugi. "Control of a flexible beam actuated by macro-fiber composite patches: I. Modeling and feedforward trajectory control". In: *Smart Materials and Structures* 20 (2010), pp. 1–7 (cit. on pp. 47, 48, 56, 83).

[80] J. Schröck, T. Meurer, and A. Kugi. "Motion planning for piezo-actuated flexible structures: Modeling, design, and experiment". In: *IEEE Transactions on Control Systems Technology* 21 (2013), pp. 807–819 (cit. on p. 11).

[81] M. Shinbrot. "On the analysis of linear and nonlinear dynamical systems from transient-response data". In: *National Advisory Commitee for Aeronautics* Technical Note 3288 (1954) (cit. on p. 7).

[82] H. Sira-Ramírez and S. K. Agrawal. *Differentially Flat Systems*. New York: Dekker, 2004 (cit. on pp. 6, 75, 141).

[83] T. Meurer and A. Kugi. "Tracking control for boundary controlled parabolic PDEs with varying parameters: combining backstepping and differential flatness". In: *Automatica* 45 (2009), pp. 1182–1194 (cit. on p. 7).

[84] S.-X. Tang, L. Camacho-Solorio, Y. Wang, and M. Krstic. "State-of-charge estimation from a thermal-electrochemical model of lithium-ion batteries". In: *Automatica* 83 (2017), pp. 206–219 (cit. on p. 11).

[85] E.C. Titchmarsh. "The zeros of certain integral functions". In: *Proceedings of the London Mathematical Society* 25 (1926), pp. 283–302 (cit. on p. 27).

[86] L. N. Trefethen. *Spectral Methods in MATLAB*. Oxford: SIAM, 2000 (cit. on pp. 123, 146).

[87] J. Wang and M. Krstic. "Vibration suppression for coupled wave PDEs in deep-sea construction". In: *IEEE Transactions on Control Systems Technology* 29 (2020), pp. 1–17 (cit. on pp. 91, 116, 118–121, 143).

[88]   J. Wang, Y. Pi, and M. Krstic. "Balancing and suppression of oscillations of tension and cage in dual-cable mining elevators". In: *Automatica* 98 (2018), pp. 223–238 (cit. on pp. 2, 91).

[89]   Ji Wang, Shu-Xia Tang, and Miroslav Krstic. "Adaptive output-feedback control of torsional vibration in off-shore rotary oil drilling systems". In: *Automatica* 111 (2020). Article 108640 (cit. on p. 91).

[90]   X. Wei, D.-Y. Liu, and D. Boutat. "Non-asymptotic pseudo-state estimation for a class of fractional order linear systems". In: *IEEE Transactions on Automatic Control* (2016) (cit. on p. 8).

[91]   Y.-Q. Wei, D.-Y. Liu, and D. Boutat. "Innovative fractional derivative estimation of the pseudo-state for a class of fractional order linear systems". In: *Automatica* 99 (2019), pp. 157–166 (cit. on p. 8).

[92]   D. V. Widder. *The Laplace Transform.* Princeton: Princeton University Press, 1946 (cit. on p. 112).

[93]   F. Woittennek. *Beiträge zum Steuerungsentwurf für lineare, örtlich verteilte Systeme mit konzentrierten Stelleingriffen.* Berichte aus der Steuerungs- und Regelungstechnik. Aachen: Shaker Verlag, 2007 (cit. on pp. 6, 7, 13, 33, 36, 40, 41, 76, 94, 99, 155, 156).

[94]   F. Woittennek and H. Mounier. "Controllability of networks of spatially one-dimensional second order PDEs – an algebraic approach". In: *SIAM Journal on Control and Optimization* 48 (2010), pp. 3882–3902 (cit. on p. 7).

[95]   F. Woittennek and J. Rudolph. "Motion planning for a class of boundary controlled linear hyperbolic PDE's involving finite distributed delays". In: *ESAIM: Control, Optimisation and Calculus of Variations* 9 (2003), pp. 419–435 (cit. on p. 103).

[96]   X. Xu and S. Dubljevic. "Optimal tracking control for a class of boundary controlled linear coupled hyperbolic PDE systems: Application to plug flow reactor with temperature output feedback". In: *European Journal of Control* 39 (2018), pp. 21–34 (cit. on p. 93).

[97]   X. Xu, Y. Yuan, M. Wang, M. Fu, and S. Dubljevic. "Fault detection and estimation for a class of PIDE systems based on boundary observers". In: *International Journal of Robust and Nonlinear Control* 29 (2019), pp. 5867–5885 (cit. on p. 3).

Publications of the author

[98]   F. Fischer and J. Deutscher. "Algebraic fault detection and isolation for parabolic distributed-parameter systems using modulation functions". In: *2nd IFAC Workshop on Control of Systems Governed by Partial Differential Equations.* Bertinoro, Italy, 2016, pp. 164–169 (cit. on pp. 4, 8, 13).

[99]   F. Fischer and J. Deutscher. "Fault detection for parabolic systems with distributed inputs and outputs using the modulation function approach". In: *20th World Congress of the International Federation of Automatic Control.* Toulouse, France, 2017, pp. 6968–6973 (cit. on pp. 13, 42).

[100] F. Fischer and J. Deutscher. "Modulating function based fault detection for parabolic systems with polynomial faults". In: *10th IFAC Symposium on Fault Detection, Supervision and Safety for Technical Processes, SAFEPROCESS.* Warsaw, Poland, 2018, pp. 359–366 (cit. on p. 15).

[101] F. Fischer and J. Deutscher. "Flachheitsbasierte algebraische Fehlerdiagnose für einen Euler-Bernoulli-Balken mittels Modulationsfunktionen". In: *at-Automatisierungstechnik* 67 (2019), pp. 622–636 (cit. on p. 47).

[102] F. Fischer and J. Deutscher. "Flatness-based algebraic fault diagnosis for distributed-parameter systems". In: *Automatica* 117 (2020). Article 108987 (cit. on pp. 4, 5, 13, 33, 42).

[103] F. Fischer and J. Deutscher. "Flatness-based algebraic fault identification for a wave equation with dynamic boundary conditions". In: *21th World Congress of the International Federation of Automatic Control.* Berlin, Germany, 2020, pp. 7737–7742 (cit. on pp. 4, 94).

[104] F. Fischer and J. Deutscher. "Fault diagnosis for linear heterodirectional hyperbolic ODE–PDE systems using backstepping-based trajectory planning". In: *Automatica* 135 (2022), p. 109952 (cit. on pp. 4, 5, 7).

[105] F. Fischer, J. Deutscher, and T.-M. Laleg-Kirati. "Source estimation for first order time-varying hyperbolic systems". In: *23rd International Symposium on Mathematical Theory of Networks and Systems.* Hong Kong, China, 2018, pp. 78–84 (cit. on p. 8).

[106] F. Fischer, V. Todorovski, and J. Deutscher. "Fault detection for lumped-parameter LTI systems using integral transformations and trajectory planning methods". In: *5th International Conference on Control and Fault-Tolerant Systems*. Saint-Raphaël, France, 2021, pp. 79–84 (cit. on p. 4).

[107] K. Löhe, G. Roppenecker, and F. Fischer. "Modellbasierter Steuerungsentwurf für die Vertikaldynamik eines Fahrzeugs mit aktiver Federung –". In: *VDI-Berichte Nr. 2196 (VDI-Tagung Steuerung und Regelung von Fahrzeugen und Motoren - AUTOREG 2013)*. Düsseldorf: VDI-Verlag, 2013, pp. 445–450.

Software libraries

[108] F. Fischer and J. Gabriel. *A Matlab toolbox for the fault diagnosis for distributed-parameter systems*. Zenodo. Version v1.0. 2021 (cit. on pp. 47, 78, 116, 143).

[109] F. Fischer, J. Gabriel, and S. Kerschbaum. *coni - a Matlab toolbox facilitating the solution of control problems*. Zenodo. Version v1.1. 2021 (cit. on pp. 51, 78).

Advised student works

[110] S. Böckler. "k-Summationsmethode für die Trajektorienplanung". Bachelor thesis. Lehrstuhl für Regelungstechnik, Friedrich-Alexander-Universität Erlangen-Nürnberg, 2017.

[111] D. Burk. "Fehlerdiagnose für hyperbolische Systeme mittels Modulationsfunktionen". Master thesis. Lehrstuhl für Regelungstechnik, Friedrich-Alexander-Universität Erlangen-Nürnberg, 2019.

[112] J. Dahlmann. "Flachheitsbasierte Trajektorienplanung für ein verteilt-parametrisches System mit zweidimensionalem Ortsbereich". Research internship. Lehrstuhl für Regelungstechnik, Friedrich-Alexander-Universität Erlangen-Nürnberg, 2019.

[113] J. Li. "Parameteridentifikation für einen zweidimensionale Wärmeleiter". Research internship. Lehrstuhl für Regelungstechnik, Friedrich-Alexander-Universität Erlangen-Nürnberg, 2020.

[114] M. Mosé. "Fehlerdetektion und -isolation für einen Wärmeleiter". Master thesis. Lehrstuhl für Regelungstechnik, Friedrich-Alexander-Universität Erlangen-Nürnberg, 2018.

[115] S. Ostertag. "Trajektorienplanung für gewisse lineare verteilt-parametrische Systeme". Bachelor thesis. Lehrstuhl für Regelungstechnik, Friedrich-Alexander-Universität Erlangen-Nürnberg, 2017.

[116] F. Probst. "Algebraische Detektion zeitveränderlicher Fehler bei verteilt-parametrischen Systemen". Bachelor thesis. Lehrstuhl für Regelungstechnik, Friedrich-Alexander-Universität Erlangen-Nürnberg, 2016.

[117] N. Riedel. "Entwurf und Aufbau eines Versuchsstandes für einen Wärmeleiter". Bachelor thesis. Lehrstuhl für Regelungstechnik, Friedrich-Alexander-Universität Erlangen-Nürnberg, 2016.

[118] F. Stephan. "Simulation fraktionaler Diffusions-Reaktionssysteme". Research internship. Lehrstuhl für Regelungstechnik, Friedrich-Alexander-Universität Erlangen-Nürnberg, 2019.

[119] M. Thurner. "Parameteridentifikation bei Werkzeugmaschinen mittels Modulationsfunktionen". Master thesis. Lehrstuhl für Regelungstechnik, Friedrich-Alexander-Universität Erlangen-Nürnberg, 2017.

[120] O. Umbeer. "Finite-Elemente-Methode für einen Euler-Bernoulli-Balken". Bachelor thesis. Lehrstuhl für Regelungstechnik, Friedrich-Alexander-Universität Erlangen-Nürnberg, 2017.

[121] M. Zheng. "Simulation of a heat conductor with FEniCS". Research internship. Lehrstuhl für Regelungstechnik, Friedrich-Alexander-Universität Erlangen-Nürnberg, 2019.

[122] S. Zimmermann. "Algebraische Fehlerdiagnose für verteilt-parametrische Systeme mit zeitlich veränderlichen Fehlern". Bachelor thesis. Lehrstuhl für Regelungstechnik, Friedrich-Alexander-Universität Erlangen-Nürnberg, 2019.

Index